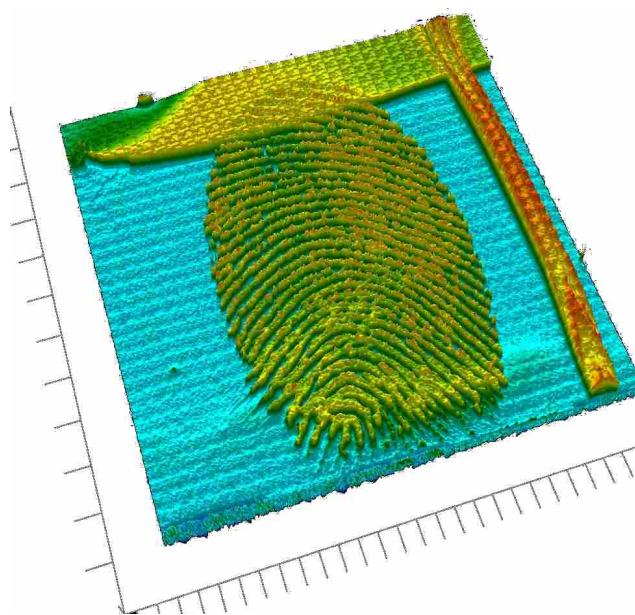# Reagents for infrared chemical imaging of fingerprints on difficult surfaces

Mark Tahtouh

A thesis submitted for the

Degree of Doctor of Philosophy (Science)

University of Technology, Sydney

May, 2008

In light of knowledge attained, the happy achievement seems almost a matter of course, and any intelligent student can grasp it without too much trouble. But the years of anxious searching in the dark, with their intense longing, their alterations of confidence and exhaustion and the final emergence into the light – only those who have experienced it can understand it.

Albert Einstein, 1933

Certificate of authorship and originality

I certify that the work in this thesis has not previously been submitted for a degree nor has it been submitted as part of the requirements for a degree except as fully acknowledged within the text.

I also certify that the thesis has been written by me. Any help that I have received in my research work and the preparation of the thesis itself has been acknowledged. In addition, I certify that all the information sources and literature used are indicated in the thesis.

Mark Tahtouh

08/12/2008

Acknowledgements

This thesis is the end product of a research project that spans several years. Over this period there have been a number of people who have contributed to the success of this project. First and foremost, I am deeply indebted to my principal supervisor Dr Brian J. Reedy. You have been the driving force behind this project since it began during my honours year (2003). You have always been supportive, encouraging and have played an enormous role in maintaining my drive and motivation. I can not thank you enough for always being helpful, supportive and encouraging throughout the highs and lows that this project has presented. You are truly the best supervisor that anyone could ask for. I am grateful to have come to know you as not only my teacher and supervisor but also as a colleague and friend.

To my co-supervisor, Dr John Kalman, I thank you for your help and support throughout this project. The organic synthetic chemistry section of this work would not have been possible without your input. I have enjoyed the many hours we have spent unlocking the mysteries of puzzling spectra and failed reactions. It has been a real pleasure and honour to work with you and I have learnt a great deal because of your involvement and enthusiasm.

To Dr Ronald Shimmon, a pseudo-supervisor, technical assistant, colleague and true friend. Your enthusiasm, commitment and helpfulness are second to none. You have made my experiences at UTS all the more enjoyable. Thanks for your help and friendship and thanks for the laughs.

To my synthetic chemistry brother, Tristan Rawling, I thank you for the laughs and good times. Thank you for never having any faith in me, my abilities or my project – you gave me motivation to prove you wrong. The organic research lab, and my experiences there, would not be complete without you. I thank you for your help and support with troublesome reactions and hereby give you credit for the 'Rawlings gamble' for improving product yield. Thank you also for your kind donation of greasy fingerprint deposits and for the gym therapy sessions that helped me though some tough times.

To my princess Kate Grimwood, thank you for being there for me and being so loving and supportive while I was being anything but. Your encouragement and patience has made more of an impact than you realise. I am happier than I have ever been because of you and I

am honoured to be walking this wonderful path through life along your side. You are my favourite and I love you. Thank you also for your greasy fingerprint deposits that, surprisingly, proved greasier than my own.

Table of contents

List of figures

List of tables

Abbreviations

A/CAA	anthracene / 2-cyanoacrylic acid adduct
A/CAA-K	anthracene / 2-cyanoacylic acid potassium salt adduct
A/CAC	anthracene / 2-cyanoacyloyl chloride adduct
A/1-CECA	anthracene / 1-cyanoethyl 2-cyanoacylate adduct
A/2-CECA	anthracene / 2-cyanoethyl 2-cyanoacylate adduct
A/ECA	anthracene / ethyl 2-cyanoacylate adduct
A/ECA-d$_5$	anthracene / pentadeuteroethyl 2-cyanoacylate adduct
A/MA	anthracene / maleic anhydride adduct
A/MCA	anthracene / methyl 2-cyanoacylate adduct
A/MCA-d$_3$	anthracene / trideuteromethyl 2-cyanoacylate adduct
ATR	attenuated total reflection
3-BPN	3-bromopropionitrile
1-CECA	1-cyanoethyl 2-cyanoacrylate
2-CECA	2-cyanoethyl 2-cyanoacrylate
2-CECAc	2-cyanoethyl cyanoacetate
DAB	diaminobenzidine
DBU	1,8-diazobicyclo[5,4,0]undec-7-ene
DFO	1,8-diazafluorene-9-one
DMAC	dimethylaminocinnamaldehyde
DMF	*N,N*-dimethylformamide
DMSO	dimethylsulfoxide
DTA	differential thermal analysis
ECA	ethyl 2-cyanoacrylate (superglue)
ECA-d$_5$	pentadeuteroethyl 2-cyanoacylate
FPA	focal plane array
FTIR	Fourier transform infrared
GS-MS	gas chromatography – mass spectrometry
HSAB	hard soft acid base
HMPA	hexamethylphosphoramide
3-HPN	3-hydroxypropionitrile
2-HPN	2-hydroxypropionitrile
IR	infrared

MCA-d$_3$	trideuteromethyl 2-cyanoacrylate
MMD	multi-metal deposition
MNF	minimal noise fraction
MS	mass spectrometry
NMR	nuclear magnetic resonance
NWSD	non-water-soluble deposit
oligo-2-CECA	oligo-2-cyanoethyl 2-cyanoacrylate
OsO$_4$	osmium tetroxide
PD	physical developer
PC	principal component
P$_2$O$_5$	phosphorus pentoxide
poly-1-CECA	1-cyanoethyl 2-cyanoacylate polymer
poly-2-CECA	2-cyanoethyl 2-cyanoacylate polymer
poly-ECA-d$_5$	pentadeuteroethyl 2-cyanoacylate polymer
poly-MCA-d$_3$	trideuteromethyl 2-cyanoacylate polymer
RTX	ruthenium tetroxide
SO$_2$	sulfur dioxide
SOCl$_2$	thionyl chloride
SPR	small particle reagent
TGA	thermogravimetric analysis
VMD	vacuum metal deposition
WSD	water-soluble deposit

Note: as a supplement to the above list of abbreviations, a fold out page at the back of this thesis contains structures, names and abbreviations for the majority of the compounds discussed.

Abstract

Fingerprints continue to be an important form of forensic evidence for individual identification. A number of techniques are currently available for the detection and enhancement of invisible or latent fingerprints. While these techniques perform well on many surfaces, there are a number of surfaces that pose problems. On such surfaces, Fourier transform infrared (FTIR) chemical imaging can provide superior results. FTIR chemical imaging involves the simultaneous collection of thousands of mid-infrared spectra across a sample using a focal plane array (FPA) detector. This allows for the collection of chemically specific spectral data while maintaining spatial information. Images can then be generated based on spectral / chemical contrast between components within a sample. A key aim of this project was to further investigate the use of FTIR chemical imaging for the detection and enhancement of latent (untreated) and developed (treated) fingerprints on a number of *'difficult'* surfaces.

During the initial development of an infrared chemical imaging technique for fingerprints, an un-optimised set of image collection parameters was used. Using these settings, the collection of an entire fingerprint image was time consuming (often several hours or days). A systematic method for the optimisation of the image collection parameters has been developed. This method allows the optimisation of parameters such as spectral resolution, number of co-added scans, spectral range, pixel aggregation and image formation parameters in order to minimise image collection time and file size while maintaining the quality of the fingerprint image produced.

A commonly-used fingerprint detection technique for latent fingerprints on non-porous or semi-porous surfaces involves fuming samples with monomeric ethyl 2-cyanoacrylate (superglue). This reagent leaves a white residue (polymeric cyanoacrylate) on the ridges of latent fingerprints, rendering them visible under white light. On some surfaces, such as polymer banknotes, however, the contrast between cyanoacrylate-developed fingerprints and the background is poor. FTIR chemical imaging of cyanoacrylate fumed fingerprints on polymer banknotes and other difficult surfaces has been shown to provide better results than optical techniques alone. During this project, further investigations into the use of FTIR chemical imaging for latent fingerprints treated with commercial cyanoacrylate monomer on a range of difficult surfaces were conducted. While excellent results were obtained on many

samples, the need for novel cyanoacrylates containing infrared absorbance in specific parts of the spectrum was identified.

A major focus of this project has been the identification, synthesis and characterisation of modified cyanoacrylates which may be used as reagents for FTIR chemical imaging of fingerprints. Monomers that contained particular functional groups that show vibrational modes in the range from $2500 - 1800$ cm^{-1} were sought. This region typically contains very few vibrational bands and therefore a reagent that could be used to give fingerprints absorptions in this range is desirable. This would provide the necessary contrast between the ridge details of the treated fingerprint and the background on which it may be located.

In total four novel cyanoacrylates were prepared. These included 2-cyanoethyl 2-cyanoacrylate (2-CECA), 1-cyanoethyl 2-cyanoacrylate (1-CECA), trideuteromethyl 2-cyanoacrylate (MCA-d$_3$) and pentadeuteroethyl 2-cyanoacrylate (ECA-d$_5$).

Each of the four novel monomers was tested a reagent for the detection and enhancement of latent fingerprints on a number of surfaces via FTIR chemical imaging. The 2-CECA monomer was found to be less volatile than conventional cyanoacrylate and thermally decomposed at the temperatures required to vaporise it. Treating latent fingerprints with this monomer at a reduced pressure yielded better results on reflective surfaces. On less reflective surfaces, such as polymer banknotes, however, the nitrile band of 2-CECA was almost undetectable and therefore could not be used for imaging the treated prints.

Fingerprints treated with the deuterated monomers (MCA-d$_3$ and ECA-d$_5$) showed characteristic bands in the region from $2300 - 1900$ cm^{-1} owing to C–D stretching vibrations. Once again, however, the relatively low intensity of these bands meant that they were only detected from prints on reflective surfaces.

The monomer that produced the best results was 1-CECA. Surprisingly the contrast between the ridge detail and the background, was not generated by the nitrile band at 2250 cm^{-1} as anticipated. Instead it appears that the absorption band for the carbonyl group in poly-1-CECA is sufficiently resolved from any absorption within this region from the background surface (such as polymer banknotes) to provide good contrast images of the treated fingerprint. High quality fingerprint images were obtained of prints treated with 1-CECA on

all difficult surfaces tested including white opaque acrylic sheets, fluorescent acrylic sheets and all areas of polymer banknotes including areas containing raised intaglio printing.

Chapter 1:

Introduction

Chapter 1:   Introduction

1.1   Fingerprints

1.1.1   Introduction and terminology

The skin on the inside surfaces of the hands and the surfaces of the feet is known as *volar skin*. It is furrowed, making it easily distinguishable from the skin on the rest of the body, (*smooth skin*) which, as its name suggests, tends to be smooth. Furthermore, smooth skin contains hair, sebaceous glands and sweat glands, while volar skin contains only sweat glands.[1]

Volar skin contains minute ridges of skin, with furrows between each ridge. These ridges have pores along their entire length that exude perspiration, but their main purpose is to increase friction between the hand or foot and any other surface they contact.[1] As a result they are commonly referred to as *friction ridges.* The friction ridges present on the surface of a finger form a pattern. These patterns fall into well-defined categories which allow them to be classified using systems such as the Henry-Galton system[2] (See Figure 1.1 below).

BASIC FINGERPRINT PATTERNS

| ARCH | TENT | LOOP | WHORL |
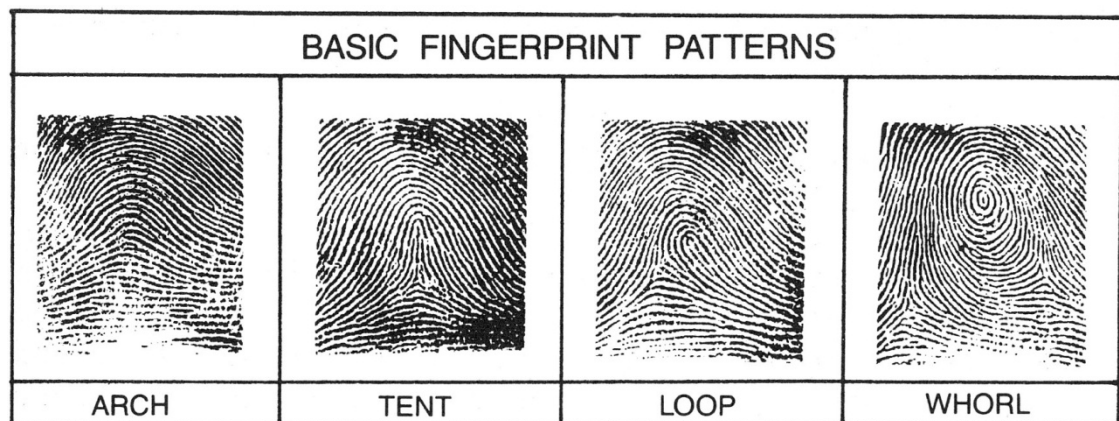
Figure 1.1:   *Classification of fingerprint patterns (from Berry and Stoney).*[3]

Friction ridges are not continuous in nature but rather are constructed of *ridge units.* The path taken by the ridges may branch, start or stop, turn, twist, or thicken and narrow independently, or as the pattern flow dictates.[1] These discontinuities are known as *ridge characteristics* or *minutiae*. Most experts recognise seven basic types of minutiae (depicted

in Figure 1.2 below).[2,3] Others consider only ridge endings, bifurcations and dots as the basic minutiae, with all other types being combinations of these.[4]
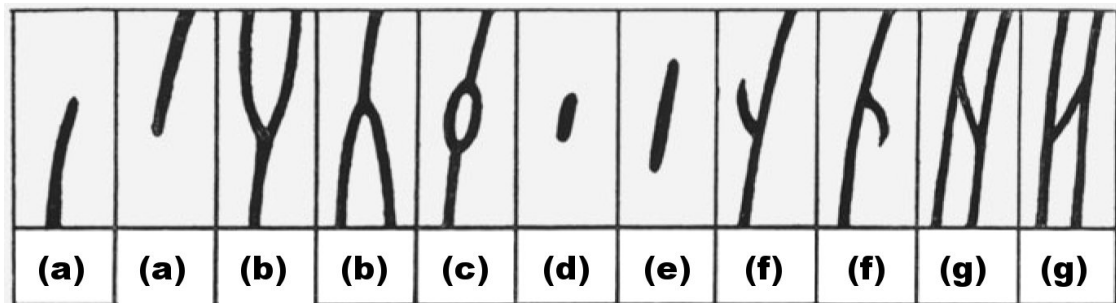
Figure 1.2:   *Seven basic types of ridge characteristics* (a) *ridge ending;* (b) *bifurcation;* (c) *enclosure or lake;* (d) *island;* (e) *short ridge or dot;* (f) *spur or hook;* (g) *crossover or ridge crossing. Image adapted from Knowles and Saferstein.*[2,5]

It is the unique pattern of friction ridge characteristics present on the surface of a finger which allows for identification (see Section 1.1.3 below). An impression which is made of the friction ridge pattern on the surface of the finger is known as a *fingerprint*. This is generally in reference to an impression made with ink or similar medium that produces a clear representation of the ridge characteristics.

The surface of a finger contains secretions and / or other contaminants, and when a finger is placed in contact with a surface, some of the material may be transferred leaving a *mark* or *fingermark*.   It is important to note here the distinction between a finger*print* and a finger*mark.* The terms finger*print* or *print* are commonly used to describe *all* impressions left by the friction ridge skin on a finger's surface. They are also commonly used in place of the terms finger*mark* and *mark*. Champod et al. suggest that the term finger*print* *"…be employed for a record or comparison print taken for identification, exclusion, or database purposes (sometimes referred to as a "known" print), whereas* [finger*mark*] *should only concern traces left (unknowingly) by a person on an object (sometimes referred to as the "unknown," "latent," or "questioned" mark)".*[4] As mentioned earlier, this distinction is not always made and the term finger*print* has been used to describe the friction ridge skin itself as well as *any* impression made by it (be it visible or latent, known or unknown). In fact, even Champod et al. are inconsistent with the use of these terms and still refer to the detection of latent fingermarks as "finger*print* detection". They also use "finger*print* residue" or "finger*print* deposit" in reference to what, according to their own definition, should be referred to as a finger*mark.*[4] In this reference, and indeed almost all publications concerning fingerprints /

fingermarks, the terms "fingermark" or "mark" and "fingerprint" or "print" are used interchangeably or in combination, often within the same sentence or paragraph. Furthermore, the use of the term finger*mark* seems to be a recent trend and its use is largely restricted to the authors of the aforementioned book. Throughout this thesis, in order to remain consistent with the bulk of the current literature in this area, the term finger*print* is used almost exclusively to describe any impression made by the friction ridge skin on the surface of a finger (including visible, latent, known and unknown prints). To prevent confusion, the use of the term finger*mark* is avoided.

Other terms which are commonly (and incorrectly) used interchangeably in the fingerprint literature are *detection* and *development* (or *enhancement*). In a recent review of the fingerprint literature from a physicist's point of view, Voss-de Hann distinguishes these terms. The purpose of *detection* is to simply locate a latent fingerprint, ideally preserving the trace completely. *Development*, however, is aimed at making all details of a located print recordable in optimal quality.[6] There exist techniques that can simultaneously search a large area for latent fingerprints and develop any that are located. For this reason, in certain contexts, a technique that is capable of fingerprint *detection* and *development* is abbreviated as simply a fingerprint *detection* technique.

1.1.2   History of friction ridge identification

The origins of using the unique patterns of friction ridges as a means of personal identification dates back thousands of years. In Mesopotamia (circa 3,000 B.C.), for example, finger imprints were purposely indented into the clay bricks used in the construction of the king's storehouse.[3] There is also evidence that, over 5,000 years ago, the ancient Chinese commonly endorsed legal contracts by embedding a fingerprint in clay seals.[3] These early examples and other similar artefacts not only suggest some recognition of the individuality of fingerprints but also that fingerprint identification (albeit in a simple or primitive form) appears to have been practiced in this early period. Despite this, the history of fingerprint identification and the appreciation of fingerprints' individuality is fragmented and murky. So too is the use of fingerprinting in criminal investigations. Several historical perspectives on these matters have been published and the reader is referred to these references for detailed accounts.[1,3,4] Presented below is a brief summary of the use of friction ridges for personal identification with particular focus on two pioneers who have each contributed significantly to the science of friction ridge identification. In fact, the work of Sir William J. Hershel and Dr

Henry Faulds and their relative contributions have been the subject of much debate. The books by Ashbaugh[1] and Berry and Stoney[3] provide a thorough treatment of this debate and other historical issues, Ashbaugh puts the debate into perspective by saying *"Both men are true pioneers and their main contribution was in the passing on of an ancient Oriental science".*[1]

Sir William J. Hershel is commonly credited as being the first fingerprint pioneer to realise the uniqueness of friction ridges. This, however, is largely the result of his own bold claims that he was the first to use friction ridge skin prints for personal identification purposes. In the 19th century, Herschel, working in the Indian Civil Service, adopted a local Indian practice for the 'signing' of contracts with an inked finger or palm. In a contract with a local native, Radyadhar Konai, Herschel asked Konai to apply his right palm print in ink. Herschel claimed that this contract, made in 1858, was this first use of friction ridges for identification. This is, of course, contradicted by the hundreds of years of use in India, China and other oriental counties. Furthermore, in his anatomical atlas published in 1788, Dr. J.C.A. Mayer of Germany states *"…the arrangement of skin ridges is never duplicated in two persons…"*. This clearly demonstrates that the concept of uniqueness was understood over 70 years prior to the Konai contract. Ashbaugh suggests that a more accurate description of Herschel's role in the history of fingerprint identification is that he *"...was likely the first man in the British Empire to understand the value of friction ridge for personal identification*".[1] Whatever the case, the science of friction ridge identification has evolved gradually since the late 19th century, with contributions from many fingerprint pioneers.

Dr Henry Faulds was born in Scotland but worked briefly in India before opening a missionary hospital in Tokyo, Japan. He may have been exposed to the use of fingerprints during his time in India but began an in-depth study on the subject in 1879. In 1880 Faulds wrote a letter to Charles Darwin telling him about his studies and published a letter to the editor of *Nature* entitled "On the Skin – Furrows on the Hands". These letters contain many insights into friction ridges including the permanence / immutability of fingerprints and the apprehension of criminals by locating fingerprints at a crime scene.

Faulds pushed for the establishment of a fingerprint bureau at Scotland Yard but was rejected. During this time Bertillon's anthropometry overshadowed the development of fingerprinting as a means of identification of individuals. Before fingerprints could be established as a more reliable means of proving an individual's identity, an accurate and

reliable means of classifying prints was needed. The work carried out by Sir Francis Galton in England, Edward Henry in India and Juan Vucetich in Argentina made it possible to classify and describe prints in such a way that matches could be reliably confirmed or rejected.

The science of friction ridge comparison has developed into an important forensic tool for the identification of individuals. Despite some initial hurdles, the admissibility of fingerprint evidence in a legal context has been proven in many cases around the world. The acceptance of fingerprint evidence by the courts has been the result of three fundamental principles which have been successfully established as fact. Saferstein identified the three principles below:

First Principle: A fingerprint is an individual characteristic; no two fingerprints have yet been found to possess identical ridge characteristics.

Second Principle: A fingerprint will remain unchanged during an individual's lifetime.

Third Principle: Fingerprints have general ridge patterns which permit them to be classified.[5]

The third principle indicates a method by which fingerprints can be classified. The identification of fingerprints, however, does not rely solely on general ridge patterns. Identification is instead based on a careful study and comparison of a fingerprint's ridge characteristics or minutiae.

1.1.3   Friction ridge identification

The purpose of friction ridge identification is to individualise, a process that Ashbaugh defines as *"the elimination of all similar items in the world, leaving only one possible source"*.[1] The identification process used by fingerprint examiners is often viewed by lay people as non-scientific and the acceptance of fingerprint evidence as being scientific in nature has been the subject of a *Daubert* hearing in the U.S. (see U.S. v. Mitchell, U.S. District court for the Eastern District of Pennsylvania, Criminal No. 96-407). This challenge and other recent hearings have affirmed that fingerprint evidence does pass the *Daubert* test and judicial notice was given to the fact that fingerprints are permanent and unique.[4]

It is the uniqueness of fingerprints that allows their use for individualisation and it has a fundamental scientific basis, which comes from our understanding of the growth and development of volar friction ridge skin. This is a topic that has been studied over many years, or even centuries, and provides a biological basis for friction ridge pattern variability. This biological research provides evidence for two cornerstones to the use of fingerprints as a means of personal identification; permanence (persistence or durability) and the uniqueness of friction ridge skin. These principles and the scientific premise behind them are covered in great detail by Ashbaugh and he summarises the fundamental premise of the uniqueness of friction ridge skin as follows; *"The friction ridges are constructed of ridge units. The number of ridge units that make up a ridge is established at random. Where a ridge starts and stops, the factors that designate its length are completely dependent on differential growth. The location of the ridge unit where a branching develops is also established at random. Due to the plethora of genetic and physical variances the ridge units are subjected to during friction ridge formation and the numbers of units involved, the paths of friction ridges are unique to that area of friction skin"*.[1] Ridge units are also subjected to a random growth factor in relation to their shapes which means they may vary in shape, size, alignment and whether they fuse to the next ridge or not. The location of the pore opening on a ridge unit is also established by random forces through differential growth. These factors enhance the uniqueness of friction ridge skin.

The processes, protocols and flow charts which are employed by fingerprint examiners are detailed in a number of references.[1,4,7] There are four parts to the friction ridge identification methodology known as "ACE-V", these being Analysis, Comparison, Evaluation and Verification. The initial step in the ACE-V protocol, Analysis, calls for the in-depth analysis of the latent friction ridge print itself. Since this thesis is concerned with latent fingerprint detection and enhancement, some attention will be drawn to this part of the comparison process. The Comparison, Evaluation and Verification stages of the ACE-V protocol involve the comparison of a latent friction ridge print (from an unknown source) with a fingerprint from a known source. A discussion of this part of the procedure is beyond the scope for this thesis and the reader is referred elsewhere for detailed information.[1,4,7]

In discussing the analysis of a latent fingerprint, it is important to understand how the uniqueness of fiction ridge skin is translated to the fingerprint impression. This is measured in terms of *clarity*. Friction ridge skin is a three-dimensional (3-D) structure and the print that it makes on a surface is only two-dimensional (2-D). Many of the minute details that make

small areas of friction skin unique do not survive the transition from ridge to print. How well the details from 3-D ridges that are reproduced in the 2-D print is referred to as the *clarity* of the print.[1] As mentioned earlier, when we are discussing the friction ridge skin, it can be said that the friction skin is unique in a very small area. This statement, however, only applies to a friction skin *print* if clarity is present.[1] During the comparison process, print clarity is described using three levels of detail:

First Level Detail: describes the overall friction ridge pattern which may be repeated and therefore grouped. This allows us to narrow down the prospective group to be compared. The frequency with which first level details are encountered is described in *degrees of rarity* (e.g. arch patterns are rarer than whorl patterns).[1]

Second Level Detail: describes the specific path deviations of friction ridges, also known as minutiae, points of identification or Galton characteristics.[1,4] Second level detail has individualising power and is described in *degrees of uniqueness*.

Third Level Detail: refers to intrinsic ridge shapes and relative pore locations. Third level detail is also described in *degrees of uniqueness*.

This terminology is useful for describing the clarity of a developed latent fingerprint and the effectiveness of fingerprint development techniques can be assessed in terms of the clarity of the resulting prints. The terms first, second and third level details are used in the balance of this thesis.

1.1.4   Types of fingerprint evidence

Fingerprint evidence which may be encountered at a crime scene may exist as either *visible fingerprints* or *latent fingerprints.* Visible fingerprints, as the term suggests, are visible without any particular treatment. Such prints may be:

Positive: where an image is formed by fingerprint ridges contaminated with a coloured substance such as blood, ink, paint, etc.;

Negative: where the fingerprint ridges remove surface material such as dust and soot; or

Indented (moulded/plastic): caused by the contact of the finger with a malleable substance (putty, candle wax, wet paint, etc.) that subsequently retains a three-dimensional image of the print.[4]

In routine forensic casework, latent fingerprints are by far the most commonly encountered type of trace and the one which poses the most problems. Latent fingerprints are present on a surface after it has been touched but they are invisible. These prints must be treated by some technique in order to visualise them. This has meant that a great deal of research and effort has gone into the development of techniques which can reveal or enhance latent fingerprint deposits. To gain an appreciation of how certain techniques operate, we must firstly understand the chemical make-up of latent fingerprints (or fingerprint deposits). A brief discussion on this matter is given in Section 1.1.5 below.

1.1.5   Composition of latent fingerprints

The latent fingerprint, deposited on a surface by the ridges of the finger or palm, is a complex mixture of natural secretions and environmental contaminants.[4] The natural secretions that form part of a fingerprint deposit originate from three main sources:

- eccrine glands (sudoriferous),
- apocrine glands (sudoriferous) and,
- sebaceous glands

A general description of the inorganic and organic constituents of these three glands is provided in the following table which has been adapted from several references:[2,4,8]

Source	Location	Constituents		Solubility
		Inorganic	**Organic**	
Eccrine Glands	All over the body, but the only type of glands on the palms of the hands and soles of the feet	chlorides metal ions (Na^+, K^+, Ca^{2+}) sulfates phosphates ammonia water (> 98%)	amino acids urea uric acid lactic acid sugars creatinine choline	Mainly water soluble
Apocrine Glands	Localised to the pubic, mammary and anal areas	iron water (>98%)	proteins carbohydrates sterols	Mainly water soluble
Sebaceous Glands	Mainly around the forehead, chest, back and abdomen		glycerides fatty acids wax esters squalene sterol esters sterols	Mainly non-water soluble

Table 1—1: *Constituents of fingerprint deposits.*[2,4,8]

Although sebaceous material is common in fingerprints, there are actually no sebaceous glands located within the finger/palm regions. These constituents are most likely transferred from contact with sebum-producing regions of the body such as the face, neck and hair. Most of the lipids on the skin come from these sebaceous glands. Only eccrine glands are located on the palm and finger regions. Eccrine sweat does not contain a significant quantity of lipid material but is largely comprised of water with trace amounts of salts, free amino acids, urea, ammonia etc.[9]

The information above and the extensive studies which have been reported in the medical literature give us a clear picture of the composition of human perspiration. Ramotowski has reviewed the composition of latent print residue from a forensic perspective and comments that *"Knowing the precise contents of the various skin glands does not accurately represent the nature of what is actually secreted onto substrates from the fingers and palms"*.[8] The latent print deposit is complex because it is made up of the secretions from glands present on

the finger surface and elsewhere on the body as well as cosmetics, perfumes, food residues and other environmental contaminants. Furthermore, the secreted material is almost immediately altered by oxidative and bacterial degradation mechanisms that become more significant as the age of the deposit increases.[8]

An understanding of the composition of latent print residue and the likely degradation products can help us to determine the most suitable and effective methods for the visualisation of latent prints. Many fingerprint detection techniques target one or more fingerprint constituent(s) (e.g. amino acids). Research is now beginning to focus on the degradation products formed when a latent print is exposed to environmental conditions in the hope of identifying new target compounds for chemical treatment and visualisation.[10-19]

1.1.6 Current fingerprint detection techniques

The term *latent* refers to something which is present but practically invisible to the human eye. A number of fingerprint enhancement techniques are currently available to the forensic scientist to reveal and image latent fingerprints. These techniques may be grouped into three main areas:

Physical detection methods: these include techniques like powders, small particle reagent (SPR) and vacuum metal deposition (VMD) etc

Chemical detection methods: these include techniques such as ninhydrin (and ninhydrin analogues including 1,8-diazafluorene-9-one (DFO)), silver nitrate, ruthenium tetroxide (RTX) etc

Physico-chemical detection methods: these include physical developer (PD), iodine and cyanoacrylate fuming.

The type of fingerprint detection method employed is dependent on a number of considerations. Of primary importance are the surface characteristics of the substrate on which the fingerprint residue has been transferred. Surfaces bearing latent fingerprints can be divided into three categories: porous, semi-porous and non-porous. Champod et al. summarise these types of surfaces and their interaction with latent fingerprint deposits in the following table (Table 1—2) and figures (Figure 1.3 and Figure 1.4).

Types of Surfaces		
Porous	**Semi-porous**	**Non-porous**
Porous surface absorbs the WSD very quickly (within seconds) after deposition The NWSD stays on top of the surface for a longer period (a half day to a day) A small amount of the NWSD stays on the surface for a significant period	Semi-porous surface absorbs the WSD slowly after deposition (minutes to h) The NWSD stays on top of the surface much longer (a day to several days) A small amount of the NWSD stays on the surface for a significant period	Non-porous surface does not absorb any part of the latent fingerprint deposit The WSD and NWSD, as an emulsion mixture, stays on top of the surface for a very long time (until degraded) Latent deposits remain on the surface and are very fragile (marks are easily smudged)
Typical examples: • paper • cardboard • some fabrics (e.g., cotton) • untreated wood, etc.	**Typical examples:** • certain types of plastic • waxed surfaces • certain types of wall paints and wallpapers • varnished wood, etc.	**Typical examples:** • certain types of plastic • glass • metal surfaces • glazed ceramics • glossy paints, etc.
Note: WSD = water-soluble deposit, NWSD = non-water-soluble deposit		

Table 1—2: *Types of surfaces and their interactions with latent fingerprint deposits – adapted from Champod et al.*[4]

Emulsion of water-soluble and water-insoluble components

porous surface

(A) Cross section of latent deposit immediately after deposition

Water-insoluble component   Water-soluble component

porous surface

(B) Minutes/hours after deposition

Water-insoluble component   Amino acids   Urea, salt, etc.

porous surface

(C) Weeks/months after deposition
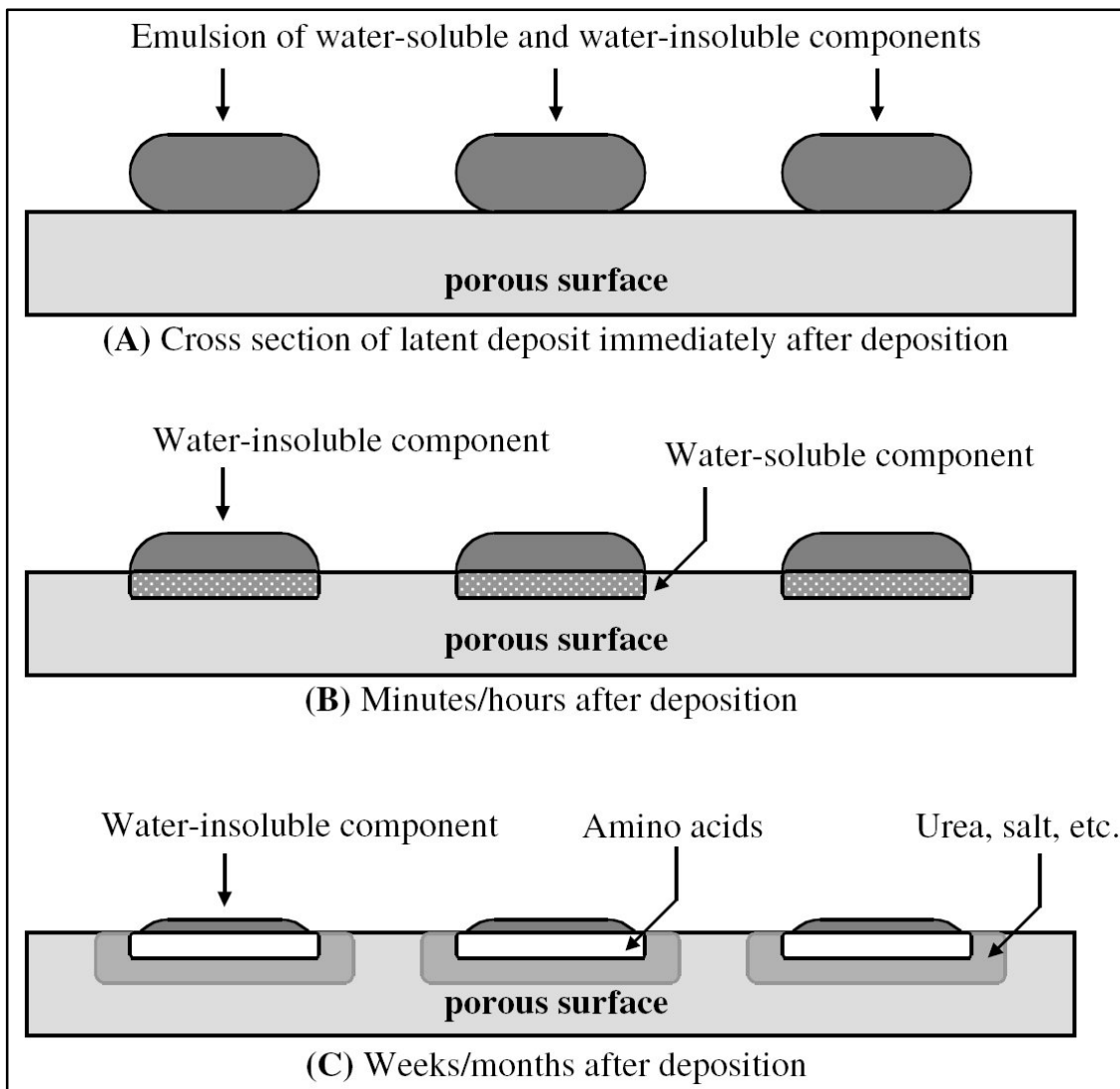
Figure 1.3:   *Aging of a latent fingerprint on a porous substrate (e.g. paper) - adapted from Champod et al.*[4]

(A) Cross section of latent deposit immediately after deposition

(B) Several weeks/months after deposition
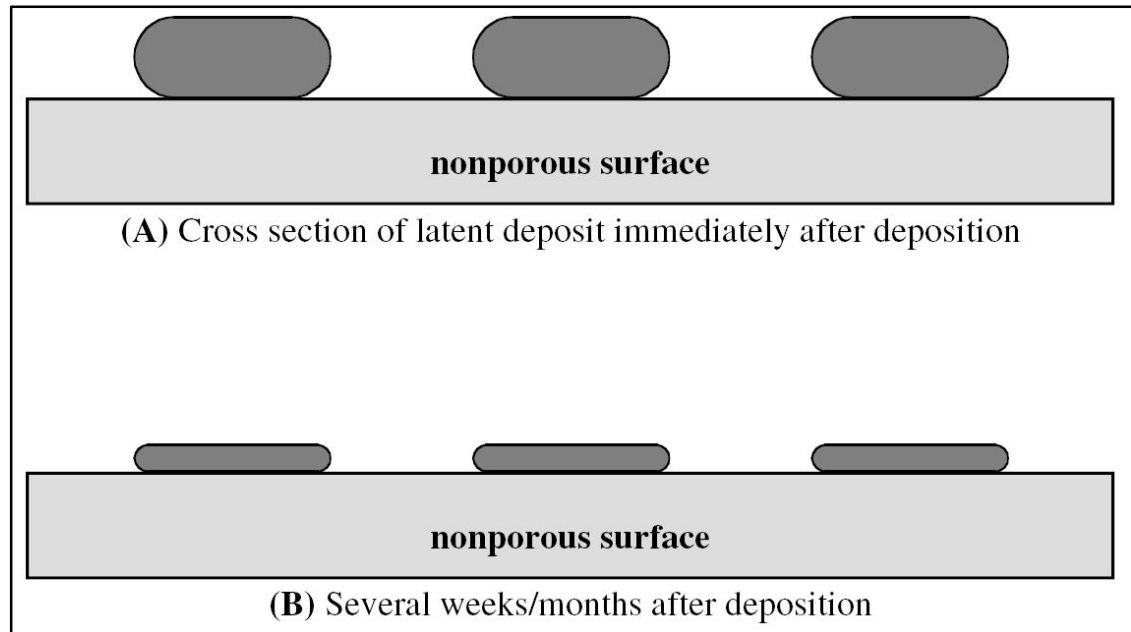
Figure 1.4: *Aging of a latent fingerprint on a non-porous substrate (e.g. glass) - adapted from Champod et al.[4]*

The type of fingerprint enhancement technique employed also depends on the environmental conditions that the substrate has been subjected too. For example, many techniques produce poor results on substrates which have been wetted. A number of reviews of fingerprint detection techniques have been published[2,4,6,20] and it is not the intention of this thesis to explore each current technique. Instead, a brief discussion of the most commonly used fingerprint detection techniques for each surface type is provided below.

1.1.6.1   Detection techniques for porous surfaces

In 1954, a compound named ninhydrin was found to be a useful reagent for the detection of latent fingerprints. It has since become the most commonly used technique for fingerprint detection on porous surfaces. Ninhydrin reacts with primary or secondary amines (including amino acids, proteins and peptides) to form a dark purple product known as Ruhemann's purple (Figure 1.5).

Figure 1.5: *Chemical reaction between ninhydrin and a primary or secondary amine that produces the dark purple product known as Ruhemann's purple (one of four resonance structures show).*

The use of ninhydrin for the detection of latent fingerprints is discussed in detail in a number of recent books and reviews.[4,20-22] The general method of application involves dipping the substrate in a solution of ninhydrin (typically 0.5% w/v in a mixture of organic solvents) followed by air drying. The development process is allowed to proceed at room temperature over 24 to 48 hours. Heating can accelerate the rate of development but is generally not recommended due to the background colouration which can result. A solvent-free application of ninhydrin involving sublimation directly onto the substrate has also been reported[23] and is of particular use for thermal paper.

Ninhydrin developed prints are dark purple in colour and are best photographed under white light with the appropriate camera filter. The prints are luminescent but only when cooled to liquid nitrogen temperatures. A secondary treatment with zinc or cadmium metal salt solutions results in a change in colour (orange for zinc and red for cadmium). This colour change is due to the formation of a 1:1 co-ordination complex between the Ruhemann's purple and the metal salt.[24] These complexes also show room temperature luminescence and can therefore yield superior results to the use of ninhydrin alone.

A number of researchers have explored the synthesis and use of ninhydrin analogues in attempts to improve the optical and luminescent properties of ninhydrin.[21,22,25-35] Many of these analogues have shown improved properties but none are yet to replace ninhydrin as the standard fingerprint reagent for latent fingerprint development on porous surfaces.[21]

Two compounds which are structurally related to ninhydrin and worthy of note are 1,2-indanedione (Figure 1.6) and 1,8-diazafluorene-9-one (DFO) (Figure 1.7). Both these compounds react with amino acids to give a coloured product and, although the product formed by 1,2-indandione is still under investigation, their structures are believed to be analogous to that of Ruhemann's purple. Unlike ninhydrin however, DFO-developed

fingerprints are highly fluorescent without secondary treatment with metal salts.[21] There are discrepancies in the literature as to the relative performance of 1,2-indanedione and ninhydrin, and work is continuing in this area.[36-40]

Figure 1.6:   *Structure of 1,2-indanedione.*

Figure 1.7:   *Structure of 1,8-diazafluorene-9-one (DFO).*

Another technique for the development of fingerprints on porous surfaces is physical developer (PD). PD, based on a photographic physical developer, is an aqueous solution containing silver ions, a ferrous/ferric redox (reduction/oxidation) system, a buffer (citric acid), and a cationic surfactant (generally *n*-dodecylamine acetate).[4] When a document is placed in the PD reagent, silver slowly deposits from solution. PD-developed prints appear dark grey to black due to the preferentially heavier deposition of silver metal along the ridges. PD targets the water-insoluble portion of the latent print residue and hence can be used after treatment with an amino acid-sensitive reagent (ninhydrin, 1,2-indanedione, DFO or their analogues) or on articles which have previously been wet. PD has been used since the mid-1970s and there are a number of suggested formulations and procedures. Cantu and Johnson have recently reviewed the most commonly employed procedures and modifications of the PD method.[41]

A technique which can be applied to a range of surfaces, including porous and non-porous, is multi-metal deposition (MMD). MMD involves a two-step process; treatment with colloidal gold solution (having a pH ~ 2.7) followed by a weak solution of silver physical developer.

The colloidal gold particles are highly negatively charged and thus bind strongly with the target species to form catalytic nucleating sites for silver physical development.[41] Both PD and MMD suffer a number of disadvantages; the reagents are delicate and time-consuming to prepare and apply, the solutions have a short shelf life, the chemicals required are expensive and these processes can only be used at the end of a detection sequence. Nevertheless, PD and MMD are sensitive techniques that can give results where other techniques fail.[4,41]

1.1.6.2   *Detection techniques for non-porous surfaces*

The traditional method for the detection of fingerprints on smooth non-porous surfaces is powdering. The principle behind fingerprint development is the physical adherence of the fine powder particles to the humid, sticky or greasy substances in the latent fingerprint deposit. Powdering is relatively simple and inexpensive and little experience is necessary to obtain satisfactory results.[4] Despite these advantages, powdering is an insensitive detection method and its application is limited to crime scene use on fixed surfaces or on objects that cannot be readily transported back to the laboratory.

Fluorescent powders are commercially available and are useful on reflective or multi-coloured surfaces where contrast may be problematic with conventional powders. Magnetic powders are also available and their use avoids the brushing, and hence the destruction, of fragile fingerprints. Note that this technique is simply an alternative method for applying the fingerprint powder whereby the applicator is comprised of a magnet rather than a brush. Although the fingerprint powder in this case is magnetically attracted to the applicator, the physical adherence between the powder and the latent print residue follows the same principles as ordinary fingerprint powder. Improved magnetic powders combined with applicators which contain stronger rare earth magnets have largely resolved problems with the application of this technique on vertical surfaces.

Fingerprints on non-porous surfaces can be developed via a 'wet powdering' method involving immersion in an aqueous suspension of an insoluble powder (e.g. molybdenum disulfide) followed by rinsing with water. Unlike conventional powdering, this method, referred to as small-particle reagent (SPR), is effective on surfaces that are wet.

Two other fingerprint detection techniques for non-porous surfaces are cyanoacrylate fuming and vacuum metal deposition (VMD). Cyanoacrylate fuming is an important technique in the context of this thesis and is given special attention in Section 1.1.6.2.1 below. Vacuum metal deposition (VMD) is a technique commonly used for the deposition of thin metallic films. This process is hindered by the presence of surface contamination such as fingerprint residue and has therefore proved a valuable and extremely sensitive technique for fingerprint development on some difficult surfaces. Champod et al. discuss the principles and application of VMD[4] and a recent review by Voss-de Haan notes the success of VMD on surfaces such as milk cartons, leather, fabrics, plastic bags and paper banknotes.[6] Of particular note in the context of this thesis is the success of VMD for the detection of fingerprints on polymer banknotes[42] (see Section 1.1.7 below).

1.1.6.2.1 *Cyanoacrylate fuming of latent fingerprints*

The use of monomeric cyanoacrylate (often referred to as *Super Glue* or *superglue*) for the detection and enhancement of fingerprints on non-porous surfaces was first demonstrated by the Criminal Identification Division of the Japanese National Police Agency in 1978.[20] At this stage it was seen as a rather exotic method of detection and was known only to a small section of the forensic community.[43] Since then, the cyanoacrylate fuming method has gained wide popularity and has become the method of choice for the development of prints on non-porous surfaces such as metals, electrical and adhesive tape, leather, glass, ceramics and plastics.[4,5,9,20,44] Cyanoacrylate fuming is an important technique in the context of this thesis and so some key aspects of the fuming process will be discussed here.

Firstly, the terms *cyanoacrylate* and *superglue* are used in reference to a group of compounds that are more accurately named *alkyl 2-cyanoacrylates*. Figure 1.8 shows the general formula for alkyl 2-cyanoacrylates or cyanoacrylate esters.
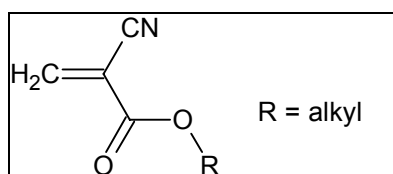
Figure 1.8:   *General structural formula for alkyl 2-cyanoacrylates.*

There are a number of cyanoacrylate esters that are commercially available, most finding use as instant adhesives. The two most common cyanoacrylates are the methyl and ethyl esters (Figure 1.9). Ethyl 2-cyanoacrylate is the most commonly used for fingerprint detection.
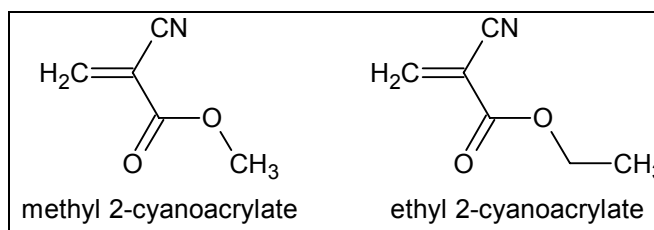
Figure 1.9:   *Structures of methyl 2-cyanoacrylate and ethyl 2-cyanoacrylate.*

The cyanoacrylate fuming method involves exposure of the evidential object to cyanoacrylate vapours in a cabinet designed for this purpose. The monomeric cyanoacrylate vapour preferentially polymerises on the ridges of latent fingerprints, usually producing a white deposit. Initially, an enclosure such as a fish tank was used to expose evidentiary items to low concentrations of the cyanoacrylate vapour. Ambient temperature and pressure was used to develop latent prints using this method.[20,45] Long exposure times were needed and there were often problems with high background polymerisation. A number of techniques have since been developed to accelerate the fuming process and minimise background development.

The simplest acceleration method involves the introduction of a small fan or air-circulating pump into the fuming chamber to increase the circulation of and more uniformly distribute the monomeric vapour. In the early 1980s work was carried out by Kendall and Rehn into a rapid fuming method.[45] This method involved placing the cyanoacrylate monomer onto an absorbent cotton treated with sodium hydroxide. Using this method, the development time was reduced to about 1 hour.[45] Around the same period, reports appeared describing the use of heat as an alternative means of accelerating the fuming process. This technique still finds widespread use today. Heating allows for faster print development without the build-up of a polymer background.

Yet another acceleration method currently used in some countries is vacuum deposition. Vacuum deposition allows for latent print development in the absence of heat.[46] The cyanoacrylate monomer is placed inside a vacuum chamber along with the item to be fumed. A vacuum pump reduces the pressure inside the closed system to approximately 1 torr. Once this pressure has been reached, the container is opened, allowing the cyanoacrylate

monomer to vaporise at room temperature under reduced pressure. The use of heated poly-cyanoacrylate (which thermal depolymerises to yield the original monomeric cyanoacrylate) has also be demonstrated as an alternative fuming technique.[47] Furthermore, a number of these acceleration / fuming methods may be combined (e.g. heating combined with fume circulation).

There is a lack of consensus in the literature on the relative merits of the various cyanoacrylate fuming methods. Considerations such as the speed (and hence operational costs) and the expense of the equipment must be balanced with the quality of the fingerprint development achieved. Champod et al. and Lee et al. discuss the various cyanoacrylate fuming methods currently used and their relative advantages and disadvantages.[4,20] Watkin et al. directly compare vacuum cyanoacrylate fuming with the heat / humidity method.[48] They report, based on blind tests by 54 forensic identification specialists, that in the majority of cases, the vacuum chamber results equalled or exceeded those from the heat and humidity chamber.[48]

A study by Burns et al. compared the effectiveness of methyl, ethyl, propyl and butyl 2-cyanoacrylate monomers using both visual and instrumental methods.[44] This team from Ireland used conventional assessment of developed prints by a panel of fingerprint experts and also employed reflectance/absorbance Fourier transform infrared (FTIR) spectroscopy to measure the extent of polymer deposition as a more accurate, semi-quantitative and less subjective means of determining polymer deposition. They found that the greatest degree of polymer deposition on latent prints was produced by the methyl 2-cyanoacrylate ester. The study also found that prior fuming with ammonia leads to a greater deposition of polymer on the fingerprint ridges for all monomers tested.[44] This finding can be easily explained with some understanding of the chemistry involved in the cyanoacrylate fuming process.

The exact mechanisms involved in the polymerisation of cyanoacrylates has been the subject of much debate and are the focus of another section (Section 4.1.1). Most of this research has been based on either bulk or solution polymerisation.[49-68] Studies on the vapour phase polymerisation of cyanoacrylates (the process involved during the fuming of latent fingerprints) are rare. It is agreed, however, that the polymerisation of cyanoacrylates (whether bulk, solution or vapour) can be initiated by a wide range of bases and that free radical polymerisation is also possible but is less common.[49,69-73] The extreme reactivity of

cyanoacrylates is due to the stability of the propagating carbanion, which, in turn, is due to the presence of two electron-withdrawing groups (−C≡N and −COOR) (Figure 1.10)
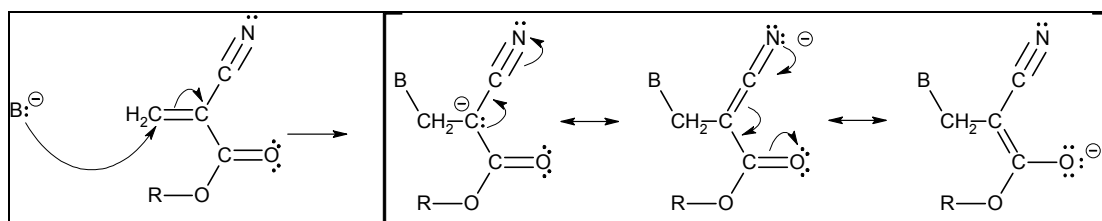
Figure 1.10: *Initiation of cyanoacrylate polymerisation – the resulting carbanion is resonance stabilised due to the presence of electron-withdrawing groups.*

The unique resonance caused by the nitrile and alkoxycarbonyl groups stabilises the anion and this allows the propagation to proceed to high molecular weight polymer[74] (Figure 1.11).
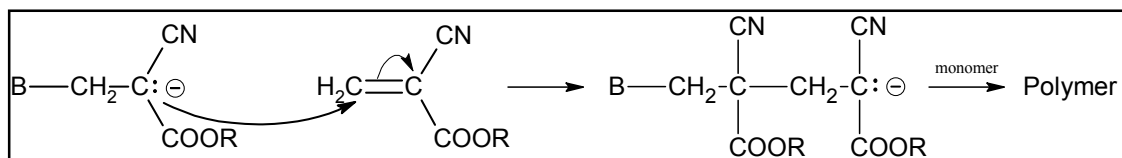
Figure 1.11: *Propagation of carbanion to form poly-cyanoacrylate.*

The base-activated polymerisation of cyanoacrylate esters has been the subject of much study from a materials and adhesion point of view for some time, and given the mechanism of polymerisation outlined above, it is not surprising that the prior treatment of latent fingerprints with ammonia leads to increased polymer deposition.

The study by Burns et al. also found that the cyanoacrylate polymer deposits onto the ridges up to a certain extent and then starts to deposit in the 'troughs' of the fingerprint, leading to a loss of contrast between the fingerprint ridge details and the background.[44] Since the polymerisation process is very rapid, care must be taken to avoid overdeveloped prints. This point is also expressed by Lewis et al., who suggest that the amount of time required to develop high quality latent prints is 2 minutes.[9] In reality, the optimal development time is influenced by a number of factors, including surface characteristics, donor, age of the latent fingerprint residue, humidity and the experimental set-up for the fuming process (i.e. heat, vacuum, fume circulation etc).

Lewis et al. carried out studies to establish the processes involved in the development of latent fingerprints using the cyanoacrylate fuming method.[9] They observed both macroscopic and microscopic differences in the ethyl 2-cyanoacrylate polymer formation on *'clean'* (representative of print deposits from a child or an individual with freshly cleaned hands) and *'oily'* (representative of print deposits from an individual with sebum-coated fingers) fingerprints. They also noted differences in the effectiveness of polymer deposition on aged fingerprints:

"Aged prints lose the grainy-white appearance, and become more translucent, which greatly reduces the contrast between the ridge and background area."[9]

This point illustrates the aforementioned drawback of the cyanoacrylate fuming method (and indeed many fingerprint detection techniques), namely the limitations of creating contrast between fingerprint ridges and the background using the visible light spectrum. The use of FTIR chemical imaging has already demonstrated that these problems can be resolved using the mid-infrared region to create "chemical contrast".[75,76] This project is a continuation of this research and a number of novel cyanoacrylates that may further improve fingerprint contrast will be investigated (see section 1.3 below).

The findings of Lewis et al. must be considered cautiously. Geller, in a commentary response to the article published by Lewis et al., is highly critical of both the article itself and the study on which it was based.[43] Geller not only questions the methodologies employed by Lewis et al., but is also highly critical of their results and the conclusions which are drawn from them. In particular, Geller identifies several factors which can affect the 'quality' of a developed latent fingerprint. Geller states:

"…when experimenting with latents, the only way to come to more or less conclusive results is to minimize, from the beginning, the number of variables.
… it seems to me that the authors [Lewis et al] *did not take this fact into account."*[43]

This is an important consideration and is addressed in the context of this project in Section 1.1.9 below.

Following the work by Lewis and Burns, a number of more recent articles have focused on understanding the chemistry behind the fingerprint fuming process and the components of the latent fingerprint that may be involved.[14,77-79] Czekanski[77] presents a 'model' for the

superglue fuming of latent fingerprints but this article contains numerous errors from both chemical and forensic perspectives. It also suffers from poor methodology and reaches conclusions that are either unsubstantiated or have been reported previously elsewhere. Wargacki et al. examined the chemistry of cyanoacrylate polymerisation in the context of fingerprint fuming using two model systems – one containing the lactate ion, a common compound in eccrine sweat, and the other containing alanine, the most abundant amino acid in fingerprint residue.[14] They also investigated the effect of varying pH on these systems. Both ions were capable of initiating cyanoacrylate polymerisation, each giving a polymer of similar quantity and molecular weight. Lowering the pH had no effect on the amount of poly-cyanoacrylate accumulated, but decreased molecular weights were observed. Increasing the pH led to a larger accumulation of polymer and an increase in molecular weight.[14] Once again, this finding is not surprising given that an increase in polymerisation initiation (and a decrease in termination) is expected at high pH (due to the additional OH^- ions which are themselves capable of initiation) and an increase in termination is expected at low pH (due to the additional H^+ ions which are capable of chain termination).

Using Raman spectroscopy, Edwards and Day provide evidence of unreacted monomer within cyanoacrylate-fumed fingerprints.[78] These authors also report the identification of exogenous materials within latent[80] and cyanoacrylate-fumed fingerprints[81] using Raman spectroscopy. The presence of monomeric cyanoacrylate within fumed fingerprints has implications for the spectral identification of exogenous materials but the implications for the fuming and visualisation of fingerprints are not very clear. This finding may, however, explain observations made by others that fingerprints can appear (or develop further) after the article has been removed from the fuming chamber. Presumably, this may be the result of post-treatment polymerisation of the unreacted monomer. Furthermore, this may also explain the common practice of allowing cyanoacrylate-fumed articles to cure or harden for 24 hours prior to photography or further treatment.[4] The mechanism of cyanoacrylate polymerisation is discussed later in this thesis (see Section 4.1.1).

Mankidy et al. have recently investigated the processes involved during the cyanoacrylate fuming of latent fingerprints from a unique point of view. This group showed that the morphology of the poly-cyanoacrylate formed was dependent on the relative humidity (RH) during fuming and the initiating species.[79] At very high RH (>95%), polymerisation was rapid and the formation of high aspect ratio nanofibres was observed.[79] At low RH (< 30%) only film-like polymer or no polymer at all, was generated.[79] The research by Mankidy et al.

reflects earlier work by Lewis et al. who describe 'noodle-like' structures on prints that had higher moisture content while more oily prints showed 'capsule-type' formations.[9] Mankidy hypothesise that varying the RH effectively varies the rate of polymerisation, thereby resulting in variations in the morphology of the polymer obtained. They also found that certain fingerprint constituents, such as sodium chloride, stearic acid, palmitic acid and amino acids, can act as nucleophilic initiators to trigger polymerisation but the morphology of the polymer formed by any one of these initiators differs from that formed from a fingerprint containing a mixture of these components. Individual substances led to the growth of short nanofibres that were sparsely populated on the surface and did not resemble the neat nanofibres observed on fingerprints. Mankidy et al. explain this finding as follows:

"These results indicated that the growth of high aspect ratio, densely populated nanofibres arises from the complex composition of fingerprint interacting with the monomer vapour at high humidity. The non-initiating components of the fingerprint at high humidity play a major role in dispersing the initiators to favour the formation of the nanofibres."[79]

These authors go on to provide proof for this theory by preparing a mixture of a non-initiating component, linoleic acid, and a known initiator, sodium chloride, to synthetically mimic a fingerprint deposit. Using this mixture, this group was able to fabricate the same long, high aspect ratio nanofibers that they had previously observed on real fingerprint samples.[79] Another interesting finding from this research was that the polymers formed by initiation with sodium hydroxide, potassium hydroxide and potassium acetate resulted in a film with 'tortellini-like' morphological features while initiation with ammonium hydroxide formed spheres of polymer.[79]

In an even more recent publication from the same group, Mankidy et al. investigated the influence of initiators on the growth of these nanofibres.[82] A correlation between the hardness-softness character (according to the Hard Soft Acid Base (HSAB) theory) of the initiators and the observed morphology was noted.[82] Typically, a harder anion (i.e. small, slightly polarisable species) with a more rapid interaction with the hard acid centre of the monomer would result in the formation of a film type morphology whereas a softer anion (i.e larger, easily polarisable species) with a slower interaction with the hard acid centre of the monomer would result in the formation of nanofibres.[82] This trend was also evident in the molecular weight of the samples with the polymer film morphology showing higher molecular weight than the nanofibres.[82]

This group is interested in these results from a materials perspective where in polymeric films of a certain desired morphology can be selectively deposited on regions of a surface by careful control of the initiating species (which may 'printed' on the surface) and the fuming conditions. However, from a forensic perspective, this research is extremely useful in understanding the complexities involved in the cyanoacrylate fuming of fingerprint samples. It is clear that the success of cyanoacrylate fuming is influenced by fuming conditions, which may be controlled, and the composition of the fingerprint deposit itself, which is complex, variable and impossible to control. The complexity of the cyanoacrylate fuming procedure is not only a result of the complexity of the fingerprint residue matrix itself but also the complexity of the cyanoacrylate polymerisation process, which is still not clearly understood (see Section 4.1.1 below).

Cyanoacrylate fuming is often followed by staining of developed fingerprints with a suitable coloured and/or luminescent stain (e.g. basic yellow 40, rhodamine 6G and adrox 970-P10). The staining procedure can improve contrast between developed prints and their background.

1.1.6.3 Detection techniques for semi-porous surfaces

Semi-porous surfaces, which may include waxed paper, glossy paper, matte painted surfaces, leather and some rubber/latex gloves, are often problematic for fingerprint detection. Techniques that work well for porous surfaces (e.g. ninhydrin, DFO) and those which work well for non-porous surfaces (e.g. cyanoacrylate fuming, VMD) often yield inferior results on semi-porous surfaces. The success of individual techniques is highly dependent on the particular semi-porous surface in question and it is generally recommended that tests be conducted on similar surfaces before proceeding with the treatment of an evidential item.[4]

1.1.6.4 Miscellaneous detection techniques

There is a plethora of miscellaneous detection techniques that have been reported which have application on specific surface types, target certain contaminants (fingerprints in blood for example) or are simply preferred by certain law enforcement agencies. Details of these methods can be found in the books by Champod et al.[4] and Lee and Gaensslen[20] and the references therein. Some of these techniques are listed below:

- Iodine / benzoflavine

- Dimethylaminocinnamaldehyde (DMAC)

- Osmium tetroxide (OsO_4)

- Ruthenium tetroxide (RTX)

- Silver nitrate

- Diaminobenzidine (DAB)

- Gentian violet

- Sticky-side powder

1.1.7   Difficult surfaces

The aim of all fingerprint detection techniques is to create contrast between the fingerprint ridge detail and the background on which it is located. There are numerous fingerprint detection techniques which are effective in this respect. A purple, ninhydrin-developed fingerprint on a common porous surface such as white copy paper, or a cyanoacrylate-fumed fingerprint (with white polymeric deposits on the ridges) on a common non-porous surface such as clear window glass are examples where the contrast between the developed fingerprint and the background is sufficient. There are, however, a number of surfaces that present problems for fingerprint detection. The problems encountered may be due to one or more of a number of reasons. For example, the surface characteristics may inhibit the transfer, adherence and/or persistence of the fingerprint residue itself. Furthermore, the surface characteristics may hamper the application and successful implementation of commonly used fingerprint techniques. Surfaces which are classed as semi-porous (see Section 1.1.6.3 above) are obvious examples but certain porous surfaces (such as textured or untreated wood) and certain non-porous surfaces (such as some ceramics and plastics and surfaces which are highly curved or textured) also belong to this category. The term that is generally used within the fingerprint community to describe surfaces on which fingerprint detection is difficult or problematic is *difficult surfaces*.

Difficult surfaces also include surfaces that contain some optical property which interferes with the visualisation of the developed fingerprint. The surface may, for example, be highly coloured or fluorescent under the lighting conditions normally employed for the visualisation of the developed fingerprint. The simplest example of this is the relatively low contrast observed for cyanoacrylate-fumed fingerprints on white backgrounds. Other difficult surfaces may contain a number of colours or inks in the form of a picture, writing or

background pattern which may obscure the fingerprint detail. Newspaper, magazine paper, aluminium drink cans, banknotes, cheques and other security documents are all examples of difficult surfaces.

One difficult surface which has been a focus of this project is the polymer banknote. A large volume of high quality counterfeits of the 1966 series Australian $10 rag paper banknote prompted a search for alternative substrates. The Reserve Bank of Australia (RBA), together with the Commonwealth Scientific and Industrial Research Organisation (CSIRO), developed this technology over a twenty year period. In 1988, Note Printing Australia (NPA), a wholly owned subsidiary of RBA, produced the first polymer note (a $10 note marking Australia's Bicentenary). By 1996, Australia had issued the world's first complete series of circulating polymer banknotes.[83] By the end of 2004, twenty-two (22) countries from all major regions of the world were using polymer notes in their national currencies.[84]

Polymer banknotes provide a number of advantages over traditional rag paper, including improved security, durability, cost effectiveness, improved processability and environmental responsibility. Unfortunately, the polymer banknotes have proven to be a difficult surface on which to develop latent fingerprints. This surface possesses a number of the undesirable surface and optical qualities discussed above and is a prime example of a difficult surface.

The polymer banknote substrate is known as *Guardian^TM* and is based on Biaxially Orientated Polypropylene (BOPP).[85] This substrate is produced by Securency (a joint venture of RBA and the Belgium-based UCB) and is solely used for the production of polymer banknotes.[83] Its exclusivity is an essential security feature. This transparent core is coated on both sides with an opacifying coating. Depending on how this coating is applied, areas of the banknote that are either transparent or semitransparent can be created. Once coated, the polymer banknote can be printed on using conventional print processes similar to that of producing paper banknotes, such as the offset process, intaglio, and letterpress printing.[83] Furthermore, Diffractive Optically Variable Devices (DOVDs), highly reflective foil based devices, can be incorporated into the banknote for improved aesthetics and increased security. The polymer banknotes are covered with two clear overcoat layers (a primer and an overcoat) to protect the note from soiling and provide a feel.[85] The primer coat is applied to improve the adhesion of the matt coat. Each of these coatings are UV-cured polymers. The polymerisation process results in a surface that prevents (or certainly limits) the absorption of residues such as moisture, oils, sweat and beverages. Figure 1.12 below shows a cross

section of a polymer banknote and the approximate thicknesses of each layer / printing technique.

SECTION THROUGH - POLYMER BANKNOTE

intaglio 10 - 50 micron

offset 1.5 micron   gravure 2 x 3 micron   ovd gloss patch coat 1.5 micron

ovd 3 micron

polyolefin skin 0.2 micron

polypropylene 2 x 37.5 micron

primer varnish 2 micron
matt varnish 2 micron

polyolefin skin 2 x 0.1 micron
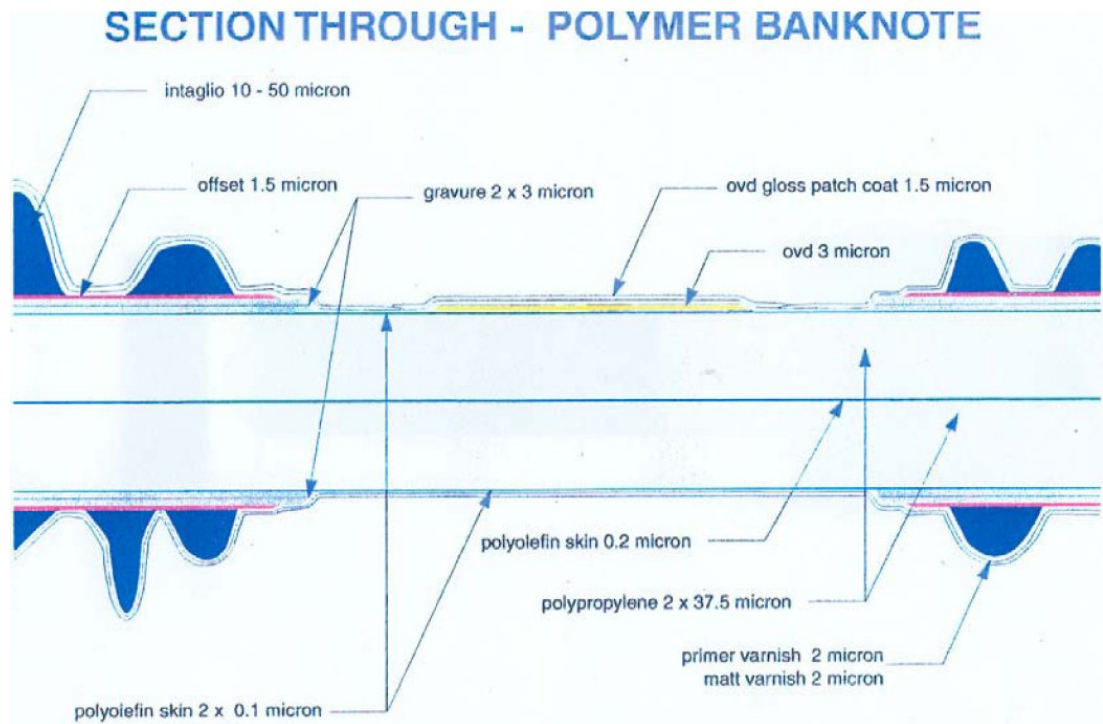
Figure 1.12:   Cross section of polymer banknote.[85]

Banknotes are commonly encountered in forensic case work in, for example, drug cases or armed robberies. Flynn et al. investigated a number of techniques for the detection and enhancement of latent fingerprints on polymer banknotes.[86] This was a preliminary study but they concluded that the semi-porous nature of the surface led to significant problems when conventional techniques are applied. It was recommended that cyanoacrylate fuming be carried out immediately to "fix" any latent prints. VMD was also identified as a promising technique. Jones et al. continued this research and recommended a sequence of techniques which included immediate cyanoacrylate fuming followed by VMD treatment and luminescent staining.[42] The wear of the note was also found to influence the success of fingerprint development. Jones et al. successfully developed one-year-old prints on new banknotes and one-month-old prints on used notes. More recently, the use of infrared chemical imaging has been demonstrated as a promising technique for the imaging of cyanoacrylate-fumed fingerprints on polymer banknotes.[75,76]

1.1.8   Need for new fingerprint development techniques

Although there are a number of currently used fingerprint detection techniques, most suffer from one or more of the following disadvantages:

- lack of sensitivity (i.e. does not detect all fingerprint e.g. older fingerprints, fingerprints from poor donors etc.)
- expensive
- time consuming / labour intensive
- use of toxic solvents / chemicals
- use of solvents / chemicals which can damage the environment
- occupational health and safety (OH & S) risks
- lack of portability (cannot be performed at a crime scene)
- preclude further evidence collection (e.g. document examination, DNA analysis etc.).

Furthermore, there are particular surfaces on which it is difficult or impossible to develop fingerprints. Champod et al. discuss the desire for the development of new or improved methods that can:

- offer increased sensitivity and signal-to-noise ratio
- be readily deployed at crime scenes
- be introduced in sequences of detection techniques or in sequence with other forensic investigation methods (e.g., DNA profiling)
- simplify the detection process by reducing the number of steps or allowing automation
- reduce the overall cost of fingerprint processing
- avoid the use of hazardous chemicals.[4]

1.1.9 Considerations for the preparation of fingerprint samples

As mentioned in Section 1.1.6.2 above, when dealing with fingerprints, it is important to minimise the variables which can affect results in latent fingerprint development. Many factors which affect the 'quality' of prints developed by cyanoacrylate fuming (the major fingerprint development technique employed during this project) can be identified. Some of these factors include:

- age of fingerprint prior to development

- moisture content within the latent fingerprint

- information about the donor e.g.:

  - skin structure

  - nutritional habits / diet

  - smoking habits

  - medication

  - diseases

  - sex

  - age

  - racial origin

  - professional occupation

  - emotional status at the moment of print application

- application surface (rough or smooth, porous or non-porous etc)

- background colouration (or fluorescence in the case of subsequent fluorescent dying of treated prints)

- clean or contaminated donor fingers

- force or pressure

- velocity of lifting finger from surface etc

- environmental factors:

  - temperature

  - humidity

  - exposure to dust, wind, sun, snow and water

Although many of these factors cannot be controlled, it is important to keep the number of variables to a minimum. For those factors which cannot be effectively controlled, an attempt should be made to measure and document that factor. In 2001, Jones et al. noted some parameters that researchers should consider when conducting fingerprint studies.[87] While this article raises awareness about the difficulties involved in conducting fingerprint research, it does little to address the real issues of how to overcome these difficulties. The major point that Jones et al. make is that it is important to control (or at least take note of) the various parameters involved, such as those listed above. With this kind of information available, a real assessment of a particular reagent's performance can be made. During this project, an attempt has been made to limit the number of variables involved in the development process and to accurately note as much information as possible regarding the donors used, the deposition of latent fingerprints, the surface characteristics of the samples and the treatment

and imaging conditions used. Details of the actual materials and methods used can be found in the relevant sections throughout this thesis (see Sections 2.2 and 4.2).

1.2   FTIR (spectral) chemical imaging

1.2.1   Introduction and terminology

Infrared (IR) spectroscopy deals with the interaction of electromagnetic radiation in the infrared region with matter. This region is comprised of wavelengths that are longer than those associated with visible light but shorter than those associated with microwaves. The radiation in the infrared region is typically referred to in terms of *wavenumber* (expressed as reciprocal centimetres – cm^{-1}) but *wavelength* (expressed as μ or μm) may be encountered in older literature. The wavenumber units are preferred because they are directly proportional to energy (a higher wavenumber corresponds to a higher energy).[88] The infrared region covers wavenumbers ranging from 12,800 to 10 cm^{-1}. This range can be divided into three regions, *near-infrared* (12,800 – 4,000 cm^{-1}), *mid-infrared* (4000 – 400 cm^{-1}) and *far-infrared* (400 – 10 cm^{-1}).[89]

The mid-infrared region is by far the most widely used for the qualitative and quantitative determination of molecular species. Any compound having covalent bonds, whether organic or inorganic, absorbs in the mid-infrared (note that the suffix *'mid-'* is commonly omitted) region, with the exception of homonuclear diatomic molecules and ions. Radiation in this energy range corresponds to the range encompassing the stretching and bending vibrational frequencies of the bonds in most covalent molecules.[88] In the absorption process, those frequencies of infrared radiation which match natural vibrational frequencies of the molecule in question are absorbed, and the energy absorbed serves to increase the amplitude of the vibrational motions of the bonds in the molecule.[88]

Every non-linear molecule of N atoms has $3N – 6$ normal modes of vibration ($3N – 5$ for linear molecules). Depending on molecular symmetry, a number of these modes are IR-active, and give rise to absorption bands. Many normal modes are effectively isolated to particular functional groups and have frequencies that vary within a narrow range and which are therefore characteristic of the functional groups. These characteristic vibrational frequencies are called *group frequencies*. Other normal modes will involve considerable participation by

each of the atoms within a molecule. This combination of characteristic group frequencies and non-localised normal modes allows the *infrared spectrum* (the term given to the infrared absorption pattern of a compound) to be used to identify functional groups and to distinguish between closely related compounds. Thus, as Pavia et al. put it, *"the infrared spectra can be used for molecules much as a fingerprint can be used for humans".*[88]

The infrared spectrum shows the frequencies of infrared radiation absorbed by the molecule and the proportion of incident light that passes through the molecule without being absorbed. The identification of an unknown compound via infrared is made possible by the collection and comparison of infrared absorption, reflection and emission spectra.   The spectrum of the unknown compound may be searched against a library of known spectra. More commonly however, the mid-infrared spectrum is used to determine structural information about the compound. A molecule absorbs a set of infrared frequencies which are unique to its structure, so by identifying the absorption bands present in the spectra, the types of bonds present can be identified.

Until the 1980s, the most widely used instruments for infrared measurements were dispersive spectrophotometers. Now, however, this type of instrument has been largely replaced by *Fourier Transform Infrared (FTIR)* spectrometers. FTIR spectrometers are based upon the Michelson interferometer, which uses a moving mirror to create an interference pattern, or *interferogram*, from which all resolution elements are determined simultaneously. FTIR instruments offer better speed, reliability and convenience while providing high resolution, sensitivity and unparalleled wavelength precision and accuracy.[89]

Infrared spectroscopy can be used for a wide variety of samples including solids, liquids and gases. Coupling an FTIR spectrometer to a microscope has greatly increased the applicability of FTIR analysis, particularly in areas such as forensic science. This technique, known as *FTIR microspectroscopy*, allows the rapid analysis of micro-sized samples or small features of interest within larger samples (in the $10 - 500$ μm range) with little or no sample preparation. This is particularly attractive from a forensic point-of-view, where the quantity of sample is often limited and non-destructive techniques are preferred.

Coupling FTIR spectrometers with a microscope also allowed for the collection of full spectral molecular images in which an IR absorption spectrum is collected at every pixel in the image. This allows for the identification of the various molecular species within a sample as well as

their spatial characteristics, such as particle size and distribution. This type of imaging, known as *FTIR chemical imaging*, is part of a more general class of techniques known broadly as *hyperspectral imaging*, *spectral imaging, spectrochemical imaging* or *chemical imaging*. These terms are often used interchangeably, but some authors have a preference for one or another. Imaging using the mid-infrared range involves the collection of spectra from which we are able to distinguish different molecular functional groups and hence chemical differences. Therefore, for FTIR imaging, any one of the aforementioned terms is fitting since the images generated are due to spectral differences that are in turn due to chemical differences. For simplicity, the terms *FTIR chemical imaging* or simply *infrared chemical imaging* are used for the balance of this thesis.

Applications of hyperspectral (chemical) imaging have included (but are not limited to) remote sensing,[90] histopathology,[91-94] food and agriculture sciences,[95-97] microbiology,[98] polymers[99] and pharmaceutical quality control and other biomedical studies.[100,101] A range of types of hyperspectral / chemical imaging have been applied to forensic science (among other areas). These include remote sensing,[102] UV-visible / fluorescence imaging,[103-108] near infrared (NIR) imaging,[106,109,110] Raman mapping and imaging,[111,112] and FTIR chemical imaging.[15,75,76,113-119]

All spectral / chemical imaging techniques involve the collection of a spectrum (be it infrared, UV, visible or otherwise) at each pixel within a sample. Alternatively, the data generated may be viewed as an image at every wavenumber (or wavelength) within the spectral range being used. Figure 1.13 shows a representation of the data generated by these imaging techniques; this can be thought of as a *datacube.* The datacube ($x \times y \times$ wavenumber) can be visualised as a collection of images of the sample, with one image for each wavenumber resolution unit. These images, or slices through the datacube, are often presented as 'false colour maps', formed by attributing an arbitrary colour to each pixel according to the spectral intensity at the frequency (wavenumber value) selected. Most commonly, a colour scale from high intensity (= red) to low intensity (= blue) is employed, but a greyscale can also be used.[75]

Spectrum at each pixel

Pixel

Image / 'false colour map' at
each wavelength / wavenumber
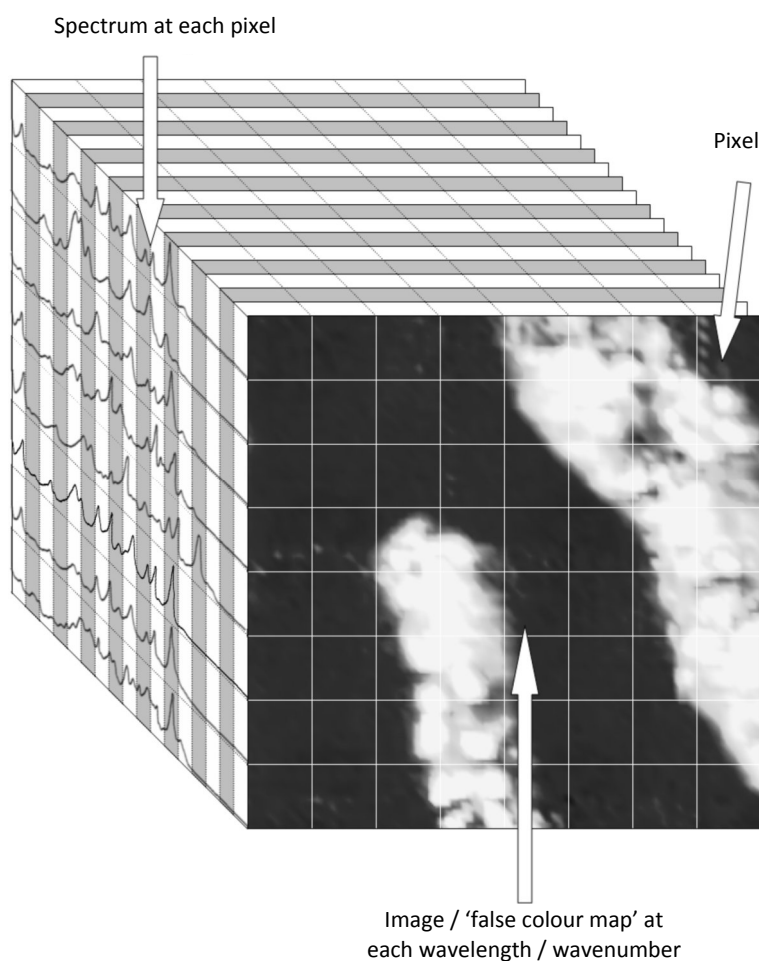
Figure 1.13: *Diagrammatic representation of 'datacube' generated by chemical imaging techniques.*

The focus of this thesis is on FTIR chemical imaging and discussion is therefore limited to this technique. Further information on the other chemical imaging techniques listed above may be found in the relevant citations and the references therein.

There are three methods for collecting FTIR chemical images. The first utilises a motorised stage to acquire spatially resolved infrared spectra across a sample in a point-by-point manner.[93,120-125] This method, known as FTIR mapping, is inherently slow and has largely been superseded. A second method uses a linear array detector made up of a row of eight or more pixels (or multiple rows of offset pixels). Using a linear array decreases the time taken to acquire an image (relative to mapping) by a factor equal to the number of pixels. A 16-pixel linear array detector, available in the Perkin Elmer Spotlight 300 system, for example, is the most common type encountered. The third method of FTIR chemical imaging uses a focal plane array (FPA) detector that can collect a full spectrum at each pixel simultaneously. The most common FPA is comprised of 64×64 pixels arranged in a grid pattern, although larger

(256 × 256) detectors are available. A 64 × 64 pixel image can be rapidly collected using this type of detector and the resulting image contains 4096 spatially resolved infrared spectra.

We will now consider the various FTIR techniques discussed above and their application to forensic science.

1.2.2 FTIR spectroscopy and microspectroscopy

FTIR spectroscopy is a widely utilised and accepted technique for the analysis of a range of forensic samples. It can be used to provide both quantitative and qualitative information, is rapid, requires little or no sample preparation and is generally non-destructive. FTIR spectroscopy is used to identify unknown materials or to establish whether two samples could come from the same source.

As mentioned in Section 1.2.1 above, coupling a microscope to a FTIR spectrometer increased the range of samples which could be analysed. Prior to the introduction of FTIR microspectroscopy, forensic FTIR analysis was limited to the analysis of bulk samples such as drugs,[126] although analysis of other forensic evidence had also been reported. FTIR microspectroscopy has found many applications including the identification of polymer contaminants, imperfections in polymer films, and individual layers of laminated polymer sheets in the materials industry, characterisation of single fibres in the textile industry and identification of contaminants on electronic components.[89] Forensic science has also benefited greatly from the development of FTIR microspectroscopy. It has enabled analysts to obtain chemical information, in the form of an objective infrared spectrum, from microscopic samples. FTIR microspectroscopy has found uses in the analysis and comparison of paint,[127-133] fibres,[134,135] hair,[136] drugs,[133,137,138] explosives,[139] adhesive tapes,[140-142] documents (including inks, toners and paper analysis)[142-148] and drugs in hair[149,150] among others. A number of books and reviews discuss the application of FTIR spectroscopy and microspectroscopy to forensic science.[126,139,151-153]

1.2.3 FTIR mapping

The collection of spatially resolved chemical information using an FTIR microscope was first made possible with the development of *FTIR mapping*.[154] This technique found many

applications in the study of polymers,[121,122] biological (organic) samples[120] and inorganic materials.

FTIR mapping involves the point-by-point collection of individual spectra across a sample using a computer–controlled stage with accurate sample positioning capabilities. This allows large areas to be examined in a predetermined manner using apertures and systematic movement. While FTIR mapping brings valuable spatially resolved information to the analyst, it suffers from a few fundamental deficiencies. Firstly, sample areas are limited to squares of side length larger than 15 μm because smaller apertures cause diffraction of longer wavelengths. Secondly, the accuracy of the data can be compromised by these diffraction effects and stray light. Lastly, and perhaps most notably, the time taken to collect an appreciable number of data points is very high. Koenig et al. comment that *'an area a fraction of a millimetre takes many hours'*.[154] Nevertheless, FTIR mapping has been applied to the analysis of drugs in hair[123,149,150] and paint cross-sections.[124] Bhargava et al. provide a comparison of FTIR mapping and imaging techniques and highlight the value of each analytical tool in specific situations.[125]

1.2.4   FTIR chemical imaging

The limitations which are inherently obvious in FTIR mapping have been overcome with the development of FTIR imaging using a linear array or (more commonly) a Focal Plane Array (FPA) detector. FPA detectors consist of a large number of small detectors (pixels) laid out in a grid pattern. Each single pixel detector is capable of the simultaneous collection of an infrared spectrum from a specific area on the sample.[154]

During collection, the entire sample area in the field of view of the detector is illuminated by the source. A 'snapshot', or image is taken; this consists of information collected from all areas at the same time, as opposed to a point-by-point examination of the sample area (as in FTIR mapping). FTIR imaging allows the collection of thousands of spectra with high spatial resolution ($\sim$ 6 μm pixel size but real resolution is poorer, especially bellow 2000 cm^{-1}) within minutes.

As mentioned above, a false colour map can be used to represent the sample according to the intensity of selected spectral features at each pixel. This can be done in a number of different ways. In the simplest application, the image can be constructed by selecting a

frequency slice of the data cube. The frequency slice method produces an image based on the vibrational peak intensity at a given wavelength/frequency (frequency slice). For example, pixels that have a high intensity at the specified wavelength may be attributed a warm colour (such as red) and pixels with a low intensity at that same wavelength are attributed a cool colour (such as blue). All the pixels in the array are coloured according to their relative intensities forming an image which gives spectral information in a spatially resolved manner. The data can also be represented using the intensities across a range of wavelengths (peak areas) or using ratios of peak intensities. Multivariate analysis of the data can also be useful in some circumstances to highlight features which are not immediately obvious from the raw data.

The main advantages of FTIR imaging are its non-invasiveness, fast data collection and the ability to create visually appealing and informative displays.[154] FTIR imaging provides an insight into the spatially resolved chemical composition of samples. With the ability to collect thousands of spectra simultaneously, FTIR imaging can also be used to analyse multiple samples simultaneously rather than exploring the spatial heterogeneity of a single sample.[155] It also makes it possible to monitor the spectral information of multiple spatial locations in parallel and provides superior image fidelity.[155]

1.2.4.1 *Development of FTIR chemical imaging*

FTIR chemical imaging is an emerging technique and reports, journal articles and information regarding this technique are being quickly outdated. In 2002 Kidder et al. described the emergence and development of FTIR imaging instrumentation. They identified the lagging of the development of IR array detectors (for spectroscopic applications) due to their strategic importance in a military context. This has meant that the availability and development of these detectors were initially restricted to military rather than commercial needs. Miseo and Wright also acknowledge the initial development of FPAs for military use (heat-seeking missiles and night vision heads-up displays for aircraft and ground vehicles) but claim that multispectral imaging systems were first demonstrated in 1979 and that *"chemists were slow to notice the technology, and it took twenty-five years for them to use it in a laboratory setting"*.[156] Whether this comment is a reflexion of physicists' animosity towards chemists or reality, the truth remains that the first commercial chemical imaging instrument in a chemical laboratory was not introduced until 1995. Despite these setbacks, many different types of FPA detectors have been developed over the past decade. Although a range of array

detectors are now commercially available, not all are suited for chemical imaging. Detectors need to be assessed based on their cost, availability, spectral coverage, sensitivity and operating temperatures (i.e. cooled or uncooled).

The grid pattern arrangement of FPAs was made possible by separating the critical parts of the detector into two semiconductor layers. One layer of this "hybrid detector" carries out photon detection, while the other carries out signal collection. Separating out these layers allows each to be manufactured from a material which is optimal to its task. The two layers are electrically and mechanically fused together by 'bumps' of a soft metal such as indium. Each individual bump-bonded entity is referred to as a pixel and functions as a discrete detector within the array.[155] A problem for early versions of these detectors was that the two layers would delaminate, but advances in technology has largely eradicated this issue.

The first commercial infrared chemical imaging instrument utilised a *indium-antimonide (InSb)* 128 × 128 pixel FPA detector which suffered from a limited spectral range (4000 – 2000 cm^{-1}).[157] Other detectors, such as a *silicon-arsenic (SiAs)* FPA are sensitive throughout the mid-infrared region but require cooling to liquid helium temperature (4 K).[155,158] To avoid the use of such low temperature while still working in the mid-infrared region, the next generation of mid-infrared chemical imaging systems (such as that released by Digilab in 1997) employed a *mercury-cadmium-telluride (MCT)* FPA detector that is sensitive from 4000 – 900 cm^{-1}.[155,156] The *64 × 64 pixel* format MCT FPA detector (commonly referred to as the Lancer or Javelin detector after the U.S. army's heat-seeking Javelin missile for which it was developed) has become the most common FPA detector used for mid-infrared chemical imaging. [155,156] This detector collects 4096 IR spectra simultaneously and is the type of detector fitted to the instrument used during this project. Further information regarding detector types and the development of detector technologies may be found in the following articles and the references therein.[155,156]

Early FTIR imaging instruments used a *Michelson step-scan interferometer* to modulate a broad band IR light source and focus it onto the sample using a series of optics. In this instrument, the IR light impinges on the sample, and the transmitted or reflected light is subsequently focused onto the FPA, preserving spatial information.[155]

Using the step-scan implementation, the flow of data is controlled by the rate of stepping of the interferometer's moving mirror. Each time the interferometer mirror is stepped into a

new position, an image frame is collected by the FPA. The mirror is held in place long enough for sufficient signal to reach the FPA which gathers and subsequently reads out the data. This is a truly hyperspectral technique, in that multiple wavelengths are detected from multiple sample locations simultaneously.

The step-scan method of data collection was first used by Lewis et al. in 1995 and is still in use today.[159] This method has, however, largely been replaced by a technique called *rapid-scan*. The rapid-scan approach was first demonstrated by Bennett et al. who used this approach to collect FTIR imaging data sets.[160] Snively et al. later reported a modification of the rapid-scan approach which allowed for rapid data collection without decreasing the data quality.[161,162]

The rapid scan instrumentation operates in a similar fashion to conventional FTIR microscopic instruments although mirror movement, and thus the rate of data acquisition and readout, is marginally slower. Rapid-scan allows faster imaging than the step-scan approach and hence it gives more time for averaging imaging data cubes (spatial data collected at every frequency), leading to more accurate spectra and images.[154,163]

At the time Bennett first demonstrated this technique, the electronics and technology involved in a rapid-scan spectrometer coupled to an FPA-equipped microscope were too costly to be commercially viable. The rapid-scan technology, however, developed very quickly to the point where the rapid-scan instruments are now used almost exclusively for FTIR imaging. Further information regarding the development of instrumentation for FTIR chemical imaging may be found in the aforementioned references as well as the following articles by Bhargava et. al.[164-167]

The FTIR chemical imaging instrument that has been used in this project is the Digilab Stingray system, which is comprised of an FTS 7000 FTIR spectrometer coupled with a UMA 600 infrared microscope and a Lancer 64 × 64 Mercury Cadmium Telluride (MCT) focal plane array (FPA) detector. In addition to the imaging capabilities of this detector (i.e. the ability to collect 4096 spectra simultaneously with spatial resolution) it also has the added ability to 'stitch' together or tile a number of images, so that larger samples (such as an entire fingerprint) can be imaged. This process is referred to as *mosaicking.* Details of the instrumental parameters used during the current research can be found in the relevant

sections throughout this thesis (see Sections 2.2 and 4.2) and Chapter 2 describes the optimisation of these parameters.

1.2.4.2   *Forensic applications of FTIR chemical imaging*

Since the introduction of commercial FTIR chemical imaging instruments, this technique has been demonstrated in many areas including polymeric materials, biomedical and pharmaceutical applications and high-throughput analysis.[91-94,98,100,158,168-170] Biological studies have ranged from lipid analysis in obesity research,[171] to research into factors affecting bone development[172] among others.[91,92,94,168,173] Bhargava et al. reviewed the uses and applications of FTIR imaging for biological tissue samples.[168] This article presents a review of instrumental configurations for both data collection and processing aspects and presents several biological applications. The utility, potential and future directions of FTIR imaging as an important analytical procedure are discussed.[168] More recently FTIR chemical imaging has become an important tool for and cancer histopathology,[91,94,120,173] and microbiology and prion research[98]. The use of ATR-FTIR chemical imaging for biomedical samples has also been reported.[100]

The quick data acquisition offered by FTIR imaging allows the examination of multiple samples simultaneously and certain processes can be viewed in real time. FTIR imaging has been used for the analysis and study of polymer laminates, semicrystalline polymers and their blends, polymer-liquid systems, polymer-liquid crystal systems and determination of phase diagrams.[99,174,175] These applications range from simple visualisation of the distribution of chemical entities to the complex analysis of multiphase systems.[154,155] FTIR chemical imaging has also been demonstrated for pharmaceutical samples.[176,177]

While the technique of FTIR chemical imaging is over a decade old, its value to forensic science is only now being realised. Its application to the detection and enhancement of latent fingerprints was reported in early 2005.[75] The use of FTIR chemical imaging for the imaging of fingerprints is discussed in detail in Section 1.2.4.3 below. Prior to the publication of this article, the use of FTIR chemical imaging for forensic samples had been reported only as part of conference proceedings. For example, in 2002, at the International Association of Forensic Sciences conference, Bartick et al. presented preliminary work on the hyperspectral imaging of untreated latent fingerprints on aluminium-coated microscope slides.[178] They provided preliminary results of whole fingerprints imaged using visible and near-infrared

(NIR) hyperspectral imaging but only partial prints in the mid-infrared range.[178] These authors were mainly concerned with gaining a better understanding of the chemical composition of latent fingerprints (particularly the difference between adults' and childrens' fingerprints) so that new methods of developing fingerprints could be explored. There have been reports on the use of single detector FTIR microscopy[10,13,179,180] and synchrotron infrared[11,12] for this purpose. More recently, Ricci et al. have reported the use of attenuated total reflection (ATR) infrared chemical imaging for the analysis of latent fingerprint residue under controlled humidity and temperature.[15]

Bartick et al. have also presented results on the detection of trace amounts of the explosive RDX located within a latent fingerprint deposit.[181,182] This is an area that has been receiving increased attention. Several authors have reported the identification of exogenous material in fingerprints via Raman spectroscopy[80,81,183,184] and FTIR spectroscopy.[185,186] In addition to the work by Bartick et al., Kazarian and co-workers at Imperial College London have demonstrated the application of ATR-FTIR chemical imaging for the detection of trace materials (such as drugs) within fingerprints, on the finger surface and on adhesive or lifting tapes used to recover such traces.[114,118,187,188] Recently, Ricci et al. reported the use of FTIR chemical imaging for the analysis of counterfeit antimalarial tablets.[189,190] Work has also focused on the application of FTIR chemical imaging to the analysis of other forensic trace evidence such as paint chips,[116] fibres[117], and hair.[191] Recently, Bojko et al. have reported the use of ATR-FTIR chemical imaging for determining the sequence of intersecting lines in forensic document examination.[113]

1.2.4.3   *FTIR chemical imaging of fingerprints*

When Bartick et al. presented images of partial fingerprints obtained using FTIR chemical imaging, they noted that *"the distinct [mid-infrared] absorption bands from chemical functionality make this spectral region most promising for fingerprint imaging"*.[178] Indeed infrared chemical imaging has the potential to solve many of the background interference problems encountered in the visualisation of fingerprints on difficult surfaces using conventional methods. As outlined in Section 1.1.7 above, "difficult" surfaces can contain pictures or text that obscure the ridge details of a latent or pre-treated fingerprint. On such surfaces, infrared imaging can provide significantly improved results because the contrast is not based on the response of the surface or print to lighting conditions but rather is based on spectrochemical differences. This chemical contrast allows the imaging of fingerprints on

surfaces where conventional fingerprint detection and enhancement methods prove difficult or impossible. While the work by Bartick et al. considered only untreated (latent) fingerprints, Tahtouh et al. demonstrated that FTIR chemical imaging can also produce superior results with cyanoacrylate-fumed fingerprints.[75] In this study, untreated fingerprints on glass or infrared reflective surfaces were easily imaged with good ridge detail using the C-H stretching frequency of the lipids and other organics from in the latent print deposit. It was noted, however, that the success of this experiment relied on the absence of any significant absorption bands in this region from the substrate which may interfere with the peak used to form the image of the latent fingerprint. Prints on difficult surfaces, such as polymer banknotes, were successfully imaged by fuming with ethyl cyanoacrylate (superglue) prior to FTIR chemical imaging.[75]

In this case, ethyl cyanoacrylate was chosen for two main reasons. Firstly, it is a commonly used fingerprint detection technique and is known to selectively deposit poly-cyanoacrylate on the ridges of a latent fingerprint. Secondly, ethyl cyanoacrylate (and hence poly-ethyl cyanoacrylate) contains a $C\equiv N$ (nitrile) functional group whose fundamental vibration frequency ($\sim$2250 cm^{-1}) is located in a part of the infrared spectrum which is generally void of any major absorption peaks. Common background surfaces therefore should not interfere with the absorption band present on the treated fingerprints and hence good contrast between the treated print and the substrate was anticipated. Unfortunately, although an absorption band at $\sim$2240 cm^{-1} is present in monomeric cyanoacrylate, the frequency for this absorption is shifted to a slightly higher wavenumber upon polymerisation and decreases significantly in intensity. This phenomenon is discussed further in Section 4.1.1 below. Despite the loss of the $C\equiv N$ peak, the $C=O$ (ester) peak from the poly-cyanoacrylate proved to be sufficiently isolated from an interfering peak in the spectrum of the polymer banknote substrate and FTIR chemical images of the cyanoacrylate-fumed fingerprints were obtained.[75]

Using a combination of lifting tape (commonly used for the recovery of traces such as fingerprints) and ATR-FTIR chemical imaging, Ricci et al. were able to image fingerprints recovered from curved surfaces such as a door handle, a mug handle, a curved glass surface and a computer screen.[119] It should be noted that the size of the images obtained by the ATR-FTIR technique used by Ricci et al. are limited by the sizes of ATR crystal and FPA detector and the instrumental configuration and optics. The largest image possible with this technique is approximately 4.7 × 6.3 mm^2. This area represents only a few ridges of the entire fingerprint.

Crane et al. have recently reported the FTIR chemical imaging of latent fingerprints on various porous and non-porous substrates including trash bags, a soda can, duct tape, copier paper, cigarette butt paper, a U.S. dollar bill and a postcard.[115] They also report the recovery of a blue fibre from one of the latent fingerprints. The fibre was not analysed *in situ* but was removed, rolled and mounted for conventional FTIR analysis.[115] Chapter 2 of this thesis explores the optimisation of parameters for FTIR chemical imaging of fingerprints. This work has recently been published[76] and some of the results obtained in our hands differ from those reported by Crane et al. Most notably, Crane et al. provide FTIR chemical images of a number of fingerprints on porous surfaces. As discussed in Section 2.3.3 below, we have been unable to image fingerprints on porous surfaces for two main reasons i) the paper substrate is highly absorbing in the infrared and therefore the signal-to-noise ratio is very low and ii) the amount of fingerprint material present (even after treatment with a fingerprint detection reagent such as ninhydrin) is very low and below the limit of detection via this method. The fact that Crane et al. were able to form images of latent (unprocessed) fingerprints on porous surfaces may be a result of a more sensitive detector. The system used by Crane et al. is a Spectrum Spotlight 300 FTIR microscope system which is fitted with a 16-pixel linear array, as opposed to the 64×64 pixel MCT-FPA detector described earlier, which is used in this research. Another factor is that many of the fingerprints imaged by Crane et al. were *slightly visible by eye*[115] prior to FTIR chemical imaging. This could suggest that the surface of the finger was contaminated with some foreign material prior to deposition onto the substrate. Full details of the results obtained in the current study can be found in Chapter 2 and Chapter 4 of this thesis and the corresponding publication.[76]

1.3 Project aims

The primary aim of this project is to use FTIR chemical imaging to obtain good quality images of untreated or treated latent fingerprints on a variety of surfaces and backgrounds. Of particular interest are fingerprints on surfaces and backgrounds which have posed particular problems for the forensic investigator. Some of these "difficult" surfaces include polymer banknotes, painted or multicoloured surfaces and substrates with complex background patterns (see Section 1.1.7 above).

At the outset of the current research project, the application of FTIR chemical imaging for the detection and enhancement of latent fingerprints had already been demonstrated.[75] The current project aims were to further investigate the potential for FTIR chemical imaging for

this purpose. To this end, a number of key areas of investigation were identified and now form the contents of this thesis. These include:

- optimisation of parameters used for the FTIR chemical imaging of fingerprints

- imaging of latent (untreated) and developed (treated) fingerprints on a number of difficult surfaces

- identification, synthesis and characterisation of modified cyanoacrylates which may be used as reagents for FTIR chemical imaging of fingerprints

- the enhancement of latent fingerprints on difficult surfaces using novel cyanoacrylates and subsequent FTIR chemical imaging

The novel cyanoacrylate monomers are based on the generalised structure for alkyl 2-cyanoacrylates (see Figure 1.8 above) and so still retain the active vinyl moiety. Hence they are expected to react with fingerprint residue in the same manner as conventional cyanoacrylates. The R groups were selected to contain a functional group that would produce a vibrational band in a region of the mid-infrared that is generally free of absorption bands from common surfaces on which the fingerprint may lie. Figure 1.14 shows the approximate regions where various common types of bonds absorb in the mid-infrared.
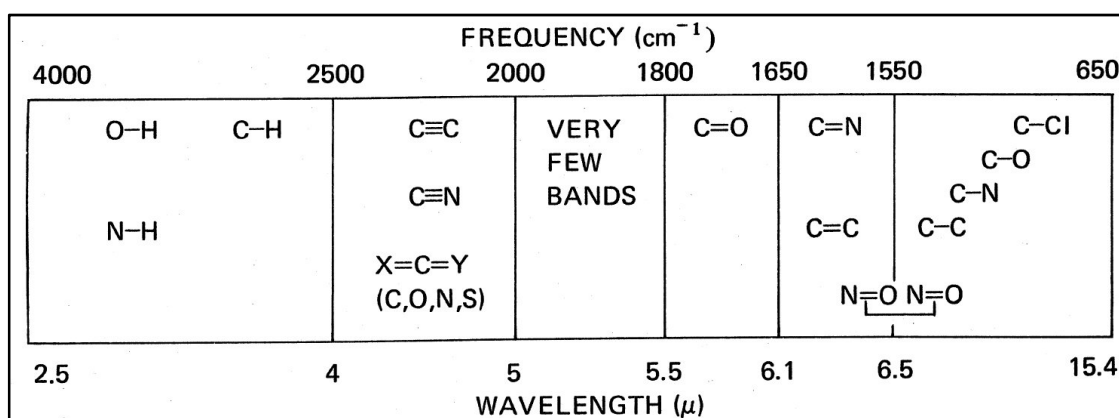
Figure 1.14:   *The approximate regions where various common types of bonds absorb (stretching vibrations only).*[88]

The range from 2500 – 1800 cm^{-1} contains very few vibrational bands, the notable exception being triple bonds such as C≡C and C≡N. It is desirable to have a reagent that contains a functional group that absorbs within this region (referred to herein as the "region of interest"). This would provide the necessary contrast between the ridge details of the treated fingerprint and the background on which it may be located. Table 1—3 lists some

functional groups, with their corresponding vibrational frequencies, that fall within this range.

Functional group / assignment	Origin	Vibrational frequency range
aliphatic nitrile	–C≡N	2280 – 2240 cm^{-1}
aromatic nitrile	–C≡N	2240 – 2220 cm^{-1}
cyanate	–O–C≡N	2260 – 2240 cm^{-1}
isocyanate	–N=C=O	2276 – 2240 cm^{-1}
thiocyanate	–S– C≡N	2175 – 2140 cm^{-1}
isothiocyanate	–N=C=S	2150 – 1990 cm^{-1}
terminal alkyne (monosubstituted)	–C≡C	2140 – 2100 cm^{-1}
medial alkyne (disubstituted)	–C≡C	2260 – 2190 cm^{-1}
deuterated	–C–D	2100 – 2235 cm^{-1}
thiol	–S–H	2600 – 2550 cm^{-1}

Table 1—3: *Target functional groups and corresponding vibrational frequency range (stretching mode only). All vibrational frequency ranges taken from Coates[192] except for C–D stretch taken from Ley et al.[193] and Tadokoro et al.[194]*

Compounds that contain the nitrile (C≡N) functional group are immediately obvious candidates for the FTIR chemical imaging of fingerprints. Not only is the C≡N stretching frequency of this functional group isolated and free from interferences but it is also present in conventional cyanoacrylate. Unfortunately, as noted in Section 1.2.4.3 above and discussed in detail in Section 4.1.1 below, the intensity of the nitrile band in conventional cyanoacrylate decreases significantly upon polymerisation. For this reason, an R group containing a second nitrile moiety on the ester chain of the cyanoacrylate molecule was selected.

It was hoped that the band arising from this nitrile group would be retained in the FTIR spectrum of the polymer and would therefore be useful for the FTIR chemical imaging of the treated fingerprints.   Other considerations for the R group are the availability of starting materials and the molecular weight / size of the group. Since fingerprints are developed by exposing the sample to vapours of cyanoacrylate monomer, it is important to maintain the volatility of the monomer. For this reason a low molecular weight R group was selected. With these criteria in mind, 2-cyanoethyl 2-cyanoacrylate (Figure 1.15) was selected as a target compound for this purpose.
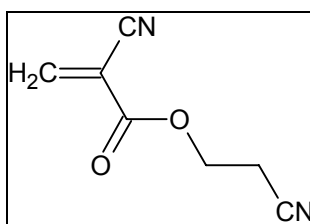
Figure 1.15:   *Structure of target compound: 2-cyanoethyl 2-cyanoacrylate.*

During the course of the project, a number of other novel cyanoacrylate monomers, which also contained one of the target functional groups listed in Table 1—3 above, were synthesised. These are discussed in Chapter 3 below.

The following is a summary of the contents of the subsequent chapters of this thesis, which address the primary aims of the project:

Chapter 2: explores the optimisation of parameters used for the FTIR chemical imaging of fingerprints.   This includes a systematic methodology for the selection, testing and optimisation of all relevant imaging parameters. This work assists in finding conditions which produce optimal results from new reagent / surface combinations in the most time-efficient manner.

Chapter 3: discusses the synthesis and characterisation of a number of novel cyanoacrylate monomers that have potential as reagents for the FTIR chemical imaging of fingerprints. Also included in this section is a history of the synthesis of cyanoacrylates, difficulties involved in their synthesis and a discussion of the thermal degradation of poly-cyanoacrylates.

Chapter 4: discusses the application of the novel cyanoacrylates to the detection and enhancement of latent fingerprints on a number of surfaces via FTIR chemical imaging. Also included in this section is a discussion of the kinetics and mechanisms involved in the polymerisation of cyanoacrylates.

Chapter 5: provides conclusions and discusses areas for further work.

Chapter 2: Optimisation of parameters for infrared spectral imaging of fingerprints

Chapter 2:   Optimisation of parameters for infrared spectral imaging of fingerprints

2.1   Introduction

The infrared spectral imaging of latent fingerprints was first demonstrated by Bartick et al.[178] These images of latent fingerprints on aluminium-coated glass microscope slides were formed using spectral bands indicative of the chemical components of the deposited material.[115] Tahtouh et al. demonstrated that latent fingerprint images were easily obtained from highly reflective surfaces such as metals due to the high signal to noise ratio of the infrared spectra collected.[75] On surfaces which are less reflective, such as glass or polymers, it is difficult to image untreated latent fingerprints. For such surfaces, ethyl cyanoacrylate (superglue) pre-treatment was found to produce high quality fingerprint images. In this case, the contrast of the treated latent prints were based on the carbonyl stretching mode of the ethyl cyanoacrylate polymer at around 1743 cm^{-1}.

During the initial development of an infrared chemical imaging technique for fingerprints, an un-optimised set of image collection parameters were used. Using these settings, the collection of an entire fingerprint image was time consuming (often several hours or days). Developing a systematic method for the optimisation of the image collection parameters became a focus of the current project.

FTIR spectral (chemical) imaging typically employs a focal plane array (FPA) detector that collects images which consist of thousands of pixels, with an infrared spectrum at each pixel. Typical FTIR chemical images are a fraction of a millimetre in size with a near-diffraction-limited real spatial resolution of $10 - 20$ μm.[158] We have described strategies for the imaging of larger samples such as whole fingerprints.[75] These strategies are instrument-dependent but often involve the combination or mosaicking of a number of single images, known as tiles, (e.g. in the Digilab/Varian or Bruker systems). When combined with expanded field of view optics, this allows the collection of images of up to several centimetres in size. As an example, the Digilab Stingray system is capable of producing mosaics of up to 4096 (64 × 64) tiles, representing an image area of 4.48 × 4.48 cm. Note that the Digilab Stingray system employed in this study produces square mosaics of particular sizes, whereas other systems,

such as the PerkinElmer Spotlight 300 system or the Bruker Hyperion imaging system can generate images of any size and aspect ratio.[195,196]

Collecting an image larger than a few millimetres introduces a number of challenges in terms of image collection time and file size. It is often necessary to reduce the spectral resolution and number of scans to achieve a practical image collection time. Likewise, spectral resolution and spectral range often need to be minimised in order to yield a manageable data file which can be processed with relative ease. Another strategy to reduce the file size involves the aggregation or averaging of neighbouring pixels. This reduces the total number of spectra (and hence the file size) at the expense of spatial resolution.

For the infrared imaging of fingerprints, it is necessary to optimise spectral resolution, number of scans, spectral range and pixel aggregation for every new surface and/or fingerprint pre-treatment tested. A technique for the systematic optimisation of these parameters is presented in this chapter. Latent fingerprints on aluminium drink cans which have been treated with cyanoacrylate (superglue) fumes have been selected as a model reagent / surface combination to demonstrate this optimisation process. While fingerprints treated in this manner are often visible to the naked eye and may be photographed using conventional techniques, some sections of aluminium drink cans are difficult to image under white light. In such cases, FTIR chemical imaging can yield superior results.

Also presented here is a continuation of previously published work[75] on the applicability of FTIR chemical imaging to other difficult non-porous surfaces such as polymer banknotes, as well as porous surfaces such as copy paper, thermal paper and masking tapes. The work presented in this chapter is the subject of a recently published article.[76]

All infrared chemical imaging measurements conducted during the current research were made in microreflection mode. Spectra collected in this manner may display artefacts such as specular reflectance due to dispersion in a sample's refractive index (known as *anomalous dispersion*). Anomalous dispersion is due to the changes in the refractive index of the sample as the wavelength (or wavenumber) changes near an absorption band.[197] It manifests itself as a tendency for some of a band's intensity to become negative and thus give the appearance of a first derivative spectrum in severe cases. In other situations, it may simply result in a small shift in the apparent peak position. While some specular reflectance was observed from some samples, the majority of samples did not display these artefacts. Furthermore,

attempts to correct for these artifacts (using a Kramers-Kronig correction algorithm built into the Win IR software) often failed to improve the results and generally introduced more artifacts.

It is also important to note that, in the current project, there was generally little interest, from a traditional spectroscopic perspective, in the actual spectral information collected from a fingerprint sample. Rather, what was of more concern was whether the spectra could be used to highlight differences between the fingerprint ridges and the background and hence provide images with sufficient contrast between these two regions. Many of the spectra collected, particular those from poorly reflective surfaces such as polymer banknotes, had a low signal to noise ratio, sloping baselines and were generally of poor quality. Despite this, chemical images formed from these spectra still produced fingerprint images of acceptable contrast in most cases.

2.2   Materials and methods

Fingerprints were prepared and deposited on a range of surfaces by thoroughly washing, rinsing and drying hands before swiping a cleaned finger across an oily region of the face (forehead, nose or neck) and finally placing the mark on the desired surface. The surfaces used during this study include clean, dry glass microscope slides, infrared reflective (metal oxide-coated) microscope slides (Kevley Technologies), freshly cleaned and dried circulated Australian polymer $5 banknotes, a range of white A4-sized copy paper, and various masking tapes, thermal paper and aluminium drink cans.

Freshly deposited latent fingerprints were developed using a purpose-designed forensic cyanoacrylate fuming cabinet (Carter-Scott Design, Australia). Approximately 1 mL of ethyl cyanoacrylate (Selleys® Supa Glue) was used for each treatment. Glass slides and aluminium drink cans were fumed until ridge development was obvious (an average of ten minutes). Samples where ridge development was not obvious were fumed simultaneously with a glass slide containing a freshly deposited print and fuming was stopped when ridge development on the glass slide was obvious but not overdeveloped (approximately 10 − 30 minutes). Polymer banknotes were fumed for an average of sixty minutes. Although ridge development on the banknotes was not visible to the naked eye at this point, a reference fingerprint on a glass slide began to show signs of over-development at fuming times in excess of sixty

minutes. Samples on porous or semi-porous substrates were treated with ninhydrin, 1,8-diaza-9-fluorenone (DFO) or 1,2-indanedione according to accepted methods.[4]

Infrared chemical imaging of fingerprints was carried out using a Digilab Stingray system, which comprised an FTS 7000 FTIR spectrometer coupled with a UMA 600 infrared microscope and a Lancer 64 × 64 focal plane array (FPA) detector. Images and spectra were collected and processed with Digilab Win IR Pro software. All samples were imaged in reflection mode using the expanded field of view (EFOV) setting, in which each individual image tile is approximately 700 × 700 µm in size. Other parameters such as spectral resolution, number of co-added scans, number of image tiles (image size), pixel aggregation factor and raw data processing methods were varied and optimised during this study. A full description of this optimisation procedure is provided in Section 2.3.1 below.

2.3 Results and discussion

2.3.1 Optimisation of parameters

The optimisation of large sample images, such as entire fingerprint images, involves a balance between various spectral and image collection parameters. The main parameters which need to be considered include:

- spectral resolution
- number of co-added scans
- spectral range
- pixel aggregation
- number of image tiles (image size)
- image formation parameters

The selection of these parameters will affect:

- image collection time
- file size
- spatial resolution and image quality

Table 2—1 summarises the effects of varying each parameter on image collection time, file size and image quality. The selection and optimisation of the various parameters is discussed below.

	Image collection time	File size	Spatial resolution and image quality
Spectral resolution	✓	✓	#
Number of co-added scans	✓	✗	#
Spectral range	✗	✓	✗
Pixel aggregation	✗	✓	✓
Number of image tiles (image size)	✓	✓	✗
Image formation parameters	✗	✗	✓

✓ = does have an effect, ✗ = does not have an effect, # = may have an effect

Table 2—1:   *Effect of various parameters on image collection time, file size and image quality.*

2.3.1.1   *Spectral resolution and number of co-added scans*

In most FTIR spectroscopic analyses, the selection of spectral resolution and number of co-added scans is routine. There is a trade-off in that higher resolution enables the separation of more closely spaced peaks, but at the expense of longer collection times for the same signal to noise quality. This is because at higher resolution (e.g. 1 cm^{-1} as opposed to 4 cm^{-1}), the signal to noise of an individual scan is poorer (less light is allowed through to the detector) and because each scan takes longer (interferometer mirror must move a greater distance).

Depending upon the sample, a modern FTIR spectrometer can collect a spectrum in seconds and rarely takes longer than a few minutes to collect an exploitable infrared spectrum of reasonable spectral resolution and quality. This time period is reasonable for most routine

single point infrared spectroscopic applications but can become a critical factor when combining a number of individual measurements as in FTIR mapping or image mosaicking. It is obvious that reducing the spectral resolution and the number of co-added scans reduces the time taken to collect each individual spectrum (or image tile) and thus the overall time of analysis.

Relative to IR mapping techniques, FTIR chemical imaging using an FPA detector has greatly reduced the time taken for the collection of up to several thousand infrared spectra across a sample. For the collection of images larger than a few millimetres, it is necessary to form a mosaic of many smaller images. This technique is analogous to the acquisition of many single IR spectra in IR mapping, but in this case each individual measurement (tile) is an image in its own right, consisting of up to thousands of spectra. The issues involved with data collection time are the same for mapping or mosaicking and thus the remedy is similar. For the collection of a large IR chemical image, such as that of an entire fingerprint, it is necessary to reduce the spectral resolution and the number of co-added scans to reduce the collection time of each individual image tile and thus minimise the time taken to acquire the larger overall image.

Table 2—2 shows the approximate time taken by the Digilab Stingray system for the collection of a 1024-tile FTIR image with various resolutions and scan numbers. This will produce an image the size of a typical fingerprint (up to 2.24 × 2.24 cm).

Co-added scans	Spectral resolution	
	16 cm^{-1}	**32 cm^{-1}**
4	3 hrs	2 hrs 30 mins
16	5 hrs 30 mins	4 hrs 15 mins
64	18 hrs	11 hrs 15 mins

Table 2—2: *Typical image collection times (2.24 × 2.24 cm image) for various combinations of spectral resolution and number of co-added scans.*

Table 2—2 shows that improving spectral resolution or increasing the number of co-added scans leads to an increase in image collection time. It also highlights the importance of selecting a reasonable combination of these two parameters. A resolution higher than

16 cm^{-1} (e.g. 8 or 4 cm^{-1}) becomes problematic due to impractical image collection times and unmanageable image data files. Increasing the spectral resolution by a factor of two leads to a corresponding twofold increase in file size since there are twice as many data points collected. The overall file size can be minimised somewhat by reducing the spectral range (see Section 2.3.1.3 below) but problems may still be encountered due to limits in computer processing capabilities. In general we have found that for the efficient FTIR imaging of entire fingerprints, the operator is limited to a spectral resolution of 16 or 32 cm^{-1}. It should be noted that it is possible to obtain images of smaller sections of fingerprints (e.g. 1.12 × 1.12 cm) with higher resolution settings (e.g. 8 cm^{-1}) where necessary. The use of attenuated total reflection FTIR imaging has also been demonstrated for high resolution imaging of fingerprints but this is also limited to small sections (typically less than a few millimetres).[15,118,119] Future advances in computer processing ability may resolve the problem of handling larger images with these settings. Advances in detector sensitivity are also anticipated and this would also improve the timely collection of images with higher spectral resolution due to the faster scan rates possible.

A similar limitation has been found for the selection of the number of co-added scans for the imaging of large sample areas. Increasing the number of co-added scans beyond 64 leads to image collection times which are impractical, so the number of scans collected is normally lower than 64. It should be noted that while the spectral resolution has a large effect on the image file size, the co-added scans are averaged to produce the final data set and therefore do not affect the final file size. Once again, a higher number of scans should become more feasible with improvements in detector sensitivity.

When optimising an image collection method for a new reagent / surface combination, a resolution of 16 cm^{-1} and 64 co-added scans is a good starting point. If exploitable fingerprint images are generated using these settings, then the same sample can be used to test 32 cm^{-1} resolution with 64 scans. If the results are still satisfactory then the number of scans can be reduced. Optimal settings are reached when exploitable fingerprint images are produced in the shortest timeframe (i.e. the lowest number of scans and the lowest resolution while maintaining ridge detail).

2.3.1.2   Number of image tiles (image size)

One obvious factor which will affect the image collection time and file size is the size of the final image. This is dictated by the number of individual image tiles which are pieced together to form the final image. The number of image tiles required is dependent on the particular instrument used and the size of the latent print (often unknown). Table 2—3 summarises the approximate image size options for the Digilab Stingray system used during this study. An image consisting of 16 image tiles (4×4) allows the sampling of a few ridges of a latent fingerprint. This size is reasonable for method optimisation of new surface / reagent combinations since it allows an assessment of the contrast achieved between the ridges and the background in the shortest space of time. Since method optimisation often involves the collection of a number of images using a range of settings, using a 16 tile image (compared to 256 or larger) also minimises the file size of the data collected.

Number of tiles	Sample area (in expanded field of view mode)
1 (1 × 1)	700×700 µm
4 (2 × 2)	1.4×1.4 mm
16 (4 × 4)	2.8×2.8 mm
256 (16 × 16)	1.12×1.12 cm
1024 (32 × 32)	2.24×2.24 cm
4096 (64 × 64)	4.48×4.48 cm

Table 2—3:   *Typical image sizes using expanded field of view optics on the Stingray FTIR imaging system.*

Once other parameters such as spectral resolution and number of co-added scans have been optimised, an image consisting of 1024 tiles (2.24 cm $\times$ 2.24 cm) is usually appropriate for the imaging of an entire fingerprint.

2.3.1.3   Spectral range and pixel aggregation

Although the spectral range acquired in FTIR spectroscopy does not affect the collection time, it does affect the size of the data file generated. One full range (400 – 4000 cm^{-1}), high resolution infrared spectrum has a negligible file size on a modern desktop computer, but in

FTIR imaging the file size can approach or exceed one gigabyte if many image tiles (each with thousands of spectra) are used to form a mosaic. Apart from disk space issues, files of this size are difficult to process because of limitations of memory and /or the computer operating system. Truncation of the spectral range to a small region of interest (e.g. the C=O stretching region of cyanoacrylate for fumed fingerprints) reduces the image file size, although it may have no effect on raw image data files that the imaging software may additionally produce.

Pixel aggregation is the averaging of spectra at adjacent pixels to form larger pixels. This has the advantage of reducing the file size (fewer spectra) of the images produced, at the expense of spatial resolution. It is an effective strategy if the spatial resolution sacrificed is unnecessary for the satisfactory imaging of the sample. Table 2—4 shows the effect of aggregating pixels on the pixel size (and hence spatial resolution) of the final image. The pixel size of images formed using the standard mode optics are shown here for completeness but EFOV optics were used exclusively during this project.

Pixel aggregation	Pixel size (μm) (Standard mode)	Pixel size (μm) (EFOV mode)
1	5	11
4	9	22
16	19	44
64	38	88
256	75	175
1,024	150	350
4,096	300	700

Table 2—4: *Resolution (pixel size) with variations in pixel aggregation.*

For the imaging of fingerprints, our results indicate that a spatial resolution of 44 μm can still produce images with sufficient clarity for the resolution of detail down to the third level (resolution of pore structure). For this reason, we have found that a pixel aggregation of 16 (which results in a pixel size of approximately 44 μm using EFOV optics) provides good quality fingerprint images and manageable file sizes. Increasing the pixel aggregation produces images with poorly resolved ridge detail while reducing the pixel aggregation gives files which are too large to process. For example, an image consisting of 1024 (32 $\times$ 32) mosaicked tiles (image size 2.24 $\times$ 2.24 cm) with a spectral resolution of 16 cm^{-1} and a pixel aggregation of 4 produces a total file size of ~ 5.7 GB, which is too large to process. This may be reduced to a

more manageable size ($\sim$ 1.4 GB) by setting the pixel aggregation value to 16. If the spectral resolution is also reduced to 32 cm^{-1}, the total file size is further reduced to $\sim$710 MB.

2.3.1.4   Image formation parameters

The parameters discussed here represent the most important choices when it comes to maximising the spectrochemical contrast between fingerprint ridges and their background. At a minimum, most chemical/hyperspectral imaging software allows the user to form images based on (i) simple spectral intensity at a single frequency (wavelength), (ii) the integrated intensity (area) under a spectral peak, usually baseline corrected or (iii) ratios of intensities at two different frequencies. A monochrome or coloured image can be created based on these intensities, using either a brightness (black to white) or a false colour scale (e.g. blue, through green and yellow, to red). As with many samples, fingerprints on an ideal, featureless background can be imaged simply using method (i), or, with better results, (ii). For example, it is trivial to form an image of a latent fingerprint on glass or metal using the C-H stretching or bending peaks in the spectrum of the oily sebaceous material in a fingerprint. Method (ii) is usually superior because of the baseline correction involved and because it is less susceptible to noise, spikes and band overlap. Method (iii) is problematic in many cases because intensity ratios often take on extreme values at random pixels due to noise or baseline effects. These extremes cause a flattening of the contrast in the rest of the image.

However, there are many situations where the fingerprint background has infrared absorption peaks that are similar in frequency to those of the latent fingerprint, and overlap occurs. This spectral overlap can reduce or destroy image contrast, and so the methods listed above can struggle or fail. The overlap between the C=O stretching vibration in cyanoacrylate-fumed fingerprints and that in the intaglio printing on Australian polymer banknotes is an example of this.[75] In some cases, experimentation with baseline and / or integration bandwidth within method (ii) can yield satisfactory results, particularly where spectral overlap is not complete and the peak desired for imaging is sufficiently resolved as a shoulder, for example. However, the best results in this situation are obtained through the use of second and fourth order derivative spectra when forming the images.

A disadvantage of derivative spectra is that they are noisier than the original spectra. Taking odd-order (e.g. first or third) derivatives of a spectrum splits each absorbance peak into positive and negative components, with zero intensity at the original peak maximum. For this

reason, odd-order derivative spectra are usually not useful for imaging purposes, but even-order derivatives have some important advantages. One advantage of computing the second derivative of the spectra in a hyperspectral image is that overlapping peaks can be more easily resolved from each other, since they are much narrower than the original peaks. Indeed, this technique is often used in spectroscopy to find the true position of overlapping bands. Another advantage of second derivative spectra is that they are generally devoid of many of the baseline and offset artefacts that may afflict the original spectra. The result is that images based on second (or higher even-order) derivative spectra generally provide the best contrast possible between a fingerprint and its background.

The frequencies that yield the best images can be found easily by "playing" through the derivative spectrum and observing the images that are formed at each consecutive frequency. This can be done with images formed using single frequency spectral intensities (method (i) above), because method (ii) offers little advantage with the "baseline-corrected" second derivative spectra. Playing through all of the available frequencies is recommended as good fingerprint contrast can be achieved at unexpected frequencies, thanks to the resolution of small shoulder bands, etc, in the second derivative spectra. Since second derivative spectra have negative peaks where there were positive peaks in the original spectra, the images formed may be negatives, but can be "flipped" using image editing software or by negating the derivative spectra. Note that in certain cases (if the original spectra were collected with sufficient resolution), taking the second derivative of the second derivative spectrum (i.e. the fourth derivative) can resolve more peaks and provide better image contrast.

The abundance of information contained in hyperspectral images often lends itself to chemometric (multivariate statistical) analysis or interpretation. An example of this is the application of principal component (PC) imaging or hierarchical cluster analysis (HCA) (and other clustering techniques) to group pixels according to spectral similarity. For fingerprints, the obvious aim would be to group spectra into ridge and background classes (clusters) based on the comparison of entire spectra, rather than discrete frequencies or peaks. While we have attempted this type of analysis of hyperspectral fingerprint images with some success, in our experience there is generally no advantage to these techniques over the methods described above. To paraphrase this, we have found that if appropriate fingerprint contrast cannot be achieved using second derivative spectral imaging, then chemometric techniques will probably not yield a better result because the information required to differentiate the

fingerprint from its background probably does not exist. This is only an empirical observation, but it can be explained at least partly (in the case of cyanoacrylate-fumed prints) by (i) the fact that during fuming, a small amount of cyanoacrylate is deposited between ridges as well as on them, and (ii) the high variability of the fingerprint background, such that the background spectra cannot all be classified into one cluster.

2.3.2 Example of optimisation of parameters – FTIR chemical imaging of fingerprints on aluminium drink cans

The method optimisation procedure discussed in Section 2.3.1 above will be outlined here by way of an example. The same procedure can be applied to any new surface and reagent combination. The example used is that of cyanoacrylate-fumed fingerprints on aluminium drink cans.

Text and images printed on aluminium drink cans can make the imaging of fingerprints using conventional methods difficult, even after cyanoacrylate development and subsequent fluorescent staining. However, the high infrared reflectivity of metal surfaces means that it is very easy to rapidly obtain high signal-to-noise spectra of thin coatings on the metal.

Since the infrared imaging process involves placing the sample on a motorised microscope stage, it is important that the sample is flat and relatively smooth. For this reason, aluminium cans used in this study were 'flattened' by cutting the top and bottom off the can and cutting a vertical slit along the length of can (Figure 2.1).
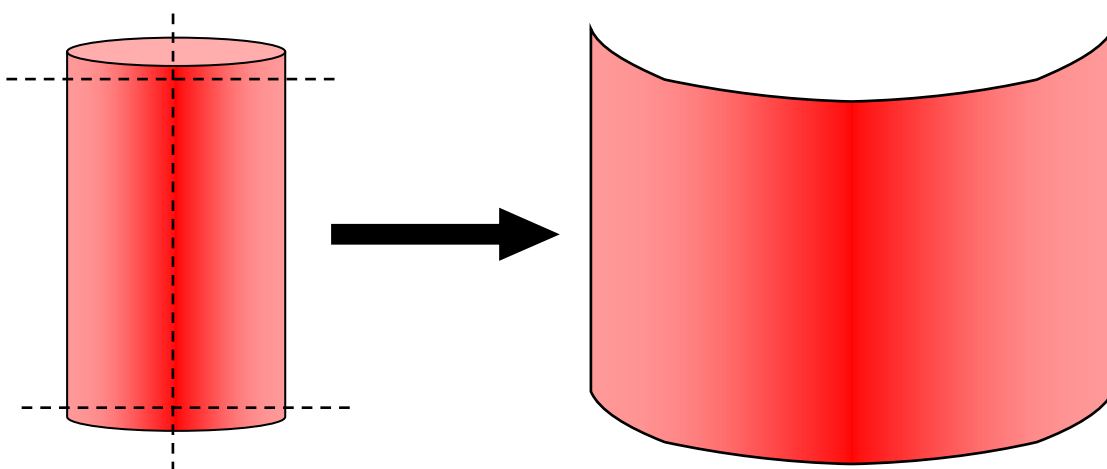
Figure 2.1: *Schematic showing how aluminium cans were prepared for FTIR chemical imaging.*

The can was then unrolled and held flat in a specially designed clamp. This clamp consisted of two sheets of Perspex hinged on one side and held flat against one another (with the aluminium can in-between) with the aid of fold back paperclips. The upper side of the clamp had a viewing hole through which the target fingerprint could be analysed, while a microscope slide was fixed to the underside of the clamp so that it could be mounted directly onto the motorised microscope stage (Figure 2.2). This clamp was also useful for flattening and holding polymer banknotes and document samples for imaging.
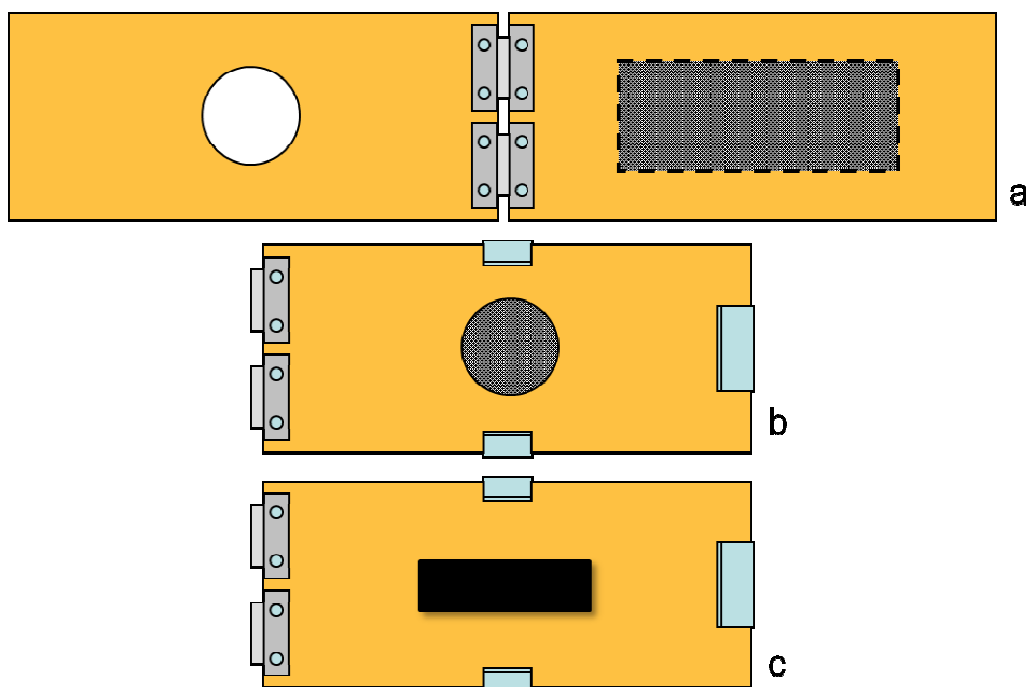
Figure 2.2: *Clamp for flattening and holding samples for subsequent FTIR chemical imaging: **(a)** opened position **(b)** top view showing sample viewing window **(c)** bottom view showing microscope slide used to attach clamp to motorised microscope stage.*

For the optimisation process an image size consisting of 16 tiles (2.8 × 2.8 mm) was selected as this allowed the imaging of a few ridges of the treated print while minimising the collection time and data file size.

The first step in the optimisation process was to find a suitable combination of spectral resolution and number of co-added scans which produced exploitable fingerprint images in the shortest timeframe. As mentioned above, a good starting point for a new reagent / surface combination is a resolution of 16 cm^{-1} and 64 co-added scans. Figure 2.3*a* shows an image of a small section of a cyanoacrylate-fumed fingerprint on an aluminium Coke can which was produced using these settings. It is clear that the second and third level

fingerprint ridge detail is of sufficient quality for subsequent comparison. Next the resolution was set to 32 cm^{-1} while the number of scans was maintained at 64 (see Figure 2.3*d*). Since the results with these settings were also satisfactory, further images were collected in which the number of scans was reduced (Figure 2.3*b, c, e* and *f*).
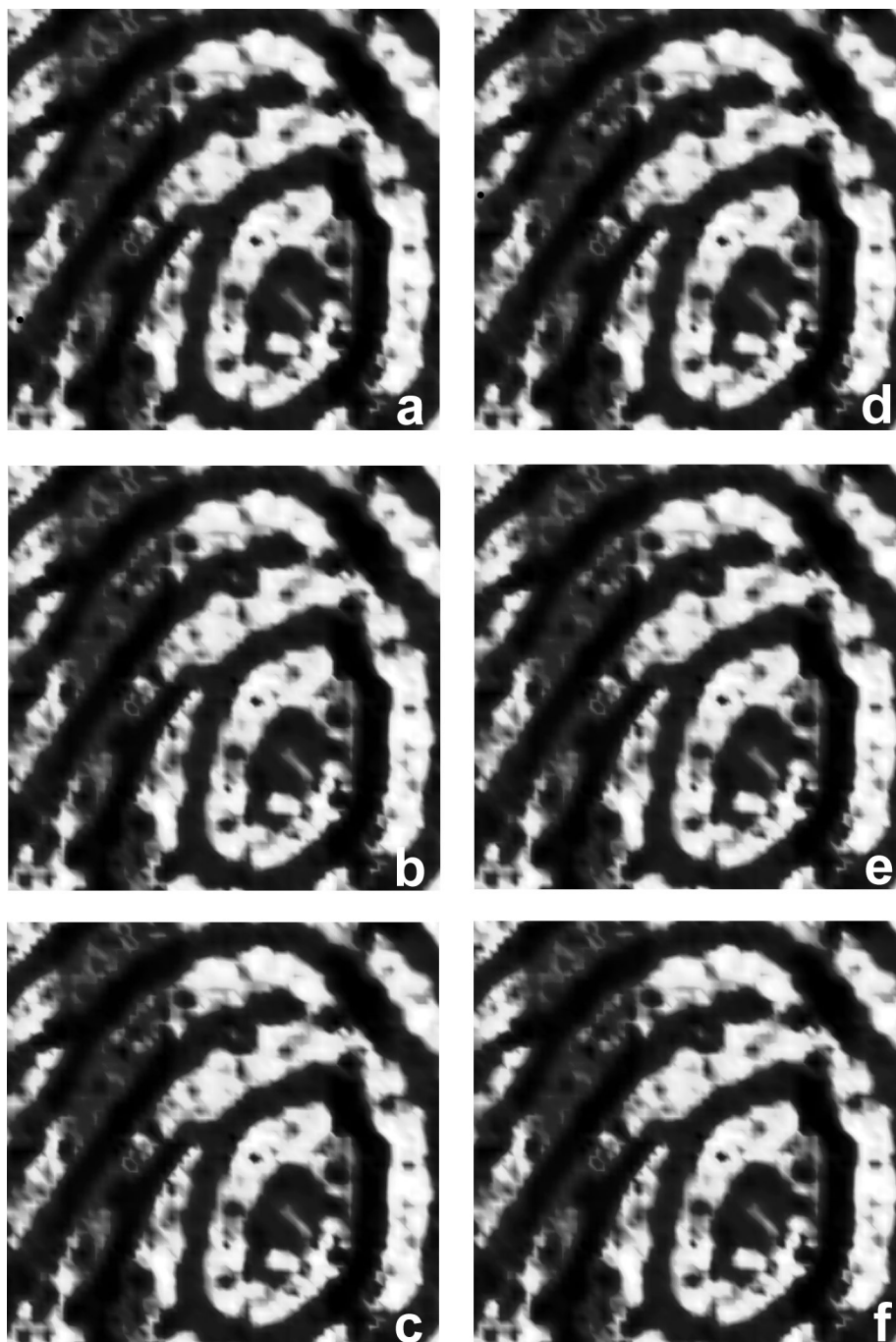
Figure 2.3: *FTIR chemical images of ethyl cyanoacrylate fumed fingerprint on aluminium drink can collected using various settings for spectral resolution and number of co-added scans: **(a)** Resolution 16 cm^{-1}, 64 co-added scans **(b)** Resolution 16 cm^{-1}, 16 co-added scans **(c)** Resolution 16 cm^{-1}, 4 co-added scans **(d)** Resolution 32 cm^{-1}, 64 co-added scans **(e)** Resolution 32 cm^{-1}, 16 co-added scans **(f)** Resolution 32 cm^{-1}, 4 co-added scans.*

The optimal settings were chosen based on the settings which produced an image of an exploitable fingerprint in the shortest timeframe (i.e. the lowest number of scans and the lowest resolution while maintaining ridge detail). From the images in Figure 2.3*a-f*, it is clear that the quality of fingerprint image produced is not diminished when the resolution and number of scans are reduced. For this reason, the settings which gave the shortest image collection time and smallest image file size (resolution $32cm^{-1}$, 4 co-added scans – Figure 2.3*f*) were selected for future infrared chemical imaging of cyanoacrylate fumed fingerprints on aluminium drink cans.

As discussed above, we have found that a pixel aggregation value of 16 (which gives a spatial resolution of about 44 μm) produces good quality fingerprint images. This is demonstrated by the quality of the images shown in Figure 2.3, which were all formed using a pixel aggregation of 16. Figure 2.4 shows a comparison of images formed using a pixel aggregation of 16 (∼ 44 μm pixel size – Figure 2.4*a*) and 64 (∼ 88 μm pixel size – Figure 2.4*b*). It is clear from these results that useful fingerprint detail is lost with a pixel size of 88 μm (or higher). For the imaging of entire fingerprints, a pixel size of less than 44 μm may result in files which are too large to process.
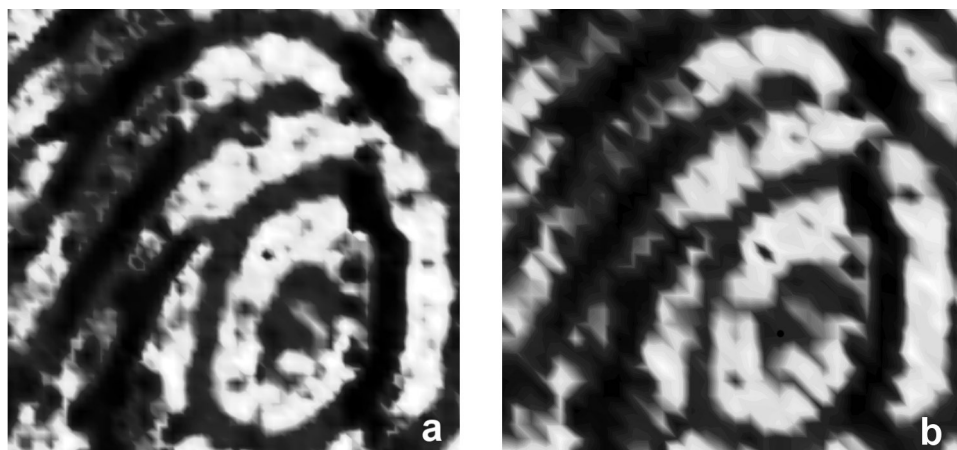
Figure 2.4:   *FTIR chemical images of ethyl cyanoacrylate fumed fingerprint on aluminium drink can collected using a pixel aggregation value of **(a)** 16 (pixel size ∼44 μm) and **(b)** 64 (pixel size ∼88 μm).*

The final stage in the optimisation process is to explore the possibility of narrowing the spectral range in order to reduce the total file size of fingerprint images. This step was performed in combination with the optimisation of image formation parameters. Initially the entire spectrum was collected during the optimisation of spectral resolution and number of co-added scans. Using this data, it became clear that the best contrast between the fumed

print and the background was achieved at certain frequencies in the region between 1750 – 1800 cm^{-1} (C=O stretching frequency). Certain frequencies below this region also produced images of the print but the region above 1900 cm^{-1} failed to produce images of any practical value. For this reason the spectral range was truncated between 1900 – 900 cm^{-1} for the imaging of further samples in order to minimise the overall file size of the image data. The best images were formed using a frequency slice within the region of 1750 – 1800 from the 2nd or 4th derivative data.

Table 2—5 shows a summary of the optimised method for the infrared chemical imaging of cyanoacrylate-fumed fingerprints on aluminium drink cans.

Parameter	Optimised settings
Spectral resolution	32 cm^{-1}
Number of co-added scans	4
Spectral range	1900 – 900 cm^{-1}
Pixel aggregation	16
Number of image tiles (image size)	1024 (2.24 × 2.24 cm)
Image formation parameters	Frequency slice within the range 1750 – 1800 cm^{-1} from the 2nd or 4th derivative data

Table 2—5: *Optimised settings for the infrared chemical imaging of cyanoacrylate-fumed fingerprints on aluminium drink cans*

2.3.3   FTIR chemical imaging of fingerprints on porous surfaces

The success of FTIR imaging of fingerprints on non-porous and semi-porous surfaces, such as glass, polymer banknotes and drink cans, led us to investigate the possibility of using this technique to image fingerprints on porous surfaces that had been developed using established reagents such as ninhydrin and DFO.

The problem usually encountered in reflectance infrared spectroscopy of paper-based surfaces is the high absorbance of cellulose components of the paper over much of the spectrum. Attempts to collect infrared reflectance spectra of inks (for example) on paper

backgrounds usually fail because the ink spectrum is swamped by the paper. Attenuated total reflectance (ATR) measurements are more successful in detecting some inks on paper,[113] but ATR imaging of an area as large as a fingerprint is not technically feasible at the time of writing. The question addressed in this work was whether the products formed by the reaction of fingerprint reagents and amino acids in fingerprints could be detected by ordinary reflectance infrared imaging on the following surfaces, some of which are less porous than ordinary paper: masking tape, thermal paper and white copier paper.

Unfortunately the answer to this question for all combinations of reagents and surfaces was in the negative. This is probably not surprising when the difficulty of paper backgrounds is considered along with the low concentrations of amino acids in fingerprints, which have been reported to be between 0.3 and 2.59 mg/L in sweat. This corresponds to an average amino acid content of 250 ng per print.[21] The amount (in molecular terms) of product formed in fingerprints developed using ninhydrin or DFO must be less than or equal to the original number of amino acid molecules, whereas cyanoacrylate development of fingerprints has the advantage of amplification; i.e. many cyanoacrylate monomer units are deposited for each initiating species present in a fingerprint. Therefore, any reagent that might be proposed for the development of fingerprints for subsequent infrared chemical imaging should either produce an amplification effect, or have an infrared absorbance that is strong and isolated enough (in the spectrum, relative to paper) for it to be detected at very low levels.

As mentioned in Section 1.2.4.3 above, Crane et al. have recently reported the FTIR chemical imaging of fingerprints on some porous surfaces including copier paper, cigarette butt paper, a U.S. dollar bill and a postcard.[115] Reasons why the results here differ from those obtained by Crane et al. have been discussed in Section 1.2.4.3 above.

2.3.4   Infrared chemical imaging of large sample areas

2.3.4.1   Untreated Fingerprints

We have previously published FTIR chemical images of untreated latent fingerprints on IR reflective slides.[75] These images were the results of preliminary findings and show only show a small section of the untreated fingerprint. An FTIR chemical image of an entire fingerprint is shown in Figure 2.5. This image was generated using the C-H stretching frequency at about 2921 cm^{-1}. The ability to generate FTIR chemical images of fingerprints using this region of

the spectrum is limited to backgrounds which do not absorb in this region. The imaging of untreated fingerprints via this technique is therefore most successful on surfaces such as metals and ceramics.
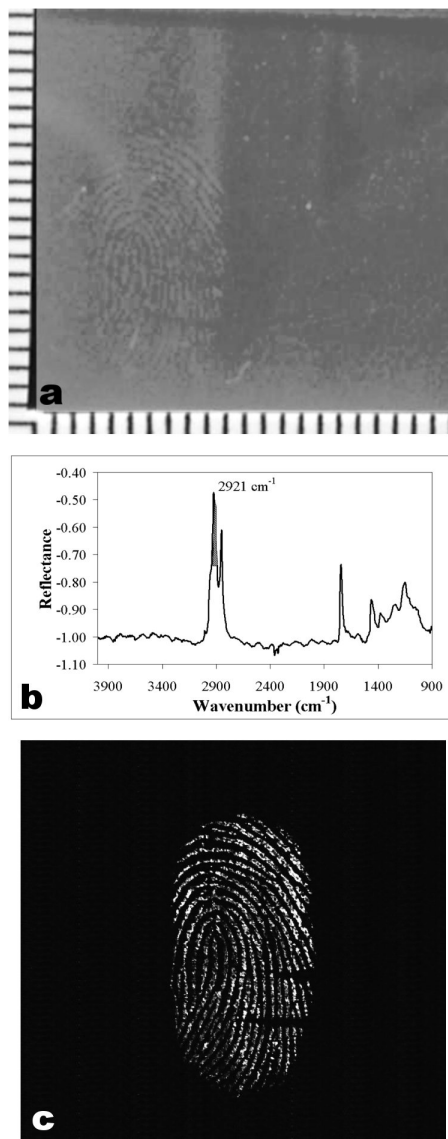
Figure 2.5: *Untreated fingerprint on infrared reflective slide: (a) White light photograph. (b) Infrared spectrum of fingerprint residue showing peak area selected to form the FTIR chemical image (c) Monochrome representation of FTIR chemical image.*

One area of interest is the detection of trace materials within untreated fingerprint deposits. For example, fingerprints contaminated with explosives have been analysed using a Raman spectrometer.[183] The feasibility of using FTIR chemical imaging for the determination of trace materials within untreated fingerprints has already been demonstrated.[114,115,186] Related research has shown that Raman spectroscopy may be used for the detection of drugs of abuse in latent fingerprints.[80,81] Although the technique was successful in obtaining spectral

identification of several drugs of abuse in fingerprints, the authors note that there were difficulties involved in visually locating these substances in the latent prints. This is a problem which may be overcome using chemical imaging techniques combined with spectral searching. Work conducted in our laboratory has shown that FTIR chemical imaging can be used to find and identify illicit substances present as contaminants in latent fingerprints. This work is not the focus of this thesis but results from this study (including the detection and identification of pharmaceuticals, drugs and explosives) will be published elsewhere.

2.3.4.2 *Cyanoacrylate fumed fingerprints on polymer banknotes*

By the end of 2004, twenty-two (22) countries from all major regions of the world were using polymer notes in their national currencies.[84] Our original work on the FTIR chemical imaging of fingerprints focused on Australian polymer banknotes because of the difficulties which had been encountered in visualising latent fingerprints on these notes using conventional methods. Since this initial work, we have been able to improve the image collection process so that larger fingerprint images can be obtained in a shorter period of time. This was achieved by reducing the spectral resolution from 16 cm^{-1} to 32 cm^{-1} and reducing the number of scans from 64 to 16. The images obtained with these settings (32 cm^{-1} resolution and 16 scans co-added) are comparable to those obtained using the previously published settings (16 cm^{-1} resolution and 64 scans co-added). Using the new settings, an image measuring 2.24 cm $\times$ 2.24 cm can be collected in just over four hours. This compares with an image collection time of about 18 hours using the previous un-optimised settings. The new image collection method is best demonstrated by the successful imaging of aged fingerprints. Figure 2.6 shows an image of a one month old fingerprint on an Australian $5 note which has been fumed with ethyl cyanoacrylate. The FTIR chemical image of this print (Figure 2.6*b*) has been formed using a frequency slice at 1735 cm^{-1} (C=O stretch) from the 4th derivative spectrum. The fingerprint ridge detail is exceptional for a 30 day-old print on such a difficult background.
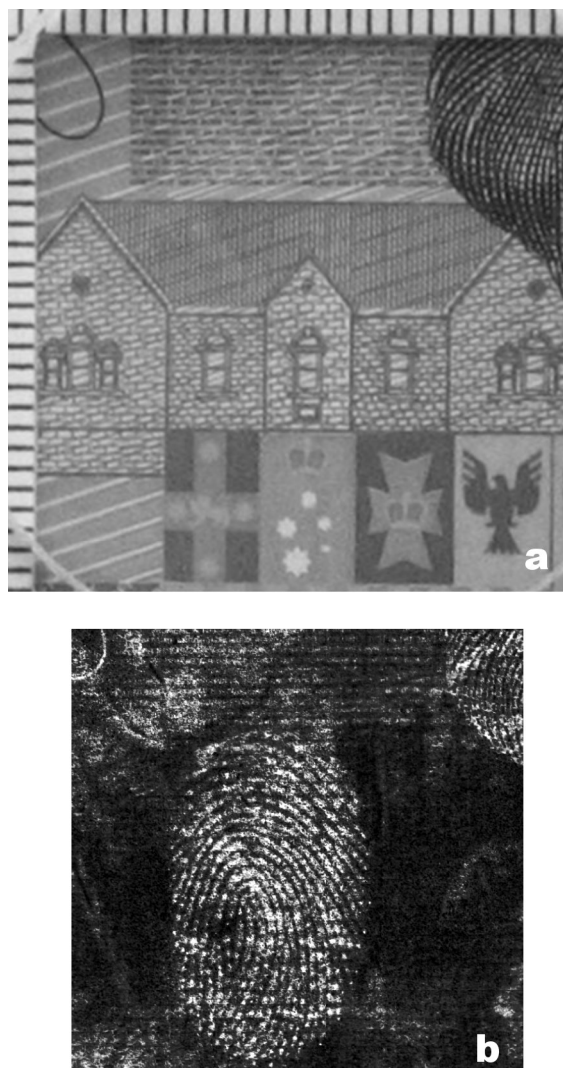
Figure 2.6:   *Ethyl cyanoacrylate fumed fingerprint on $5 note (aged one month prior to fuming):* ***(a)*** *White light photograph.* ***(b)*** *Monochrome representation of FTIR chemical image.*

2.3.4.3   *Cyanoacrylate fumed fingerprints on aluminium drink cans*

The procedure used for optimising the image collection method for cyanoacrylate fumed fingerprints on aluminium drink cans is discussed above. Figures 2.7 – 2.9 show a number of FTIR chemical images of cyanoacrylate fumed fingerprints on various aluminium cans collected using this optimised method. The most noteworthy results were on sections of the aluminium can where ridge detail was obscured by coloured patterns or text under white light. In these cases, FTIR chemical imaging was able to produce superior fingerprint images where the background pattern or text was completely eliminated and the ridge details of the fingerprint were pronounced. As can be seen in Figure 2.8*a* and Figure 2.9*a*, the

cyanoacrylate-fumed fingerprints were often difficult or impossible to image using traditional white light photography.
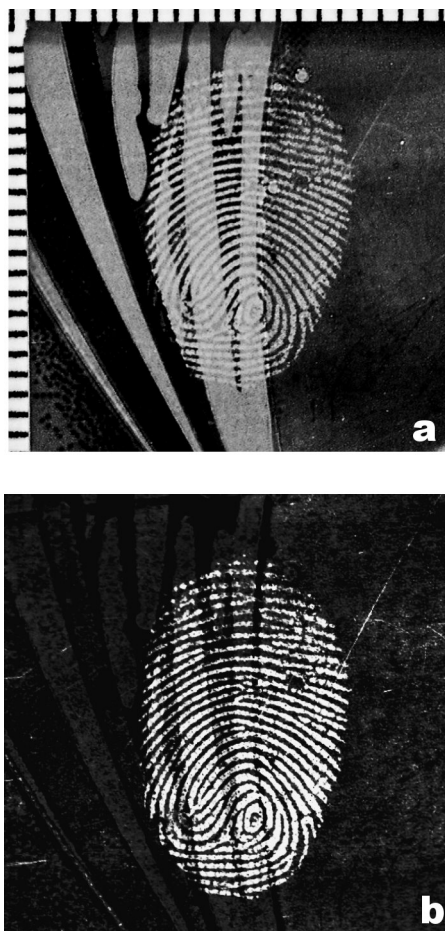
Figure 2.7: *Ethyl cyanoacrylate fumed fingerprint on Coke aluminium drink can. **(a)** White light photograph. **(b)** Monochrome representation of FTIR chemical image.*
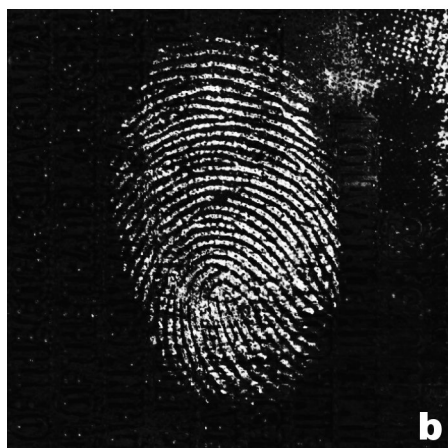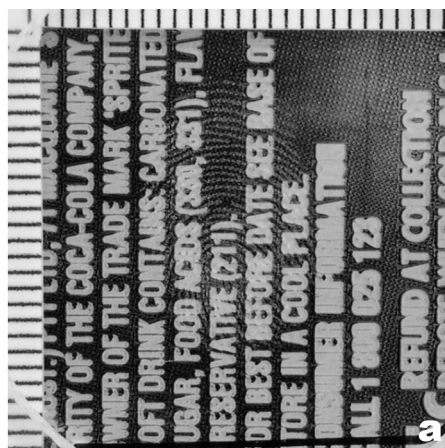
Figure 2.8: *Ethyl cyanoacrylate fumed fingerprint on Sprite aluminium drink can. **(a)** White light photograph. **(b)** Monochrome representation of FTIR chemical image.*
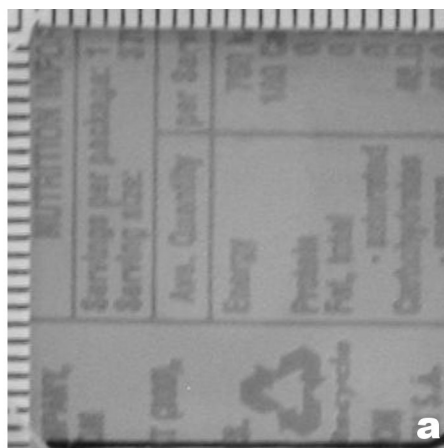
Figure 2.9:   *Ethyl cyanoacrylate fumed fingerprint on Lift aluminium drink can. **(a)** White light photograph. **(b)** Monochrome representation of FTIR chemical image.*

2.3.5   Practical considerations and limitations of the method

This research was carried out using a Digilab Stingray system equipped with a Lancer 64×64 FPA detector.   Although FTIR imaging instruments vary between manufacturers (e.g. Digilab/Varian vs Perkin-Elmer), the process of optimisation discussed has wide applicability. Provided "pixel aggregation" can be related to a pixel size (as we have done), and provided that the different sensitivity of different detectors is taken into account, the optimisation process is general to most instruments because spatial and spectral resolution are standard parameters.

As discussed in 1.2.4.3 above, attenuated total reflection (ATR) FTIR imaging has also been demonstrated for the imaging of fingerprints on lifting tapes (use to recover the print from curved surfaces).[119] The size of images obtained by the ATR-FTIR technique is limited by the dimensions of ATR crystal and the FPA detector, and the instrumental configuration and

optics. The largest image possible with this technique is currently approximately 4.7×6.3 mm^2.[119] This area represents only a few ridges of an entire fingerprint. ATR-FTIR chemical imaging does offer the potential for rapid image collection and improved signal-to-noise. It is envisaged that ATR-FTIR chemical imaging of larger areas (such as an entire fingerprint) may soon become a reality with advances in ATR crystals, instrumentation, optics and detectors. To date however, the imaging of entire fingerprints is only possible using a reflection / mosaicking technique such as that described in this thesis.

It is also envisaged that there will be marked improvements in other aspects of FTIR chemical imaging instruments. The next generation of FPA detectors, for example, should offer increased sensitivity and possibly (in combination with advances in optics and instrumentation) increased image sizes. These advances, together with advances in computer processing, will lead to faster image collection times and higher quality spectral data, which, in turn, will lead to higher quality infrared chemical images of fingerprints on a range of surfaces.

Chapter 3: Synthesis of novel cyanoacrylates

Chapter 3: Synthesis of novel cyanoacrylates

3.1 History of cyanoacrylate synthesis

In 1945, Long reported the synthesis of a novel compound, methyl 2-cyanoacrylate, but the monomer itself was not successfully isolated and the product was *"obtained in polymeric form as a hard glasslike solid"*.[198] This was perhaps an early insight into the inherent difficulties of synthesising these reactive compounds. It was not until 1949 that Ardis, working for the B.F. Goodrich Company, proposed the first successful method for obtaining monomeric alkyl-cyanoacrylates.[199,200] In that year, Ardis published two concurrent patents describing the synthesis of alkyl-cyanoacrylates. The first of these patents described the synthesis of monomeric 2-cyanoacrylates by reaction of alkyl cyanoacetate with an alkali metal alcoholate such as sodium ethoxide and then with chloromethyl acetate,[199] while the second describes the synthesis of alkyl-cyanoacrylates by reacting an alkyl cyanoacetate with formaldehyde in aqueous solution in the presence of a basic catalyst.[200] The principles involved in the latter method are still used today for the commercial synthesis of a wide range of cyanoacrylate monomers.

The most common method of cyanoacrylate synthesis involves the Knoevenagel condensation of alkyl cyanoacetates with formaldehyde in the presence of a base catalyst. This reaction should, in principle, yield the desired monomeric alkyl cyanoacrylate but the extreme reactivity of these monomers precludes direct synthesis via this method. The actual product formed is an oligomer of the desired cyanoacrylate, which necessitates the additional step of thermal depolymerisation to isolate the monomeric alkyl cyanoacrylate. This thermal depolymerisation step is usually performed in the presence of one or more polymerisation inhibitors to prevent the polymerisation of the distilling monomer. The initial alkyl cyanoacetate can be obtained by esterification of cyanoacetic acid and the corresponding alcohol. This method can be represented as a three-step process involving esterification, Knoevenagel condensation and thermal depolymerisation (Figure 3.1).
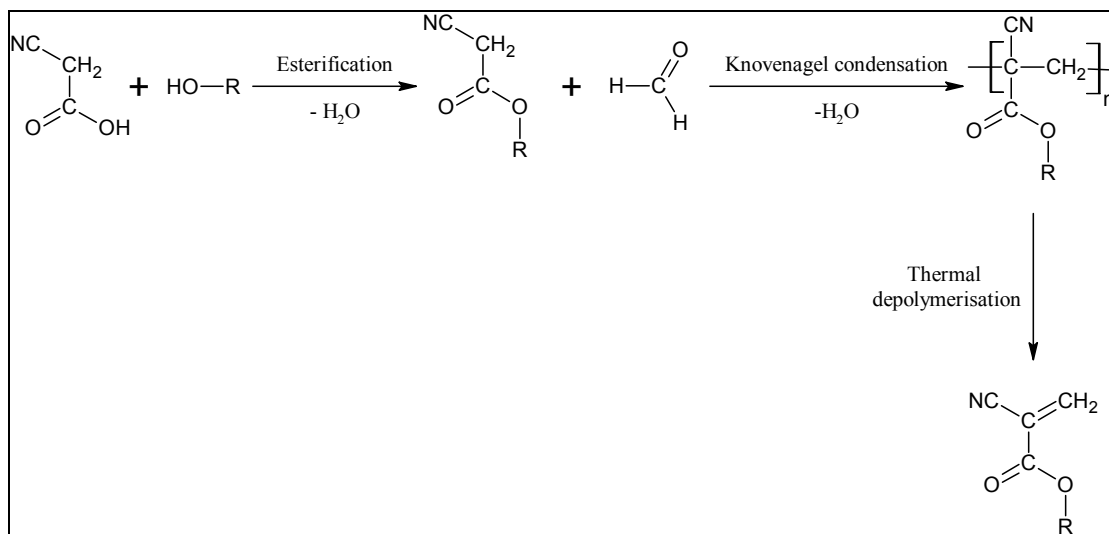
Figure 3.1:   *Most common route for cyanoacrylate synthesis.*

Although monomeric cyanoacrylates were first isolated in 1949, their potential as instant adhesives was not realised until the mid 1950s. The adhesive properties of these monomers was discovered accidentally by workers at the Eastman Kodak Company who fused together the prisms of an Abbe refractometer while measuring the refractive index of the highly purified ethyl-2-cyanoacrylate.[74]   These researchers then realised that alkyl cyanoacrylate esters could effectively perform as one-part liquid adhesives which would cure rapidly at room temperature without the need for an initiator or curing agent. This discovery was followed by several patents by Joyner, Coover, Jeremias, Hawkins, Dickey and Shearer that detailed improved methods of synthesis as well as compositions containing cyanoacrylate monomers for use as adhesives.[201-208]

The Eastman Kodak Company was also the first to market this new range of instant adhesives initially sold as *Eastman 910*®.[74,209]   This product, released in 1958, utilised the methyl cyanoacrylate ester but was mainly aimed at industrial applications due to expense. Although the cost was somewhat offset by the very small amounts required to form a good bond, the product remained largely a laboratory curiosity.[209]

The properties that make the alkyl cyanoacrylates unique and sets them apart from conventional adhesives are the ability to polymerise rapidly at room temperature without the addition of a catalyst and the ability to give a high bond strength between a wide variety of adherents. In the decades following their initial discovery, there were many improvements and modifications to the synthetic procedure originally proposed by Ardis. These

improvements and modifications were essential for the efficient manufacture of commercially viable cyanoacrylate monomers. There was an obvious demand for methods that produced higher yields, improved purity, greater stability and greater shelf life while being simple and reproducible.

To understand how and why improvements were made to the original method, it is important to understand the chemistry and reactivity of cyanoacrylate monomers. The exact mechanisms involved in the polymerisation of cyanoacrylates has been the subject of much debate and are the focus of another section (Section 4.1.1). It is agreed, however, that the polymerisation of cyanoacrylates can be initiated by a wide range of bases and that free radical polymerisation is also possible but is less common.[49,69-73] The extreme reactivity of cyanoacrylates is due to the stability of the propagating carbanion, which is due to the presence of two electron-withdrawing groups ($-C\equiv N$ and $-COOR$) (Figure 3.2).
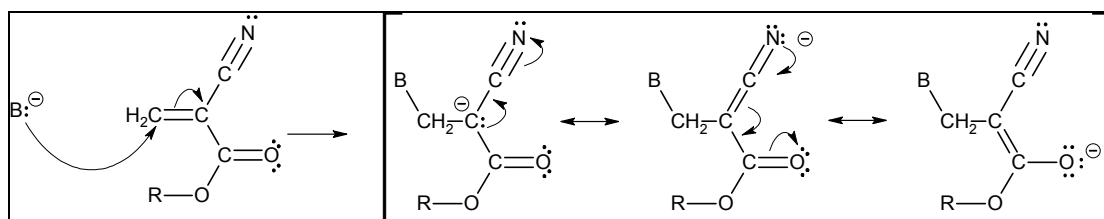
Figure 3.2: *Initiation of cyanoacrylate polymerisation – the resulting carbanion is resonance stabilised due to the presence of electron-withdrawing groups.*

The unique resonance caused by the nitrile and alkoxycarbonyl groups stabilises the anion which allows for the propagation to proceed to high molecular weight polymer[74] (Figure 3.3).
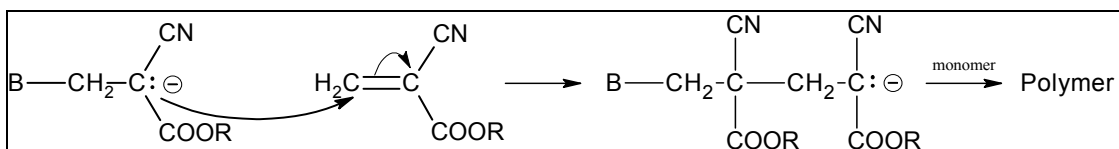
Figure 3.3: *Propagation of carbanion to form poly-cyanoacrylate.*

The first improvement to the cyanoacrylate synthesis procedure was proposed by Joyner in 1955 and involves the use of a non-aqueous organic solvent for the condensation reaction.[201] Using a non-aqueous organic solvent, the water formed during the reaction can be distilled off with the solvent, leaving a polymer with very low moisture content. The advantages of this technique are that the polymer depolymerises more readily and the monomeric product

is more stable. This is due to the fact that even a residual amount of water can initiate the polymerisation of monomeric cyanoacrylate, thus decreasing the yield.

Coover was the first to propose the addition of polymerisation inhibitors such as sulfur dioxide (SO_2) gas and hydroquinone to improve the stability and shelf life of the synthesised adhesive without impairing the speed or strength of the adhesive bond.[202] Jeremias proposed the use of a combination of SO_2, hydroquinone and phosphorus pentoxide (P_2O_5)[204] and these three polymerisation inhibitors remain the most common inhibitors used in cyanoacrylate manufacture. These inhibitors are not only used during the depolymerisation step in cyanoacrylate manufacture but are also present in trace amounts in the final adhesive composition. SO_2 and P_2O_5 are both acidic polymerisation inhibitors while hydroquinone (a free radical scavenger) prevents polymerisation via free radical initiation.

Other polymerisation inhibitors that have been suggested include nitric oxide,[199] phosphoric anhydride,[201,205] pyrogallol,[210-214] hydroquinone monomethyl ether,[207,215] acetic anhydride,[211] phosphoric acid,[211,216,217] 3-sulfolene,[218] polyphosphoric acid,[212-214,219,220] hydrochloric acid,[221] sulfur trioxide,[222] *p*-toluenesulfonic acid[69,223-225] and acetic acid.[223]

Other advances in the synthesis of cyanoacrylates include:

- using high-boiling, heat transfer medium (usually triesters of phosphoric acid) during depolymerisation[201,204,205]
- controlling the pH in the condensation step[204]
- controlling the cyanoacetate / formaldehyde ratio to obtain a more readily processed and depolymerised polymer intermediate[217,220]
- neutralising and removing the base catalyst prior to depolymerisation[220]
- processing the product in a dry environment to keep the water concentration below 200 ppm[219]

A number of other modifications / variations on the general procedure described above have been reported.[211,221,226] Alternative methods have also been described. In general these routes have been used to synthesise cyanoacrylates that are difficult or impossible to synthesise via the normal condensation-depolymerisation method. These include

fluorinated, higher alkyl and di-functional or bis-cyanoacrylates. The most notably alterative preparative methods include:

- the use of acid catalysts for the condensation reaction between alkyl cyanoacetates and formaldehyde[212-214,216]
- Diels-Alder protection and de-protection[227-237]
- esterification of 2-cyanoacryloyl chloride and an alcohol or diol (for bis cyanoacrylates)[238]
- direct transesterification of methyl cyanoacrylate with a diol to form the corresponding bis-cyanoacrylate[239]
- condensation of either methyl or ethyl cyanoacetate with paraformaldehyde followed by transesterification of the intermediate oligomer with a higher alkyl alcohol and subsequent thermal depolymerisation[240]
- oxidation of a phenylselenide precursor[241,242]
- condensation of diethyl dicyanoglutarate (from the waste residue of large scale cyanoacrylate synthesis) with paraformaldehyde and subsequent depolymerisation[243,244]

3.2 Cyanoacrylate monomers

In both industrial and consumer applications, there are millions of end users of cyanoacrylate monomers. Although their use is generally in drop-by-drop quantities, their versatility and the large number of users means that annual cyanoacrylate production is in multi-ton quantities.[209] It follows that there exists a large commercial interest in these compounds. This is also reflected in the relatively large number of patents that have been issued over the past 50 years.

The first cyanoacrylate instant adhesive, Eastman 910®, which utilised methyl cyanoacrylate, was marketed in 1958.[245] Since then, a large range of cyanoacrylate adhesives has been marketed but the most widely-used cyanoacrylate monomer is the ethyl ester (see Figure 3.4).
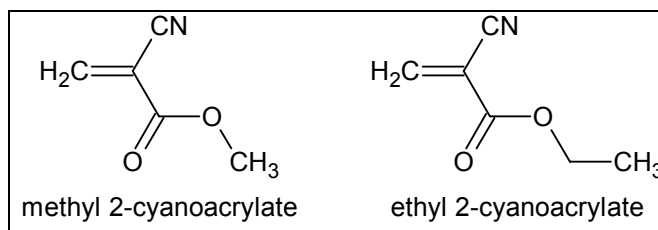
Figure 3.4: *Structures of methyl and ethyl 2-cyanoacrylate.*

Alkyl 2-cyanoacrylate adhesives have found unique application for the instantaneous bonding of a wide variety of materials such as metals, alloys, plastics, rubbers and ceramics.[74,209,245-248] They are widely used in the automotive and appliance industry, the electronics industry and as consumer adhesives useful for arts, crafts, and home repairs. A typical commercially available cyanoacrylate adhesive comprises 80 – 95% cyanoacrylate ester, 5 – 15% thickener, and 0.5 – 2% inhibitor. Cyanoacrylates are applied as liquids and cure within seconds to minutes at room temperature by reacting in the presence of moisture or weakly alkaline materials, forming inert, hard, polymeric solids.
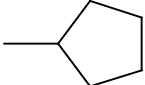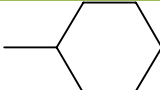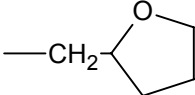
Cyanoacrylates also have important medical applications including the treatment of intracerebral aneurysms, as an alternative to the surgical clipping approach, fixing the cranial bone flap after craniotomy, closing skin wounds, and performing suture-less cardiac techniques.[249-253]   The pharmaceutical industry has recently investigated the use of cyanoacrylates as colloidal drug carriers of antibiotics, hormones and cytostatics and as biodegradable insulin nanocapsules.[254-256]
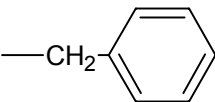
In addition to methyl and ethyl cyanoacrylate, several other esters have been reported and find uses as adhesives in their own right and / or as components in adhesive preparations consisting mainly of the methyl or ethyl esters. Some provide improvements on the common esters for specific applications such as improved heat resistance,[246,257-259], impact resistance,[260] toughness[261] and stability and biocompatibility.[210,249,250,252,262,263]   Table 3—1 provides a summary of the various cyanoacrylate monomers that have been reported and their respective boiling points.
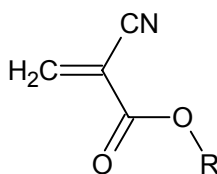
Monomer	R	Boiling point °C (mmHg)Ref
NORMAL		
methyl	——CH$_3$	55 (4)[210] 58-60 (1.0)[216] 48-49 (2.5-2.7)[209]
ethyl	——CH$_2$CH$_3$	60 (3)[210] 60-62 (1.0)[216] 54-56 (2.6-3.0)[209]
propyl	——CH$_2$CH$_2$CH$_3$	80 (6)[210] 60-62 (1.0)[216]
butyl	——CH$_2$CH$_2$CH$_2$CH$_3$	68 (1.8)[210] 68-72 (0.8)[216] 83-84 (3.0)[209] 92-94 (8.5-9.2)[209]
pentyl	——CH$_2$CH$_2$CH$_2$CH$_2$CH$_3$	80-84 (0.9)[216] 113 (5.4)[210]
hexyl	——CH$_2$CH$_2$CH$_2$CH$_2$CH$_2$CH$_3$	90 (1.6)[210] 108-110 (1.2)[216]
heptyl	——CH$_2$CH$_2$CH$_2$CH$_2$CH$_2$CH$_2$CH$_3$	125 (1.2)[210] 108-110 (1.0)[216]
octyl	——CH$_2$CH$_2$CH$_2$CH$_2$CH$_2$CH$_2$CH$_2$CH$_3$	118-120 (1.5)[216] 117 (1.8)[210] 105-106 (0.6-0.7)[214]
BRANCHED		
iso-propyl	——CH(CH$_3$)CH$_3$	59-62 (1.2)[216] 53-56 (2.0-2.5)[209]
iso-butyl	——CH$_2$CH(CH$_3$)CH$_3$	72-75 (1.4)[216] 71-73 (1.9-2.2)[209] 76-81 (3.2-4.0)[209]
sec-butyl	——CH(CH$_2$CH$_3$)CH$_3$	89-90 (4.0)[216] 64-66 (1)[209]
iso-pentyl	——CH$_2$CH$_2$CH(CH$_3$)CH$_3$	82-84 (1.4)[216]
neo-pentyl	——CH$_2$C(CH$_3$)(CH$_3$)CH$_3$	45-49 (0.1-0.3)[209] Solid at RT M.P. 36-39 °C

2,2-dimethyl butyl	$-CH_2\overset{\overset{\displaystyle CH_3}{|}}{\underset{\underset{\displaystyle CH_3}{|}}{C}}-CH_2CH_3$	85-87 (2.9)[209]
2-octyl	$-CH_2\overset{}{\underset{\underset{\displaystyle CH_3}{|}}{CH}}-CH_2CH_2CH_2CH_3$	94-96 (0.3)[216] 110-111 (2.8)[209]
2-ethyl hexyl	$-CH_2\overset{}{\underset{\underset{\displaystyle H_2C-CH_3}{|}}{CH}}-CH_2CH_2CH_2CH_3$	92-94 (0.3)[216] 121-125 (4)[209]
CYCLO		
cyclopentyl		72-74 (0.5)[216]
cyclohexyl		90-93 (1.0)[216] 111-112 (3.4-3.7)[209]
ALKENYL / ALKYNYL		
allyl	$-CH_2CH=CH_2$	78 (6)[264] 74 (4.2)[210] 62-63 (1.5)[216] 78-82 (6)[209]
crotyl	$-CH_2CH=CH-CH_3$	64-66 (1.4) [216]
propargyl	$-CH_2C\equiv CH$	68 (2)[264] 62-63 (1.4)[216]
1-methyl-2-propinyl	$-\overset{}{\underset{\underset{\displaystyle CH_3}{|}}{CH}}-C\equiv CH$	72 (2)[264]
1-propyl-2-propinyl	$-\overset{}{\underset{\underset{\displaystyle CH_2CH_2CH_3}{|}}{CH}}-C\equiv CH$	80 (2)[264]
ALKOXY		
2-methoxy ethyl	$-CH_2CH_2O-CH_3$	88-92 (1.0)[216]
2-ethoxy ethyl	$-CH_2CH_2O-CH_2CH_3$	92-96 (1.1)[216] 100-102 (3)[224]
2-butoxy ethyl	$-CH_2CH_2O-CH_2CH_2CH_2CH_3$	124-128 (1.0)[216]
1-methoxy propyl	$-\overset{}{\underset{\underset{\displaystyle O-CH_3}{|}}{CH}}-CH_2CH_3$	84-86 (0.9)[216]
tetrahydrofufuryl		108-111 (1.5)[224]
allyloxyethyl	$-CH_2CH_2O-CH_2CH=CH_2$	93 (3)[246]
HALO		
2-chloroethyl	$-CH_2CH_2Cl$	96-98 (0.3)[216]
3-chloroethyl	$-CH_2CH_2CH_2Cl$	100-104 (0.3)[216]
2,2,2,-trifluoroethyl	$-CH_2CF_3$	83-84 (13)[212,214] 73 (2)[236]

2-(1,1,1-trifluoro)propyl	—CH–CF_3
	    |
	    CH_3
		83-85 (17)[212]

1-(2,2,3,3-tetrafluoro)propyl	—$CH_2CF_2 \cdot CF_2 \cdot H$	89-90 (0.3)[212]
1-(2,2,3,3,3-pentafluoro)propyl	—$CH_2CF_2 \cdot CF_3$	98-100 (15)[212] 60 (1)[236]

2-trifluoromethyl-2-propyl	CH_3
	    |
	—C—CF_3
	    |
	    CH_3
		B.P. not reported[214]

2-(2,2,2-trifluoroethoxy)ethyl	—CH_2CH_2O—CH_2CF_3	98-100 (0.2)[214]
1-(2,2,3,3,4,4,5,5-octafluoro)pentyl	—$CH_2CF_2 \cdot CF_2 \cdot CF_2 \cdot CF_2 \cdot H$	91-95 (0.2-0.4)[212]
2,2,3,3,4,4,5,5,6,6,7,7-Dodecafluoroheptyl	—$CH_2CF_2 \cdot CF_2 \cdot CF_2 \cdot CF_2 \cdot CF_2 \cdot CF_2 \cdot H$	B.P. not reported[214]
2-(1,1-dihydroperfluorobutoxy)ethyl	—CH_2CH_2O—$CH_2CF_2 \cdot CF_2 \cdot CF_3$	100-103 (0.8)[213]
ARYL		
benzyl	—CH_2-⟨benzene ring⟩	118-120 (0.6)[216]
SILYL		

trimethylsilyl methyl	CH_3
	    |
	—$CH_2 Si$—CH_3
	    |
	    CH_3
		67 (2)[260]

trimethylsilyl ethyl	CH_3
	    |
	—$CH_2 CH_2 Si$—CH_3
	    |
	    CH_3
		B.P. not reported[260]

trimethylsilyl *n*-propyl	CH_3
	    |
	—$CH_2 CH_2 CH_2 Si$—CH_3
	    |
	    CH_3
		B.P. not reported[260]

Table 3—1: *List of cyanoacrylate monomers and their boiling point.*

Details regarding specific cyanoacrylate analogues, including their synthesis and use, may be found in the corresponding reference(s). In addition, a number of reviews have been published regarding the synthesis of cyanoacrylates and their application[70,74,209,245,247-249,265-267] and the reader is referred to these references (and others contained throughout this thesis) for further details. As a general guide, the properties of polymerised cyanoacrylate monomers may be summarised as follows:

- *Hardness* generally decreases with an increase in size of the ester group.

- *Tensile break* (the forces required to break the material) decreases with increasing size of the ester group.

- *Elongation* shows little change with ester group size until reaching C-5 and C8 esters.

- *Stiffness* (as measured by flexural modulus) decreases with increased size of the ester group. Chain branching increases this value above that of the corresponding *n*-alkyl homologue.

- *Brittleness:* all the polymers are brittle. Brittleness decreases with increasing size of the ester group.[209]

3.3   Difficulties involved in cyanoacrylate synthesis

As mentioned previously, cyanoacrylate monomers are among the most reactive monomers known. It follows that the synthesis of these reactive monomers is fraught with difficulties. In addition to this, the commercial nature of cyanoacrylate monomers means that potential manufacturers must pass a number of legal hurdles before beginning production. In his review of acrylic adhesives, Lees says: *"Production is fraught with hazards. The many difficulties faced have probably done more to curb the number of would-be manufacturers than the ever present threat of litigation. In the period of 20 years* [up to 1979] *only a handful of companies have ever succeeded in negotiating their way through the net of restrictive patents and at the same time establish a technical position which would allow them to cope with the intractable nature of the unstabilised cyanoacrylate monomer"*.[265] Although mass production is not part of the aims of this project, the difficulties encountered are the same. In fact, the difficulties are further complicated by attempting to synthesise small quantities of monomer rather than the vast amounts that are typically reported in the patent literature. Below is a discussion on some of the difficulties involved in cyanoacrylate synthesis.

3.3.1   Patents vs journal articles

As mentioned in Section 3.2, the literature on cyanoacrylate synthesis is dominated by patents rather than academic literature such as journal articles. Of the literature reviewed for the purposes of this project, there are 27 references to the synthesis of cyanoacrylates via the Knoevenagel condensation method (see Table 3—2 for references). Of these, 20 (74%) are patents compared to only 7 (26%) journal articles. The patent literature poses some

problems for the development of a synthetic procedure for a novel cyanoacrylate. Due to the commercial nature of patents, the synthetic procedures tend to be less detailed than those found in peer-reviewed journal articles. Furthermore, since patents are generally aimed at improved methods for the large scale production of cyanoacrylate adhesives, the quantities and equipment used often prohibit adaptation to the much smaller scale production of a novel monomer. In fact, most journal articles also describe the synthesis of cyanoacrylate monomers on large / industrial scales. Below is a table summarising the scale of reaction employed by the same 27 references.

Scale (moles cyanoacetate)	Grams equivalent (ethyl cyanoacetate)	Frequency
0.05	5.66 g	1[260]
0.16	18.1 g	2[215,225]
0.33	37.3 g	1[268]
0.50	56.6 g	1[200]
1.00	113 g	5[212,214,218,221,226]
1.05	119 g	1[223]
1.25	141 g	1[204]
1.75	198 g	1[219]
2.00	226 g	2[213,224]
2.65	300 g	1[217]
3.00	339 g	1[69]
4.00	452 g	3[207,220,269]
5.00	566 g	1[210]
7.50	848 g	1[201]
12.5	1414 g	1[211]
Not quoted	Not quoted	4[216,246,264]
	TOTAL	**27**

Table 3—2: *Scale of reaction used from various references*

Table 3—2 shows that it is rare to find a published method for the synthesis of small quantities of cyanoacrylate monomers.

3.3.2 Thermal degradation of cyanoacrylates

In order to understand the problems associated with the obtaining monomeric cyanoacrylate via this method, it is useful to investigate the thermal behaviour of the polymers (or oligomers) of cyanoacrylates (note that for the purposes of this discussion the term polymer (or poly-) refers also to low molecular weight polymers or oligomers (oligo-)). The thermal degradation of poly-cyanoacrylates has been the subject of much research.[49,210,223,270-280] While many researchers have been more concerned with the thermal stability of poly-cyanoacrylate from a materials and adhesion perspective, it is also of relevance for the isolation of cyanoacrylate monomers from the intermediate polymer.

Rooney originally described the thermal degradation of lower alkyl cyanoacrylate oligomers as *"a chemically simple process involving end-group initiation and depropagation to a residue which can be distilled from the system"*.[270] The experimental results of this research, however, suggest that the overall rate of thermal degradation is somewhat more complex, involving factors such as the rate of diffusion (or mass transfer) of the distilling monomer through the layer of decomposed polymer.[270]

Birkinshaw and Pepper confirmed the end-initiated unzipping reaction and identified that the nature of the end group (initiating species from the preceding stage of anionic polymerisation) and the molecular weight also influence the rate of thermal degradation.[272] In a more recent study, Hickey et al. found that the degradation can indeed be initiated at the chain-end containing the polymerisation initiator residue, as previously reported, but this is not always the case.[280] When triphenylphosphane (TPP) was used as the initiating species, there was evidence to suggest that the chain end containing the TPP residue was not the initiation site for the degradation. Furthermore, conducting the degradation in a vacuum oven led to a greater mass loss (i.e. more complete degradation) while the presence of excess initiator was found to significantly reduce the thermal degradation of the polymer.[280] These observations may be explained in terms of the same mass transfer factors that earlier research had identified[270] but Hickey et al. provide an alternative possibility. It is possible that the excess initiator species (or the released terminal groups) are involved in a depolymerisation / repolymerisation reaction such as that proposed by Ryan and McCann[277] and Robello et al.[279] for solution degradation. In fact these groups go on to describe poly-cyanoacrylates that have been base-initiated as *"inherently unstable"* and as being present in

a dynamic equilibrium with their monomer, causing severe degradation of the molecular weight of the polymer by an order of magnitude or more.[279] It should be noted that the majority of work conducted by Ryan and McCann and Robello et al. was in solution but there was also evidence to suggest that the degradation in molecular weight even occurred slowly in the solid state[279] and can indeed occur while the polymer is in a melt phase during thermal treatment.

Negulescu et al. investigated the thermal behaviour of a series of poly-cyanoacrylates and found that the temperature at which degradation is initially observed increases slightly as the alkyl group size increases.[274] This slight increase in apparent thermal stability for higher homologues is probably the result of a decrease in volatility of the distilling monomer. In other words, a higher onset temperature is observed simply because the less volatile monomers take longer to diffuse through the degrading polymer. This point has been noted previously[270] but it is further supported by this group, who showed that there was little difference in the temperature at which the degradation rate is at a maximum for the methyl, ethyl and propyl cyanoacrylates.[274] In experiments where the diffusion of the monomer can be ignored (achieved by analysing thin polymer film samples) the type of poly-cyanoacrylate has been found to be a contributing factor to thermal stability, with lower alkyl esters being less thermally stable.[275]

Bulk polymer samples of the lower alkyl cyanoacrylates show little difference in their thermal behaviour. However, as the size of the alkyl group increases, the decreased volatility of the higher alkyl monomers becomes a significant factor. The synthesis of these higher alkyl cyanoacrylates via the Knoevenagel condensation / depolymerisation route has proved difficult or impossible.[241,242] If the monomers are obtained via this method, the yields are generally very poor. This can be explained, at least partially, by their low volatility, which means that the liberated reactive monomer is more likely to re-polymerise. There is also some evidence that there is an increase in volatile side products during the depolymerisation of polymers with larger ester alkyl groups.[275] Once again their low volatility means the liberated monomer would remain trapped in the viscous polymeric melt where it is likely to decompose further before it can be distilled and isolated.

Functionalised cyanoacrylate monomers, such as allyl 2-cyanoacrylate, which contain an additional unsaturated group on the ester chain, also give poor yields when synthesised from

their intermediate polymer. This is due to the fact that the additional allylic group is capable of forming cross-links between polymeric chains after the initial polymerisation has taken place or during thermal treatment.[274,278] The polymers are therefore more thermally stable.[278] The monomer is much harder to distil from the crosslink polymer and further decomposition can occur,[278] again leading to poor yields.

As mentioned above, residual (or liberated) base can inhibit the thermal degradation of poly-cyanoacrylates. This was noticed by early researchers looking at improving the large scale manufacture of cyanoacrylate monomers. As mentioned in Section 3.1 above, this led to improvements such as controlling the pH in the condensation step[204] and neutralising and removing the base catalyst prior to depolymerisation.[220] Stein showed how these steps can help, by investigating the influence of pH during polymerisation on the thermal behaviour of poly-cyanoacrylates.[276] The pH did not seem to affect the onset temperature of the degradation but the softening temperature increased with ascending pH during polymerisation. Chorbadjiev and Novakov showed that the activation energy was not influenced by the presence of acid and radical inhibitors, but that these substances accelerate the thermal degradation by stabilising the liberated monomer.[275] Basic compounds caused both an increase in activation energy and an inhibition of the thermal degradation.[275]

The study conducted by Chorbadjiev and Novakov in 1991 is perhaps the most comprehensive and systematic analysis of the thermal degradation of cyanoacrylate polymers (and oligomers).[275] By performing Thermogravimetric Analysis (TGA) on a series of poly-cyanoacrylates, this study was able to confirm and draw together a number of the previously published views on the factors that influence decomposition temperatures and monomeric product yields. The summary below and the corresponding figures outline the major factors influencing the thermal degradation of poly-cyanoacrylates:

- Diffusion through the polymer film is the kinetically limiting stage of thermal degradation. When the degradation is carried out in thin layers, the diffusion can be ignored. As the thickness of the layers increases, the temperature range, the activation energy and the probability of side reaction also increase (see Figure 3.5)

- There is an optimal molecular weight for each type of poly(alkyl α-cyanoacrylate) at which the rate of thermal degradation is highest and the probability of side reaction is least (see Figure 3.6).

- The activation energy of degradation (independent of the diffusional process) is affected primarily by the type of poly(alkyl α-cyanoacrylate) with lower alkyl esters having a lower activation energy and therefore lower thermal stability (see Figure 3.6).

- The inhibitors of anionic and radical polymerisation accelerate the thermal degradation by blocking the polymerisation of the liberated monomer. They do not influence the diffusional-independent degradation process (see Figure 3.7 and Figure 3.8).

- Basic substances inhibit the degradation. They affect primarily the first stages of the process (the liberation of monomer) and probably increase the extent of the accompanying side reactions (crosslinking, cyclisation involving the CN groups).[275]
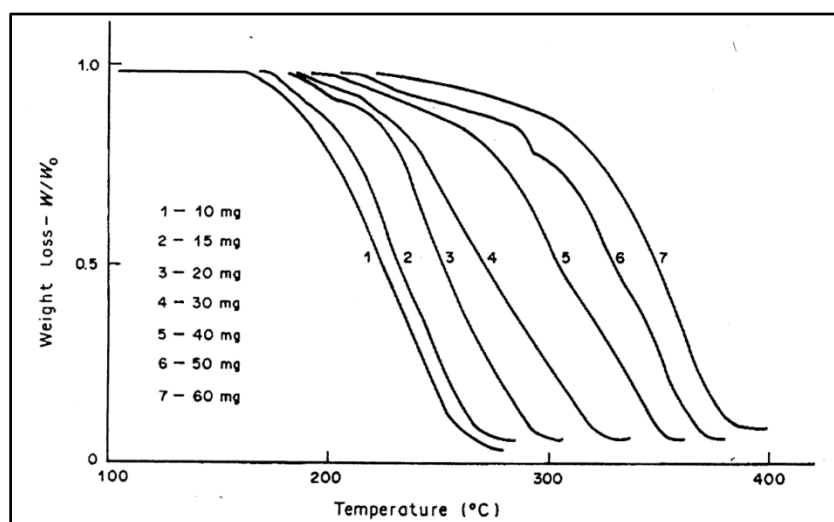
Figure 3.5: *Thermogravimetric curves of poly(ethyl α-cyanoacrylate) with various initial sample weights (W_0). Heating rate, 5 °C/min; W, transient sample weight.*[275]
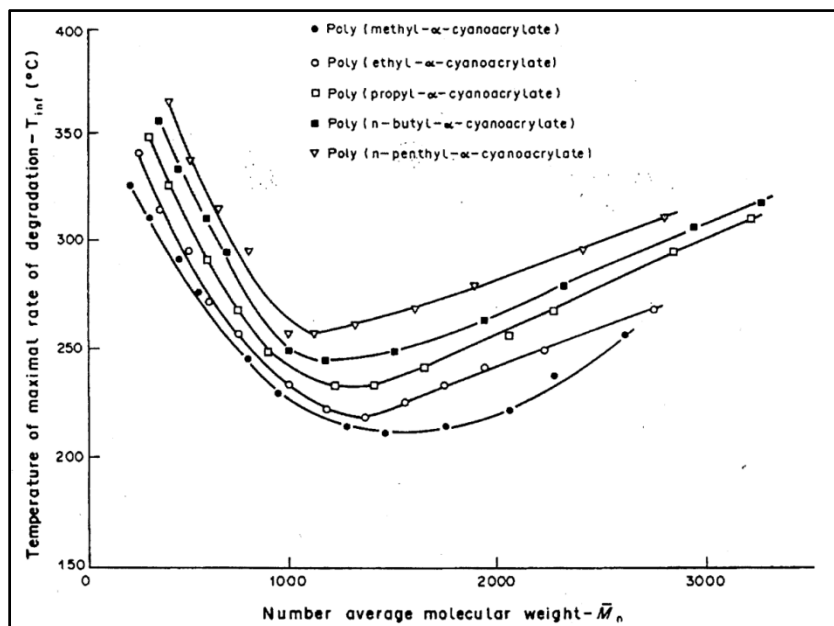
Figure 3.6:   *Temperature of maximal rate of degradation for poly(alkyl α-cyanoacrylates) with different molecular weights ($\overline{M}_n$). Conditions: heating rate = 5 ℃/min, initial sample weight (W$_0$) = 10 – 15 mg, area of polymer sample = 2 cm^2.*[275]
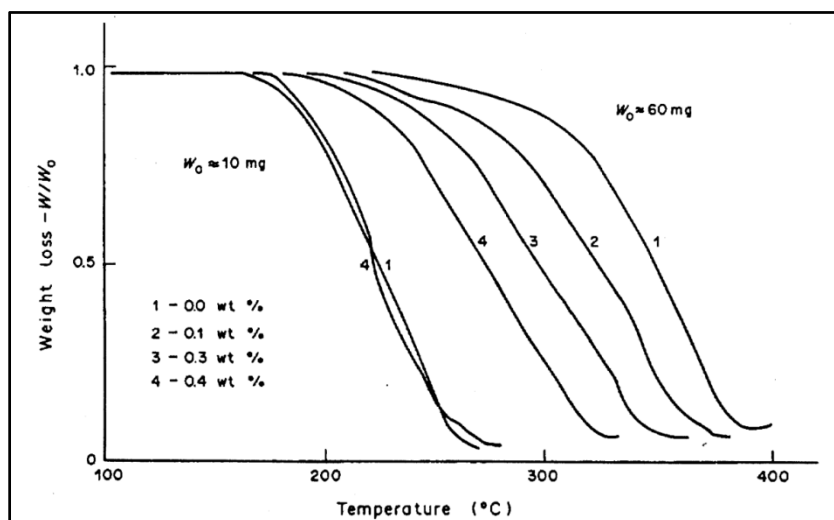
Figure 3.7:   *Thermogravimetric curves of poly(ethyl α-cyanoacrylate) for various quantities of H$_2$SO$_4$ (acid) in the polymer sample. Conditions: heating rate = 5 ℃/min, initial sample weight (W$_0$) = 10 mg or 60 mg, area of polymer sample = 2 cm^2.*[275]
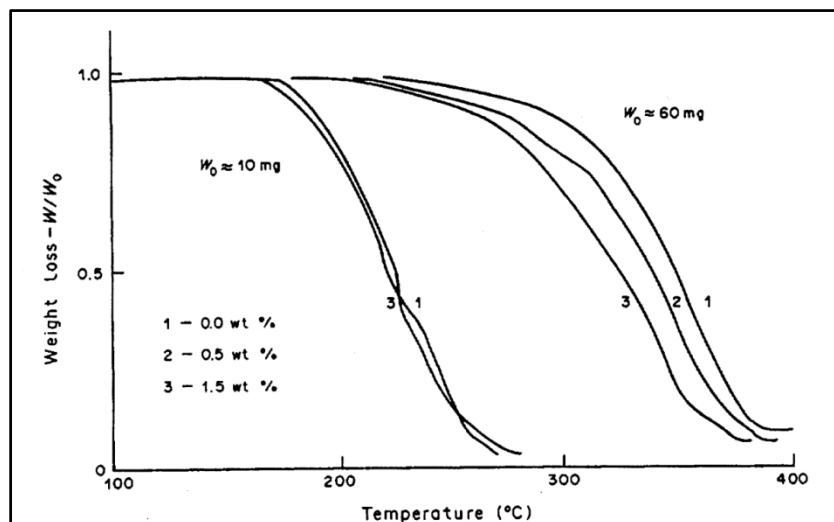
Figure 3.8: *Thermogravimetric curves of poly(ethyl α-cyanoacrylate) for various quantities of hydroquinone (radical polymerisation inhibitor) in the polymer sample. Conditions: heating rate = 5 °C/min, initial sample weight (W_0) = 10 mg or 60 mg, area of polymer sample = 2 cm^2.[275]*
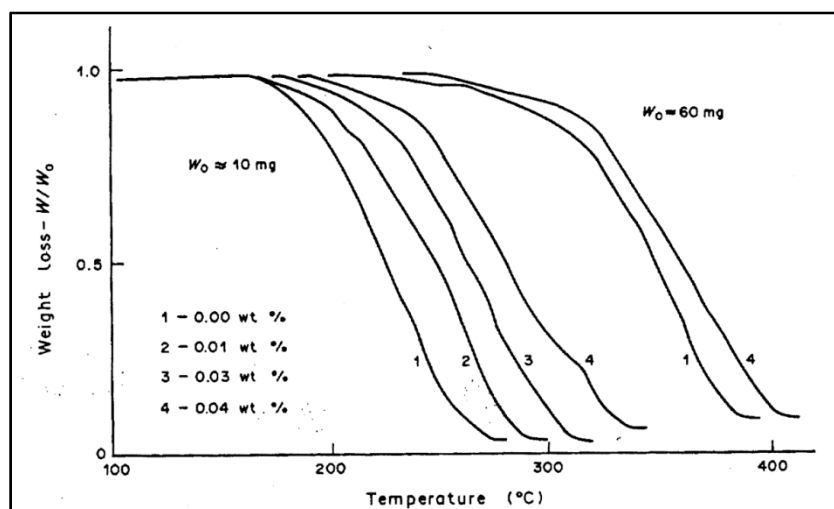
Figure 3.9: *Thermogravimetric curves of poly(ethyl α-cyanoacrylate) for various quantities of pyridine (base) in the polymer sample. Conditions: heating rate = 5 °C/min, initial sample weight (W_0) = 10 mg or 60 mg, area of polymer sample = 2 cm^2.[275]*

It is clear that the thermal depolymerisation of poly-cyanoacrylates is a complex process and there are certain conditions whereby the depolymerisation temperature and the chance of side reactions are at a minimum. In terms of the synthesis of cyanoacrylate monomers (particularly novel cyanoacrylates), it is difficult or impossible to optimise the preceding Knoevenagel condensation (polymer-forming) step to obtain a product that is easily depolymerisable. The extreme reactivity of the intermediate monomer means that the molecular weight of the obtained polymer may be larger than the optimal size for the

depolymerisation step. Furthermore, the oligomeric product is likely to have a high polydispersity that further complicates the depolymerisation step. These factors, together with the presence of even trace amounts of base or water and the need to maintain a sufficient amount of polymerisation inhibitor, mean that the temperature for depolymerisation is often high enough for unwanted thermal degradation and side reactions to occur.

In the following section (Section 3.4), attempts to synthesise novel cyanoacrylates via the common Knoevenagel condensation / depolymerisation process will be discussed. For reasons that have been outlined above, difficulties were encountered during the depolymerisation stage of this process and so alternative routes were investigated and these are presented here too.

3.4   Approaches to the synthesis of novel cyanoacrylates

The following section discusses approaches to the synthesis of novel cyanoacrylates. Throughout this section a number of compounds are referred to by their acronyms. To assist the reader, a fold-out page at the back of this thesis contains structures, names and abbreviations for the majority of the compounds discussed here.

3.4.1   Knoevenagel condensation

For reasons that are detailed in Section 1.3, the compound 2-cyanoethyl 2-cyanoacrylate (2-CECA) (Figure 3.10) was a target compound for this project.
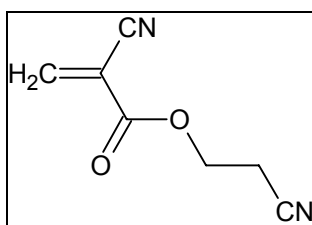
Figure 3.10:   *2-cyanoethyl 2-cyanoacrylate (2-CECA).*

As mentioned in Section 3.1 above, the most common route for cyanoacrylate synthesis is via the Knoevenagel condensation of a cyanoacetate with formaldehyde followed by thermal

depolymerisation (Figure 3.1). At the outset of this project, attempts were made to isolate 2-CECA via this route. The precursor compound, 2-cyanoethyl cyanoacetate (2-CECAc), was successfully synthesised in high yield (~73%) via the acid-catalysed esterification of cyanoacetic acid and 3-hydroxypropionitrile (3-HPN). Although this compound has been previously reported in the patent literature,[281] no analytical data is provided. Furthermore, the authors describe the use of chloroform as the solvent for this reaction and employ a mixed alkanesulfonic acid catalyst. In our hands, this method proved unsatisfactory. An alternative method employing benzene as the reaction solvent and sulfuric acid catalyst has also been reported,[282] however, no yield is given and the final product is characterised by its melting point (41 °C),[282] boiling point (171 – 173 °C / 1 mmHg)[282] and elemental analysis only. The method described by these authors also proved unsatisfactory, but an alternative procedure,[283] using benzene and Amberlyst 15 cation exchange resin, proved successful. The crude product was distilled at reduced pressure and yielded 2-CECAc of sufficient purity at 73% theoretical yield. The product was found to have a boiling point of 154 – 156 °C (1 mmHg). This product was characterised by its ^{1}H and ^{13}C NMR spectra as well as IR, MS and elemental analysis data, which all supported the proposed structure.

The next step in this synthetic route involved the Knoevenagel condensation of 2-CECAc with paraformaldehyde to form oligo-2-CECA. This reaction proved difficult for a number of reasons. Firstly, the nature of the formed product (a highly viscous oligomer) necessitates the use of an overhead mechanical stirrer for agitation. This in turn has implications for the scale on which the reaction can be performed, since small scale reactions are impossible with this sort of apparatus. Upon formation of the oligomeric product, the apparatus often became jammed, leading to incomplete reaction and difficulties in handling and recovering the formed product. Despite these difficulties, oligomeric 2-CECA was obtained in crude form.

The final step in this synthetic route involves the thermal depolymerisation of the oligomer. Since the monomeric cyanoacrylate is highly reactive, this step must be performed in the presence of polymerisation inhibitors such as phosphorus pentoxide and hydroquinone. In attempts to depolymerise the oligomeric product, both these inhibitors were added to the crude oligomer prior to depolymerisation. Phosphorus pentoxide and hydroquinone were also added to the collection flasks for the distilling monomer. Two types of depolymerisation techniques were trialled, namely vacuum distillation and vacuum Kugelrohr distillation.

During vacuum distillation, the oligomer was heated to temperatures in excess of 200 °C under a reduced pressure of 0.4 mmHg or better. No evidence of distilling monomer was observed. The mixture was observed to boil vigorously and gradually darken. Eventually the reaction mixture blackened and charred completely.

In a separate attempt to depolymerise this product, the crude oligomer was placed in a Kugelrohr distillation flask and the phosphorus pentoxide and hydroquinone polymerisation inhibitors were added. Phosphorus pentoxide and hydroquinone were also charged into the collection flask. The oven on the Kugelrohr apparatus was preheated to 150 °C before placing the flask into the oven and applying a vacuum of 0.4 mmHg or better. As with the vacuum distillation, no monomeric product was observed in the analysis of the distillate, either by GC-MS or ^{1}H NMR. Both analyses of the distillate collected during the attempted depolymerisation indicated the presence of significant amounts of 2-CECAc and 3-hydroxypropionitrile. Both these compounds were absent from the analysis of the crude oligomer and so it follows that they have been produced during the attempted depolymerisation process. The exact mechanism for the formation of these by-products is not clear.

The difficulties encountered here have also been reported by numerous groups. For example, Denchev et al report difficulties in depolymerising oilgo-allyloxyethyl cyanoacrylate even when it is heated to temperatures in excess of 300 °C.[246] Similarly, Kotzev et al. were unable to isolate the following cyanoacrylate monomers: 2-methyl-2-propenyl, 2-butenyl and 1-propyl-2-propenyl[264] and Vijayalakshmi et al. report difficulties in obtaining *tert*-butyl and undecyl cyanoacrylate.[216] Using a molar excess of the cyanoacetate in the condensation step, Denchev et al. were able to obtain a more easily depolymerisable product, but the yields were still comparatively low.[246]

3.4.2   Alternative approaches

Due to the difficulties encountered in the attempted synthesis via the common route, which involves a depolymerisation step (outlined in Section 3.4.1 above), alternative procedures for the synthesis of cyanoacrylates were investigated. As discussed in Section 3.1 above, a number of alternative methods have also been published. These routes have been used to synthesise cyanoacrylates that are difficult or impossible to synthesise via the normal

condensation-depolymerisation method. These include fluorinated, higher alkyl and di-functional or bis-cyanoacrylates.

From the range of alternative preparative methods available, the first obvious choice was the use of acid catalysts for the condensation reaction between alkyl cyanoacetates and formaldehyde. The use of an acid catalyst would theoretically inhibit (or at least limit) the polymerisation of the formed cyanoacrylate leading to a product that may be more easily depolymerised / distilled. This approach has been employed by several authors for the synthesis of fluoroalkyl,[212-214] allyl and haloalkyl 2-cyanoacrylates.[216] Typical acid catalysts include piperdine hydrochloride and glacial acetic acid, which are often used in combination,[212-214,216] but other acids such as phosphoric acid,[213] hydrochloric acid,[212,214] sulfuric acid,[212,214] bis-(2-chloroethyl) amine hydrochloride[214] and morpholine hydrochloride[214] have also been reported.

Attempts were made to synthesise 2-CECA (or oligo-2-CECA) using the Knoevenagel condensation of 2-CECAc with paraformaldehyde in the presence of the dual catalysts piperidine hydrochloride and glacial acetic acid. The reactants were heated under reflux in benzene under a positive pressure of sulfur dioxide (SO_2) polymerisation inhibitor. No reaction was observed after several hours. In one attempt, no reaction was observed using the acidic conditions described above, so, following the complete addition of paraformaldehyde and several hours reflux, the reaction mixture was treated with piperidine (base) and the reaction proceeded as per previous attempts using basic catalysts. This confirmed that the reagents themselves were satisfactory and that the acids had failed to catalyse the reaction. For this reason the use of acid catalysts was deemed ineffective in this case and further attempts were abandoned.

The majority of the remaining alternative approaches for the synthesis of cyanoacrylates are either poorly documented,[239] involve the use of extremely reactive intermediates (such as 2-cyanoacryloyl chloride),[238] involve a complex multi-step synthesis[241,242] and / or still involve a depolymerisation step.[240,244] The exception is the Diels-Alder protection and de-protection route that was first described in a patent by Ray and Doran in 1969.[228] This method involves the synthesis of monomeric 2-cyanoacrylates by heating a mixture of the corresponding ester of cyanoacetic acid, formaldehyde, anthracene and a basic catalyst in an inert, non-aqueous organic solvent to give the adduct of the monomeric ester and anthracene. The monomeric

cyanoacrylate can then be displaced from the anthracene adduct by heating the adduct alone or in the presence of a dienophile such as maleic anhydride.[228]

The two steps in this procedure can be thought of as a protection and de-protection of the reactive vinyl group. During the protection step a diene (usually anthracene) is involved in a Diels-Alder reaction with the reactive intermediate of the Knoevenagel condensation reaction (the alkyl 2-cyanoacrylate), which acts as a dienophile (see Figure 3.11 below). The anthracene adduct that is formed undergoes thermal degradation at elevated temperatures to yield anthracene and monomeric alkyl 2-cyanoacrylate. If this adduct is heated with maleic anhydride (a more reactive dienophile) then the liberated anthracene may be trapped as the anthracene / maleic anhydride adduct (A/MA) and the monomer can be isolated in an anhydrous environment (see Figure 3.12 below).
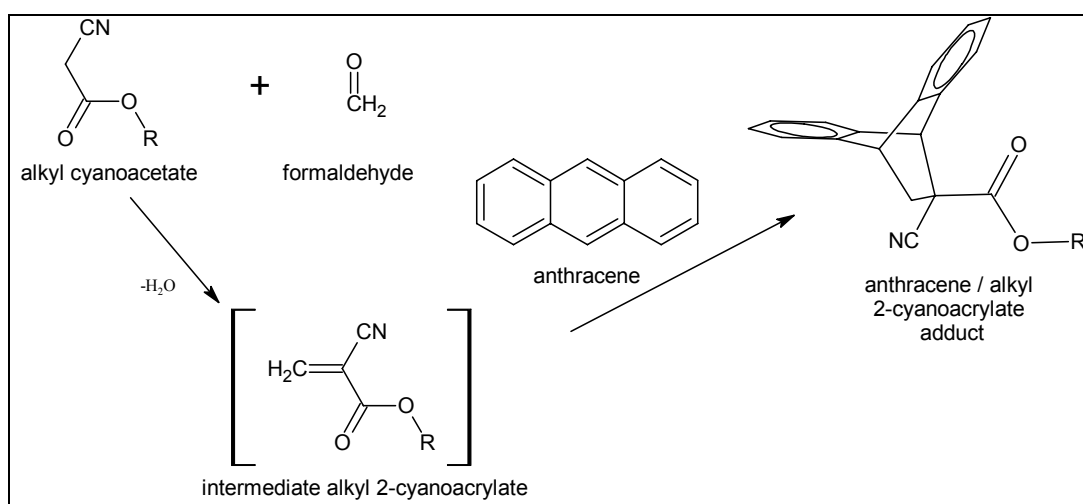
Figure 3.11: *Simultaneous Knoevenagel condensation and Diels-Alder 'protection' yields an anthracene / alkyl 2-cyanoacrylate adduct.*
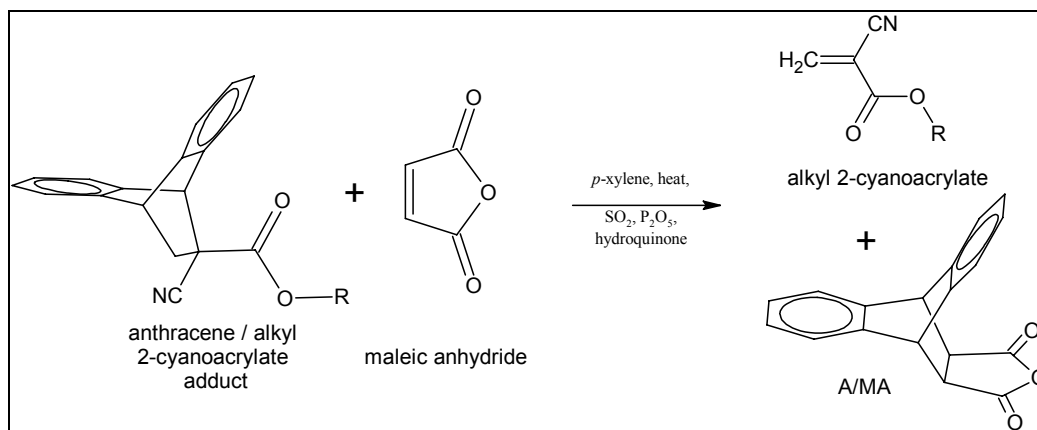
Figure 3.12:   *Retrograde Diels-Alder ('de-protection') of anthracene / alkyl 2-cyanoacrylate adduct yields monomeric alkyl 2-cyanoacrylate.*

This method avoids the formation of an oligomeric intermediate and therefore does not require a depolymerisation step. Furthermore, the anthracene adduct precursors are stable crystalline compounds at room temperature. They can therefore be isolated in reasonable purity by recrystallisation. Ray and Doran used this method for the synthesis of mono-functional cyanoacrylates such as ethyl cyanoacrylate.[228] Giral et al. describe a modification of this method that employs acidic catalysts for the synthesis of fluorinated cyanoacrylates.[236] As mentioned above, however, acidic catalysts fail to effect the Knoevenagel condensation of 2-CECAc with paraformaldehyde.

An advantage of Ray and Doran's protection / de-protection method of particular appeal in the context of this thesis is that it is amenable to much smaller quantities than those normally employed for the Knoevenagel condensation / depolymerisation method. This was demonstrated by De Keyser et al., who used this method to synthesise approximately 300 mg of isobutyl [3-^{14}C] cyanoacrylate.[233]

The anthracene adduct of 2-cyanoethyl 2-cyanoacrylate (A/2-CECA) was successfully synthesised from equimolar quantities of 2-cyanoethyl cyanoacetate (2-CECAc), paraformaldehyde and anthracene. The reaction was performed in refluxing benzene in the presence of piperidine catalyst and the water formed was azeotropically removed. The product was isolated as a crystalline solid that was recrystallised from methanol. The overall yield for the reaction was quite poor (approx. 14%). Furthermore, the product was often contaminated with residual amounts of anthracene, which were difficult to remove by recrystallisation alone. Small quantities of anthracene could be removed by sublimation at

reduced pressure using sublimation apparatus fitted with a cold finger. This, however was difficult and time-consuming with larger samples.

In an attempt to improve the yield, the reaction was repeated, replacing the benzene solvent with either *p*-xylene or an 80:20 mixture of toluene and benzene. These solvent systems gave similar results at best. Changing the method of addition of the reactants also had no effect on the yield. Using a 2.5 – 3 molar excess of anthracene led to improvements of yield to a maximum of approximately 30%. The product obtained from these reactions however, was still contaminated with significant amounts of unreacted anthracene.

Initial attempts to isolate 2-cyanoethyl 2-cyanoacrylate (2-CECA) by treatment of the A/2-CECA (produced by this method) with maleic anhydride in either tricresyl phosphate or *p*-xylene led to a polymeric or charred product. The monomeric product was finally isolated in crude form when the reaction was performed under strictly anhydrous conditions. This included pre-treatment of glassware with a silanating agent and using anhydrous *p*-xylene, which was inhibited with a strong stream of sulfur dioxide (SO_2). The reaction was also conducted under SO_2 in the presence of other polymerisation inhibitors including phosphorus pentoxide (P_2O_5) and hydroquinone. The reaction was monitored via NMR of regularly withdrawn 100-µL aliquots.

Despite the success of isolating 2-CECA via this method, the product was not pure and only a limited amount was obtained due to the difficulty of obtaining the precursor anthracene adduct in a high yield (and purity). An alternative method for the synthesis of the precursor (A/2-CECA) was therefore investigated.

In a slight modification of the Ray and Doran method, Buck demonstrated that the protection / de-protection approach is useful for the synthesis of di-functional or bis(2-cyanoacrylate) monomers having the general formula shown in Figure 3.13 below.[230,234]
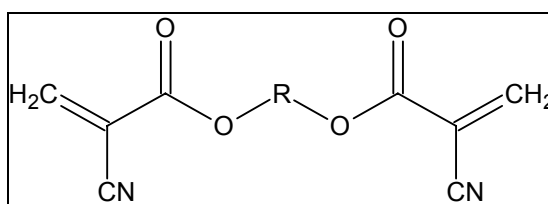
Figure 3.13:   *General structural formula for alkyl bis(2-cyanoacrylate) monomers.*

Buck describes the Diels-Alder reaction of either isobutyl 2-cyanoacrylate (IBCA) or ethyl 2-cyanoacrylate (ECA) with anthracene to form the corresponding anthracene adduct (A/IBCA or A/ECA). Saponification of this adduct yielded the anthracene/2-cyanoacrylic acid adduct (A/CAA). Further conversion to the alkali metal salt or acid chloride derivative followed by esterification reactions with an organic dihalide or glycol gave the bis-anthracene adduct precursors to the bis(2-cyanoacrylate) monomers. Heating the bis-adducts with excess maleic anhydride in refluxing xylene effected the same retrograde diene scission described above, which, in this case, yielded the bis(2-cyanoacrylate) monomers in up to 80% overall yields.[234] The overall reaction scheme reported by Buck is shown in Figure 3.14 below. Note that the esterification step can be achieved in a number of ways and can produce mono-functional or di-functional products depending on the reagents used. Kronenthal and Schipper report the direct esterification of A/CAA with a haloalkane (or dihalide in the case of bis-adducts) in the presence of triethylamine[231] (see broken line in Figure 3.14 below). As mentioned above, Buck describes the treatment of the alkai metal salt of A/CAA such as the anthracene / 2-cyanoacrylic acid potassium salt (A/CAA-K) with a dihalide (or haloalkane). Alternatively, anthracene / 2-cyanoacryloyl chloride adduct (A/CAC), which may be formed by treating A/CAA with thionyl chloride in the presence of pyridine, can be treated with a dihalide (or haloalkane) in the presence of triethylamine.
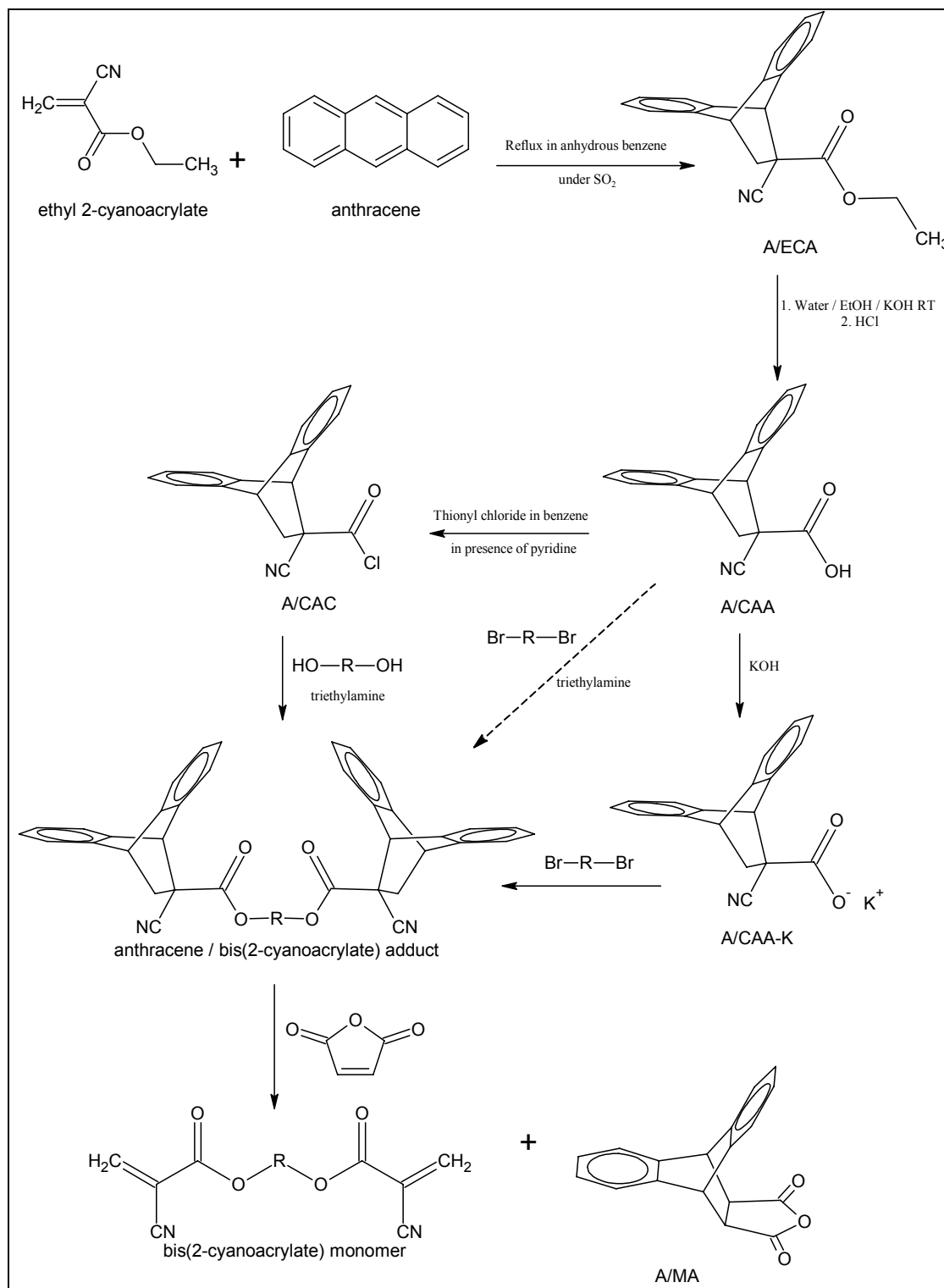
Figure 3.14: *Reaction scheme for the synthesis of alkyl bis(2-cyanoacrylates) reported by Buck.*[234]

This method has also been used by other authors for the synthesis of thiocyanoacrylates,[229] carbalkoxyalkyl 2-cyanoacrylates[231] and cyanoacrylate-capped polyisobutylenes.[235] Warrener

has also reported a number of anthracene / 2-cyanoacrylate adducts but the corresponding cyanoacrylate monomers were not isolated.[232]

Using the method reported by Buck, A/ECA was synthesised by reaction of ethyl 2-cyanoacrylate (in the form of commercial superglue) with anthracene in refluxing benzene under SO_2. The A/ECA was used in its crude form for the next step – saponification with potassium hydroxide (KOH) in a mixture of ethanol and water at room temperature. At this stage, a convenient purification step became apparent and involved simple filtration of the insoluble residual anthracene and (poly) ethyl 2-cyanoacrylate. Subsequent acidification to pH 2 yielded A/CAA as a white crystalline powder in high purity and yield. Adjusting the pH of a solution of A/CAA in acetone with methanolic potassium hydroxide (40% w/v) to pH 9.5 and subsequent filtration yielded A/CAA-K. Alternatively, A-CAC could be isolated by treatment of A/CAA with thionyl chloride ($SOCl_2$) in benzene in the presence of pyridine. All products were characterised by melting point, FTIR, ^{1}H and ^{13}C NMR and elemental analysis. All data corresponded to those previously reported (where available) and were consistent with the proposed structures. A/CAC was found to react with atmospheric moisture, reverting back to A/CAA. For this reason, it was prepared immediately before use. During the conversion from A/CAA to A/CAC, the reaction was heated in a water bath that was not allowed to exceed 60 °C. Heating above this temperature was found to cause de-protection of the anthracene adducts producing anthracene that was difficult to remove from the product. Furthermore, due to the extreme reactivity of $SOCl_2$ used in the conversion, strictly anhydrous conditions were necessary and fresh $SOCl_2$ gave the best results. Figure 3.15 shows a summary of these reactions and the average yield of A/CAA, A/CAA-K and A/CAC. These three compounds were produced in very high yield and high purity and provide convenient precursors for the synthesis of anthracene-protected cyanoacrylate esters via esterification.
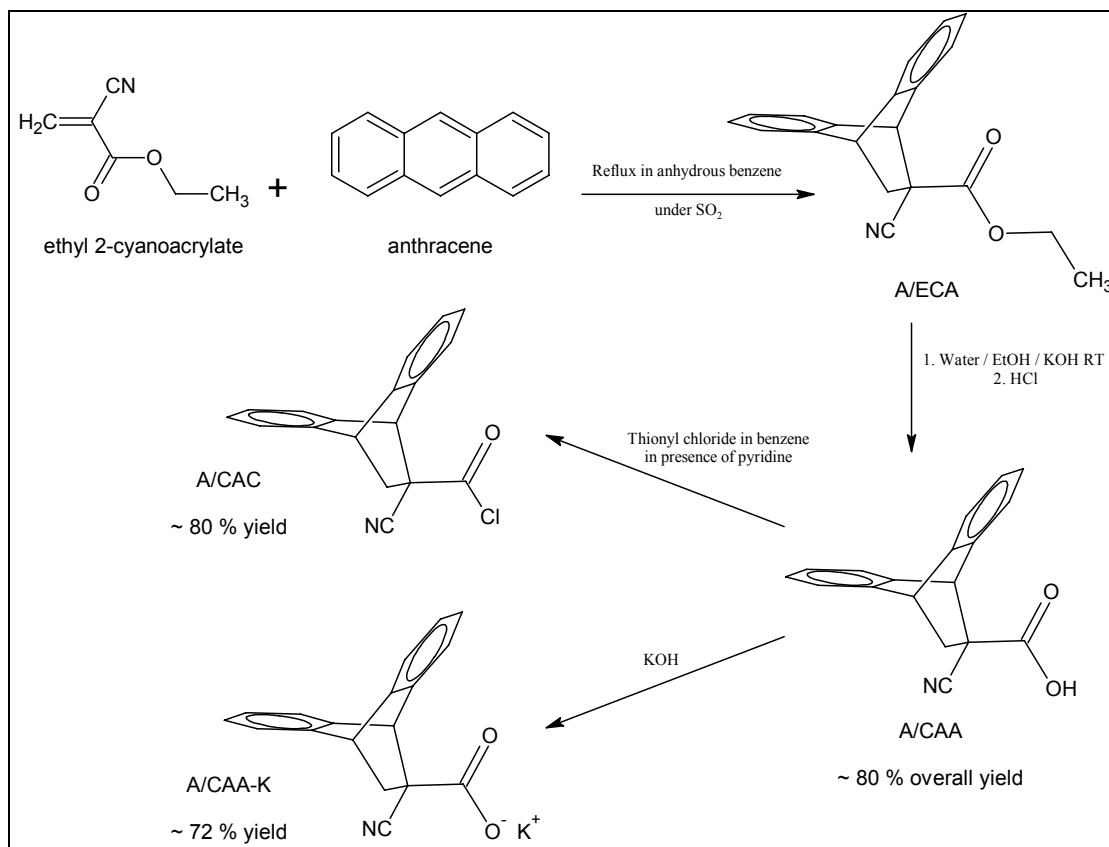
Figure 3.15: *Synthesis of A/CAA, A/CAC and A/CAA-K and average percentage yields obtained.*

Having successfully synthesised these three precursors, attempts were made to synthesise the anthracene / 2-cyanoethyl 2-cyanoacrylate adduct (A/2-CECA) via esterification. As mentioned above, there are three main pathways (from each of the three precursors) for the esterification reaction. A number of attempts at the direct esterification of A/CAA were made. The first of these was based on the success of the esterification between cyanoacetic acid and 3-hydroxypropionitrile (3-HPN) to form 2-cyanoethyl cyanoacetate (see Section 3.4.1 above). A/CAA was refluxed in benzene with 3-HPN in the presence of Amberlyst 15 cation exchange resin. A Dean-Stark reflux trap was used to remove any water formed by this reaction. Following 15 hours of reflux, no signs of reaction were observed. The failure of this reaction is thought to be due to steric effects caused by the hindered acid.

In 1978, Ono et al. discovered that treatment of carboxylic acids with 1,8-diazobicyclo[5,4,0]undec-7-ene (DBU) and alkyl halides in benzene at room temperature or reflux affords the ester in good yields.[284] Later, Rao reported that acetonitrile could be used in place of benzene. This not only reduced the toxicity and flammability hazards but was also found to increase the rate of reaction and produce essentially quantitative yields of

the esters.[285] The reaction between equimolar portions of A/CAA, 3-bromopropionitrile (3-BPN) and DBU was conducted in benzene. Analysis via NMR after stirring at room temperature for several hours showed only trace amounts of the desired product (A/2-CECA). The reaction was repeated in acetonitrile but this solvent also failed to produce the DBU-promoted esterification that has been reported.

Carboxylic acid salts, including hindered acids, are reported to react rapidly with primary or secondary bromides or iodides at room temperature in polar aprotic solvents, such as hexamethylphosphoramide (HMPA), to give high yields of the carboxylic ester.[286,287] Other polar aprotic solvents such as dimethylsulfoxide (DMSO) and *N,N*-dimethylformamide (DMF) have also been used.[287,288] Buck reports that A/CAA-K reacts with dihalides in DMF to produce the desired bis-anthracene adducts of bis(2-cyanoacrylate).[234] Following the method reported by Buck, A/CAA-K was stirred with an equimolar amount of 3-BPN in dry DMF and heated at 100 °C for two hours before quenching the reaction in water. The ^{1}H NMR spectrum of the precipitate collected showed mainly peaks due to the starting materials with only traces of the desired product (A/2-CECA).

Buck also reports a method for esterification with A/CAC. Following this method, to a stirred solution of 3-HPN with an excess of triethylamine in dry DMF at room temperature was added, over 30 minutes, a solution of freshly prepared A/CAC in dry DMF. The suspension of triethylamine hydrochloride was poured into water and the orange precipitate was extracted with benzene. A/2-CECA was successfully synthesised via this method with yields of approximately 35% prior to recrystallisation. Yields were increased to ~75% (crude) / ~60% (after recrystallisation) by conducting the reaction in anhydrous benzene. A summary of the esterification reactions tested is shown in Figure 3.16 below.
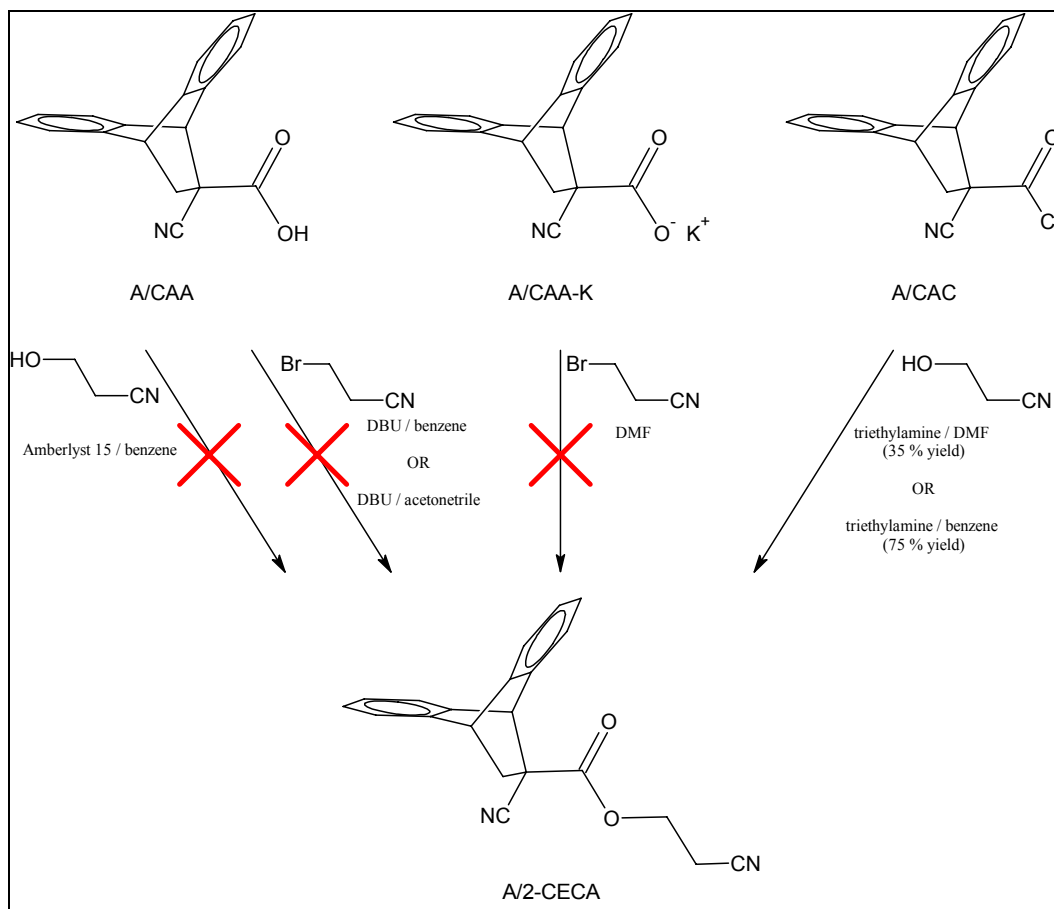
Figure 3.16: *Esterification reactions tested for the synthesis of A/2-CECA.*

The method described above has a number of advantages over the Ray and Doran simultaneous Knoevenagel condensation / Diels-Alder protection method previously employed for the synthesis of A/2-CECA. Firstly, the overall yield for the reaction was higher (25 – 30% over 4 steps). Secondly, the purity of the final product is much higher. This is due to the purity of the A/CAA precursor, which, in turn, is due to the filtration of the aqueous solution prior to acidification. This is very effective at removing the major contaminant, anthracene, from the A/CAA. The formation of anthracene is avoided in the reactions that follow due to the mild reaction conditions employed. Lastly, and perhaps most importantly, the new method allows for the convenient synthesis of other anthracene / alkyl 2-cyanoacrylate adducts (and hence other cyanoacrylate monomers) by simply changing the alcohol used in the reaction with A/CAC. The overall reaction sequence is shown in Figure 3.17 below.
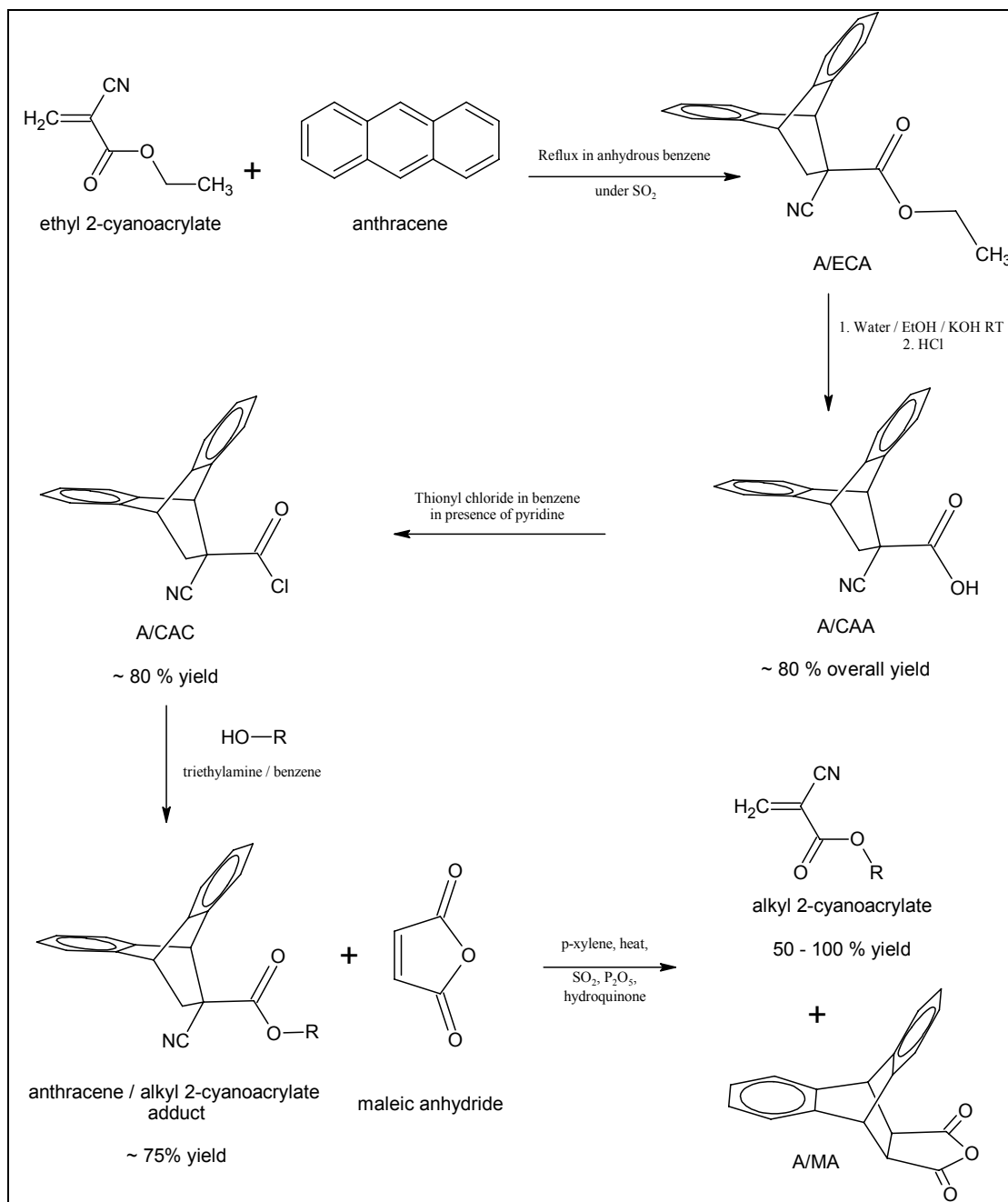
Figure 3.17: *Overall reaction sequence for synthesis of novel alkyl 2-cyanoacrylates.*

Using this reaction scheme, 4 novel anthracene / alkyl 2-cyanoacrylate adducts were prepared. These include anthracene / 2-cyanoethyl 2-cyanoacrylate (A/2-CECA), anthracene / 1-cyanoethyl 2-cyanoacrylate (A/1-CECA), anthracene / trideuteromethyl 2-cyanoacrylate (A/MCA-d$_3$) and anthracene / pentadeuteroethyl 2-cyanoacrylate (A/ECA-d$_5$) – see Figure 3.18.
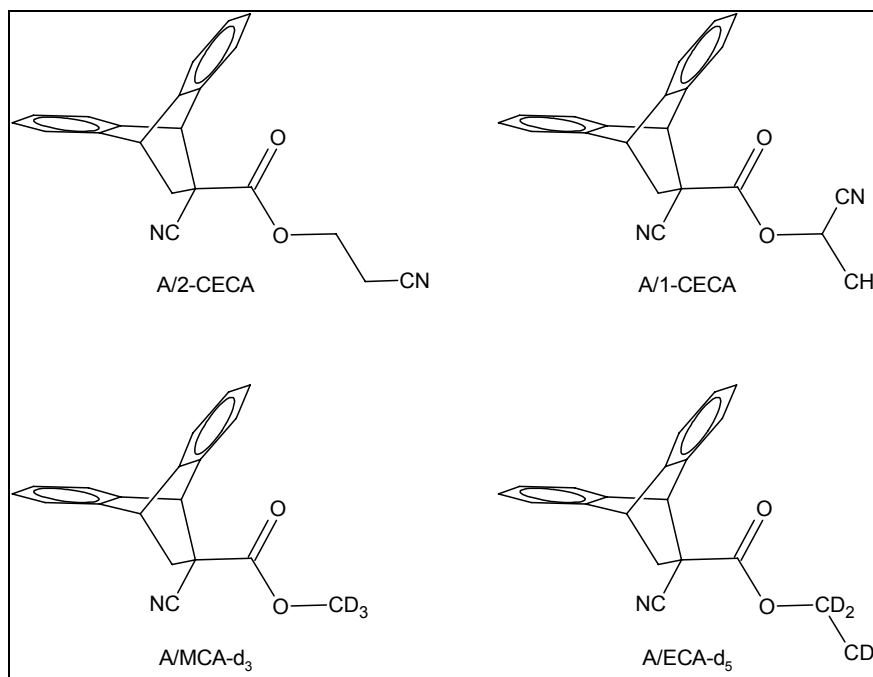
Figure 3.18: *Structures of novel anthracene / alkyl 2-cyanoacrylate adducts.*

From these adducts the following novel alkyl 2-cyanoacrylates were isolated: 2-cyanoethyl 2-cyanoacrylate (2-CECA), 1-cyanoethyl 2-cyanoacrylate (1-CECA), trideuteromethyl 2-cyanoacrylate (MCA-d$_3$) and pentadeuteroethyl 2-cyanoacrylate (ECA-d$_5$) – see Figure 3.19.
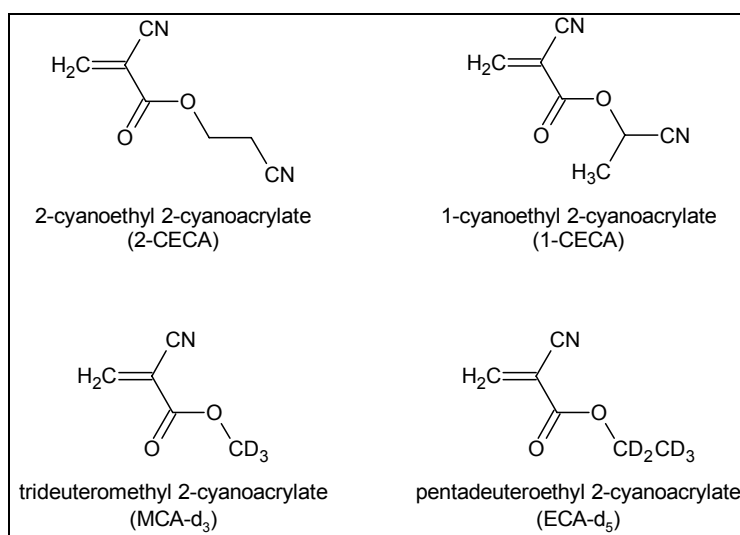
Figure 3.19: *Structures of novel alkyl 2-cyanoacrylate monomers.*

As noted previously, the isolation of monomeric cyanoacrylate from its anthracene adduct was conducted in silanated and oven dried glassware. The reaction medium was anhydrous *p*-xylene, which had been inhibited with a strong stream of SO_2 and the reaction was conducted under SO_2. The presence of other polymerisation inhibitors such as phosphorus pentoxide (P_2O_5) and hydroquinone did not improve results and hence these were eliminated from subsequent reactions. The reaction was monitored via NMR of regularly withdrawn 100-μL aliquots. The reaction was typically allowed to proceed for 48 − 72 hours, at which point the level of monomer being produced had reached a maximum, or signs of polymerisation and loss of product were observed. Monomeric samples were contaminated with varying amounts of their anthracene adduct and (to a lesser extent) anthracene / maleic anhydride adduct (A/MA). Estimations of monomer purity were made based on the ^{1}H NMR spectra. Due to the relatively small quantities of product and the high probability of polymerisation, no attempts were made to distil or otherwise purify the monomers. The impurities present generally did not interfere with the use of these monomers for the fuming of latent fingerprints. This is discussed in detail in Section 4.3.

3.5   Analysis and characterisation of novel compounds

3.5.1   Thermal analysis of anthracene / alkyl 2-cyanoacrylate adducts

As mentioned above, the anthracene adducts of alkyl 2-cyanoacrylates thermally decompose in a retrograde Diels-Alder reaction to yield anthracene and cyanoacrylate monomer. Giral et al. have reported using this thermal degradation alone to isolate the desired monomeric product.[236] This method involves the use of glassware specially designed to trap the liberated anthracene on its inside walls by condensation while the monomeric vapours are distilled. More commonly, however, a more reactive dienophile (such as maleic anhydride) is introduced to trap the liberated anthracene as a non-volatile adduct.

Furthermore, a patent by Warrener and Yong discusses the possibility of using anthracene / alkyl 2-cyanoacrylate adducts as solid precursors for the fuming of latent fingerprints.[232] In order to investigate methods of recovering the desired monomeric cyanoacrylate from the corresponding anthracene adduct, and to evaluate the potential use of these adducts for

direct fuming of latent fingerprints, the thermal decomposition of all four novel anthracene / cyanoacrylate adducts was studied. Simultaneous thermogravimetric analysis (TGA) and differential thermal analysis (DTA) were performed on a SDT 2960 module (TA instruments) with a 10 °C/minute heating rate from ambient conditions to 600 °C. Figures 3.20 – 3.23 show the thermal analysis of the four novel anthracene adducts synthesised (blue trace DTA, green trace TGA, brown trace derivative of TGA).
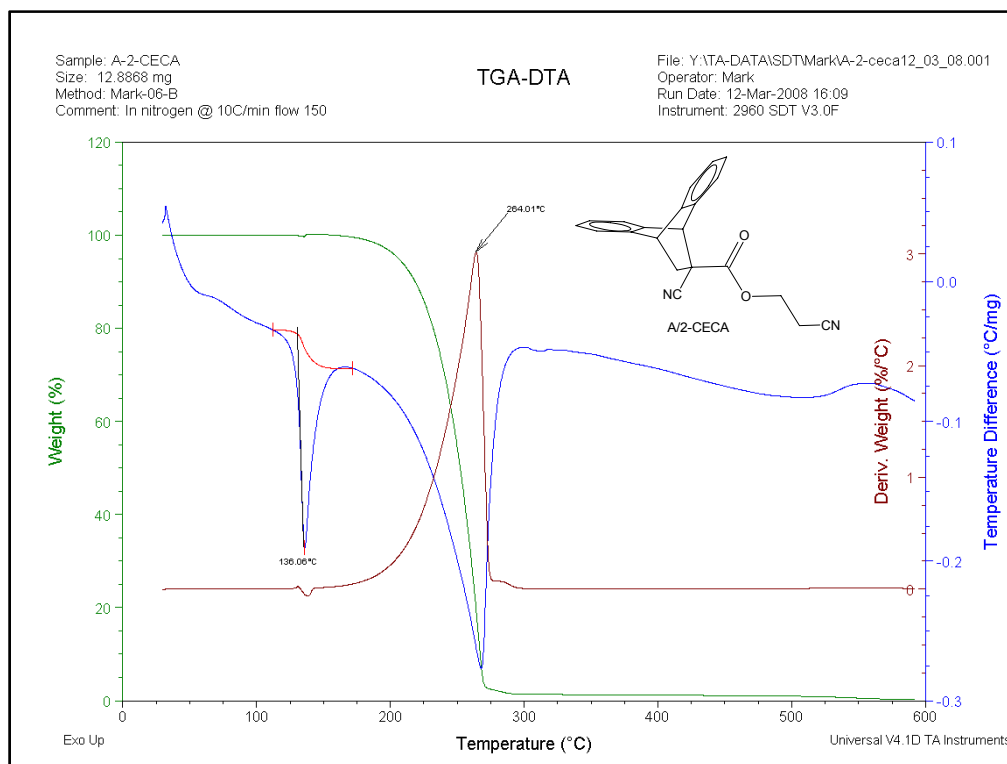
Figure 3.20: *TGA-DTA curves for anthracene / 2-cyanoethyl 2-cyanoacrylate adduct (A/2-CECA).*
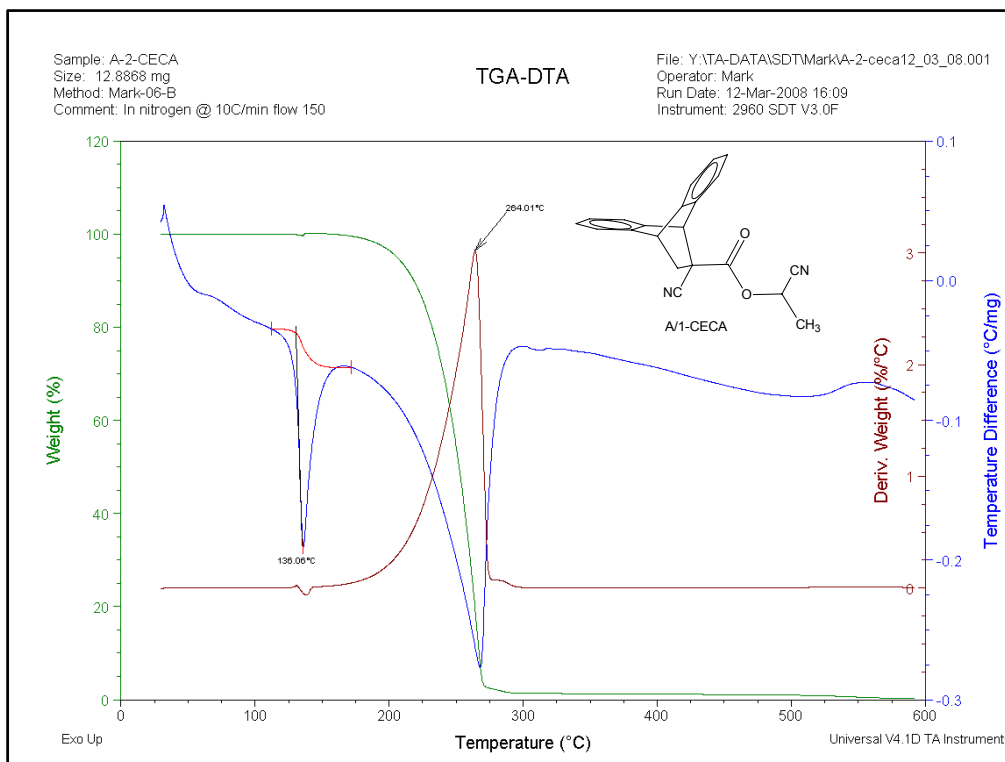
Figure 3.21: *TGA-DTA curves for anthracene / 1-cyanoethyl 2-cyanoacrylate adduct (A/1-CECA).*
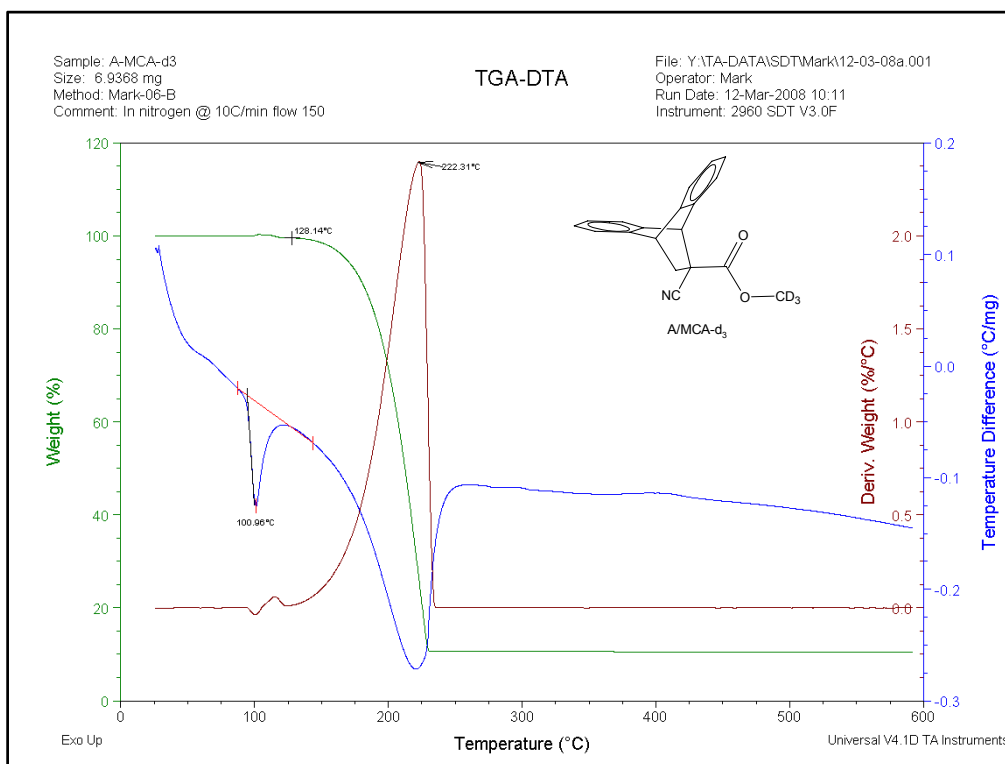
Figure 3.22: *TGA-DTA curves for anthracene / trideuteromethyl 2-cyanoacrylate adduct (A/MCA-d$_3$).*
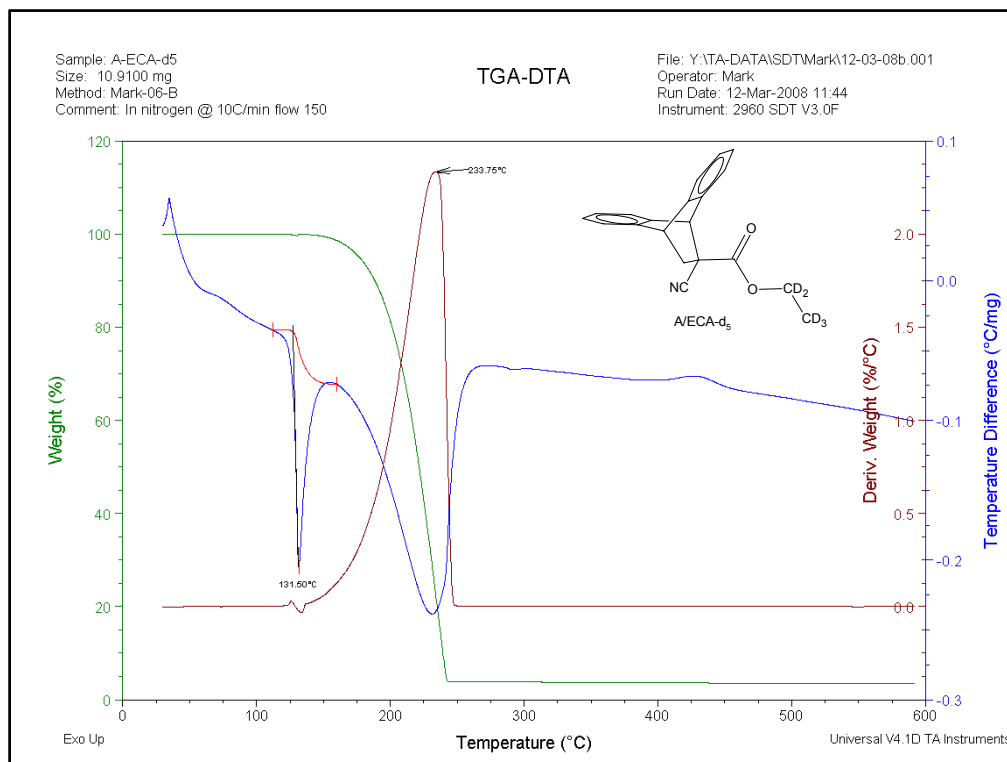
Figure 3.23: *TGA-DTA curves for anthracene / pentadeuteroethyl 2-cyanoacrylate adduct (A/ECA-d5).*

The first endotherm in the DTA traces for each of the four adducts examined represents melting and accordingly there is no corresponding mass loss in the TGA traces. The melting points for A/2-CECA, A/ECA-d5 and A/MCA-d3 are sharp (i.e. occur over a narrow temperature interval) and correspond well with that obtained using conventional melting point apparatus. In contrast, the first endotherm in the DTA trace for A/1-CECA shows melting over a wide range. This can be explained by the fact that this compound is actually a mixture of stereoisomers (see Section 3.5.2 below).

The second endotherm in the DTA traces for all four adducts corresponds to thermal decomposition. It is clear from the TGA traces that mass loss commences at temperatures slightly above the melting point, with maxima ranging between 220 – 265 °C. It is tempting to suggest that the temperature of maximum decomposition is a function of the identity of the particular cyanoacrylate evolved, but many factors need to be considered. Firstly, it is likely that two factors determine the maximum decomposition temperature i) the strength of the dienophile (monomer), with stronger dienophiles requiring higher temperatures; ii) the volatility of liberated monomer, with less volatile monomers requiring higher temperatures. It is difficult to ascertain which factor is more critical and it is likely that both are indeed

significant. Furthermore, the sample size and viscosity, which in turn can affect diffusion kinetics, may also be factors to consider. Further work is needed to draw any meaningful conclusions regarding the relative decomposition temperatures of these compounds. Nevertheless, the information gained during the thermal analysis of these compounds is useful for the isolation of the monomeric product and also became of importance for the fuming of latent fingerprints using the anthracene adduct itself (see Section 4.3.1) or the isolated (but crude) monomer (see relevant discussion in Section 4.3). Table 3—3 below summarises the melting points and the temperature at which thermal decomposition is at a maximum.

Compound	Melting point via TGA (°C)	Melting point via conventional melting point apparatus (°C)	Temperature of maximum thermal decomposition (°C)
A/2-CECA	136.1	127-129	264.0
A/1-CECA	124.1 (broad)	n/a	241.2
A/MCA-d$_3$	101.0	97-99	222.3
A/ECA-d$_5$	131.5	126-127	233.8

Table 3—3: *Summary of thermal analysis data for anthracene / alkyl 2- cyanoacrylate adducts*

3.5.2 Nuclear magnetic resonance (NMR) spectroscopy

Nuclear Magnetic Resonance (NMR) spectroscopy was used extensively for the analysis and characterisation of all compounds synthesised during this project. The ^{1}H and ^{13}C NMR resonances for all compounds are listed in the experimental section below (Section 3.6). Highlighted here are a few examples of more complex and interesting spectra.

Throughout this project, a number of Diels-Alder anthracene adducts were synthesised. The general structure for these compounds is shown in Figure 3.24. The ^{1}H NMR spectra of these

compounds show a multiplet owing to the aromatic protons (ArH_1 – ArH_8), a triplet owing to C9-**H**, a singlet owing to C10-**H** and a doublet of doublets for each of the magnetically inequivalent protons on C12 (labelled H_α and H_β). Table 3—4 summarises the ^{1}H NMR data obtained for these compounds, with the exception of A/1-CECA, which is discussed in detail below.
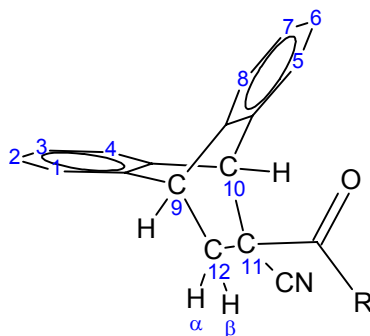
Figure 3.24: *General structure for Diels-Alder anthracene adducts.*

Adduct	R	Solvent	ArH$_1$–ArH$_8$ (m)	C9-H (t)	C10-H (s)	C12-H$_\alpha$ (dd)	C12-H$_\beta$ (dd)
A/CAC	–Cl	CDCl$_3$	7.10 – 7.60	4.45 (*J*=2.7 Hz)	5.06	2.28 (*J*=2.7, 13.5 Hz)	2.75 (*J*=2.7, 13.5 Hz)
A/CAA	–OH	acetone-d$_6$	7.10 – 7.65	4.63 (*J*=2.7 Hz)	5.08	2.21 (*J*=2.7, 12.9 Hz)	2.84 (*J*=2.7, 12.9 Hz)
A/CAA-K	–O$^-$ K$^+$	DMSO-d$_6$	6.95 – 7.40	4.33 (*J*=2.6 Hz)	4.77	1.82 (*J*=2.9, 12.5 Hz)	2.75 (*J*=2.5, 12.5 Hz)
A/MCA	–OCH$_3$	CDCl$_3$	7.10 – 7.60	4.45 (*J*=2.7 Hz)	4.91	2.25 (*J*=2.7, 12.9 Hz)	2.84 (*J*=2.7, 12.9 Hz)
A/ECA	–OCH$_2$CH$_3$	CDCl$_3$	7.10 – 7.50	4.42 (*J*=2.7 Hz)	4.87	2.19 (*J*=2.7, 13.2 Hz)	2.80 (*J*=2.7, 13.2 Hz)
A/2-CECA	–OCH$_2$CH$_2$CN	CDCl$_3$	7.10 – 7.60	4.48 (*J*=2.7 Hz)	4.96	2.26 (*J*=2.7, 13.2 Hz)	2.84 (*J*=2.7, 13.2 Hz)
A/MCA-d$_3$	–OCD$_3$	CDCl$_3$	7.10 – 7.60	4.46 (*J*=2.7 Hz)	4.91	2.24 (*J*=2.7, 13.2 Hz)	2.83 (*J*=2.7, 13.2 Hz)
A/ECA-d$_5$	–OCD$_2$CD$_3$	CDCl$_3$	7.10 – 7.60	4.46 (*J*=2.7 Hz)	4.91	2.24 (*J*=2.7, 12.9 Hz)	2.84 (*J*=2.7, 12.9 Hz)

Table 3—4: *Summary of ^{1}H NMR data for several anthracene adducts.*

Anthracene / 1-cyanoethyl 2-cyanoacrylate (A/1-CECA) contains two chiral centres, which give rise to four possible stereoisomers (see Figure 3.25).
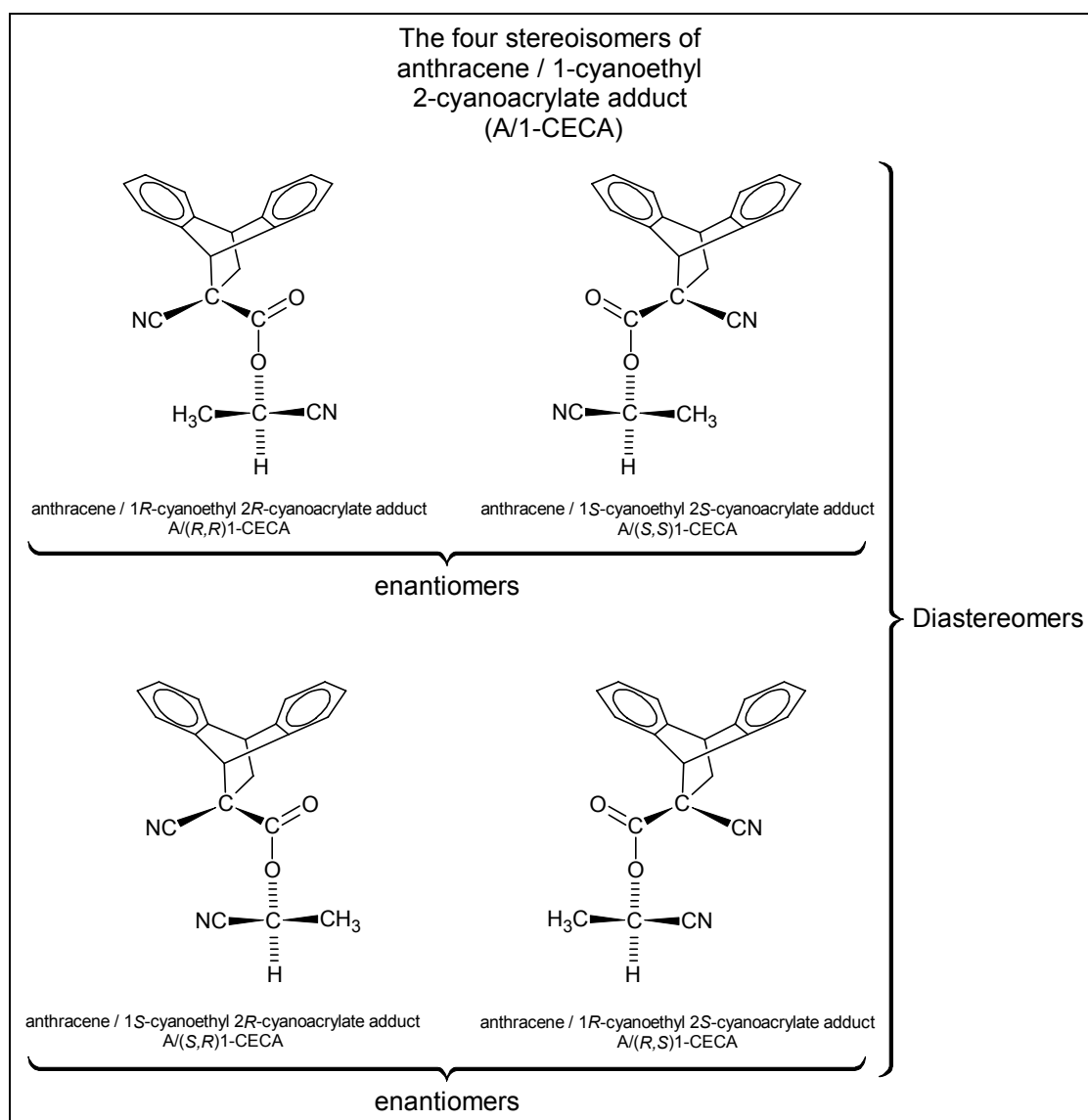
Figure 3.25: *The four stereoisomers of anthracene / 1-cyanoethyl 2-cyanoacrylate adduct (A/1-CECA).*

The NMR spectra for A/1-CECA clearly show two distinct groups of resonances, resulting from the two diastereoisomeric pairs of enantiomers (referred to as *enantiomeric pair a* and *enantiomeric pair b)*. Note that one of these pairs is the (*R,R*) and (*S,S*) pair while the other is the (*R,S*) and (*S,R*) pair (as shown in Figure 3.25) but it is not possible to distinguish which pair is which. The corresponding ^{1}H and ^{13}C spectra are shown in Figure 3.26 and Figure 3.27 respectively. In the ^{1}H NMR spectrum (Figure 3.26) for the two disastereoisomeric pairs of enantiomers, the resonances for the following proton environments are not resolved at 300

MHz: **CH**₃ (doublet at 1.67 ppm), C9-**H** (triplet at 4.49 ppm), Ar**H**₁ – Ar **H**₈ (multiplet from 7.10 – 7.60 ppm). The resonance for the protons C12-**H**α and C12-**H**β, however, appear as doublets of doublets at 2.25 and 2.83 ppm for enantiomeric pair a and at 2.30 and 2.80 ppm for enantiomeric pair b. These resonances for the enantiomeric pairs overlap but clarification of the individual resonances was obtained from a sample with a higher proportion of enantiomeric pair b (see discussion below and the corresponding spectra). The singlet peaks at 4.95 for enantiomeric pair a and at 4.89 ppm for enantiomeric pair b, assigned to the C10-**H** proton, proved useful for determining the relative amount of each pair of compounds. Finally the resonances for the C**H**CN protons appear as two partially overlapped quartets centred at 5.32 and 5.27 ppm for enantiomeric pair a and b respectively. The ¹³C NMR spectrum also shows two distinct groups of resonances appearing mostly in pairs with slight intensity differences.
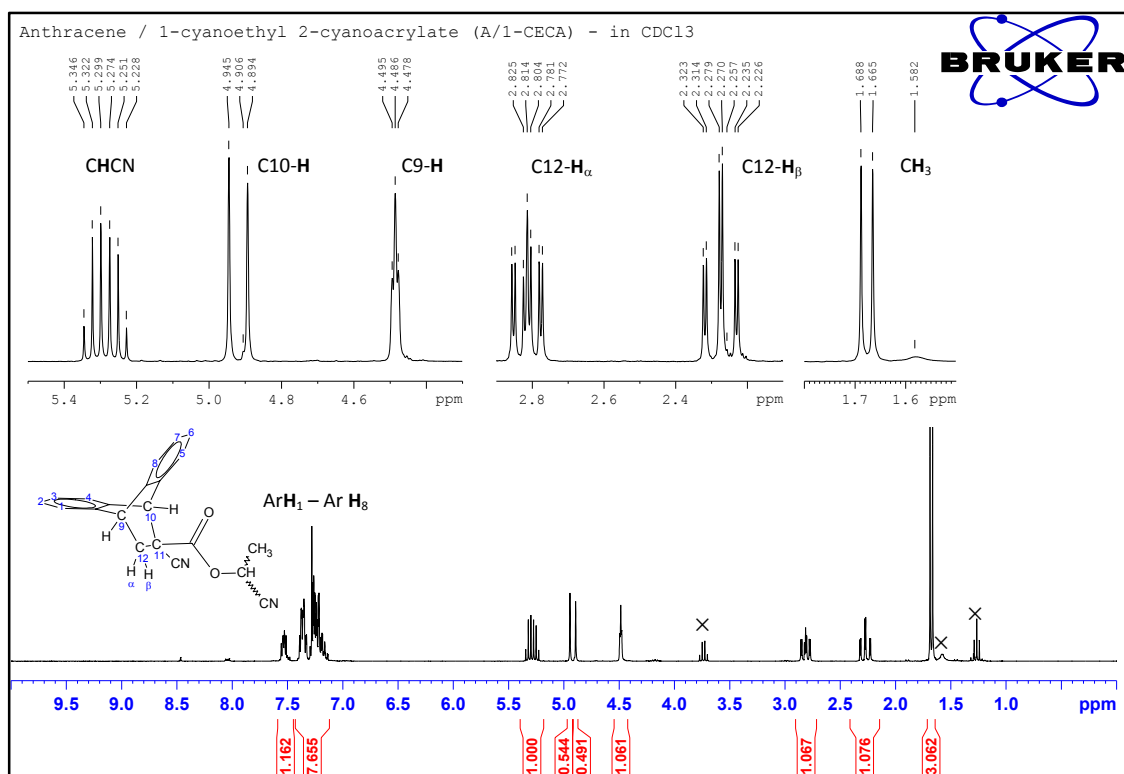
Figure 3.26: *¹H NMR spectrum of anthracene / 1-cyanoethyl 2-cyanoacrylate adduct (A/1-CECA) – resonances from residual ethanol marked with ×.*
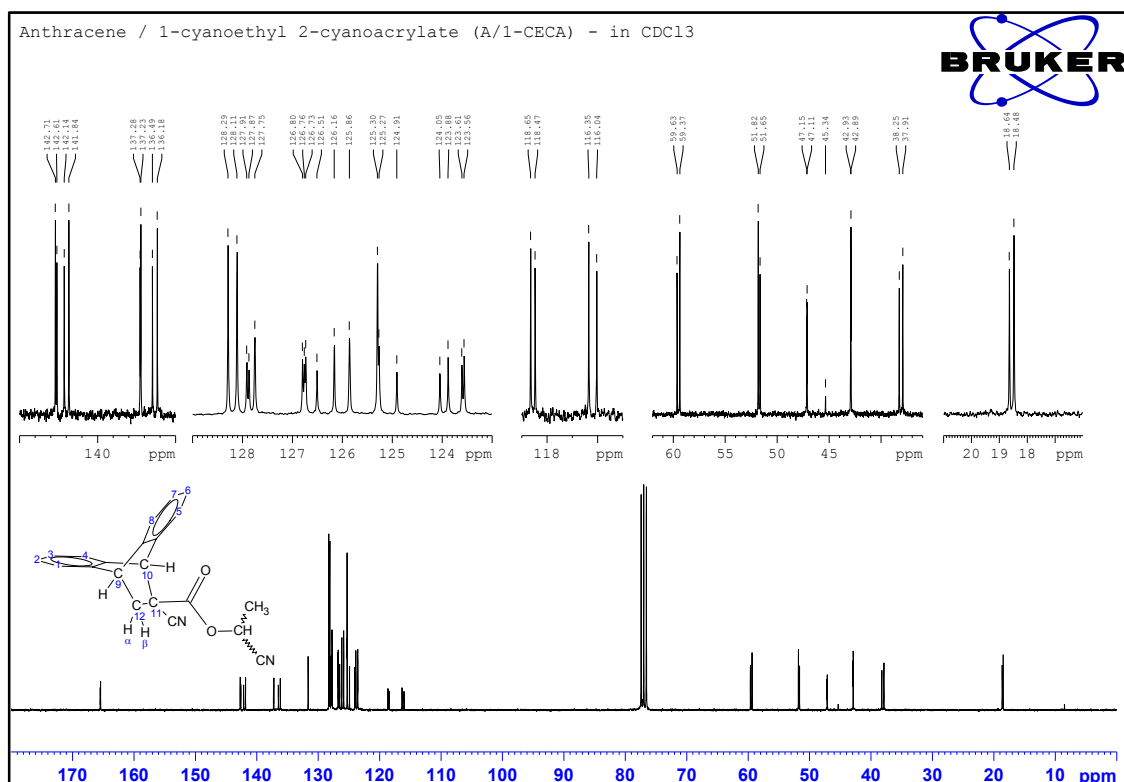
Figure 3.27: *^{13}C NMR spectrum of anthracene / 1-cyanoethyl 2-cyanoacrylate adduct (A/1-CECA).*

Upon recrystallisation of crude 1-CECA, the majority of the product oiled out of solution as a viscous mass, which solidified upon recovery and drying. The ratio of the enantiomeric pairs was determined to be approximately 53% *enantiomeric pair a* : 47% *enantiomeric pair b*. A second (smaller) crop of white crystalline compound was recovered from the mother liquor after cooling in a refrigerator overnight. The ^{1}H and ^{13}C NMR spectra for this crop (shown in Figure 3.28 and Figure 3.29 respectively) show a significant change in the ratio between enantiomeric pair a and enantiomeric pair b (calculated to be approximately 29% enantiomeric pair a and 71% enantiomeric pair b). This indicates that enantiomeric pair a is more soluble and hence remains in solution while enantiomeric pair b crystallises. This difference in solubility could be utilised to separate these two diastereoisomeric pairs of enantiomers by fractional crystallisation, but this was not attempted. Chromatographic separation is also feasible but was not investigated further as the same racemic monomeric product (1-cyanoethyl 2-cyanoacrylate) would results from each diastereomeric racemate. Nevertheless, the isolation of this small crop with a significantly higher proportion of enantiomeric pair b allowed for confirmation of the spectral assignment of the ^{1}H NMR spectra (compare Figure 3.26 and Figure 3.28) and unambiguous assignment of the ^{13}C NMR

resonances for each enantiomeric pair, based on the significant intensity differences (compare peak height differences in Figure 3.29 with those in Figure 3.27).
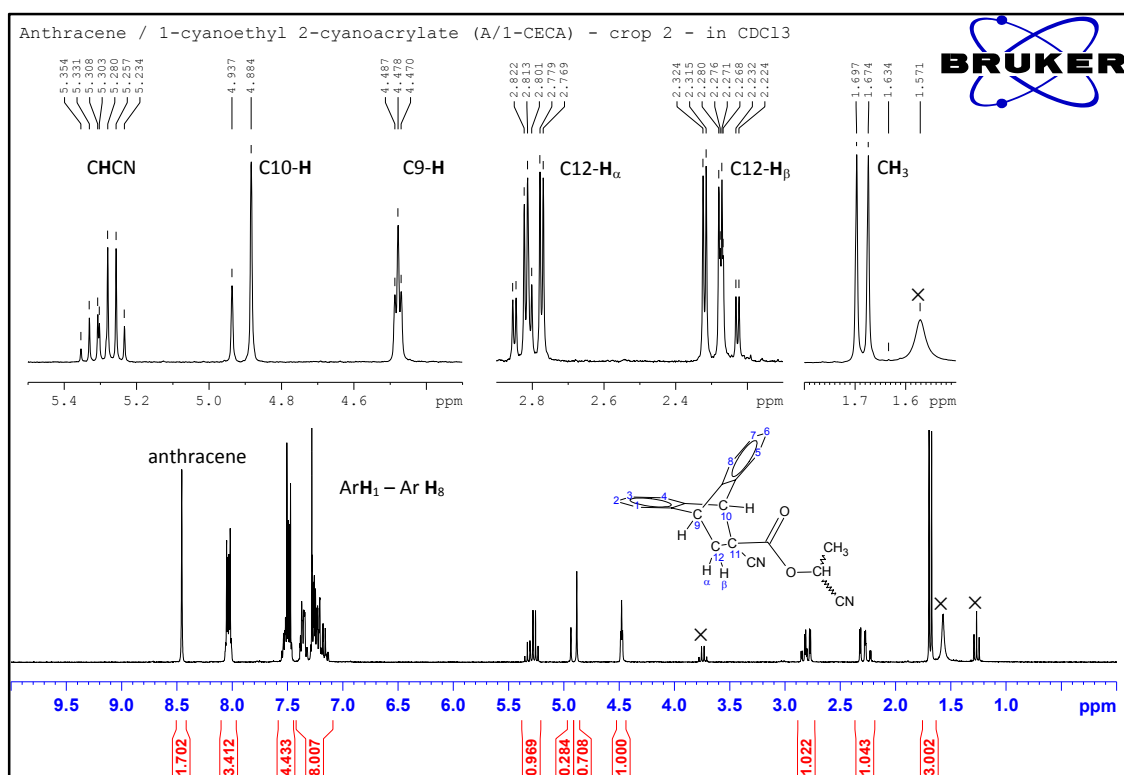
Figure 3.28: *^{1}H NMR spectrum of A/1-CECA – crop 2 – resonances from residual ethanol marked with ×.*
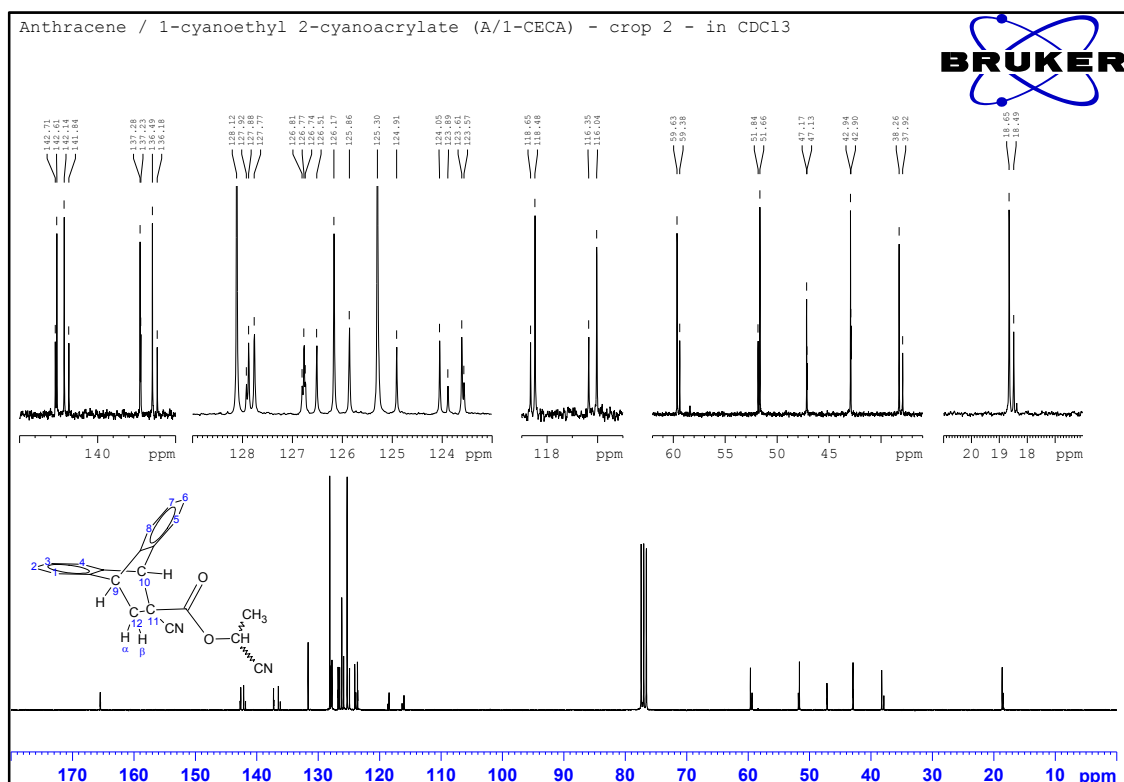
Figure 3.29: ^{13}C NMR spectrum of A/1-CECA – crop 2.

The ^{1}H NMR spectra of the deuterated compounds anthracene / trideuteromethyl 2-cyanoacrylate adduct (A/MCA-d$_3$) and anthracene / pentadeuteroethyl 2-cyanoacrylate adduct (A/ECA-d$_5$) display resonances for the protons indicated in Table 3—4 only (i.e. no resonances are observed for the deuterium atoms of the CD$_3$ / CD$_2$CD$_3$ chains). Although the absence of these resonances indicates that these groups are in fact deuterated, confirmation of the presence of the deuterium atoms was possible from the ^{13}C NMR spectra. During this experiment, the protons (^{1}H atoms) were irradiated, which leads to decoupling of ^{13}C-^{1}H interactions. However, the deuterium nuclei (^{2}H atoms) were not irradiated and hence ^{13}C-^{2}H heteronuclear coupling was observed.

The spin quantum number (*I*) for deuterium (^{2}H) is 1 and the number of allowed spin states (2*I* + 1) is therefore 3.[88] The resonance for the CD$_3$ in A/MCA-d$_3$ is therefore expected to be split into a septet with an intensity ratio of 1:3:6:7:6:3:1. The splitting of the weak ^{13}C signal into a septet makes it difficult to obtain a high signal to noise ratio. Nevertheless, a septet centred at 53.2 ppm was detected in the ^{13}C NMR spectrum of A/MCA-d$_3$ and the coupling constant *J*$_{CD}$ measured was 22.3 Hz (see Figure 3.30). Note the similarity in chemical shift to

the corresponding resonance at 53.8 ppm for the CH_3 group in the un-deuterated compound anthracene / methyl 2-cyanoacrylate adduct (A/MCA) (see Section 3.6 below).
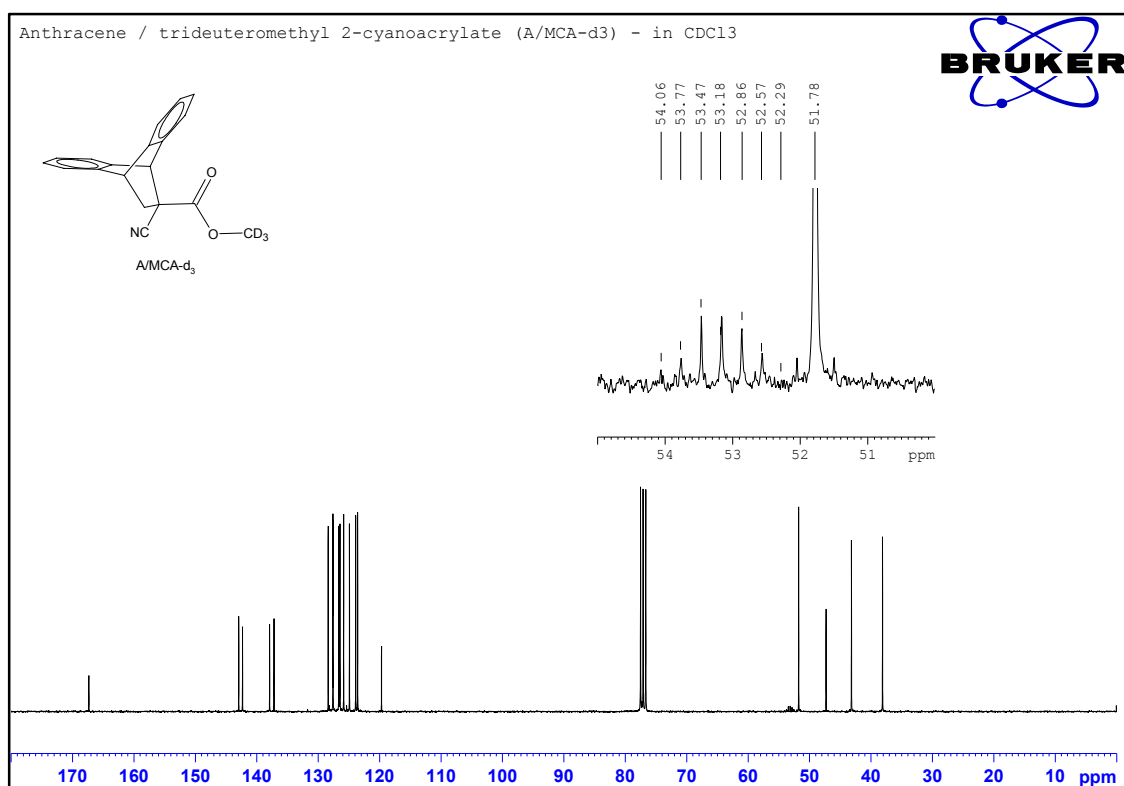
Figure 3.30: ^{13}C *NMR spectrum of anthracene / trideuteromethyl 2-cyanoacrylate adduct (A/MCA-d$_3$) showing septet (J$_{CD}$ = 22.3 Hz) for CD$_3$ group at 53.2 ppm.*

Similarly, the resonances for the CD_2 and CD_3 in A/ECA-d$_5$ are split into a quintet (intensity ratio 1:2:3:2:1) at 62.4 ppm (J_{CD}=23 Hz) and a septet at 13.0 ppm (J_{CD}=19 Hz) respectively (see Figure 3.31). The chemical shifts for these resonances also correspond well to the resonances for the CH_2 (63.2 ppm) and CH_3 (14.0 ppm) groups in the un-deuterated compound anthracene / ethyl 2-cyanoacrylate adduct (A/ECA) (see Section 3.6 below).
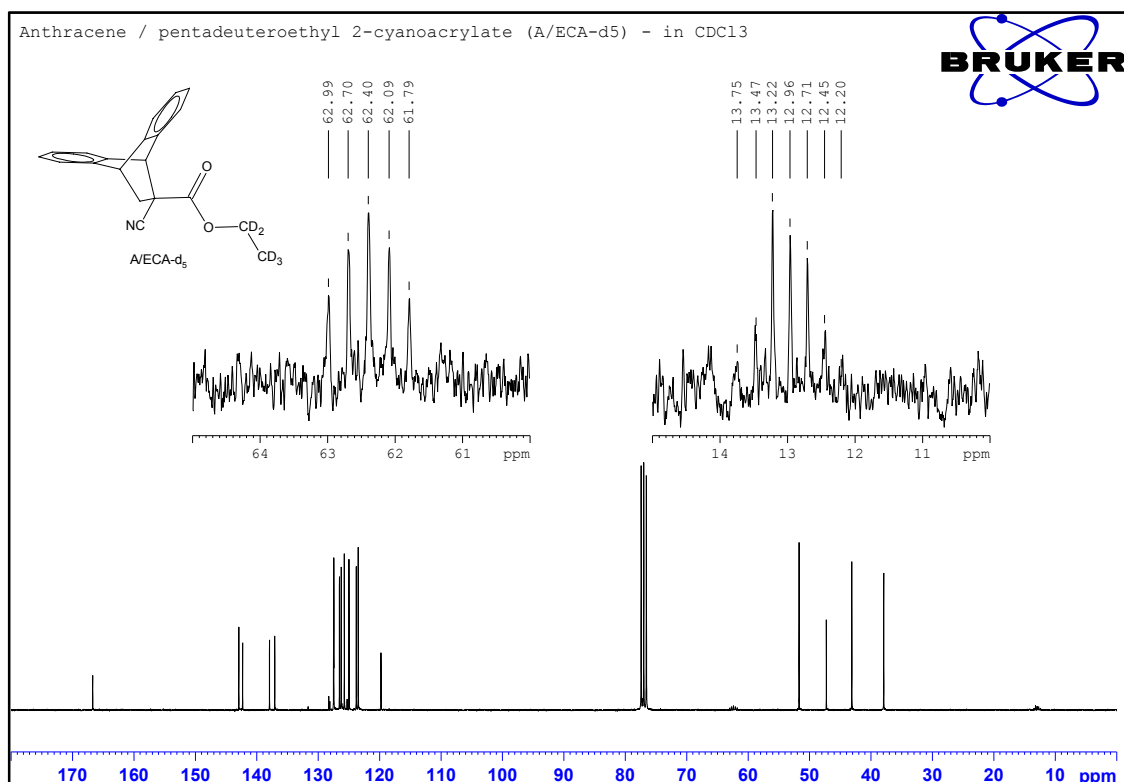
Figure 3.31: ^{13}C NMR spectrum of anthracene / pentadeuteroethyl 2-cyanoacrylate adduct (A/ECA-d$_5$) showing quintet (J_{CD}=23 Hz) for CD$_2$ group at 62.4 ppm and septet (J_{CD}=19 Hz) for CD$_3$ group at 13.0 ppm.

The ^{13}C NMR spectra of the corresponding monomers, trideuteromethyl 2-cyanoacrylate (MCA-d$_3$) and pentadeuteroethyl 2-cyanoacrylate (ECA-d$_5$), also show ^{13}C-^{2}H heteronuclear coupling. Table 3—5 summarises the chemical shifts, multiplicities and coupling constants for the four novel deuterated compounds synthesised during this project.

Compound	Assignment	Chemical shift (ppm)	Multiplicity	Coupling constant – J_{CD} (Hz)
A/MCA-d$_3$	CD$_3$	53.2	septet	22.3
A/ECA-d$_5$	CD$_2$	62.4	quintet	23
	CD$_3$	13.0	septet	19
MCA-d$_3$	CD$_3$	52.8	septet	22.6
ECA-d$_5$	CD$_2$	62.4	quintet	23
	CD$_3$	12.9	septet	19

Table 3—5: Summary of chemical shift, multiplicity and coupling constants for novel deuterated compounds.

3.5.3 FTIR spectroscopy

The FTIR spectra of all compounds synthesised were collected in transmission mode as KBr disks for solids or as thin films between two freshly pressed 13-mm KBr disks for liquids (details of instrumentation in Section 3.6 below). All spectra showed the expected vibrational bands for the functional groups present. Evidence of the reaction of the acid chloride – anthracene / 2-cyanoacryloyl chloride adduct (A/CAC) with moisture to form the corresponding carboxylic acid – anthracene / 2-cyanoacylic acid adduct (A/CAA) was provided by FTIR analysis. The FTIR spectrum of freshly prepared A/CAC is shown in Figure 3.32 below. It shows a peak at 1786 cm^{-1} for the carbonyl (C=O) stretch of the acid chloride, which is in the expected region. There is also, however, a smaller peak at 1722 cm^{-1}, which indicates that, even in this fresh sample, some A/CAA is present. Figure 3.33 shows three overlaid spectra of the same product (A/CAC) taken at various times after storage in a sealed vessel (exact time periods not recorded). The conversion from A/CAC to A/CAA is demonstrated by the appearance of a peak at ~1720 cm^{-1} corresponding to the C=O stretch of the carboxylic acid (A/CAA) (see Figure 3.34 for reference spectrum of pure A/CAA). In fact, it is possible to use FTIR to monitor the conversion by collecting an infrared spectrum of the freshly prepared A/CAC at regular time intervals. Although these kinetic experiments were not conducted, the conversion was found to begin almost immediately upon exposure to atmospheric moisture at room temperature. This highlighted the need to freshly prepare A/CAC for immediate use.
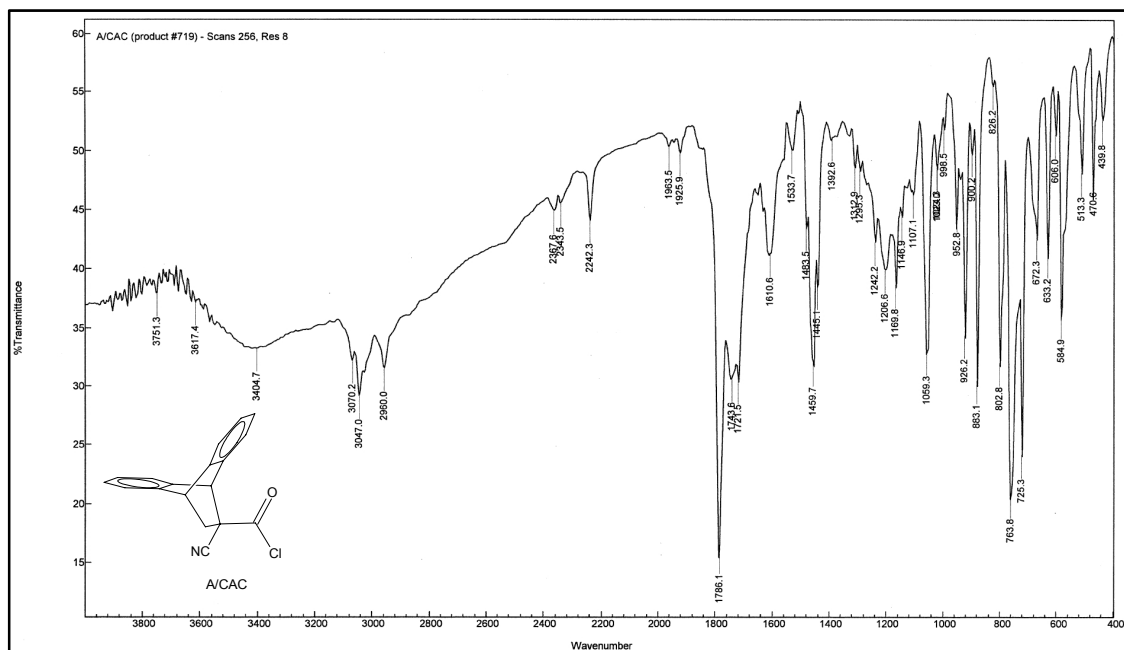
Figure 3.32: *FTIR spectrum of anthracene / 2-cyanoacryloyl chloride adduct (A/CAC).*
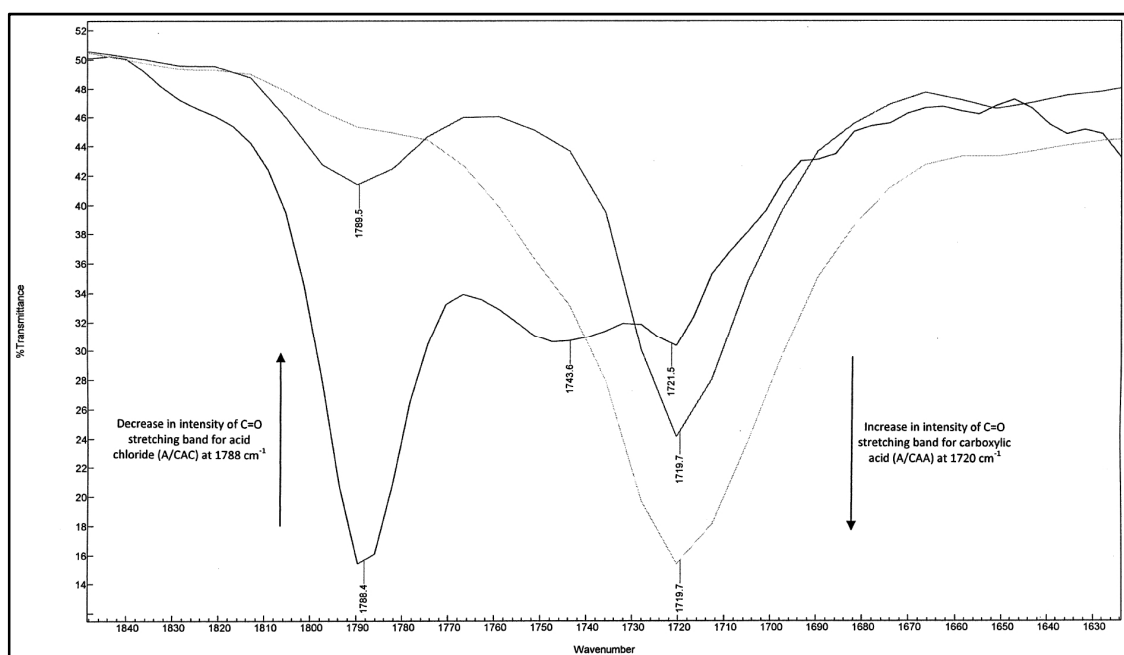
Figure 3.33: *Overlay of three FTIR spectra of A/CAC showing gradual conversion to A/CAA.*
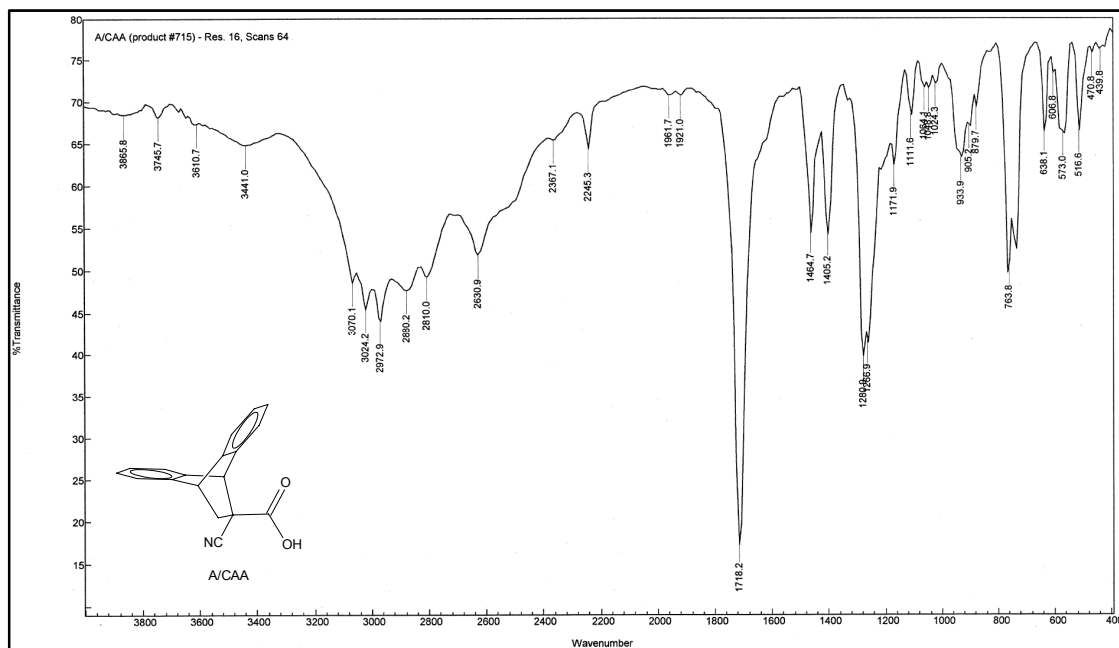
Figure 3.34: *FTIR spectrum of anthracene / 2-cyanoacylic acid adduct (A/CAA).*

As outlined in Section 1.3, the novel cyanoacrylate monomers synthesised during this project should exhibit infrared vibrational bands in the range 2500 – 1800 cm^{-1} and hence provide a target peak (or peaks) to create contrast between a treated fingerprint and the background surface. The actual substances that will ultimately be used to provide this contrast are the corresponding poly-(alkyl 2-cyanoacrylates), which are deposited (via fuming and polymerisation) preferentially on the ridges of the latent fingerprint. The infrared spectra of the poly-(alkyl 2-cyanoacrylates) are therefore of primary importance. Prior to obtaining a sample (and hence an infrared spectrum) of each of the novel poly-(alkyl 2-cyanoacrylates), the precursor anthracene / alkyl 2-cyanoacrylate adduct and the monomeric alkyl 2-cyanoacrylate are isolated. These compounds also contain the desired target functional groups and so their infrared spectra proved useful prior to the fuming of fingerprint samples. The following figures show the infrared spectra for anthracene / 2-cyanoethyl 2-cyanoacrylate adduct (A/2-CECA) (Figure 3.35), anthracene / 1-cyanoethyl 2-cyanoacrylate adduct (A/1-CECA) (Figure 3.36), anthracene / trideuteromethyl 2-cyanoacrylate adduct (A/MCA-d$_3$) (Figure 3.37) and anthracene / pentadeuteroethyl 2-cyanoacrylate adduct (A/ECA-d$_5$) (Figure 3.38).
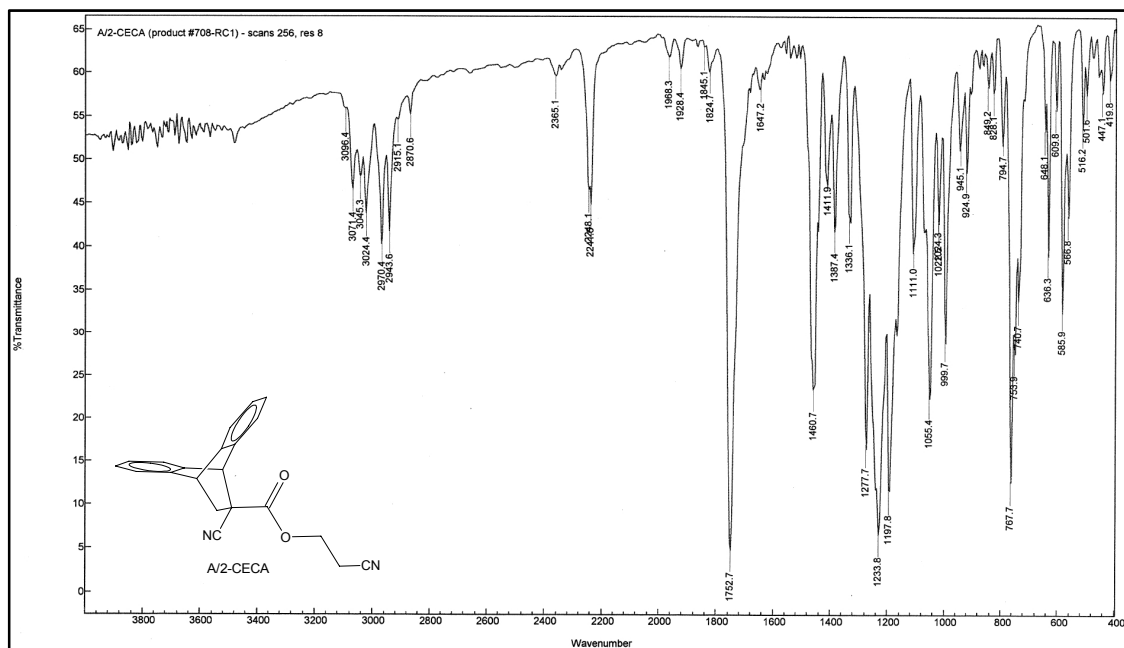
Figure 3.35: *FTIR spectrum of anthracene / 2-cyanoethyl 2-cyanoacrylate adduct (A/2-CECA).*
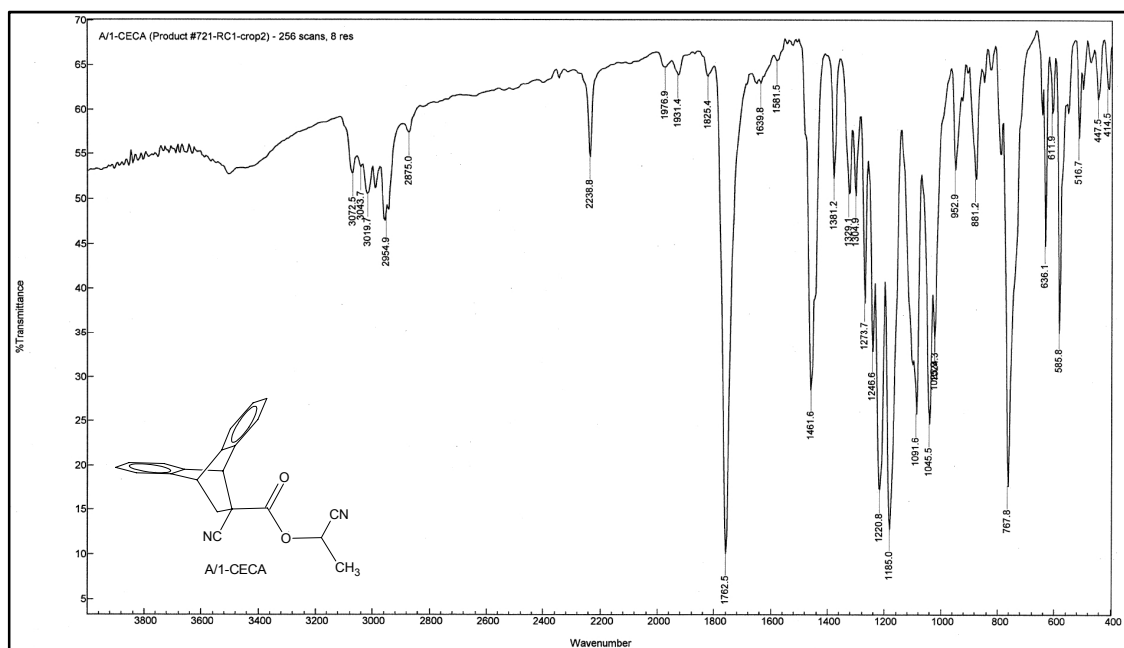
Figure 3.36: *FTIR spectrum of anthracene / 1-cyanoethyl 2-cyanoacrylate adduct (A/1-CECA).*
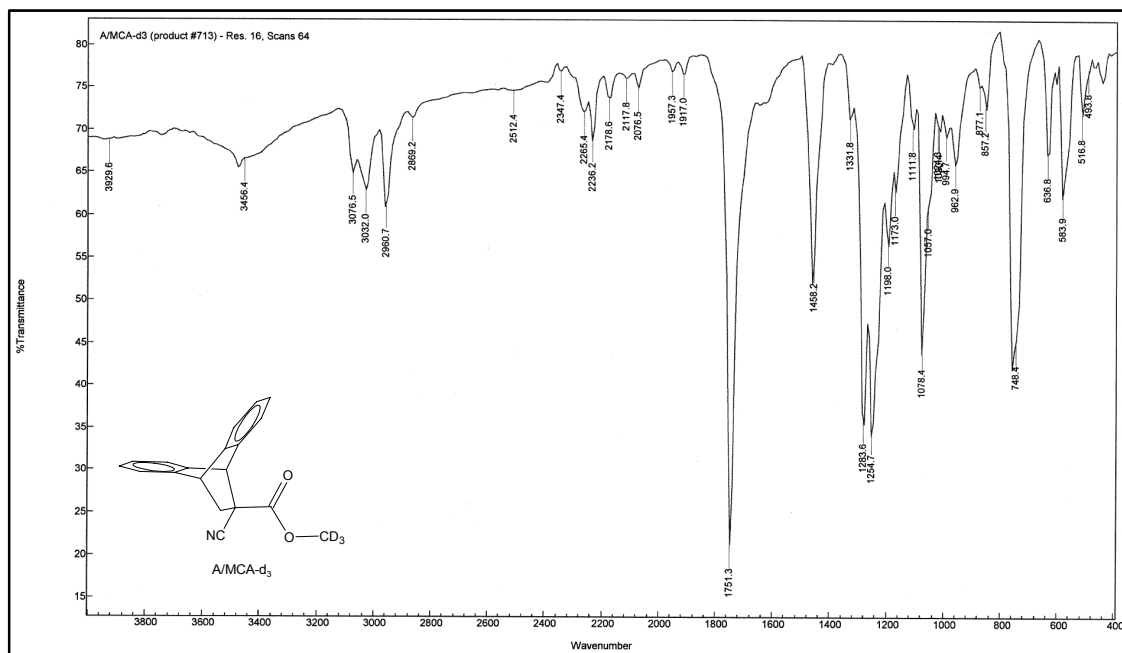
Figure 3.37: FTIR spectrum of anthracene / trideuteromethyl 2-cyanoacrylate adduct (A/MCA-d_3).
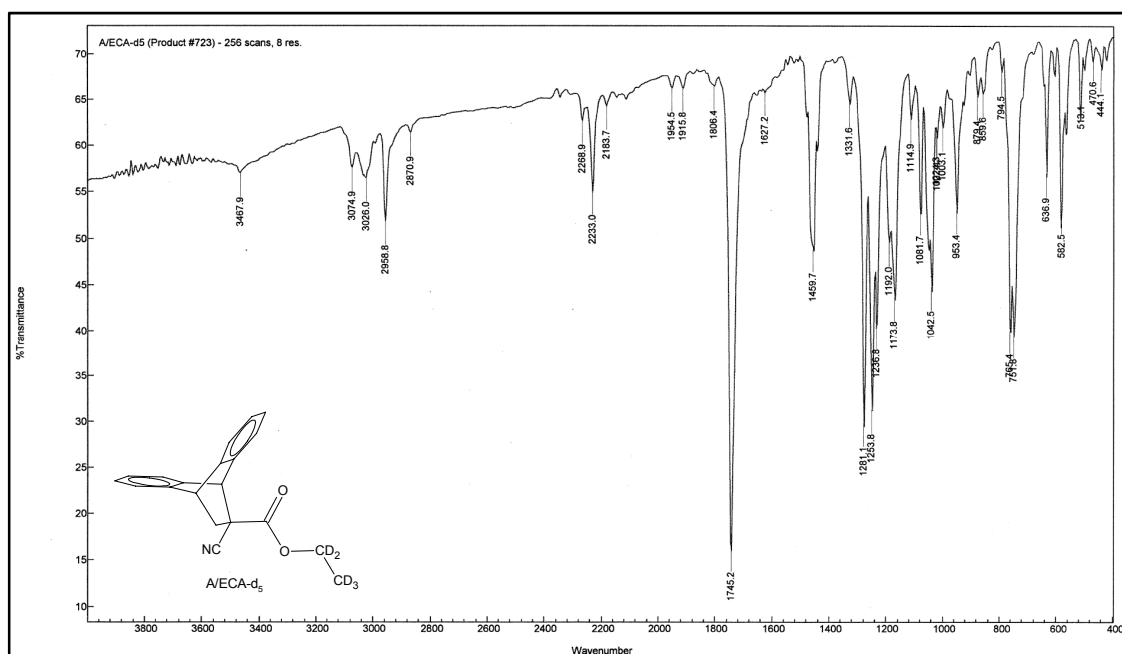
Figure 3.38: FTIR spectrum of anthracene / pentadeuteroethyl 2-cyanoacrylate adduct (A/ECA-d_5).

From these spectra, the frequency and intensity of peaks in the 'region of interest' (2500 – 1800 cm^{-1}) can be assessed. All compounds show absorbance in the expected region but the intensity of these peaks are relatively low. Nevertheless, the peaks in this area provide suitable targets for the FTIR chemical imaging of fingerprints treated with the novel

cyanoacrylates. A peak also worthy of note is the carbonyl stretch in the spectrum for A/1-CECA (see Figure 3.36). This peak appears at approximately 1763 cm^{-1}, which is 10 – 20 cm^{-1} higher than the corresponding peak in spectra of other anthracene / alkyl 2-cyanoacrylate adducts and alkyl 2-cyanoacrylate polymers. This shift to higher frequency is attributed to the close proximity of an additional electron-withdrawing group (nitrile) which strengthens the C=O bond, and thereby increases the associated stretching frequency. This shift in frequency became important for the FTIR chemical imaging of fingerprints treated with 1-CECA (see Section 4.3.4).

As outlined in Section 3.4.2 above, due to the relatively small quantities of product and the high probability of polymerisation, no attempts were made to distil or otherwise purify the novel alkyl 2- cyanoacrylate monomers. The purity was therefore not sufficient for direct FTIR analysis. After fuming latent fingerprints with the novel cyanoacrylates, however, the infrared spectrum of each polymer was obtained. This was made possible by collecting reflection spectra from the polymer deposited on the ridges of latent prints on infrared reflective slides. These spectra gave clear indications of the vibrational frequencies that may be used for infrared chemical imaging of fingerprints on more difficult surfaces and are presented and discussed in Section 4.3 below.

3.5.4   Elemental micro analysis

C, H and N elemental analysis is still considered an essential part of product characterisation and proof of product purity. During this project, a number of known and novel compounds were analysed on a Carlo Erba 1106 automatic analyser (Australian National University – Microanalytical Laboratory). The results of this analysis are reported in Section 3.6 below with the majority of analyses falling within 0.4% of the calculated values.

The elemental analysis for anthracene / 2-cyanoacryloyl chloride adduct (A/CAC) varied from the calculated for $C_{18}H_{12}ClNO$, with the calculated values being: C, 73.60; H, 4.12; N, 4.77 and the found: C, 75.09; H, 4.54; N, 5.24. This is due to the conversion of this acid chloride to the corresponding carboxylic acid (A/CAA) upon reaction with moisture as already noted in Sections 3.4.2 and 3.5.3 above.

It is important to note that the calculation of the percentage composition for the deuterated compounds anthracene / trideuteromethyl 2-cyanoacrylate adduct (A/MCA-d_3) and anthracene / pentadeuteroethyl 2-cyanoacrylate adduct (A/ECA-d_5) required a slight modification of that routinely used for compounds that do not contain deuterium. The percentage composition values for carbon and nitrogen were calculated in the usual manner, but in calculating the expected percentage composition of 'hydrogen', the deuterium atoms were considered as equivalent to hydrogen atoms. Hence A/MCA-d_3 was considered as having fifteen 'hydrogen' atoms (twelve ^{1}H atoms and three ^{2}H atoms) while A/ECA-d_5 was considered as having seventeen 'hydrogen' atoms (twelve ^{1}H atoms and five ^{2}H atoms). Using this approach, the following results were obtained:

A/MCA-d_3 – Calculated for $C_{19}H_{12}D_3NO_2$: C, 78.06; H(equivalent), 5.17; N, 4.79. Found: C, 77.81; H, 5.21; N, 4.68.

A/ECA-d_5 – Calculated for $C_{20}H_{12}D_5NO_2$: C, 77.89; H(equivalent), 5.56; N, 4.54. Found: C, 78.20; H, 5.56; N, 4.88.

The values found for these compounds corresponds well with the calculated values (within 0.34%), confirming their expected structures and indicating high purity.

It is also important to note that elemental analysis was not performed on any of the monomeric cyanoacrylate samples. As outlined in Section 3.4.2 above, due to the relatively small quantities of product and the high probability of polymerisation, no attempts were made to distil or otherwise purify the monomers. The purity was therefore not sufficient for elemental analysis. Furthermore, the reactivity of the monomers would necessitate the addition of stabilisers, which would also interfere with elemental analysis.

3.6   Experimental

Infrared spectra were recorded on a Nicolet Magna IR 760 spectrophotometer or Digilab FTS 7000 IR spectrophotometer. Liquid samples were placed directly between two freshly pressed 13-mm KBr disks and the spectra were collected in transmission. Solids were prepared as KBr disks and spectra were collected in transmission. All ^{1}H NMR spectra were obtained using a Bruker DRX NMR spectrometer operating at 300.13 MHz. Chemical shifts

are quoted on the δ scale, followed by proton integration, multiplicity (s = singlet, d = doublet, t = triplet, q = quartet, quin =quintet, sept = septet, m = multiplet, dd = doublet of a doublet, bs = broad singlet, bd = broad doublet), coupling in Hertz and proton assignment. All ^{13}C NMR spectra were obtained using the Bruker DRX NMR spectrometer operating at 75.48 MHz. Gas chromatography – mass spectrometry (GS-MS) was performed on a Hewlett Packard 5890 GC coupled to a 5970 series Mass Sensitive Detector. The fragmentation peaks for the mass spectra were reported if they had more than 10% abundance relative to the base peak. Elemental analyses were performed on a Carlo Erba 1106 automatic analyser (Australian National University – Microanalytical Laboratory). Melting points were obtained on a John Morris Electrothermal melting point apparatus and were corrected using benzoic acid (Mp. 122°C) as reference. Simultaneous thermogravimetric analysis (TGA) and differential thermal analysis (DTA) were performed on a SDT 2960 module (TA instruments) with a 10 °C/minute heating rate.

Drying of organic residues was performed using AR grade anhydrous Na_2SO_4. Benzene, toluene and *p*-xylene were dried by storing over sodium wire. Where anhydrous reaction conditions were needed, glassware was flame-dried prior to use and all reactions were performed under an atmosphere of nitrogen unless otherwise stated. Reactions were either stirred using magnetic stirring bars or IKA RW 20.n overhead mechanical stirrer.

Glassware used for the de-protection of anthracene / alkyl 2-cyanoacrylate adducts via retro-Diels-Alder reaction were treated with chromic acid cleaning solution and washed thoroughly with deionised water before being oven dried at 100 °C. The glassware was then treated with a solution of chlorotrimethylsilane (5% in toluene) followed by several washings with dry toluene an oven drying at 100 °C.

2-cyanoethyl cyanoacetate (2-CECAc)
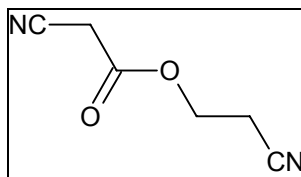
This reaction was performed in a 500-mL two-necked round bottom flask fitted with magnetic stirrer, Dean-Stark reflux trap with condenser and calcium chloride drying tube. Into the round bottom flask was charged cyanoacetic acid (85.0 g, 1.00 mol), 3-hydroxypropionitrile (79.6 g, 1.12 mol), Amberlyst 15 cationic exchange resin (6.00 g) as catalyst and anhydrous benzene (300 mL). Benzene (10 mL) was also charged into the side arm of the Dean Stark reflux trap to prevent any significant change in volume. The mixture was stirred to dissolve the cyanoacetic acid and heated via an oil bath. The oil bath temperature was slowly elevated over one hour to a maximum of 115 °C. The temperature was then maintained between 100 °C and 115 °C and the reaction progress was monitored by noting the volume of water collected. After 8 days (192 hours) approximately 14.0 mL water (78% of theoretical) had been collected and the rate of evolution has dropped significantly. The benzene was removed by rotary evaporation and the crude reaction mixture was placed under reduced pressure for a minimum of two hours to ensure complete solvent removal. The crude product was then subjected to vacuum distillation to yield 100.2 g (72.6%) 2-cyanoethyl cyanoacetate. Bp. 154 – 156 °C (1 mmHg). ^{1}H NMR (CDCl$_3$) : δ 2.79, 2H, t (*J*=6 Hz), CH$_2$**CH$_2$**CN; 3.58, 2H, s, NCC**H$_2$**COO; 4.42, 2H, t (*J*=6 Hz), **CH$_2$**CH$_2$CN. ^{13}C NMR (CDCl$_3$) : δ 18.3, 25.1, 61.3, 113.2, 116.9, 163.3. EI : *m/z* 68 (100), 54 (35), 40 (29), 41 (22), 28 (19), 27 (11). IR $\bar{v}_{max}$ (cm^{-1}): 3489, 2978, 2950, 2257, 1754, 1470, 1453, 1419, 1392, 1341, 1180, 1029. Calculated for C$_6$H$_6$N$_2$O$_2$: C, 52.17; H, 4.38; N, 20.28. Found: C, 51.46; H, 4.47; N, 20.04.

Oligo-2-cyanoethyl 2-cyanoacrylate (Oligo-2-CECA)
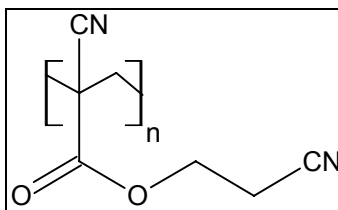
Into a 100-mL three-necked round bottom flask fitted with an overhead mechanical stirrer, dropping funnel and a Dean-Stark reflux trap equipped with a water-cooled condenser and nitrogen gas inlet was charged, under nitrogen, paraformaldehyde (3.00 g, 0.01 mol) and piperidine (0.055 g, 0.4 wt%). Next, anhydrous benzene (25 mL) was added for the azeotropic removal of water. Benzene (10 mL) was also added to the side arm of the Dean-Stark reflux trap to prevent a significant change in the volume of the reaction mixture while refluxing. At this point diethylene glycol dimethyl ether / diglyme (2.5 mL) was added to facilitate the reaction and to prevent the loss of paraformaldehyde during the reaction. To the refluxing mixture was added dropwise over 30 minutes 2-cyanoethyl cyanoacetate (0.10 mol, 13.8 g). A straw-coloured mass began to develop after just 15 minutes. Water began to collect in the Dean-Stark reflux trap after 20 minutes. The reaction was kept under reflux for two hours while removing the water formed by the reaction. The mixture was then cooled and solvent-stripped by rotary evaporation. The crude oligomer was treated with dichloromethane (20 mL) and benzene (10 mL) in order to remove the remaining diglyme and other organic impurities. The mixture separated into two layers and the top organic layer was decanted off. Two more organic extractions were performed using benzene (10 mL) for each before placing the crude oligomer under reduced pressure for a minimum of 1 hour to ensure complete solvent removal. The spectral characterisation of this compound was hampered by the presence of impurities and the nature of the compound. As discussed in Section 3.4.1 above, attempts to depolymerise this compound failed and so further attempts to isolate and characterise this compound were abandoned.

Anthracene / ethyl 2-cyanoacrylate adduct; ethyl 9,10-dihydro-9,10-

endoethanoanthracene-11-cyano-11-carboxylate (A/ECA)
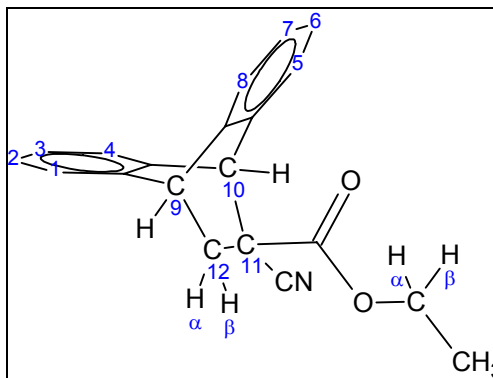
Into a 1-L two-necked round bottom flask fitted with an overhead mechanical stirrer and condenser with gas inlet valve was charged anthracene (53.5 g, 0.300 mol), ethyl 2-cyanoacrylate (41.3 g, 0.330 mol) inhibited with excess SO_2 and anhydrous benzene (600 mL) inhibited with a strong stream of SO_2 (minimum 5 minutes). The mixture was brought to reflux and the resulting solution was refluxed for a further 20 hours. The solution was cooled and 6.7 g unreacted anthracene was filtered. The benzene was then removed by rotary evaporation before placing the flask under reduced pressure for minimum of two hours to ensure complete solvent removal. The crude anthracene / ethyl 2-cyanoacrylate adduct (A/ECA) weighed 78.2 g (86%) and was used without further purification for the next step. ^{1}H NMR ($CDCl_3$) : δ 1.26, 3H, t (*J*=7 Hz), CH_2**CH₃**; 2.19, 1H, dd (*J*=2.7, 13.2 Hz), C12-**H**$_α$; 2.80, 1H, dd (*J*=2.7, 13.2 Hz), C12-**H**$_β$; 4.17, 2H, m, **CH**$_α$CH₃ and **CH**$_β$CH₃; 4.42, 1H, t (*J*=2.7 Hz), C9-**H**; 4.87, 1H, s, C10-**H**; 7.10 – 7.50, 8H, m, Ar**H**1 – **H**8. ^{13}C NMR ($CDCl_3$) : δ 14.0, 38.0, 43.2, 47.3, 51.8, 63.2, 119.8, 123.5, 123.8, 125.0, 125.8, 126.3, 126.6, 127.5, 127.6, 137.1, 138.0, 142.3, 143.0. IR $\bar{\nu}_{max}$ (cm^{-1}): 3074, 3016, 2985, 2961, 2232, 1747, 1458, 1369, 1276, 1224, 1189, 1097, 1048, 755, 637, 579.

Anthracene / 2-cyanoacrylic acid adduct; 9,10-dihydro-9,10-endoethanoanthracene-11-cyano-11-carboxylic acid (A/CAA)
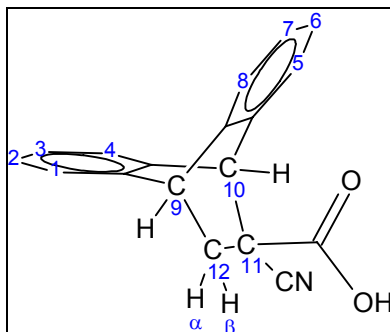
Into a 500-mL single-necked round bottom flask equipped with an overhead mechanical stirrer was charged the crude A/ECA product (78.2 g), absolute ethanol (200 mL) and potassium hydroxide (25.2 g, 0.450 mol) in water (200 mL). The resulting suspension was stirred at the ambient temperature (25 – 30 °C) for three hours Quenching of the reaction in water (1 L) and filtration afforded 8.8 g free anthracene. The orange-red filtrate was acidified to pH 2 with 10 M hydrochloric acid to precipitate the anthracene / 2-cyanoacrylic acid adduct (A/CAA) as a finely divided white solid. The A/CAA was filtered and washed with water and air dried at room temperature to yield 60.5 g (85.8%) of A/CAA. Mp. 201 – 204 °C (lit.[234] 199 – 203 °C). ^{1}H NMR (acetone-*d*6) : δ 2.21, 1H, dd (*J*=2.7, 12.9 Hz), C12-**H**$_\alpha$; 2.84, 1H, dd (*J*=2.7, 12.9 Hz), C12-**H**$_\beta$; 4.63, 1H, t (*J*=2.7 Hz), C9-**H**; 5.08, 1H, s, C10-**H**; 7.10 – 7.30, 4H, m, Ar**H**2, Ar**H**3, Ar**H**6 and Ar**H**7; 7.35 – 7.50, 3H, m, Ar**H**1, Ar**H**4 and Ar**H**8; 7.55 – 7.65, 1H, m, Ar**H**5. ^{13}C NMR (acetone-*d*6) : δ 39.0, 44.0, 48.1, 52.2, 121.0, 124.6, 124.7, 126.3, 126.7, 127.1, 127.2, 128.2, 138.8, 140.0, 144.0, 144.6, 168.2. IR $\bar{v}_{max}$ (cm^{-1}): 3070, 3024, 2972, 2880, :2810, 2631, 2245, 1718, 1464, 1405, 1281, 1267, 1171, 1112, 934, 763, 730, 638, 573, 517. Calculated for C$_{18}$H$_{13}$NO$_2$: C, 78.53; H, 4.76; N, 5.09. Found: C, 78.55; H, 4.94; N, 5.18.

Anthracene / 2-cyanoacrylic acid potassium salt adduct; Potassium 9,10-dihydro-9,10-endoethanoanthracene-11-cyano-11-carboxylate (A/CAA-K)
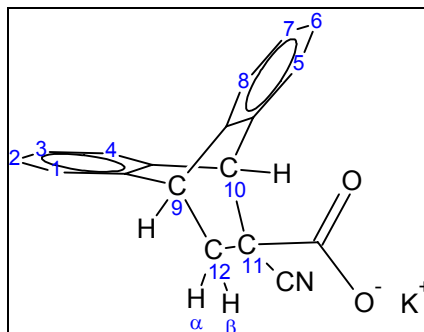
Into a 500-mL two-necked round bottom flask fitted with a mechanical stirrer and dropping funnel was charged a solution of A/CAA (27.5 g, 0.100 mol) in acetone (100 mL). The solution was stirred and neutralised from pH 2.5 to pH 9.5 by the addition of a 40% w/v solution of potassium hydroxide in absolute methanol. The suspension of white solids was stirred at room temperature for three hours, filtered, washed with 100 mL acetone and air-dried at room temperature to give 22.5 g (71.9%) of anthracene / 2-cyanoacrylic acid potassium salt adduct (A/CAA-K). Mp. 252 - 256 °C dec. (lit.[234] 250 – 260 °C). ^{1}H NMR (DMSO-*d6*) : δ 1.82, 1H, dd (*J*=2.9, 12.5 Hz), C12-**H**$_\alpha$; 2.75, 1H, dd (*J*=2.5, 12.5 Hz), C12-**H**$_\beta$; 4.33, 1H, t (*J*=2.6 Hz), C9-**H**; 4.77, 1H, s, C10-**H**; 6.95 – 7.40, 8H, m, Ar**H**1 – Ar**H**8. ^{13}C NMR (DMSO-*d6*) : δ 38.8, 43.3, 48.9, 51.4, 122.9, 123.4, 125.0, 125.3, 125.4, 125.5, 125.8, 125.8, 126.0, 140.3, 142.0, 143.7, 144.2, 165.6. IR $\bar{\nu}_{max}$ (cm^{-1}): 3471, 3073, 3028, 2961, 2938, 2862, 2238, 1615, 1458, 1352, 897, 793, 754, 642, 579, 519, 478. Calculated for $C_{18}H_{12}KNO_2$: C, 68.98; H, 3.86; N, 4.47. Found: C, 68.20; H, 3.97; N, 4.51.

Anthracene / 2-cyanoacryloyl chloride adduct; 9,10-dihydro-9,10-endoethanoanthracene-11-cyano-11-carboxylic acid chloride (A/CAC)
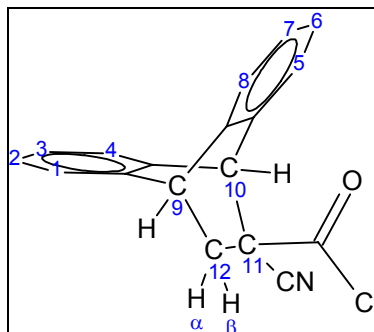
A suspension of A/CAA (41.3 g, 0.15 mol) in anhydrous benzene (150 mL) was stirred under nitrogen in a 500-mL three-necked round bottom flask fitted with overhead mechanical stirrer, dropping funnel and reflux condenser. The reaction was catalysed with a few drops of pyridine. Thionyl chloride (21.4 g / 13.1 mL, 0.18 mol) was added dropwise via the dropping funnel over a period of 20 minutes. The resulting mixture was stirred under nitrogen for one hour at 60 °C. An additional 5.95 g / 3.6 mL (0.05 mol) thionyl chloride was added and stirring continued for two hours. Further portions of thionyl chloride (2 mL) were added as required to ensure complete reaction. Since the desired product is soluble in warm benzene while the starting material (A/CAA) is not, the reactions completion was signified by the disappearance of A/CAA suspension. This typically required stirring at 60 °C for about four hours. Heating to temperatures exceeding 60 °C led to the appearance of anthracene in the final product due to a retro Diels-Alder side-reaction. The warm solution was filtered and allowed to cool. The white needles were collected and recrystallised from hot benzene to yield 19.8 g of anthracene / 2-cyanoacryloyl chloride adduct (A/CAC). A second crop (8.1 g) could be obtained by solvent-stripping the mother liquor and recrystallising the residue from hot benzene. Total yield 27.9 g (63.3%). Mp. 81 - 84 °C (lit.[234] 82 – 85 °C). ^{1}H NMR (CDCl$_3$) : δ 2.28, 1H, dd (*J*=2.7, 13.5 Hz), C12-**H**$_\alpha$; 2.75, 1H, dd (*J*=2.7, 13.5 Hz), C12-**H**$_\beta$; 4.45, 1H, t (*J*=2.7 Hz), C9-**H**; 5.06, 1H, s, C10-**H**; 7.10 – 7.30, 4H, m, Ar**H**2, Ar**H**3, Ar**H**6 and Ar**H**7; 7.30 – 7.45, 3H, m, Ar**H**1, Ar**H**4 and Ar**H**8; 7.50 – 7.60, 1H, m, Ar**H**5. ^{13}C NMR (CDCl$_3$) : δ 38.7, 43.0, 52.0, 57.9, 117.7, 123.6, 123.9, 125.4, 126.0, 126.8, 126.9, 127.9, 128.0, 135.5, 136.6, 141.7, 142.7, 168.6. IR $\bar{\nu}_{max}$ (cm^{-1}): 3070, 3047, 2960, 2242, 1786, 1744, 1722, 1611, 1460, 1445, 1242, 1207, 1170, 1059, 96, 883, 803, 764, 725, 672, 633, 585. Calculated for C$_{18}$H$_{12}$ClNO: C, 73.60; H, 4.12; N, 4.77. Found: C, 75.09; H, 4.54; N, 5.24.

Anthracene / 2-cyanoethyl 2-cyanoacrylate adduct; 2-cyanoethyl 9,10-dihydro-9,10-endoethanoanthracene-11-cyano-11-carboxylate (A/2-CECA)
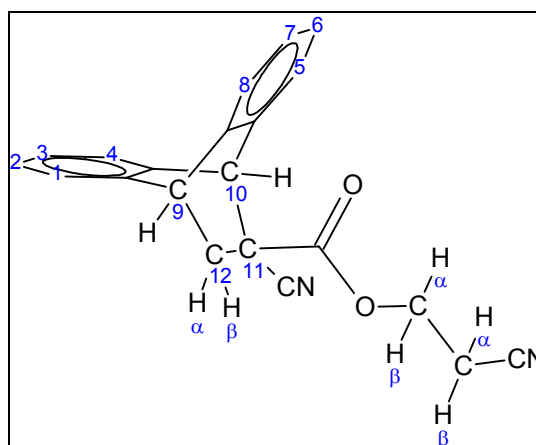
Into a 500-mL two-necked round bottom flask fitted with magnetic stirrer bar, dropping funnel and reflux condenser with gas inlet tube was charged under nitrogen A/CAC (29.5 g, 0.10 mol), triethylamine (12.1 g / 16.7 mL, 0.12 mol) and anhydrous benzene (150 mL). The solution was stirred under nitrogen and warmed to 60 °C. 3-hydroxypropionitrile (7.1 g, 0.10 mol) was added dropwise over one hour. After stirring at 60 °C for three hours, the suspension of triethylamine hydrochloride was diluted with benzene (300 mL) and extracted several times with saturated ammonium chloride solution followed by saturated sodium chloride solution. The benzene extract was collected and dried over anhydrous sodium sulfate and solvent-stripped under vacuum to yield 23.4 g (71.2%) of crude anthracene / 2-cyanoethyl 2-cyanoacrylate adduct (A/2-CECA). The crude product was recrystallised from ethanol to yield 20.8 g (63.1%) A/2-CECA. Mp. 127 – 129 °C. ^{1}H NMR (CDCl$_3$) : δ 2.26, 1H, dd (*J*=2.7, 13.2 Hz), C12-**H**$_\alpha$; 2.59 – 2.76, 2H, m, C**H**$_\alpha$CN and C**H**$_\beta$CN; 2.84, 1H, dd (*J*=2.7, 13.2 Hz), C12-**H**$_\beta$; 4.10 – 4.40, 2H, m, COOC**H**$_\alpha$ and COOC**H**$_\beta$; 4.48, 1H, t (*J*=2.7 Hz), C9-**H**; 4.96, 1H, s, C10-**H**; 7.10 – 7.30, 4H, m, Ar**H**2, Ar**H**3, Ar**H**6 and Ar**H**7; 7.30 – 7.45, 3H, m, Ar**H**1, Ar**H**4 and Ar**H**8; 7.50 – 7.60, 1H, m, Ar**H**5. ^{13}C NMR (CDCl$_3$) : δ 17.7, 37.9, 42.9, 47.2, 51.7, 61.0, 116.4, 119.1, 123.5, 124.0, 124.9, 125.9, 126.5, 126.7, 127.6, 127.7,.136.7, 137.5, 142.1, 142.7, 166.4. IR $\bar{\nu}_{max}$ (cm^{-1}): 3071, 3045, 3024, 2970, 2944, 2870, 2248, 2242, 1753, 1461, 1412, 1387, 1336, 1278, 1234, 1198, 1111, 1055, 1023, 1000, 768, 636, 586, 567. Calculated for C$_{21}$H$_{16}$N$_2$O$_2$: C, 76.81; H, 4.91; N, 8.31. Found: C, 76.67; H, 4.94; N, 8.32.

Anthracene / 1-cyanoethyl 2-cyanoacrylate adduct; 1-cyanoethyl 9,10-dihydro-9,10-endoethanoanthracene-11-cyano-11-carboxylate (A/1-CECA)
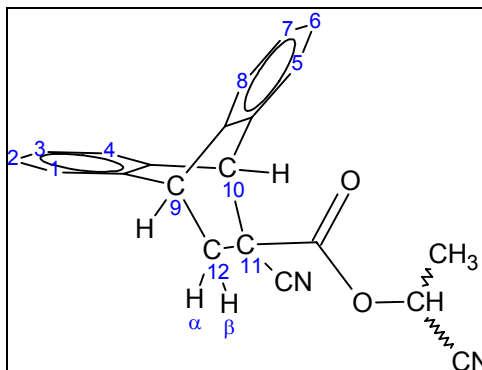
Into a 500-mL two-necked round bottom flask fitted with magnetic stirrer bar, dropping funnel and reflux condenser with gas inlet tube was charged under nitrogen A/CAC (29.5 g, 0.10 mol), triethylamine (12.1 g / 16.7 mL, 0.12 mol) and anhydrous benzene (150 mL). The solution was stirred under nitrogen and warmed to 60 °C and 2-hydroxypropionitrile (7.1 g, 0.10 mol) was added dropwise over 40 minutes. After stirring at 60 °C for three hours, the suspension of triethylamine hydrochloride was diluted with benzene (300 mL) and extracted several times with saturated ammonium chloride solution followed by saturated sodium chloride solution. The benzene extract was collected and dried over anhydrous sodium sulfate and solvent-stripped under vacuum to yield 22.9 g (69.5%) of crude anthracene / 1-cyanoethyl 2-cyanoacrylate adduct (A/1-CECA). The crude product was recrystallised from ethanol to yield a total of 18.2 g (55.3%) A/1-CECA in two crops. This product was a mixture of stereoisomers. The NMR spectra clearly show two distinct groups of resonances, resulting from two diastereoisomeric pairs of enantiomers with a ratio of approximately 53% *enantiomeric pair a* and 47% *enantiomeric pair b* (see Section 3.5.2 above for detailed discussion). ***Enantiomeric pair a:*** ^{1}H NMR (CDCl$_3$) : δ 1.67, 3H, d (*J*=6.9 Hz), C**H**$_3$; 2.25, 1H, dd (*J*=2.7, 13.2 Hz), C12-**H**$_\alpha$; 2.83, 1H, dd (*J*=2.7, 13.2 Hz), C12-**H**$_\beta$; 4.49, 1H, t (*J*=2.7 Hz), C9-**H**; 4.95, 1H, s, C10-**H**; 5.32, 1H, q (*J*=6.9 Hz), C**H**CN; 7.10 – 7.60, 8H, m, Ar**H**1 - Ar**H**8. ^{13}C NMR (CDCl$_3$) : δ 18.5, 37.9, 42.9, 47.1, 51.8, 59.4, 116.4, 118.7, 123.6, 123.9, 125.3, 125.9, 126.7, 126.8, 127.8, 127.9, 136.2, 136.2, 141.8, 142.7, 165.4. ***Enantiomeric pair b:*** ^{1}H NMR (CDCl$_3$) : δ 1.67, 3H, d (*J*=6.9 Hz), C**H**$_3$; 2.30, 1H, dd (*J*=2.7, 13.2 Hz), C12-**H**$_\alpha$; 2.80, 1H, dd (*J*=2.7, 13.2), C12-**H**$_\beta$; 4.49, 1H, t (*J*=2.7 Hz), C9-**H**; 4.89, 1H, s, C10-**H**; 5.27, 1H, q (*J*=6.9 Hz), C**H**CN, 7.10 – 7.60, 8H, m, Ar**H**1 - Ar**H**8. ^{13}C NMR (CDCl$_3$) : δ 18.6, 38.6, 42.9, 47.2, 51.7, 59.6, 116.0, 118.5, 123.6, 124.1, 124.9, 125.9, 126.5, 126.8, 127.8, 127.9, 136.5, 137.3, 142.1, 142.6, 165.5. IR

$\bar{v}_{max}$ (cm^{-1}): 3073, 3044, 3020, 2955, 2875, 2239, 1977, 1931, 1825, 1762, 1461, 1381, 1329, 1305, 1274, 1247, 1221, 1185, 1092, 1046, 1026, 953, 881, 768, 636, 586, 517. Calculated for $C_{21}H_{16}N_2O_2$: C, 76.81; H, 4.91; N, 8.31. Found: C, 76.48; H, 4.97; N, 8.35.

Anthracene / methyl 2-cyanoacrylate adduct; methyl 9,10-dihydro-9,10-endoethanoanthracene-11-cyano-11-carboxylate (A/MCA)
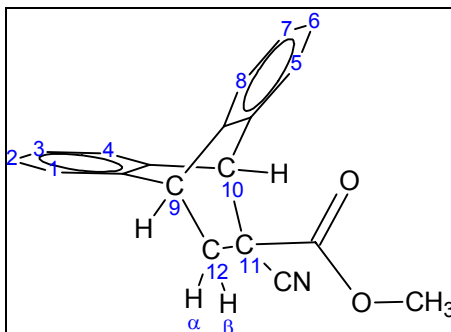

The reaction was performed under nitrogen in a 100-mL two-necked round bottom flask fitted with magnetic stirrer bar, dropping funnel and reflux condenser. A mixture of methanol (0.32 g / 0.405 mL, 0.01 mol) and triethylamine (1.52 g / 2.09 mL, 0.015 mol) in anhydrous DMF (2.5 mL) was added dropwise over 30 minutes at room temperature to a stirred solution of A/CAC (2.94 g, 0.01 mol) in anhydrous DMF (2.5 mL). The suspension of triethylamine hydrochloride was poured into water (75 mL) to precipitate the adduct as an orange gum. The latter was extracted into benzene (2×50 mL) and the extract was washed with water then saturated sodium chloride solution, filtered and solvent-stripped to a gum to yield 1.50 g (51.9%) crude anthracene / methyl 2-cyanoacrylate adduct (A / MCA). The crude product was analysed by ^{1}H and ^{13}C NMR only and the spectra were used for comparison with the spectra for the deuterated product (below). ^{1}H NMR (CDCl$_3$) : δ 2.25, 1H, dd (*J*=2.7, 12.9 Hz), C12-**H**$_\alpha$; 2.84, 1H, dd (*J*=2.7, 12.9 Hz), C12-**H**$_\beta$; 3.75, 3H, s, C**H**$_3$; 4.45, 1H, t (*J*=2.7 Hz), C9-**H**; 4.91, 1H, s, C10-**H**; 7.10 – 7.60, 8H, m, Ar**H**1 – Ar**H**8. ^{13}C NMR (CDCl$_3$) : δ 38.1, 43.1, 47.3, 51.7, 53.8, 119.6, 123.5, 123.8, 124.8, 125.8, 126.4, 126.6, 127.5, 127.5, 137.1, 137.8, 142.2, 142.9, 167.3.

Anthracene / trideuteromethyl 2-cyanoacrylate adduct; trideuteromethyl 9,10-dihydro-9,10-endoethanoanthracene-11-cyano-11-carboxylate (A/MCA-d₃)
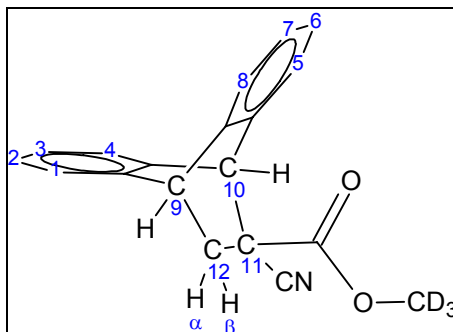
Into a 500-mL two-necked round bottom flask fitted magnetic stirrer bar, dropping funnel and reflux condenser was charged under nitrogen, A/CAC (29.5 g, 0.10 mol) and triethylamine (12.1 g / 16.7 mL, 0.12 mol) in anhydrous benzene (150 mL). Methanol-d_4 (3.61 g / 4.06 mL, 0.10 mol) was added dropwise over 10 minutes. After stirring at 60 °C for three hours, the suspension of triethylamine hydrochloride was diluted with benzene (300 mL) and extracted several times with saturated ammonium chloride solution followed by saturated NaCl solution. The benzene extract was collected and dried over anhydrous sodium sulfate and solvent-stripped under vacuum to yield 20.81 g (71.3%) crude anthracene / trideuteromethyl 2-cyanoacrylate adduct (A/MCA-d₃). The crude product was recrystallised from ethanol to yield 17.73 g (60.7%) A/MCA-d₃ in three crops. Mp. 97 – 99 °C. ^{1}H NMR (CDCl₃) : δ 2.24, 1H, dd (*J*=2.7, 13.2 Hz), C12-**H**$_\alpha$; 2.83, 1H, dd (*J*=2.7, 13.2 Hz), C12-**H**$_\beta$; 4.46, 1H, t (*J*=2.7 Hz), C9-**H**; 4.91, 1H, s, C10-**H**; 7.10 – 7.60, 8H, m, Ar**H**1 – Ar**H**8. ^{13}C NMR (CDCl₃) : δ 38.1, 43.2, 47.3, 51.8, 53.2 (sept – *J*$_{CD}$=22.3 Hz), 119.7, 123.6, 124.0, 124.9, 125.9, 126.5, 126.7, 127.6, 127.6,.137.2, 137.9, 142.3, 143.0, 167.4. IR $\bar{\nu}_{max}$ (cm^{-1}): 3077, 3032, 2961, 2869, 2265, 2236, 2178, 2118, 2077, 1957, 1917, 1751, 1458, 1332, 1284, 1255, 1198, 1173, 1112, 1078, 963, 857, 748, 637, 584, 517. Calculated for $C_{19}H_{12}D_3NO_2$: C, 78.06; H(equivalent), 5.17; N, 4.79. Found: C, 77.81; H, 5.21; N, 4.68.

Anthracene / pentadeuteroethyl 2-cyanoacrylate adduct; pentadeuteroethyl 9,10-dihydro-9,10-endoethanoanthracene-11-cyano-11-carboxylate (A/ECA-d$_5$)
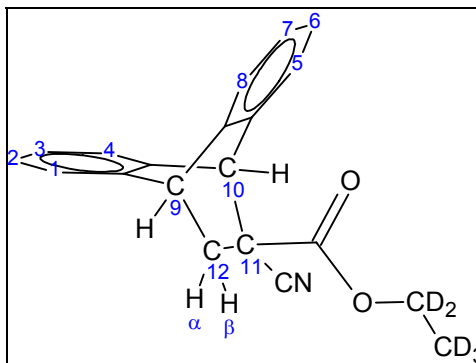
Into a 500-mL two-necked round bottom flask fitted magnetic stirrer bar, dropping funnel and reflux condenser was charged under nitrogen, A/CAC (29.5 g, 0.10 mol) and triethylamine (12.1 g / 16.7 mL, 0.12 mol) in anhydrous benzene (150 mL). Ethanol-d$_6$ (5.21 g / 5.84 mL, 0.10 mol) was added dropwise over 10 minutes. After stirring at 60 °C for three hours, the suspension of triethylamine hydrochloride was diluted with benzene (300 mL), filtered and extracted several times with saturated ammonium chloride solution followed by saturated NaCl solution. The benzene extract was collected and dried over anhydrous sodium sulfate and solvent-stripped under vacuum to yield 19.48 g (63.2%) crude anthracene / pentadeuteroethyl 2-cyanoacrylate adduct (A/ECA-d$_5$). The crude product was recrystallised from ethanol to yield 17.7 g (57.5%) A/ECA-d$_5$. Mp. 126 – 127 °C. ^{1}H NMR (CDCl$_3$) : δ 2.24, 1H, dd (*J*=2.7, 12.9 Hz), C12-**H**$_α$; 2.84, 1H, dd (*J*=2.7, 12.9 Hz), C12-**H**$_β$; 4.46, 1H, t (*J*=2.7 Hz), C9-**H**; 4.91, 1H, s, C10-**H**; 7.10 – 7.60, 8H, m, Ar**H**1 – Ar**H**8. ^{13}C NMR (CDCl$_3$) : δ 13.0 (sept - *J*$_{CD}$=19 Hz), 37.9, 43.1, 47.3, 51.7, 62.4 (quin – *J*$_{CD}$=23 Hz), 119.8, 123.5, 123.8, 124.4, 125.8, 126.3, 126.6, 127.4, 127.5, 137.1, 137.9, 142.3, 142.9, 166.7. IR $\bar{v}_{max}$ (cm^{-1}): 3075, 3026, 2959, 2871, 2269, 2233, 2184, 1955, 1916, 1745, 1460, 1332, 1281, 1254, 1237, 1192, 1174, 1115, 1082, 1043, 953, 765, 752, 637, 583, 513. Calculated for C$_{20}$H$_{12}$D$_5$NO$_2$: C, 77.89; H(equivalent) 5.56; N, 4.54. Found: C, 78.20; H, 5.56; N, 4.88.

2-cyanoethyl 2-cyanoacrylate (2-CECA)
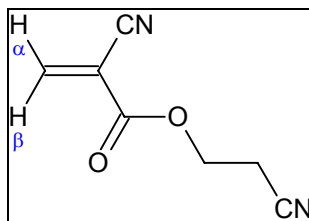
Into a 500-mL two-necked round bottom flask fitted with a small condenser, gas inlet valve, rubber septum and a magnetic stirrer was charged under SO_2, A/2-CECA (32.8 g, 0.10 mol), powdered maleic anhydride (9.81 g, 0.10 mol), phosphorus pentoxide (~1 g; based on 10 g / mole monomer), hydroquinone (~15 mg, 1000 ppm based on theoretical yield of monomer) and anhydrous *p*-xylene (300 mL) inhibited with a strong stream of SO_2 (minimum 5 minutes). SO_2 (polymerisation inhibitor) was introduced into the system via an inlet tube on top of the condenser and the reaction mixture was brought to a gentle reflux. The reaction was monitored by NMR of regularly withdrawn 100-μL aliquots in $CDCl_3$. Once NMR indicated the reaction's completion (45 hours), the mixture was allowed to cool to room temperature and the anthracene / maleic anhydride adduct (A/MA) was filtered off. The mixture was solvent-stripped at 35 − 40 °C under reduced pressure. The crude product was dissolved in anhydrous benzene (inhibited with SO_2), cooled and filtered to remove any residual crystalline A/MA. The residual xylene was removed by repeated addition and evacuation of anhydrous benzene (inhibited with SO_2) to yield crude monomer, which was stabilised with P_2O_5 and hydroquinone and kept in benzene solution (100 mL) under SO_2 until just prior to use. The purity of the crude monomer, 6.44 g (42.9%) was found by NMR to be approximately 80%, with A/2-CECA and A/MA being the only contaminants. ^{1}H NMR ($CDCl_3$) : δ 2.83, 2H, t (*J*=6.3 Hz), C**H₂**CN; 4.50, 2H, t (*J*=6.3 Hz), COOC**H₂**; 6.73, 1H, s, C=C**H**$_\alpha$; 7.13, 1H, s, C=C**H**$_\beta$. ^{13}C NMR ($CDCl_3$) : δ 17.7, 60.6, 113.8, 115.6, 116.1, 144.5, 159.8.

1-cyanoethyl 2-cyanoacrylate (1-CECA)
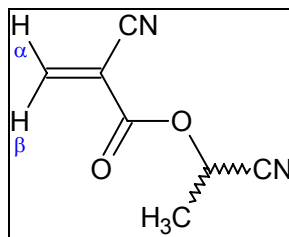
Into a 500-mL two-necked round bottom flask fitted with a small condenser, gas inlet valve, rubber septum and a magnetic stirrer was charged under SO_2, A/1-CECA (16.4 g, 0.05 mol), powdered maleic anhydride (5.88 g, 0.06 mol) and anhydrous *p*-xylene (300 mL) inhibited with a strong stream of SO_2 (minimum 5 minutes). SO_2 (polymerisation inhibitor) was introduced into the system via an inlet tube on top of the condenser and the reaction mixture was brought to a gentle reflux. The reaction was monitored by NMR of regularly withdrawn 100-μL aliquots in $CDCl_3$. Once NMR indicated the reaction's completion (71.5 hours), the mixture was allowed to cool to room temperature and the anthracene / maleic anhydride adduct (A/MA) was filtered off. The mixture was solvent-stripped at 35 – 40 °C under reduced pressure. The crude product was dissolved in anhydrous benzene (inhibited with SO_2), cooled and filtered to remove any residual crystalline A/MA. The residual xylene was removed by repeated addition and evacuation of anhydrous benzene (inhibited with SO_2) to yield crude monomer, which was kept in benzene solution (100 mL) under SO_2 until just prior to use. The crude monomer (4.57 g) was found by NMR to be a mixture of approximately 50% w/w 1-CECA and 50% w/w A/1-CECA. Based on this, the yield was taken to be ~2.3 g (~31%) 1-CECA. ^{1}H NMR ($CDCl_3$) : δ 1.78, 3H, d (*J*=6.9 Hz), C**H**$_3$; 5.50, 1H, q (*J*=6.6 Hz), C**H**CN; 6.56, 1H, s, C=C**H**$_\alpha$; 7.06, 1H, s, C=C**H**$_\beta$. ^{13}C NMR ($CDCl_3$) : δ 17.9, 59.1, 113.3, 114.5, 116.2, 144.8, 158.7.

Trideuteromethyl 2-cyanoacrylate (MCA-d₃)
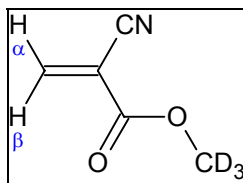
Into a 500-mL two-necked round bottom flask fitted with a small condenser, gas inlet valve, rubber septum and a magnetic stirrer was charged under SO_2, A/MCA-d₃ (15.0 g, 0.051 mol), powdered maleic anhydride (6.05 g, 0.062 mol) and anhydrous *p*-xylene (300 mL) inhibited with a strong stream of SO_2 (minimum 5 minutes). SO_2 (polymerisation inhibitor) was introduced into the system via an inlet tube on top of the condenser and the reaction mixture was brought to a gentle reflux. The reaction was monitored by NMR of regularly withdrawn 100-μL aliquots in $CDCl_3$. Once NMR indicated the reaction's completion (48 hours), the mixture was allowed to cool to room temperature and the anthracene / maleic anhydride adduct (A/MA) was filtered off. The mixture was solvent-stripped at 35 – 40 °C under reduced pressure. The crude product was dissolved in anhydrous benzene (inhibited with SO_2), cooled and filtered to remove any residual crystalline A/MA. The residual xylene was removed by repeated addition and evacuation of anhydrous benzene (inhibited with SO_2) to yield crude monomer, which was kept in benzene solution (100 mL) under SO_2 until just prior to use. The crude monomer (5.55 g) was found by NMR to be a mixture of approximately 70% w/w MCA-d₃ and 30% w/w A/MCA-d₃ with small traces of A/MA. Based on this, the yield was taken to be ~3.89 g (~66.3%) MCA-d₃. ^{1}H NMR ($CDCl_3$) : δ 7.04, 1H, s, C=**CH**$_\alpha$; 6.60, 1H, s, C=**CH**$_\beta$. ^{13}C NMR ($CDCl_3$) : δ 52.8 (sept - J_{CD}=22.6 Hz), 114.4, 116.8,143.5, 161.0.

Pentadeuteroethyl 2-cyanoacrylate (ECA-d$_5$)
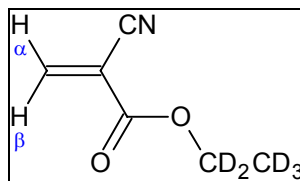
Into a 500-mL two-necked round bottom flask fitted with a small condenser, gas inlet valve, rubber septum and a magnetic stirrer was charged under SO$_2$, A/ECA-d$_5$ (30.8 g, 0.10 mol), powdered maleic anhydride (10.79 g, 0.11 mol) and anhydrous *p*-xylene (350 mL) inhibited with a strong stream of SO$_2$ (minimum 5 minutes). SO$_2$ (polymerisation inhibitor) was introduced into the system via an inlet tube on top of the condenser and the reaction mixture was brought to a gentle reflux. The reaction was monitored by NMR of regularly withdrawn 100-μL aliquots in CDCl$_3$. Once NMR indicated the reaction's completion (97.5 hours), the mixture was allowed to cool to room temperature and the anthracene / maleic anhydride adduct (A/MA) was filtered off. The mixture was solvent-stripped at 35 – 40 °C under reduced pressure. The crude product was dissolved in anhydrous benzene (inhibited with SO$_2$), cooled and filtered to remove any residual crystalline A/MA. The residual xylene was removed by repeated addition and evacuation of anhydrous benzene (inhibited with SO$_2$) to yield crude monomer, which was kept in benzene solution (100 mL) under SO$_2$ until just prior to use. Some product was lost during removal of residual solvent due to the volatility of monomer. The crude monomer (14.07 g) was found by NMR to be a mixture of approximately 50% w/w ECA-d$_5$ and 50% w/w A/ECA-d$_5$. Based on this, the yield was taken to be ~7 g (~54%) ECA-d$_5$. ^{1}H NMR (CDCl$_3$) : δ 6.61, 1H, s, C=C**H**$_\alpha$; 7.07, 1H, s, C=C**H**$_\beta$. ^{13}C NMR (CDCl$_3$) : δ 12.9 (sept - J_{CD}=19 Hz), 62.4 (quin – J_{CD}=23 Hz), 114.4, 116.8,142.9, 160.4.

Chapter 4: Use of novel cyanoacrylates for latent fingerprint enhancement

Chapter 4: Use of novel cyanoacrylates for latent fingerprint enhancement

4.1 Introduction

The use of cyanoacrylates for the detection and enhancement of latent fingerprints has been discussed in detail in Section 1.1.6.2.1. This method involves the selective polymerisation of monomeric cyanoacrylate along the ridges of latent fingerprints. On typical non-porous surfaces, such as clear glass, most plastics or metals, the latent fingerprint is rendered visible due to the white polymeric film deposited on the ridges. Other surfaces may require further treatment, such as luminescent staining, to visualise the developed print. On difficult surfaces (see Section 1.1.7), however, the cyanoacrylate-fumed print may be difficult or impossible to image using traditional optical or luminescence visualisation. In these cases infrared chemical imaging has been shown to yield superior results.[75]

For the infrared chemical imaging of fingerprints, the contrast between the fingerprint ridges and background is based on differences between the infrared spectra of areas where the ridges lie and areas void of fingerprint ridge detail (i.e. the furrows or background). Since most non-porous backgrounds on which fingerprints may be present have some mid-infrared absorption of their own, it is desirable to have a fingerprint reagent that has a mid-infrared absorption peak that is distinctive and not present in the infrared spectra of most common background materials. Key functional groups which have mid-infrared absorbance in a part of the spectrum which is generally free from interfering peaks are outlined in Section 1.3 and summarised in Table 1—3.

At first glance, cyanoacrylate appears to contain an ideal infrared absorption peak for infrared imaging, that due to the nitrile ($C\equiv N$) functional group. Unfortunately, although the peak for this functional group is present in the infrared spectrum of monomeric cyanoacrylate, its intensity diminishes to almost zero upon polymerisation. To explore this phenomenon, it is useful to consider the processes involved during the polymerisation of alkyl 2-cyanoacrylates. This is an area which has been explored by a number of authors and the following is a summary of work in this area.

4.1.1 Cyanoacrylate curing (polymerisation)

Many studies have identified various initiators of cyanoacrylate polymerisation. Below is a list of some compounds and species that can act as polymerisation initiators:

- simple anions (OH^-, CN^-, I^-, Br^-, CH_3COO^- etc)
- any traces of residual moisture, including water molecules adsorbed on the surface of a substrate
- trace metals
- bases (e.g. primary, secondary and tertiary amines, phosphines)

Photoinitiated polymerisation has also been described[65,289,290] and so too has radically initiated polymerisation[49,69-73] but these usually do not occur during general use such as adhesive bonding.[70] Polymerisation is inhibited by acids, which makes them useful as stabilisers (see Section 3.1).

The phenomenon of the decrease in intensity of the C≡N stretching band from cyanoacrylate upon polymerisation (describe above) was first noted by Shibasaki and Suetaka in 1975:

"The band arisen from the C≡N stretching vibration gradually decreased in intensity in the course of polymerisation and disappeared completely when polymerisation was completed. The C≡N groups might be changed to form C=N or C–N bonds. Further work is necessary to solve these problems".[50]

In 1977, Donnelly et al. studied the polymerisation of alkyl 2-cyanoacrylates.[51] At this time, alkyl 2-cyanoacrylates were already being used extensively as adhesives in industry and medicine. The polymerisation was assumed to be anionic in mechanism (as shown in Figure 3.2 and Figure 3.3 above) but there were no reports of quantitative comparisons with other vinyl monomers, or even systematic investigations.[51] Donnelly et al. proposed for the first time that different initiators can provoke two distinct mechanisms: (i) anionic living polymerisation initiated by conventional initiators but also by very stable anions, including simple anions such as CH_3COO^-, CN^-, I^-, Br^- (but probably not Cl^-); and (ii) polymerisation initiated by covalent organic bases in which the growing species are presumably zwitterions (see Figure 4.1).[51] A negative temperature coefficient of overall rate was found for polymerisation initiated by covalent bases, indicating that the overall rate must be a

composite rate and must include the influence of a termination process.[51] Neither type of reaction was suppressed by traces of O_2, CO_2, H_2O or CH_3OH, which would effectively "kill" the anionic polymerisation of monomers (e.g. styrene, 1- methyl styrene etc.) giving less stable anions.[51,52]
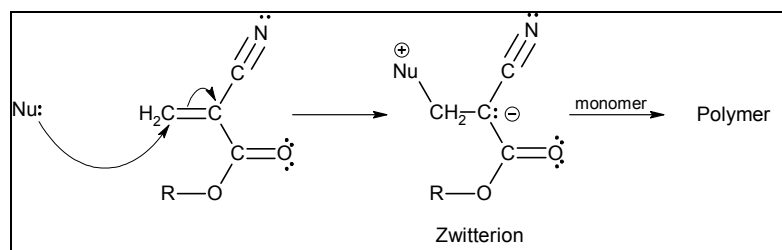
Figure 4.1: *Polymerisation of cyanoacrylate with a Lewis base as the nucleophilic initiator (Nu:) forming a zwitterion, which subsequently reacts with additional monomer to form the polymer.*

Later work provided direct evidence of a zwitterionic propagating species when initiation is via organic bases.[53] Extensive work was carried out into the kinetics and mechanisms of this process.[51-53,58,60,64,256,291-293] Also worthy of note is the work by Klemarczyk who investigated the differences in reactivity between ethyl cyanoacrylate with various phosphines and amines and succeeded in isolating and characterising a stable zwitterionic species.[67] The research in this area is beyond the scope of this thesis and the reader is referred to the aforementioned articles for a thorough treatment.

The reactivity and complexities involved in the thermal degradation / depolymerisation of alkyl 2-cyanoacrylates has been discussed in detail in Section 3.3.2 above. The observations regarding the polymerisation of alkyl 2-cyanoacrylates (primarily reported by Donnelly, Pepper, Johnston and co-workers) again highlight the extreme reactivity of alkyl 2-cyanoacrylates and the complexities involved in their behaviour. This has implications for the use of cyanoacrylates for the development of latent fingerprints and for the infrared chemical imaging of developed prints. Since latent fingerprint residue contains a number of potential polymerisation inhibitors, both the anionic and zwitterionic mechanisms of polymerisation may be at play when cyanoacrylate monomer vapours come in to contact with latent print residue. Each mechanism is governed by different kinetic factors and may give rise to a variety of polymeric structures (varying molecular weight and morphology, for example). Indeed the complexity involved in the fuming of latent fingerprints and the variations in polymer deposition has already been the subject of investigation[9,14,77-79,294] and has been discussed in detail in Section 1.1.6.2.1.

A number of spectroscopic techniques have been used to investigate and monitor the curing or polymerisation of alkyl 2-cyanoacrylates. Kusaka and Suetaka reported the use of reflection infrared (IR) spectroscopy to investigate the adhesive molecules in the first monolayer of cyanoacrylate on anodically oxidised aluminium mirrors.[54] The vibrational spectrum of this monolayer could be derived from the spectral change obtained on changing the layer thickness. On decreasing the adhesive layer thickness, shifts in band position were found. These authors reported that the C=O stretch at 1750 cm^{-1} decreases in frequency with decreasing layer thickness and the C–O–C stretch at 1250 cm^{-1} increases in frequency with decreasing layer thickness. [54] Previous work had shown that the C=O stretching frequency of an ester decreases upon hydrogen bond formation through the carbonyl group, while that of the antisymmetric stretching vibration of C–O–C group moves to a higher frequency, and so Kusaka and Suetaka reported that the hydroxy groups of the oxide layer are *"probably forming hydrogen bonds with cyanoacrylate molecule".*[54]

A subsequent article by Suetaka again suggests (based on the shifts of the C=O and C-O-C bands) that a hydrogen bond is formed between the cyanoacrylate polymer and the oxide present on the aluminium surface.[57] This band shift is also attributed to an overlapping of the band of the first monolayer and that of the subsequent layers. Suetaka reports that as the thickness of the layer increases, the centre of gravity of these two bands shifts from 1744 cm^{-1} (the frequency associated with the first monolayer) to 1751 cm^{-1} (the frequency associated with subsequent layers).[57]

In a similar study presented in two concurrent publications, Oxley[55] and Reynolds et al.[56] used Inelastic Electron Tunnelling (IET) Spectroscopy to study the orientation and bonding of the cyanoacrylate polymer at the Al$_2$O$_3$ surface. IET spectroscopy is a useful technique for the study of vibrational modes of molecules adsorbed on the surface of oxide layers in a metal-insulator-metal tunnel junction.[295] The data give useful information about the structure, bonding, and orientation of adsorbed molecules.[295]

Shifts similar to those observed via the reflectance infrared technique for the C=O and C–O–C stretching frequencies were noted in the IET spectrum of the uniform layer. Oxley draws the following conclusion based on these results in combination with theory proposed by Kusaka and Suetaka: *"the present IET spectrum confirms this position* [i.e. hydrogen bonding of the carbonyl group with the hydroxyl groups of the oxide layer] *for monolayer coverage in that the C=O and C–O–C frequencies are shifted relative to the bulk values in a manner consistent*

with hydrogen bonding".[55] This statement was latter revised after Dr W. A. Lees pointed out that the nitrile group is much more polar than the carbonyl group and could dominate in hydrogen bonding.[55,56] In fact, faced with this information, Reynolds et al. conceded that although the above hypothesis does not contradict the IET data, the apparent shifts of the C=O and C–O– bonds need to be accounted for. They go on to note that the shifts of these bonds are *"uncomfortably close to the resolution of our spectrometer"* and stress that *"IET and IR/Raman frequencies often do not correlate within this limit when one might expect they should"*.[56]

If hydrogen bonding is indeed occurring through the nitrile functionality, a consideration of the vibrational frequency of this functional group in the monomer and polymeric cyanoacrylate may provide some answers. Although Reynolds et al. did note a decrease in the intensity of the $C\equiv N$ stretching mode at 2250 cm^{-1} on curing, they attributed this to the loss of α,β unsaturation and note that in the Raman spectrum this band is always strong.[56] This is supported by Bellamy who notes that the intensities of α,β unsaturated nitriles are usually greater than in the saturated compounds.[296] Bellamy also notes that *"there is marked variation in intensity in various types of nitrile, so that the band varies from very strong to undetectable"*.[296] Furthermore, in compounds such as alkyl cyanoacrylates, where an oxygen-containing group (ester) is attached to the same carbon as the nitrile, a 'quenching' of the $C\equiv N$ absorption intensity is seen.[296] Therefore, in monomeric cyanoacrylates, the ester group has a quenching effect on the intensity of the $C\equiv N$ stretch while the vinyl group serves to increase its intensity. Upon polymerisation, the loss of conjugation with the vinyl group leads to a decrease in intensity.

In 1993, Yang used FTIR spectroscopy to study the photoinduced anionic polymerisation of ethyl cyanoacrylate.[61] To eliminate the effects of variations in sample thickness, peak areas rather than peak intensities were used and the carbonyl peak area was used as an internal standard. Yang also credits the loss of conjugation for the slight shift of the carbonyl peak upon polymerisation.[61] In a subsequent publication,[62] Yang reiterates this point and also attributes the shift in the nitrile peak from 2237 cm^{-1} to 2242 cm^{-1} to the loss in conjugation.

In the same year, Radhakrishnan and Saini used a dielectric technique to monitor the curing of cyanoacrylate and compared their results with infrared spectra of the uncured (monomer) and cured (polymer) sample.[63] Interestingly, their results clearly indicate that setting of this adhesive takes place in two stages. Radhakrishnan and Saini also correctly point out that

despite the large number of patents regarding these monomers and their extensive use for over thirty years, in 1993 there was *"practically no data available in the literature regarding the physical characterisation or specific evidence regarding the curing mechanism"*.[63] In fact, even in 2001, Klemarczyk wrote *"despite their extensive use in instant adhesive products, the chemical reactivity of alkyl cyanoacrylate monomers is still not completely understood"*.[67]

Some evidence for the two-stage curing is provided by the fact that the tensile strength of steel-steel cyanoacrylate bonds increases over time from 2005 psi at 2 hours to 3840 psi after 24 hours and reaches a maximum at 5030 psi after 48 hours.[247] Radhakrishnan and Saini interpret this (in combination with their own results) as a suggestion that a secondary process may be present after the initial fast curing step.[63] These additional processes are said to *"cause structural rearrangement on longer time scales in these resins"*.[63] The dielectric data suggest that there could be additional bond formation, either hydrogen bonding between $C\equiv N$ and $C=O$ through moisture present, or some form of crosslinking.[63]

Considering the IR spectra for cured and uncured cyanoacrylate, major differences are noted in the spectral region of $600 - 1100$ cm^{-1}.[63] The occurrence of new absorption bands at 950, 840, 730 and 680 cm^{-1} is taken as further evidence that curing does not proceed simply by polymerisation alone.[63] A peak at 1980 cm^{-1} in the uncured spectra cannot be directly assigned to any of the known frequencies for $C=C$ moieties and may be evidence of the formation of zwitterionic structures.[63] IR assignments are provided and the decrease in the nitrile absorption is again noted with suggestions that this may be the result of a secondary step via bond formation at the nitrile group.[63]

More recently, Raman spectroscopy has been used to monitor the curing of cyanoacrylate over time.[66,68] Brookes and Craston noted the decrease in the nitrile band and shift from 2235 cm^{-1} to 2245 cm^{-1} (see Figure 4.2) and conclude that *"this indicates either that the $C\equiv N$ bond is being changed chemically, i.e. new substituents are being added to the carbon, or that identical groups are in two very different environments"*.[66] Furthermore, this change gives rise to an isobestic point indicating that the two bands are very closely related and dependent upon each other (i.e. A $\rightarrow$ B conversion). These authors suggest that Raman spectroscopy may be used to monitor the extent of cure (using, for example, the decrease in intensity of the band at 840 cm^{-1}) and that the experiment could be conducted at different temperatures in order to elucidate kinetic information, but they did not perform these experiments.[66]
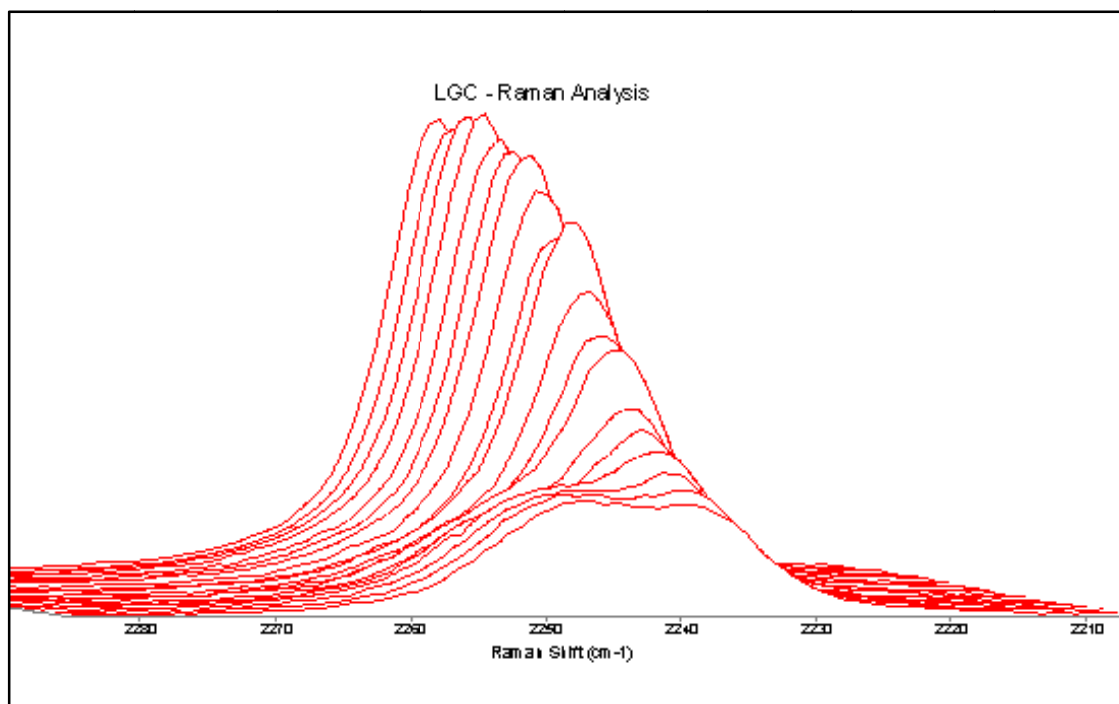
Figure 4.2: *Raman spectra of the C≡N region (range 2290 – 2210 cm⁻¹) showing the decrease in intensity of the band at 2235 cm⁻¹ and the appearance of the band at 2245 cm⁻¹ (0 hours at rear and 19 hours at front).*[66]

Edwards and Day also used Raman spectroscopy to monitor the curing of cyanoacrylate, this time in a sealed glass tube over three months.[68]   Despite the lengthy period, evidence of residual, un-polymerised monomer was found in the final spectrum.   This mimics work described in Section 1.1.6.2.1 above by the same authors regarding the formation of a 'skin' of polymerised material that protects underlying monomeric cyanoacrylate.[78]

Edwards and Day also attribute the shifts in the carbonyl and nitrile bands to the loss in conjugation but additionally note significant increases in bandwidth.   The increase in bandwidth is *"attributed to intermolecular interactions in the polymer, through which hydrogen bonding with similar groups in the three-dimensional folded network can affect local environmental conditions in the neighbourhood of the C=O and C≡N features".*[68]   Figure 4.3 shows this change in the nitrile band in Raman spectra collected by Edwards and Day.
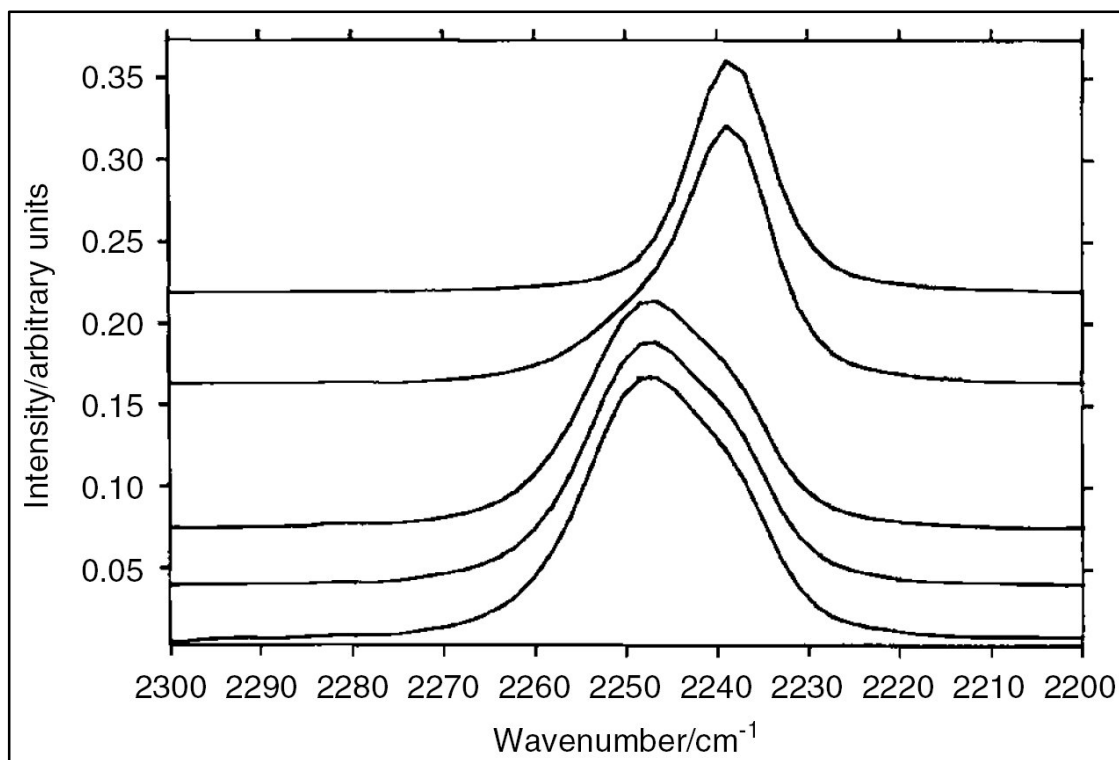
Figure 4.3: *FT-Raman spectral stack-plot of ethyl 2-cyanoacrylate undergoing slow, spontaneous polymerisation. From the top: monomer at time t = 0, 7, 67, 84 and 92 days. Total time lapse of experiment, three months. Excitation at 1064 nm, wavenumber range 2300 – 2200 cm^{-1} showing the v(C≡N) stretching mode near 2240 cm^{-1}.[68]*

The same phenomenon has recently been reported for the mid-infrared transmission spectra of curing cyanoacrylate[297,298] (see Figure 4.4). In these articles, the most recent research into the curing of cyanoacrylates, Tomlinson et al. point to the same two possibilities that previous research (discussed above) has identified; i.e. the loss of conjugation upon polymerisation or intra- and intermolecular hydrogen bonding.[297] Disappointingly, no firm position is taken as to which process is the more likely.
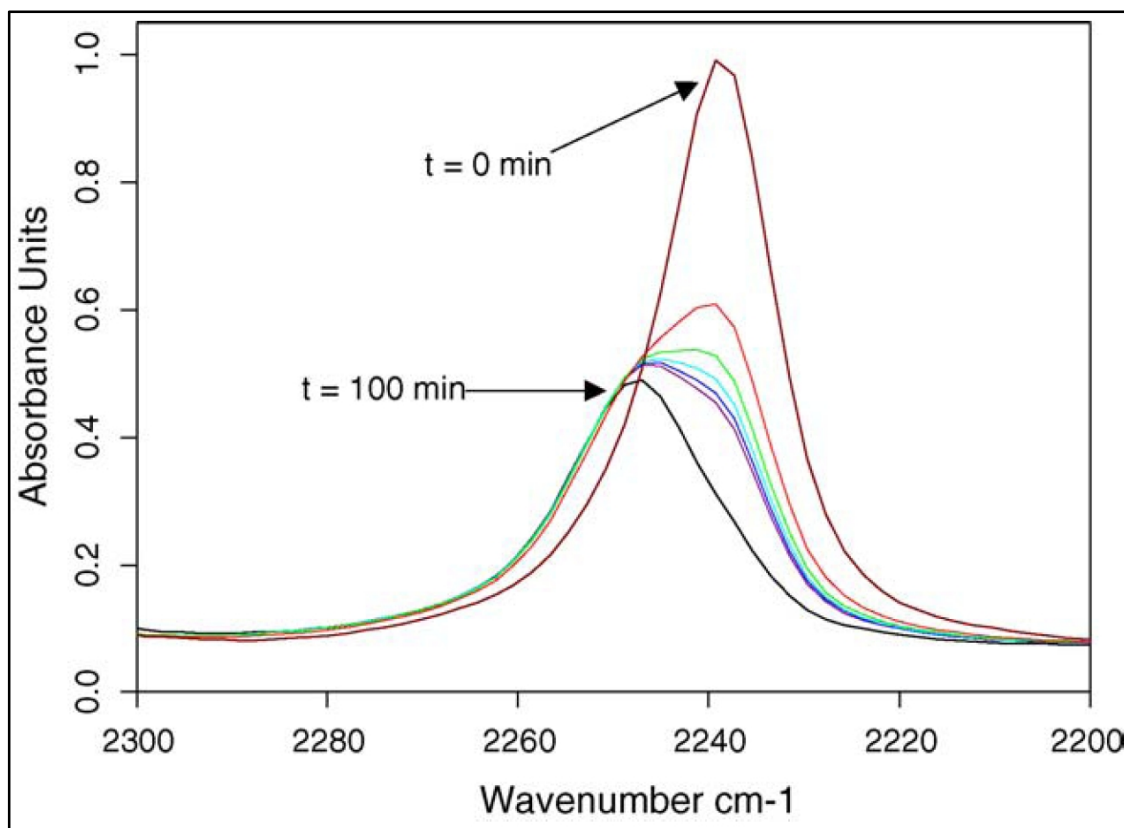
Figure 4.4: *Mid-IR transmission spectra of the curing cyanoacrylate system. Wavenumber range 2300 – 2200 cm^{-1} showing the v(C≡N) stretching mode near 2240 cm^{-1} (only spectra recorded every minute between 0 and 5 min and finally at 100 min are displayed).*[297]

Tomlinson et al. also conducted experiments in which the effect of film thickness was investigated. Cyanoacrylate samples of different thicknesses were placed on a glass substrate and the extent of cure was monitored via near-infrared reflectance spectroscopy, using the change in intensity of the overtone band for vinyl C–H at 6207 cm^{-1}. Not surprisingly, thicker films required more time to reach an equivalent extent of cure.[297] A more interesting finding was that the thicker films levelled to a slightly lower extent of cure.[297] This may be explained by the formation of an impenetrable polymeric film at the surface/adhesive and adhesive/air interfaces. As mentioned above, Edwards and Day have reported similar findings wherein monomeric cyanoacrylate is detected even after three months' curing.[68,78]

Tomlinson et al. discuss the probability that, in these situations, initiating species (such as water) are isolated from the monomer units, which are trapped underneath an impenetrable polymeric film. They also raise another important consideration:

"It is important to discuss the fact as the viscosity of the monomer–polymer mixture increases (as a function [of] *conversion) the movement of all species, not only water, in the mixture will*

become increasingly hindered. Areas of the adhesive film may be developing, in which "living" polymer-chain anions are becoming isolated in the glassy matrix of the polycyanoacrylate.[70] Any further reaction would depend on the slow diffusion of monomer molecules (and water molecules for chain transfer) to the immobile anion chains. This theory might account for some of the remaining monomer (after 100 min) in even the very thin films of cyanoacrylate used in this work".[297]

This mirrors research into the thermal degradation / depolymerisation of cyanoacrylates (discussed in detail in Section 3.3.2 above) whereby the diffusion of the distilling monomer through the polymeric film is the kinetically limiting stage of thermal degradation. Results obtained as part of the current research confirm those obtained by the aforementioned articles (see Figure 4.5). These spectra, collected in transmission mode, show the curing of a thin cyanoacrylate film between two freshly pressed KBr disks. Once again the decrease in intensity and shift to higher frequency of the nitrile band is clear and the persistence of residual monomer was observed. The final spectrum shown here is that collected after ten minutes. A spectrum collected 24 hours later (not presented here) showed a further decrease in the intensity of nitrile band.
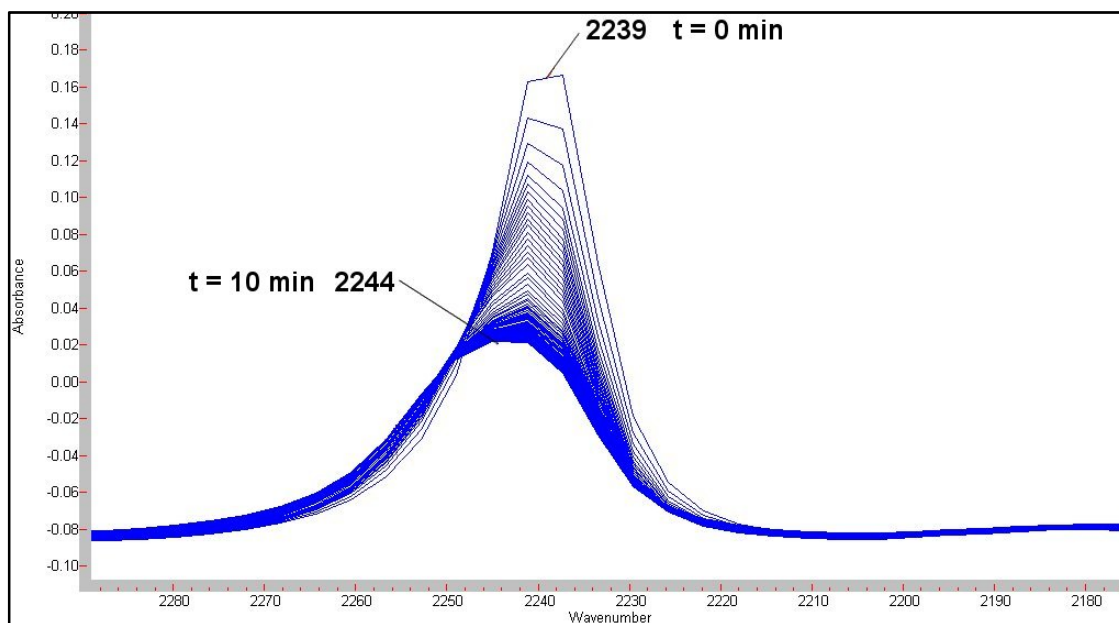
Figure 4.5:   *Mid-IR transmission spectra of curing cyanoacrylate. Wavenumber range 2300 – 2200 cm^{-1} showing the ν(C≡N) stretching mode near 2240 cm^{-1}.*

Our result, and those of other workers, indicate that there is an initial, rapid polymerisation step whereby the monomer units are rapidly consumed, as indicated by the rapid decrease in

intensity of the nitrile band (and other bands) due to the loss of conjugation. There is also indication of a slower process that leads to a further decrease in the intensity of the nitrile band. As discussed above, some authors have suggested that this may be the result of hydrogen bonding or cross-linking through the nitrile band. It is our belief that there is no direct evidence of this. A more plausible theory is that the secondary process is a result of restrictions to the migration of residual monomer through the sample that has already polymerised. This theory, suggested by Tomlinson[297] is supported by thermal degradation data (see Section 3.3.2 above) and the spectral data, which shows an A → B conversion with corresponding isobestic points. Furthermore, the infrared spectra of many cyanoacrylate monomers and polymers have been recorded.[299] To our knowledge, all cyanoacrylate polymer spectra exhibit this phenomenon (i.e. a lower intensity nitrile band in the polymer spectrum compared to the monomer spectrum). Since it is unlikely that hydrogen bonding or cross-linking occurs in *all* cyanoacrylates regardless of the identity of the ester group (or polymerisation conditions, initiator etc), the loss of conjugation and the corresponding change in chemical environment seems the most likely explanation for the loss in intensity of the nitrile band upon polymerisation.

While the loss of the nitrile band is unavoidable in conventional cyanoacrylate, the introduction of an additional nitrile band or another functional group that has an infrared absorption within the 'region of interest' (2500 – 1800 cm^{-1}) may resolve this issue and provide a suitable target peak for the FTIR chemical imaging of fingerprints. As described in Chapter 3, a total of four novel cyanoacrylate monomers were synthesised during this project. Two of these monomers contained an additional nitrile group, these were 2-cyanoethyl 2-cyanoacrylate (2-CECA) and 1-cyanoethyl 2-cyanoacrylate (1-CECA). The infrared spectrum of these monomers and the corresponding polymers were found to contain an additional nitrile band near 2250 cm^{-1}. The remaining two monomers contained deuterium (^{2}H / D) atoms, these were trideuteromethyl 2-cyanoacrylate (MCA-d$_3$) and pentadeuteroethyl 2-cyanoacrylate (ECA-d$_5$). The infrared spectrum of these monomers and the corresponding polymers were found to contain a number of additional bands in the region 2300 – 1900 cm^{-1} related to C–D stretching vibrations. In all cases, the intensities of peaks in the region of interest were relatively low. Nevertheless, the peaks in this area provided suitable targets for the FTIR chemical imaging of fingerprints treated with these novel cyanoacrylates and the results are presented here.

4.2   Materials and methods

As discussed in Section 1.1.9 above, an attempt has been made to limit the number of variables involved in the fingerprint development process and to accurately note as much information as possible regarding the donors used, the deposition of latent fingerprints, the surface characteristics of the samples and the treatment and imaging conditions used. The main aim of this part of the current work was to assess the ability of the synthesised novel cyanoacrylates to develop latent fingerprints that could subsequently be imaged via FTIR chemical imaging. In doing so, factors such as variations in the material secreted and deposited or transferred by various donors were not controlled. Instead, a number of fingerprint donors were used throughout this study to get a reasonable sample of the population. The following table (Table 4—1) summarises the donors used and their sex and age. The donor number is provided for each developed / imaged fingerprint presented here.

Donor number	Sex	Age (at time of deposition)
1	M	40
2	F	28
3	M	26
4	M	23
5	F	30
6	F	23
7	F	25

Table 4—1:   *Summary of fingerprints donors used during this study.*

Fingerprints were prepared and deposited on a range of surfaces by thoroughly washing, rinsing and drying hands before swiping a cleaned finger across an oily region of the face (forehead, nose or neck) and finally placing the mark on the desired surface. In some cases the washing, rinsing and drying of hands was omitted in order to assess a range of natural fingerprint deposits. The surfaces used during this study included clean, dry glass microscope slides, infrared reflective (metal oxide-coated) microscope slides (Kevley Technologies), aluminium foil, freshly cleaned and dried circulated Australian polymer $5 banknotes, clear

plastic zip-lock bags, opaque white poly(methyl methacrylate) (PMMA), translucent blue fluorescent PMMA, translucent green fluorescent PMMA, translucent red fluorescent PMMA, reflective gift wrap, glossy playing cards and plastic-coated playing cards.

Samples containing freshly deposited latent fingerprints were placed in a custom-made cyanoacrylate fuming cabinet based on a clear polymethylmethacrylate (PMMA / acrylic) box (500 × 750 × 600 mm). Cyanoacrylate monomers were heated using a Dick Smith temperature-controlled soldering station – model 137, with a custom-made aluminium heat block (40 × 40 × 25 mm) with wells for holding liquid monomer. The temperature of the heating block was monitored via a thermocouple and the temperatures used during fuming varied depending on the monomer and its purity. Details of fuming conditions and temperatures are discussed in Section 4.3 below.

Infrared chemical imaging of fingerprints was carried out using a Digilab Stingray system, which comprised an FTS 7000 FTIR spectrometer coupled with a UMA 600 infrared microscope and a Lancer 64 × 64 focal plane array (FPA) detector. Images and spectra were collected and processed with Digilab Win IR Pro software. All samples were imaged in reflection mode using the expanded field of view (EFOV) setting, in which each individual image tile is approximately 700 × 700 μm in size. A pixel aggregation factor of 16 (pixel size ~44 μm) was used for all images. Other parameters such as spectral resolution, number of co-added scans, number of image tiles (image size) and raw data processing methods were varied and optimised according to the methodology outlined in Section 2.3.1 above. Details of the parameters used for imaging are provided with the appropriate images.

4.3   Results and discussion

4.3.1   Anthracene adducts

As mentioned in Section 3.5.1 above, a patent by Warrener and Yong has discussed the possibility of using anthracene / alkyl 2-cyanoacrylate adducts as solid precursors for the fuming of latent fingerprints.[232] This patent, however, does not contain any images of fingerprints fumed via this method. The fuming of latent fingerprints using anthracene / 2-cyanoethyl 2-cyanoacrylate (A/2-CECA) was attempted during the current work.

Although cyanoacrylate fuming cabinets are commercially available, the unit available in our laboratory (and indeed the majority of commercial units) does not allow for adjustment of the temperature used to heat the cyanoacrylate. Thermal analysis of A/2-CECA (see Figure 3.20 in Section 3.5.1 above) indicated that its thermal decomposition, which produces anthracene and monomeric 2-cyanoethyl 2-cyanoacrylate (2-CECA), begins at approximately 200 °C and reaches a maximum at approximately 264 °C. The temperature reached by the heating well on the commercial forensic cyanoacrylate fuming cabinet (Carter-Scott Design, Australia) was measured using a thermocouple. The temperature was found to be 150 – 155 °C when the circulating fan was on (during the "evaporate" cycle) and reached a maximum of 178 °C when the fan is temporarily switched off (during the optional "refill" cycle). This temperature was determined to be too low for attempts to fume latent fingerprints using the A/2-CECA adduct, so an alternative cyanoacrylate fuming cabinet was designed and manufactured.

The custom-made cyanoacrylate fuming cabinet consisted of a clear polymethylmethacrylate (PMMA / acrylic) box (500 × 750 × 600 mm). Control over temperature was achieved by designing and manufacturing an aluminium heat block (40 × 40 × 25 mm) with wells for holding liquid monomer, which could be fitted to a commercially available soldering iron with variable temperature control (Dick Smith temperature-controlled soldering station – model 137). The dimensions of this aluminium heat block were modelled on the heating element of the commercial cyanoacrylate fuming cabinet and were modified to accommodate the soldiering iron and a thermocouple (see Figure 4.6).
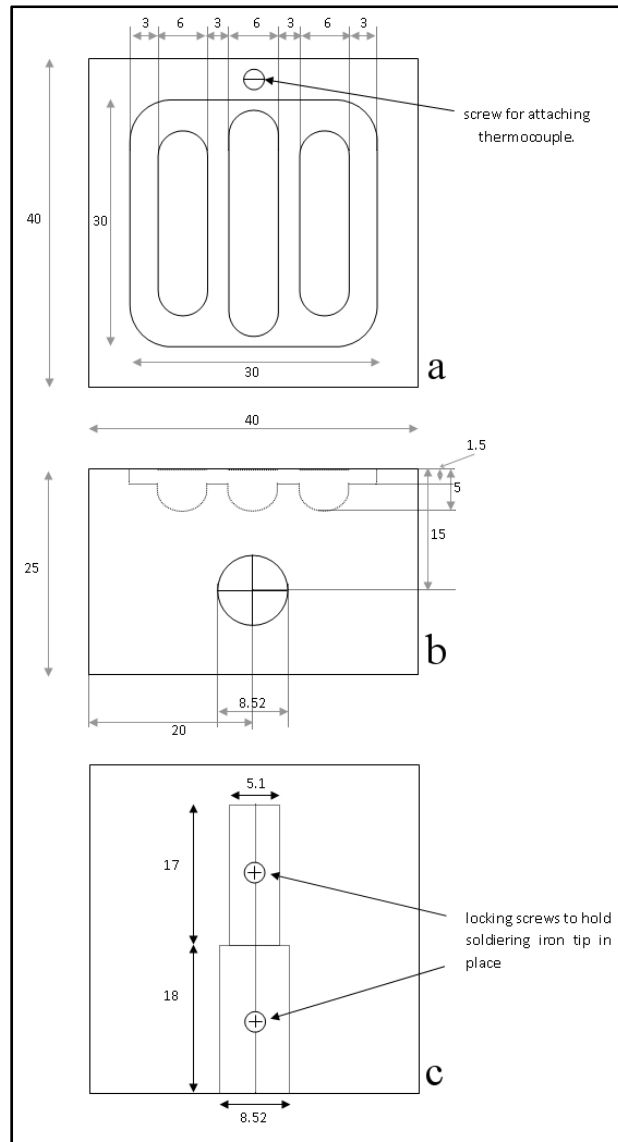
Figure 4.6: *Aluminium heating block designed to attached to soldiering iron: **a)** top view, **b)** side view, **c)** bottom view showing dimensions of hole for soldering iron.*

The aluminium heat block was housed in an insulated casing and placed inside the fuming cabinet. A small battery-operated fan was also placed inside the fuming cabinet to allow for even distribution of vapours. A shelf inside the cabinet was fitted with a number of fold back paperclips for holding samples. Figure 4.7 shows the custom-made fuming cabinet in use.
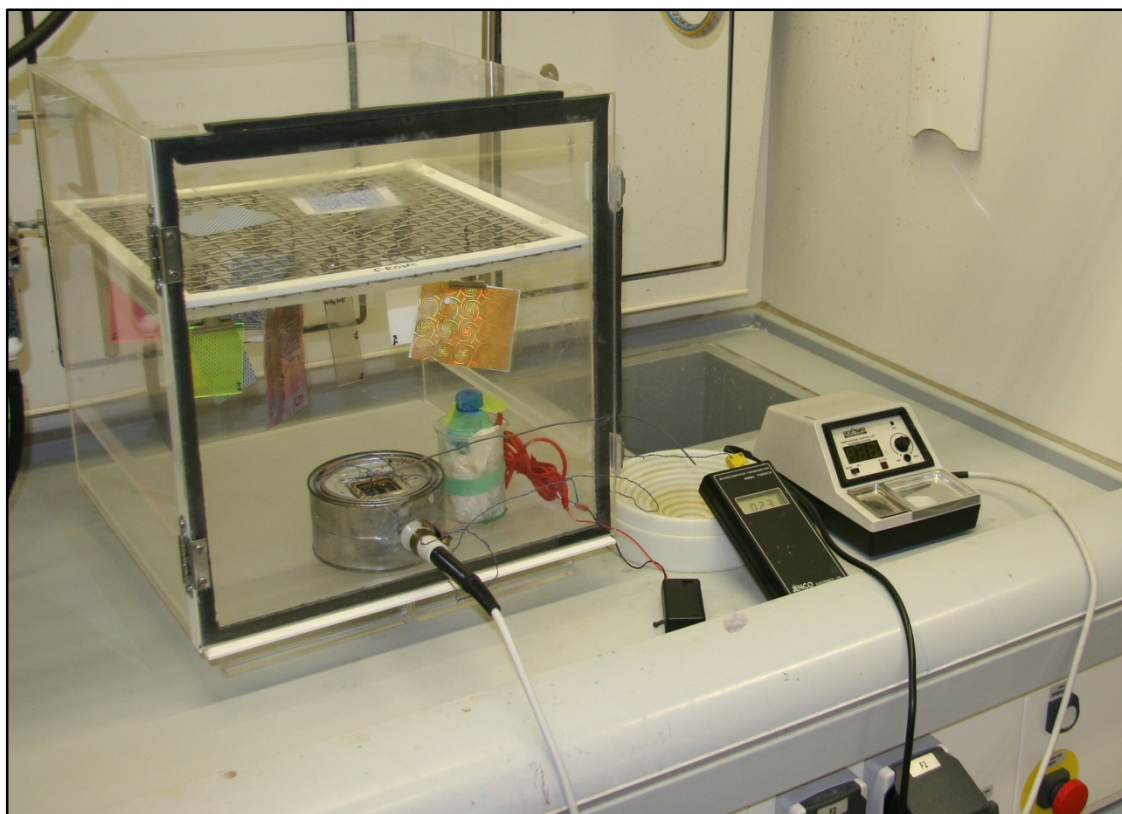
Figure 4.7: *Custom-made cyanoacrylate fuming cabinet comprised of temperature controlled soldering iron with aluminium heat block, thermocouple for monitoring temperature, fan for circulating vapours and shelf with clips for mounting samples.*

A number of samples with fresh latent fingerprints from two donors (#1 and #2) were placed inside the fuming cabinet. These samples included infrared reflective microscope slides, glass microscope slides, Australian $5 banknotes and white copy paper. The aluminium heat block was pre-heated to 100 °C and then charged with ~0.5 g of the solid anthracene adduct (A/2-CECA). The A/2-CECA melted when the heater temperature reached approximately 130 °C and signs of "fuming" were observed when the temperature reached 210 °C. The temperature was elevated to 260 °C, held at this temperature for 30 minutes and then allowed to cool. Shortly after fuming (or the thermal decomposition) began, a white crystalline powder was found to deposit on cold surfaces such as the metal insulator box housing the heater block. As the decomposition continued, this white crystalline residue deposited on all samples and on all the inside walls of the fuming cabinet. The samples were left in the sealed cabinet overnight.

The white residue deposited on samples showed fluorescence under UV illumination, which suggested it might be anthracene. A ^{1}H NMR spectrum of a sample of this residue confirmed it was indeed anthracene. FTIR chemical imaging of treated samples failed to produce any

images of fingerprints or any evidence of the 2-cyanoethyl 2-cyanoacrylate polymer. No further attempts to treat latent fingerprints with the anthracene adducts of alkyl 2-cyanoacrylates were made.

4.3.2   Oligo-2-cyanoethyl 2-cyanoacrylate (oligo-2-CECA)

Almog and Gabay have demonstrated the use of poly-cyanoacrylate for latent fingerprint development.[47] This is based on the fact that monomeric cyanoacrylate vapours are released as a result of the thermal decomposition of the polymer (see Section 3.3.2 above for detailed discussion). Using the same custom-made fuming cabinet described in Section 4.3.1 above (see Figure 4.7), attempts were made to use oligo-2-cyanoethyl 2-cyanoacrylate (obtained from the Knoevenagel condensation of 2-cyanoethyl cyanoacetate and paraformaldehyde) to fume samples bearing latent fingerprints.

A number of samples with fresh latent fingerprints from two donors (#1 and #2) were placed inside the fuming cabinet. These samples included infrared reflective microscope slides, glass microscope slides, aluminium foil and plastic zip lock bags. The aluminium heating block was pre-heated to 120 °C before charging with oligo-2-cyanoethyl 2-cyanoacrylate. The heating block temperature was gradually raised and signs of vapour emission were observed when the temperature reached 170 °C. "Fuming" continued while the temperature was raised to 220 – 230 °C. These temperatures caused a gradual charring of the oligomeric residue and so the fuming was ceased when the temperature reached 250 °C. Samples were left sealed in the fuming cabinet overnight before being analysed using FTIR chemical imaging.

None of the samples tested produced any images of fingerprints nor was there any evidence of the 2-cyanoethyl 2-cyanoacrylate polymer. This mirrored attempts to thermally depolymerise this oilgomer (see Section 3.4.1 above), wherein no monomer was obtained and evidence of other thermal decomposition products was observed. In a separate attempt to fume fingerprints using oligo-2-CECA, the temperature was held between 190 – 200 °C in order to limit the chances of adverse side reactions / thermal degradation. This did not improve the results obtained. No further attempts to treat latent fingerprints with the oligo-2-cyanoethyl 2-cyanoacrylate were made.

The poor results obtained in attempts to fume latent fingerprints with the intermediate / precursor compounds, namely A/2-CECA and oligo-2-CECA, highlighted the need to isolate

the monomeric 2-cyanoethyl 2-cyanoacrylate.   As discussed in Section 3.4.2, this was eventually achieved and three other novel cyanoacrylate monomers were obtained. The use of these monomers for the fuming of latent fingerprints and subsequent FTIR chemical imaging is discussed below.

4.3.3   2-Cyanoethyl 2-cyanoacrylate (2-CECA)

The first novel cyanoacrylate monomer to be successfully isolated during the work was 2-cyanoethyl 2-cyanoacrylate (2-CECA).   As discussed in Sections 3.4.2, 3.5 and 3.6, the monomeric products were generally contaminated with the corresponding precursor anthracene adducts. A number of batches of 2-CECA were isolated and the level of the anthracene adduct (A/2-CECA) ranged from 50 – 90 % w/w. As outlined in Section 3.4.2 above, due to the relatively small quantities of product and the high probability of polymerisation, no attempts were made to distil or otherwise purify this or any of the other monomers.

Using the same custom-made fuming cabinet described in Section 4.3.1 above (see Figure 4.7), attempts were made to use the crude monomeric 2-CECA to fume samples bearing latent fingerprints.   During several attempts, a number of samples with fresh latent fingerprints from various donors (including donors #2, #3, #4 and #5) were placed inside the fuming cabinet prior to sealing the chamber and heating the monomer. These samples included infrared reflective microscope slides, glass microscope slides, aluminium foil, plastic zip lock bags, Australian $5 polymer banknotes, white opaque poly(methyl methacrylate) (PMMA), translucent blue fluorescent PMMA, translucent green fluorescent PMMA, translucent red fluorescent PMMA, glossy playing cards and plastic-coated playing cards.

In one attempt, samples were placed inside the fuming cabinet and the aluminium heating block was pre-heated to 60 °C before charging with approximately 380 mg crude monomeric 2-cyanoethyl 2-cyanoacrylate. The temperature was gradually raised (over 18 minutes) to 185 °C, at which point the monomer appeared to have darkened. At temperatures between 185 – 210 °C, some signs of bubbling were observed but the monomer appeared to become viscous (possibly indicating polymerisation) and darken. After approximately 30 minutes, when the temperature had reached a maximum of 215 °C, the heating unit was switched off and allowed to cool. At the end of the heating period, the monomer appeared almost completely charred. Furthermore, a white crystalline residue had deposited on some

surfaces. This residue was later confirmed to be anthracene, most likely generated from the thermal decomposition of the residual A/2-CECA as discussed in Section 4.3.1 above.

Despite the obvious signs of polymerisation and thermal degradation / charring, samples bearing latent fingerprints were left sealed in the fuming cabinet overnight before being analysed using FTIR chemical imaging. None of the samples tested produced any images of fingerprints nor was there any evidence of the 2-cyanoethyl 2-cyanoacrylate polymer.

Other attempts to vaporise 2-CECA using heat gave similar results. It was concluded that monomeric 2-CECA was not as volatile as conventional superglue (ethyl 2-cyanoacrylate) and hence could not be used in the same manner for the fuming of latent fingerprints. It is surprising that such a small change in molecular weight has such a pronounced effect on the volatility of the monomer.

As discussed in Section 1.1.6.2.1 above, another common method (and one that does not require heat) for fuming latent fingerprints with cyanoacrylate vapours involves the use of reduced pressure.[46] This method, known as vacuum deposition, was appealing in this case because it avoids the use of high temperatures and therefore limits the probability of thermal degradation of the monomer and the chance of side-reactions. Commercial cyanoacrylate vacuum deposition units are available but one was not available in our laboratory. Yamashita has reported the use of a *benchtop desiccator* for vacuum cyanoacrylate treatment of latent prints.[46] In an adaptation of this approach, samples bearing latent fingerprints were placed in a sealed glass vessel that was also charged with monomeric 2-CECA. In one attempt, an infrared reflective slide with freshly deposited fingerprints from three donors (donor #1, #3 and #4) was placed inside a 250-mL round bottom flask that was also charged with approximately 860 mg 2-CECA. The system was placed under a reduced pressure (~3 mmHg), heated to 60 °C and then sealed for three hours. Subsequent FTIR chemical imaging showed evidence of preferential deposition of material on the ridges of the latent fingerprints. This particular method of cyanoacrylate deposition provided some strange and interesting results and is discussed further in 4.3.7 below.

In other attempts to treat a larger number of samples with 2-CECA using the vacuum deposition method, a one-litre reaction vessel was employed (see Figure 4.8). Using this vessel, samples bearing latent fingerprints could be fixed to the inside walls of the vessel

while monomeric 2-CECA could be placed in the base. The lower portion of the vessel could be heated on a water bath and a vacuum could be applied via the fitting on top of the vessel.
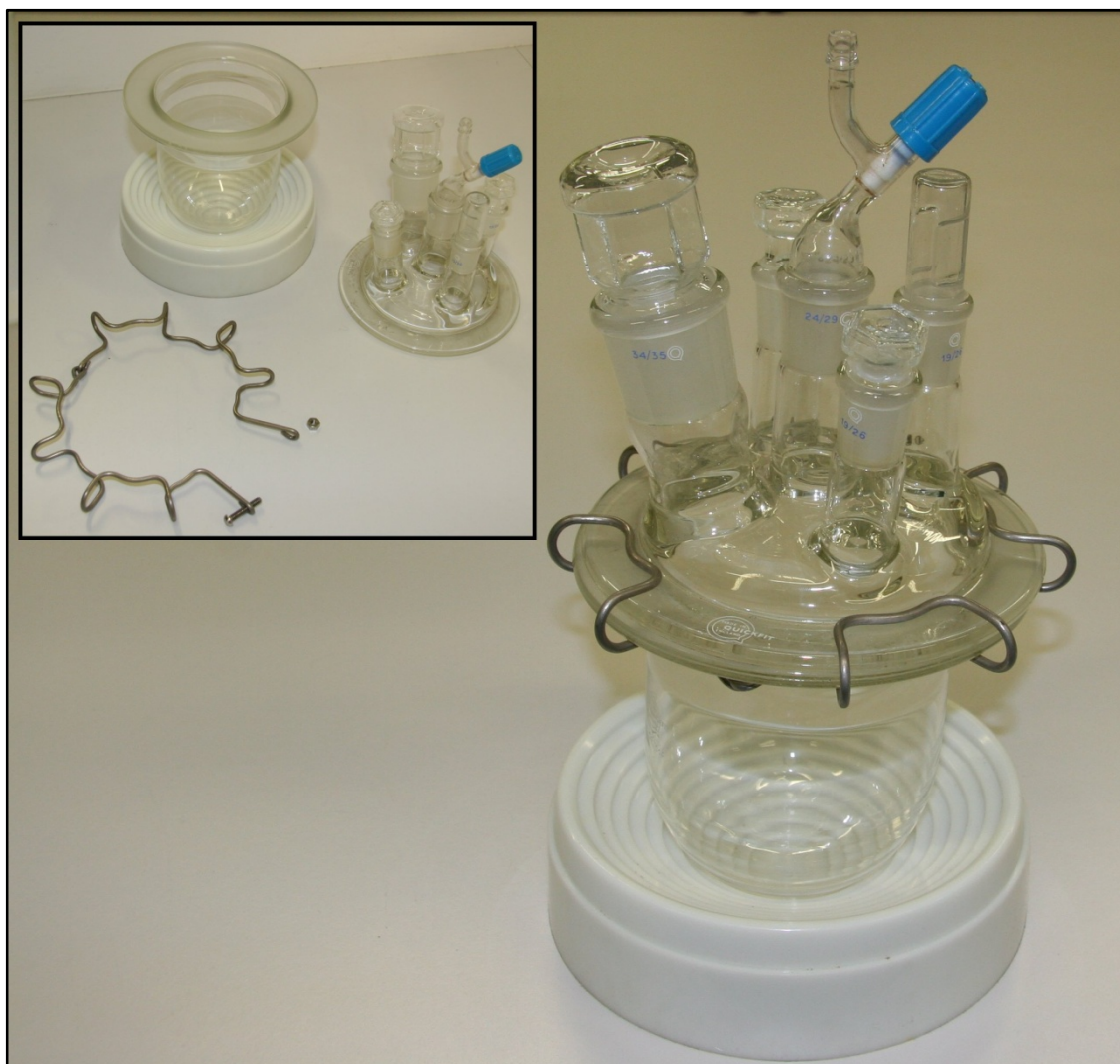
Figure 4.8:   *Reaction vessel (one-litre) used for vacuum deposition of 2-cyanoethyl 2-cyanoacrylate.*

A number of experiments involving the vacuum deposition of 2-CECA using the reaction vessel were conducted. During each experiment, 0.9 – 1.6 g of monomeric 2-CECA was used and samples treated included IR reflective sides, glass microscope slides and Australian polymer $5 banknotes. Figure 4.9 and Figure 4.10 show latent fingerprints (donor #3 and #4 respectively) that were developed with 2-CECA on infrared reflective slides. Firstly, the white light photographs (Figure 4.9*a* and Figure 4.10*a*) clearly show ridge development under white light.   This indicates that 2-cyanoethyl 2-cyanoacrylate selectively polymerises on the fingerprint ridges in a manner akin to conventional (ethyl) cyanoacrylate.   Secondly, Figure 4.9*b* shows an FTIR chemical image generated using an absorbance that corresponds

to the carbonyl (C=O) stretching mode at 1759 cm^{-1}. This too is an indication that 2-CECA has selectively polymerised on the ridges of the latent fingerprint.   This FTIR chemical image shows clear ridge detail down to the third level and mirrors results obtained using conventional cyanoacrylate on similarly reflective surfaces such as aluminium drink cans (see Section 2.3.4.3). Finally, Figure 4.9*c* and Figure 4.10*b* show the FTIR chemical images that can be produced using the nitrile (C≡N) band at ~2252 cm^{-1}. Unlike conventional cyanoacrylate, absorbance in this region is retained upon polymerisation due the extra nitrile group on the ester chain.
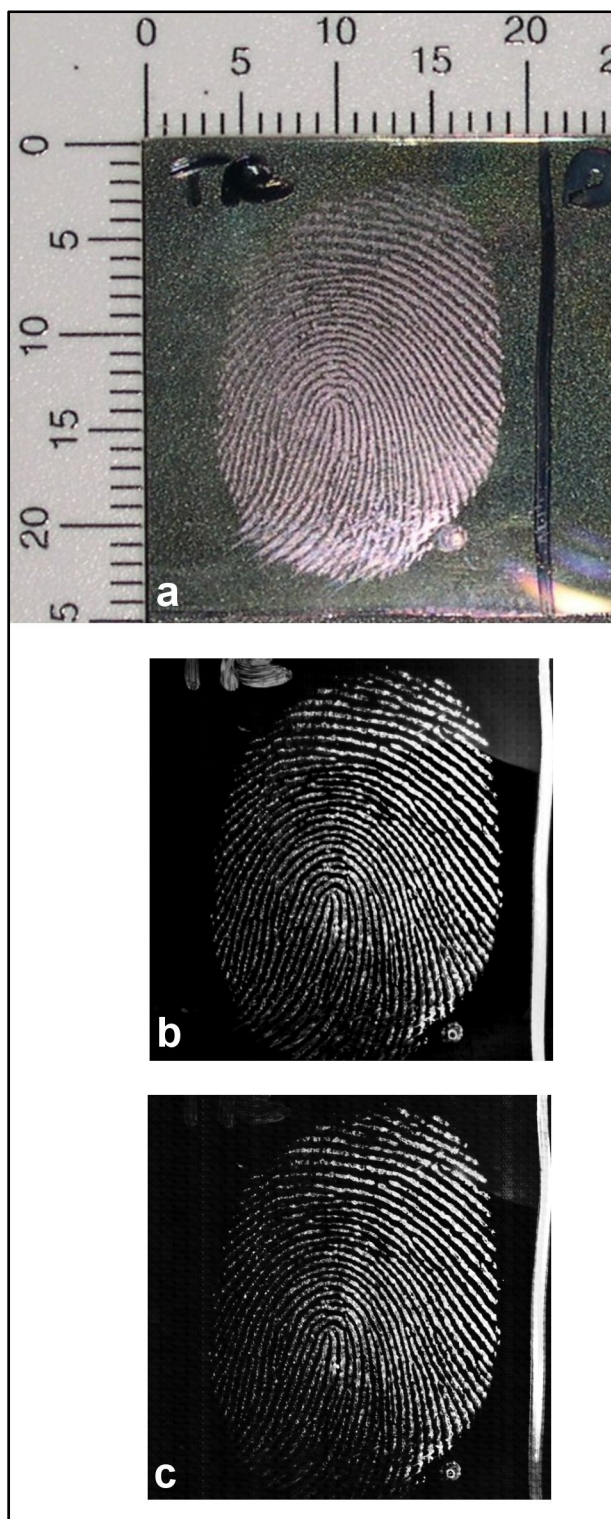
Figure 4.9: *Fingerprint (donor #3) treated with 2-cyanoethyl 2-cyanoacrylate on IR reflective slide. **(a)** White light photograph. **(b)** Monochrome representation of FTIR chemical image (second derivative, 1759 cm^{-1}). **(c)** Monochrome representation of FTIR chemical image (second derivative, 2252 cm^{-1}).*
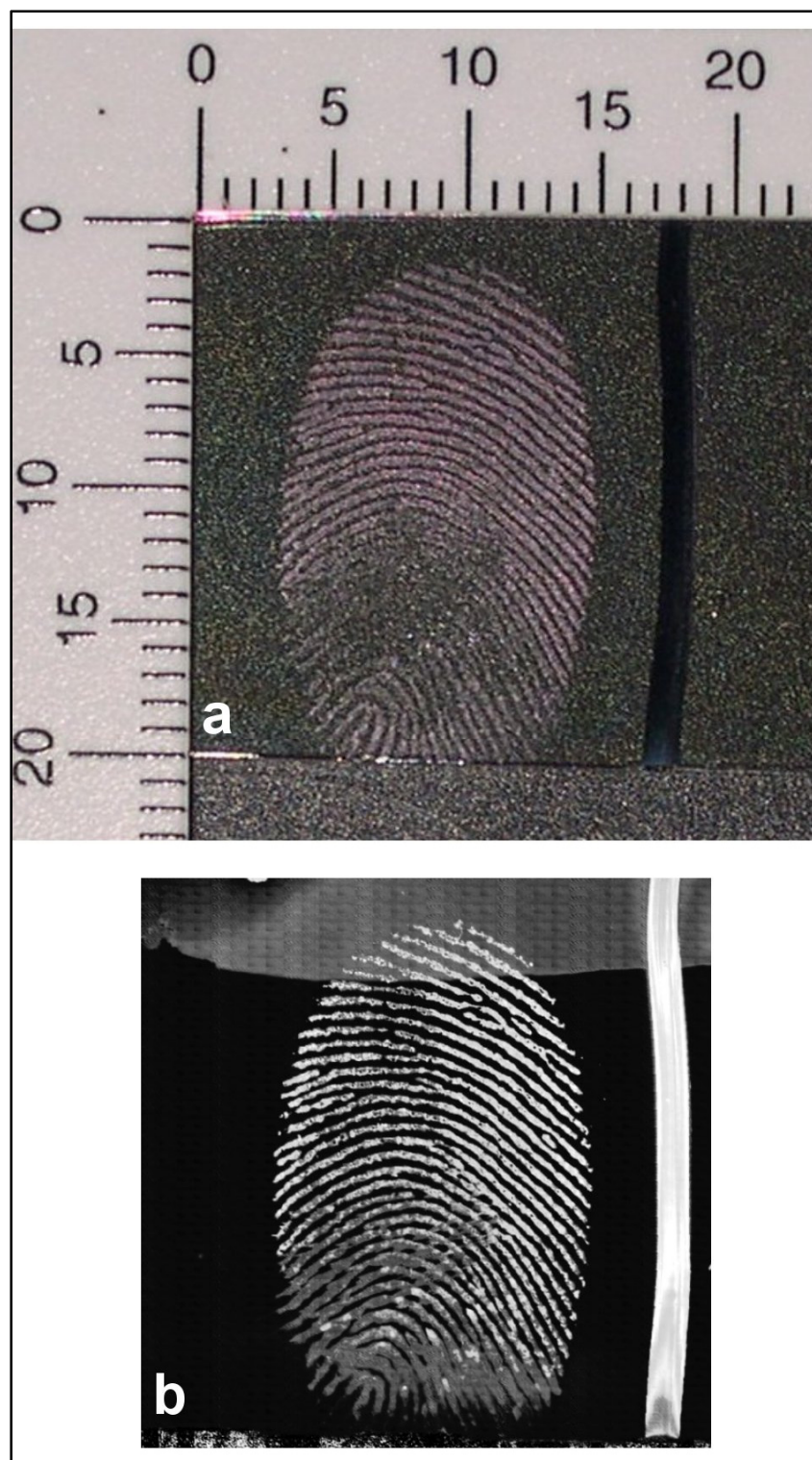
Figure 4.10:   *Fingerprint (donor #4) treated with 2-cyanoethyl 2-cyanoacrylate on IR reflective slide.* **(a)** *White light photograph.* **(b)** *Monochrome representation of FTIR chemical image (second derivative, 2252 cm^{-1}).*

Unfortunately, the intensity of the band produced by the additional nitrile group was relatively low. Figure 4.11 shows an FTIR spectrum extracted from an area on a fingerprint ridge in the FTIR chemical image shown in Figure 4.9*a,b*. The nitrile band from poly-2-CECA is

clear at ~2255 cm^{-1} but its intensity is relatively low. This meant that it could be detected in the infrared refection spectra from reflective surfaces (and hence was utilised for FTIR chemical imaging) but was generally not detectable in the weaker and noisier spectra from less reflective surfaces such as glass or polymer banknotes.
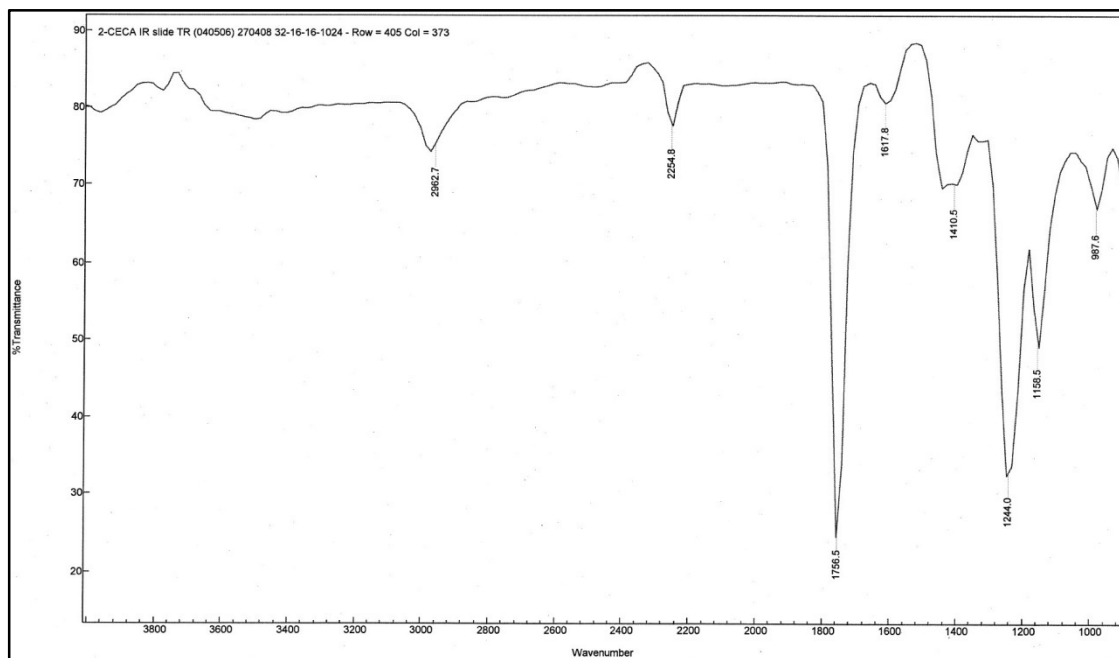
Figure 4.11: *FTIR spectrum from ridge of fingerprint on infrared reflective slide fumed with 2-CECA (poly-2-CECA).*

Figure 4.12 shows a fingerprint developed with 2-CECA (via vacuum deposition) on a glass microscope slide. In this example, the fingerprint was faint but visible under white light (see Figure 4.12*a*) and the contrast could be greatly improved using FTIR chemical imaging (see Figure 4.12*b*). The best results using FTIR chemical imaging however, came from imaging at a frequency of 987 cm^{-1}. Since glass is highly absorbing (particularly in this region), the contrast achieved may be a result of the developed fingerprint simply being more reflective than the background glass. A peak for the nitrile band could not be detected and hence could not be used to form a chemical image of this fingerprint.

In the case of the polymer banknotes, the nitrile band was generally not detected and, as with conventional cyanoacrylate, the carbonyl band from the poly-2-CECA seemed to overlap with the absorption in this region from the background polymer. As with conventional cyanoacrylate (see discussion in Section 2.3.1.4 above), in addition to second (and high order) derivative transformation, chemometric methods were also trialled. Second and higher order

derivatisation helped to resolve the overlapping peaks of the carbonyl band from poly-2-CECA and the band in this region from the background but high contrast images were not possible, particularly on area containing raised intaglio printing.

Using the ENVI software package, two chemometric methods, principal component (PC) analysis and minimum noise fraction (MNF) transformation, were trialled in an attempt to remove background interference from the raised intaglio printed area of polymer banknotes. It was also hoped that this processing could help reduce background variations within individual image tiles, which results in an overall 'tiling' effect. This artefact is thought to be due to an uneven illumination of the FPA detector, which leads to lower signal-to-noise responses in certain areas of an individual image tile. Combining a number of image tiles (i.e. mosaicking) to piece together a larger image such as an entire fingerprint can lead to a repeated background pattern, which can obscure ridge detail.

A PC analysis was conducted on FTIR chemical image data of a fingerprint on a polymer banknote fumed with 2-CECA. An image could be generated for each PC with certain PCs showing exclusively intaglio printed areas of the note while others showed partial fingerprint detail.   No individual PC gave a good quality image of the ridge detail without any interference from the background. The PCs that contained partial fingerprint detail were selected, while unwanted components (such as those containing 'background' or 'tiling artefact' or simply noise) were eliminated. An inverse PC transformation was then conducted to reconstruct the spectral data without the background interferences. The images produced did not significantly improve on results that could be obtained using second or higher even order derivatives.

A similar approach was taken using minimum noise fraction (MNF) analysis. Once again, certain components (such as the intaglio printing or partial fingerprint detail) could be extracted but no individual component yielded a high quality image of the entire print. As with PC analysis, MNF components containing some ridge detail were selected before conducting an inverse MNF transformation to reconstruct the data. This processing did not significantly improve on results that could be obtained using second or higher even order derivatives.

Figure 4.12: *Fingerprint (donor #3) treated with 2-cyanoethyl 2-cyanoacrylate on glass slide. **(a)** White light photograph. **(b)** Monochrome representation of FTIR chemical image (second derivative, 987 cm^{-1}).*

4.3.4   1-Cyanoethyl 2-cyanoacrylate (1-CECA)

Monomeric 1-cyanoethyl 2-cyanoacrylate (1-CECA) was obtained in crude form from its anthracene adduct (A/1-CECA). As reported in Section 3.6, the crude monomer was found (by NMR) to be a mixture of approximately 50% w/w 1-CECA and 50% w/w anthracene / 1-cyanoethyl 2-cyanoacrylate adduct (A/1-CECA), the precursor compound. In contrast to the problems encountered with the presence of residual anthracene adduct in 2-CECA (discussed in Section 4.3.3 above), the presence of anthracene adduct did not hinder the use of 1-CECA for the treatment of latent fingerprints. This was due to the higher volatility of the 1-cyanoethyl isomer (compared with the 2-cyanoethyl isomer).

Using the custom-made cyanoacrylate fuming cabinet described earlier (see Figure 4.7), approximately 2.15 g of crude 1-CECA was charged into the wells of the aluminium heating block. A number of samples bearing freshly deposited fingerprints from two donors (#3 and #5) were placed inside the cabinet prior to sealing the chamber and heating the monomer. The samples treated with 1-CECA included an infrared reflective slide, glossy playing cards, plastic-coated playing cards, white opaque PMMA, translucent blue fluorescent PMMA, translucent green fluorescent PMMA, translucent red fluorescent PMMA, reflective gift wrap and an Australian polymer $5 banknote.

The monomeric 1-CECA was heated to approximately 110 °C before some bubbling was observed and fumes began to evolve. Fumes continued to evolve from the heated monomer while the temperature was slowly increased to a maximum of 190 °C (after 50 minutes) before switching the heater unit off and allowing to cool. Temperatures within this range appeared sufficient to efficiently volatilise the monomeric 1-CECA. Importantly, this temperature is below the temperatures needed to thermally decompose the anthracene / 1-cyanoethyl 2-cyanoacrylate adduct (A/1-CECA) that was also present (refer to Section 3.5.1 and Figure 3.21 above). In fact, recovery and analysis of the residue (1.09 g) remaining in the heater after fuming confirmed that A/1-CECA remained behind while the monomer volatilised and developed the latent fingerprints. It was possible to recover the residual A/1-CECA and, after recrystallisation, reuse it in subsequent reactions. The mass of A/1-CECA recovered is also further evidence that the original sample was a 50:50 mixture of the monomer and anthracene adduct.

Figure 4.13*a* shows a fingerprint (donor #5) developed with 1-CECA on an infrared reflective slide. This white light photograph clearly shows the development achieved by the selective polymerisation of 1-CECA on the ridges of the latent fingerprint. This confirms that 1-CECA reacts in a manner similar to conventional cyanoacrylate and can render latent fingerprints visible to the naked eye. Figure 4.13*b* shows an FTIR chemical image of the same fingerprint. This is a high quality fingerprint with excellent second and third level detail. This FTIR chemical image was generated using a band at 2854 cm^{-1} (sixth derivative data), presumably due to a C–H stretching vibration. FTIR chemical images of this fingerprint were also obtained at a number of other frequencies including those corresponding to the carbonyl (C=O) stretch between 1780 – 1680 cm^{-1} and the ester C–O stretch at 1188 cm^{-1}. An image could be obtained using the nitrile (C≡N) band at 2253 cm^{-1} but this was of much poorer quality. As with 2-CECA, the nitrile band from the poly-1-CECA was present but had very low intensity even in spectra from reflective surfaces such as this (see Figure 4.14 and caption). On less reflective surfaces, this band was undetectable and therefore could not be used to generate any FTIR chemical images.
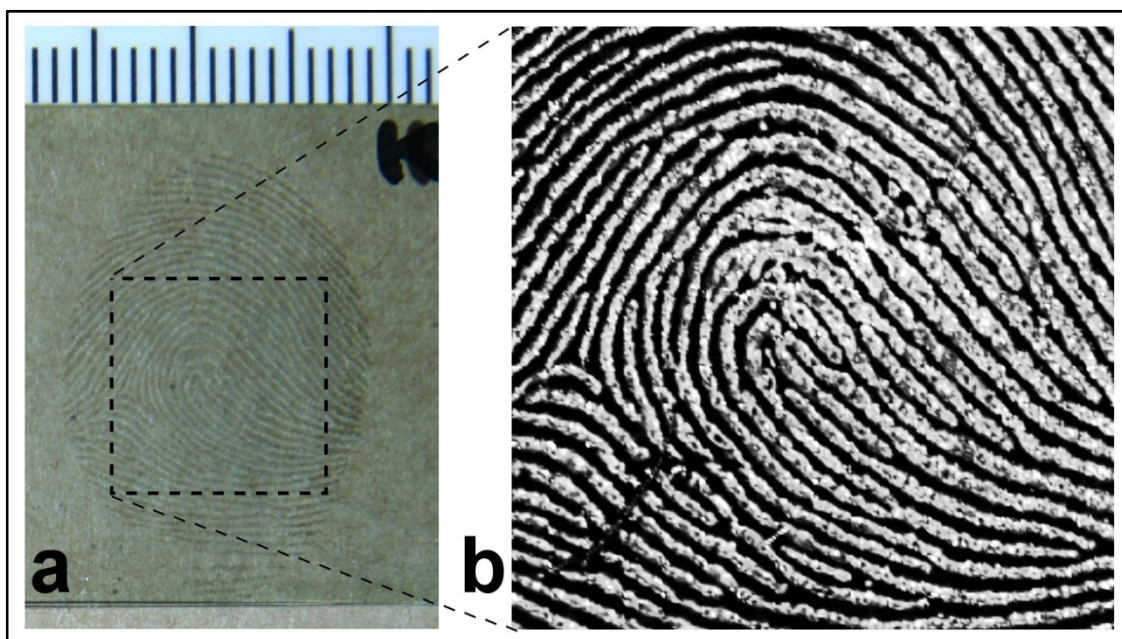

Figure 4.13: *Fingerprint (donor #5) treated with 1-cyanoethyl 2-cyanoacrylate on IR reflective slide. **(a)** White light photograph with area imaged using FTIR chemical imaging indicated. **(b)** Monochrome representation of FTIR chemical image (sixth derivative, 2854 cm^{-1}).*
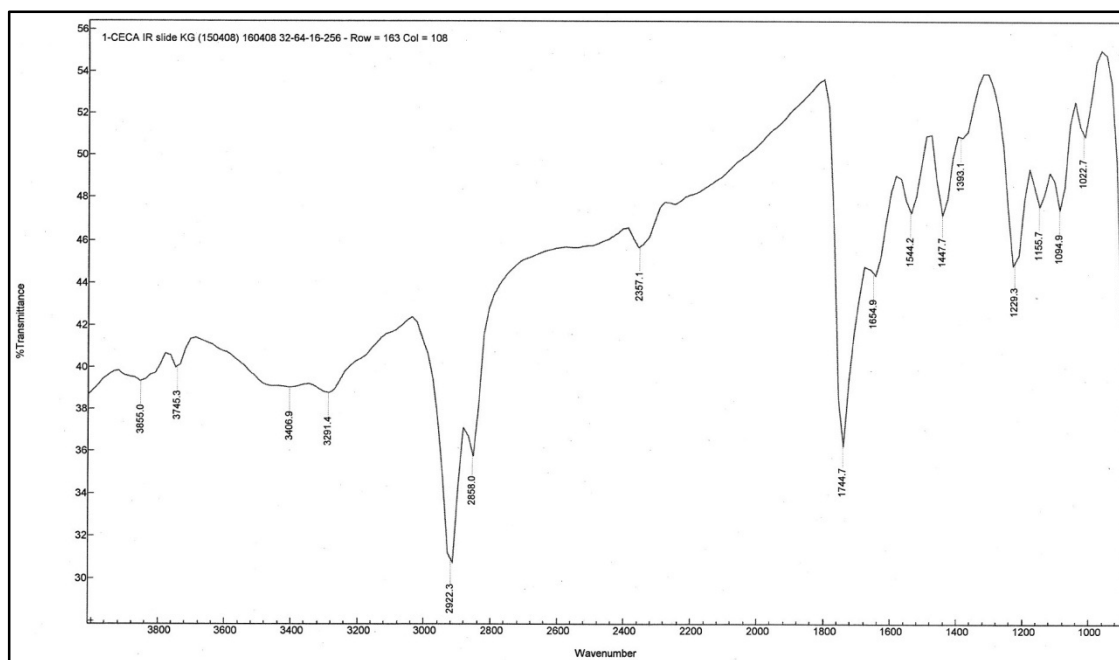
Figure 4.14: *FTIR spectrum from ridge of fingerprint on infrared reflective slide fumed with 1-CECA (poly-1-CECA).*

The absence of any considerable absorption within the 'region of interest' did not hinder the successful imaging of fingerprints developed with 1-CECA on a number of surfaces. Figures 4.15 – 4.18 show several fingerprints on a number of difficult surfaces that were developed using 1-CECA and subsequently imaged using FTIR chemical imaging. In some cases, such as in Figure 4.16*a* and Figure 4.17*a*, the developed fingerprint was partially visible under white light. Achieving good contrast between the developed print and the background was difficult using white light, however, due to the optical properties of these backgrounds. In other cases, such as in Figure 4.15*a* and Figure 4.18*a*, the developed print was almost invisible to the naked eye using conventional optical / photographic techniques. In all these cases, FTIR chemical imaging was able to provide high quality fingerprint images regardless of the optical properties of the background. All FTIR chemical images have been formed using the carbonyl band centred at around 1750 cm^{-1}. This band is not unique to this particular monomer and is indeed present in conventional (ethyl) cyanoacrylate. In fact the use of the carbonyl band of ethyl cyanoacrylate for FTIR chemical imaging of fingerprints has already been discussed in Chapter 2 above. The use of conventional cyanoacrylate and subsequent FTIR chemical imaging on these particular surfaces (i.e. various PMMA sheets, reflective gift wrap and glossy playing cards) was not tested. However, since the contrast achieved with 1-CECA was possible using the carbonyl band only, it is expected that similar results could be achieved on these surfaces using conventional cyanoacrylate.
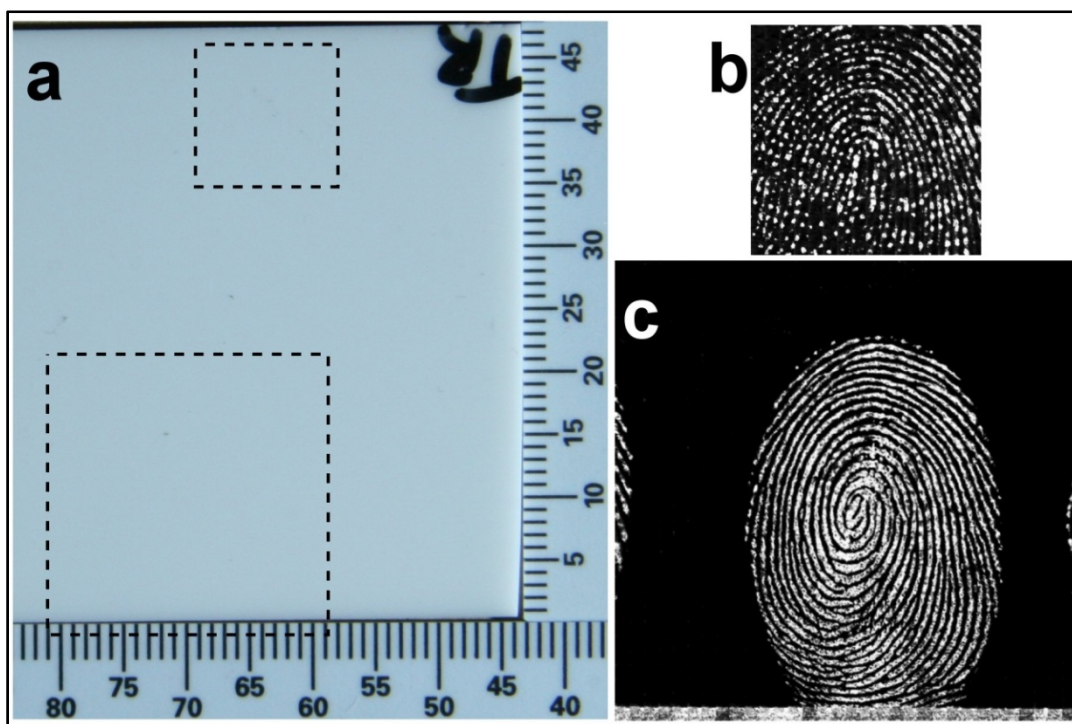
Figure 4.15: *Fingerprints (donors #3 (upper) and #5 (lower)) treated with 1-cyanoethyl 2-cyanoacrylate on opaque white PMMA. **(a)** White light photograph with areas imaged using FTIR chemical imaging indicated. **(b)** Monochrome representation of FTIR chemical image (second derivative, 1774 cm^{-1}) – FTIR image has been rotated 180° relative to white light image. **(c)** Monochrome representation of FTIR chemical image (second derivative, 1728 cm^{-1}).*
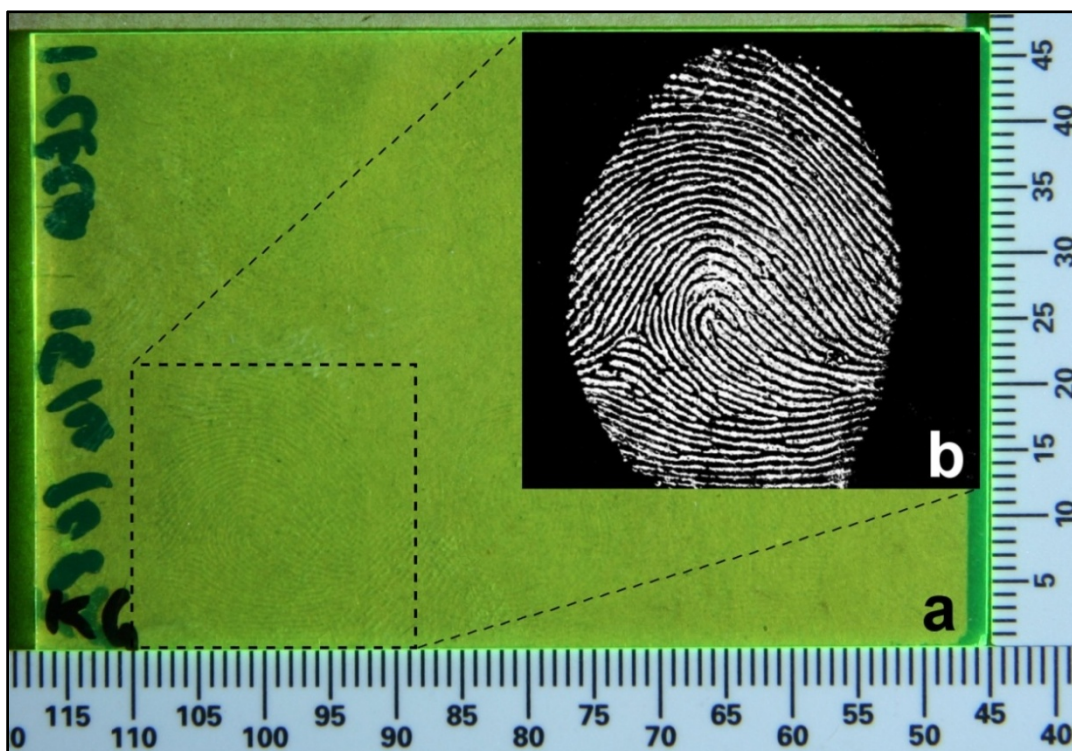
Figure 4.16: *Fingerprint (donor #5) treated with 1-cyanoethyl 2-cyanoacrylate on translucent yellow fluorescent PMMA. **(a)** White light photograph with area imaged using FTIR chemical imaging indicated. **(b)** Monochrome representation of FTIR chemical image (first derivative, 1744 cm^{-1}).*
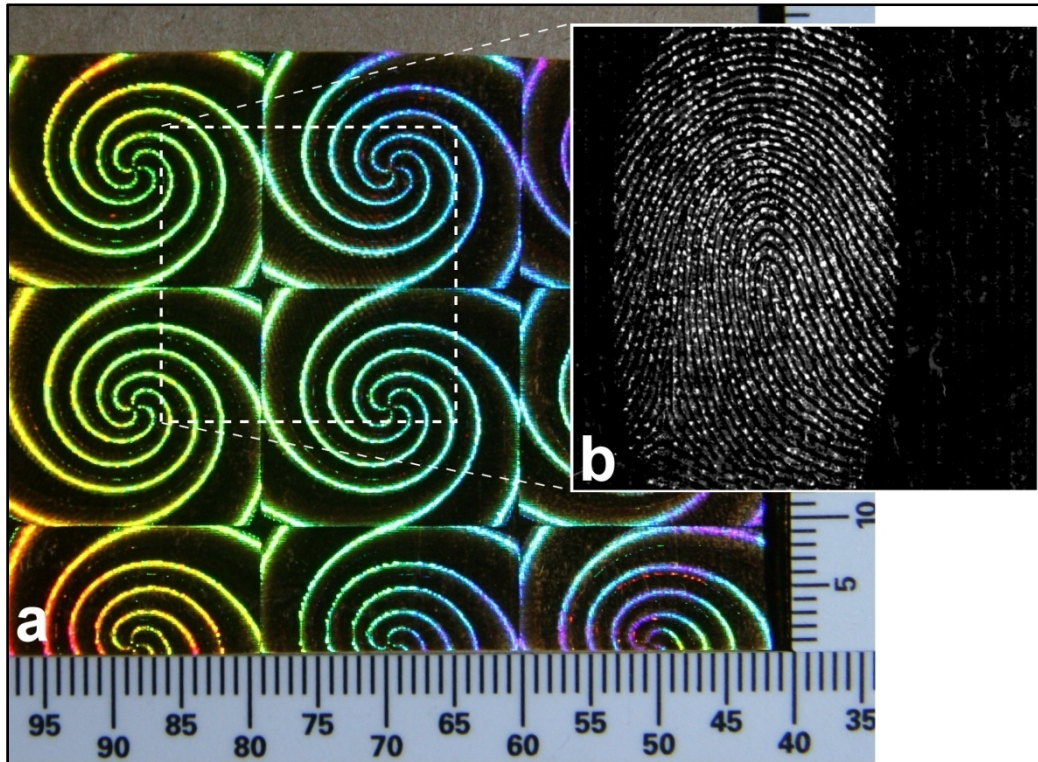
Figure 4.17: *Fingerprint (donor #3) treated with 1-cyanoethyl 2-cyanoacrylate on reflective gift wrap. (a) White light photograph with area imaged using FTIR chemical imaging indicated. (b) Monochrome representation of FTIR chemical image (sixth derivative, 1774 cm^{-1}).*
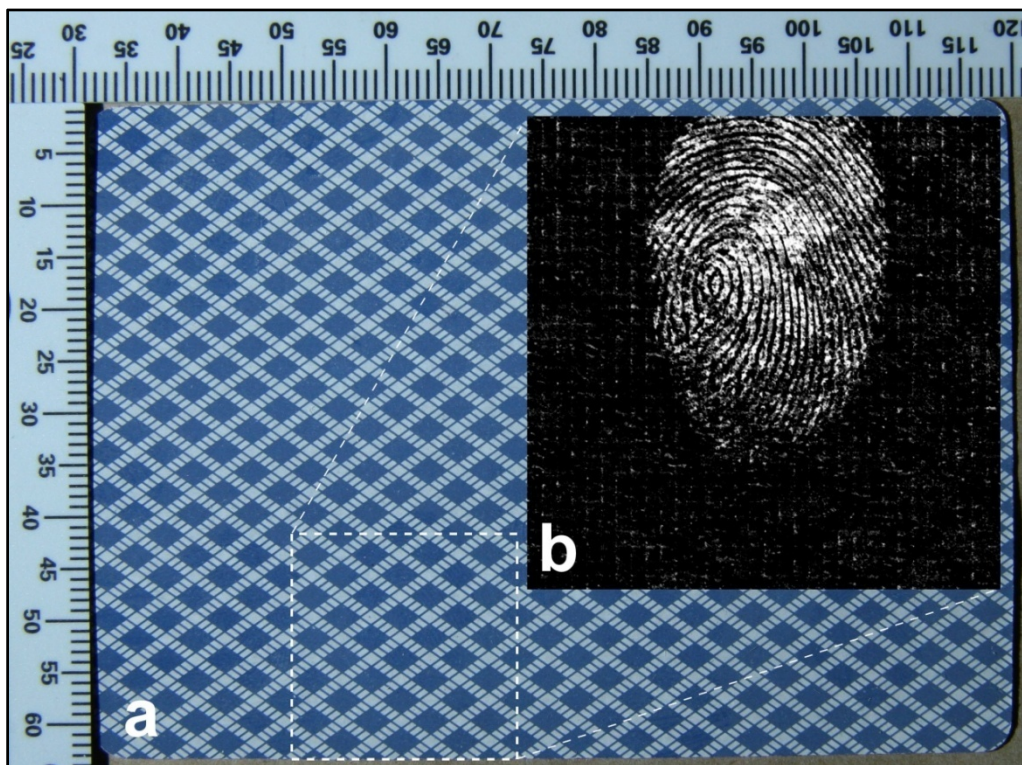
Figure 4.18: *Fingerprint (donor #5) treated with 1-cyanoethyl 2-cyanoacrylate on glossy playing card. (a) White light photograph with area imaged using FTIR chemical imaging indicated. (b) Monochrome representation of FTIR chemical image (second derivative, 1697 cm^{-1}).*

Fingerprints on Australian $5 polymer banknotes treated with 1-CECA were also successfully imaged using FTIR chemical imaging (see Figure 4.20 and Figure 4.21). The FTIR chemical imaging of fingerprints of polymer banknotes developed using conventional cyanoacrylate has been previously demonstrated (see Tahtouh et al.[75,76] and Section 2.3.4.2 above). Using the carbonyl band from conventional cyanoacrylate, good quality fingerprint images are obtained if the print is located on areas of the banknotes that does not contain raised intaglio printing. In areas that do contain intaglio printing, however, the size and intensity of an interfering peak from the background increases and contrast is difficult or impossible to achieve (see Figure 4.19 and caption).
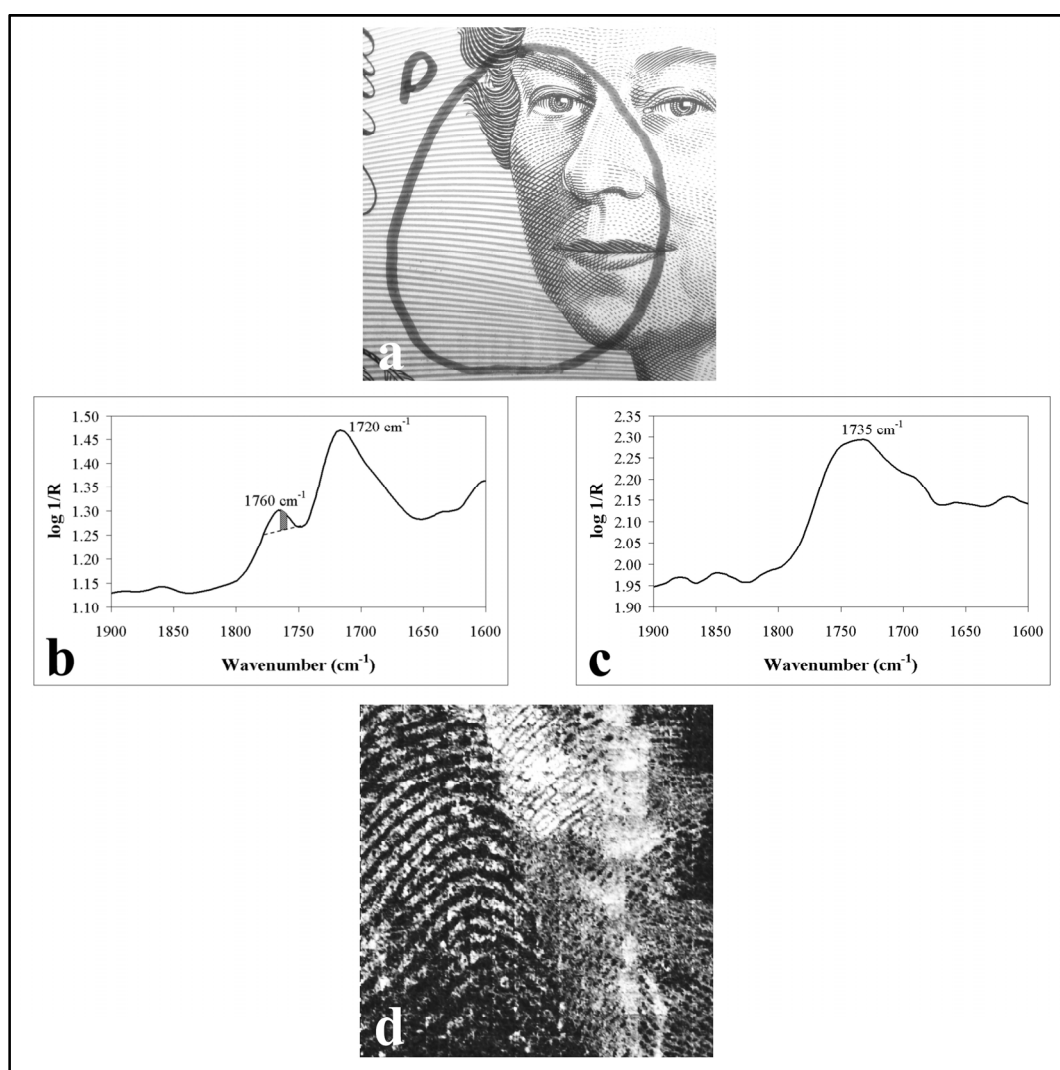
Figure 4.19: *Image adapted from Tahtouh et al.[75] showing loss in contrast between print (fumed with conventional cyanoacrylate) and polymer banknote background on areas with raised intaglio printing. **(a)** White light photograph of ethyl cyanoacrylate fumed print on $5 note. **(b)** Infrared spectrum of fingerprint ridge on area of banknote free from raised intaglio printing showing peak area at 1760 cm^{-1} used to generate image. **(c)** Infrared spectrum of area of banknote with raised intaglio printing showing increase in size and intensity of interfering background peak. **(d)** Monochrome representation of infrared chemical image (1760 cm^{-1} peak area).*

Figure 4.20 shows an Australian $5 polymer banknote treated with 1-CECA. Four areas were selected for FTIR chemical imaging and these are indicated on the white light photograph (Figure 4.20*a*) and labelled *b – e*. Area *e* is on an area that is free from any raised intaglio printing and, as with prints fumed with conventional cyanoacrylate, the FTIR chemical image of the 1-CECA fumed fingerprint in this area (Figure 4.20*e*) shows very clear ridge detail. More importantly, FTIR chemical imaging of fingerprints in areas that do contain raised intaglio printing also show very clear ridge detail (see Figure 4.20*b-d*). The intaglio printing in these areas can be almost completely eliminated in the FTIR chemical images.
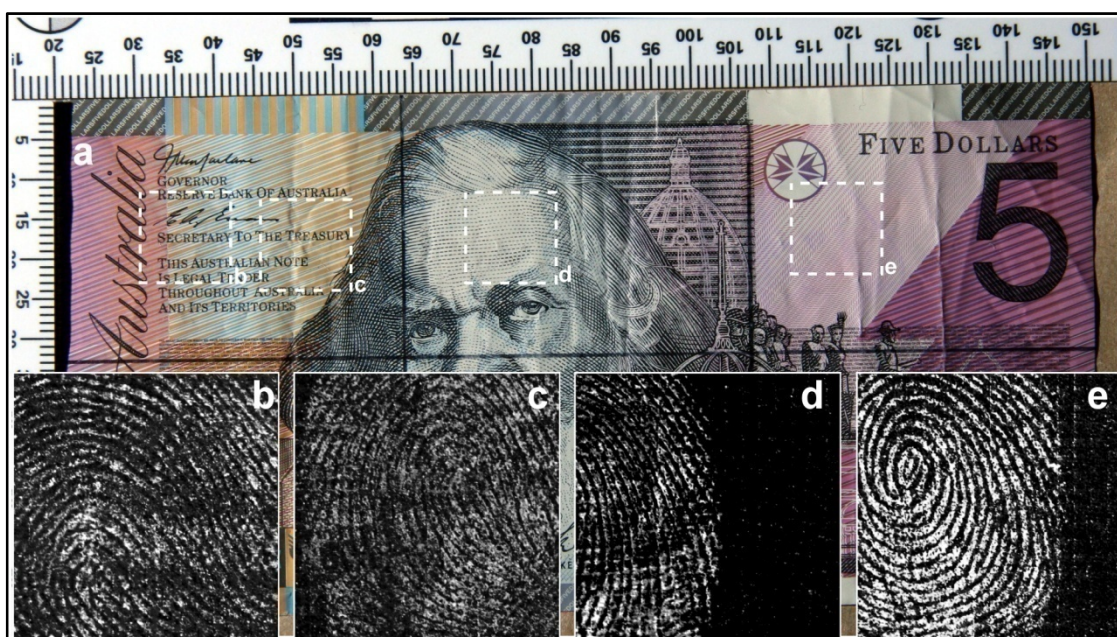
Figure 4.20:   *Fingerprints (donor #5) treated with 1-cyanoethyl 2-cyanoacrylate on Australian $5 polymer banknote. **(a)** White light photograph with areas imaged using FTIR chemical imaging indicated. **(b - e)** Monochrome representations of FTIR chemical images using: **(b)** second derivative, 1697 cm^{-1}, **(c)** eighth derivative, 1682 cm^{-1}, **(d)** eighth derivative, 1713 cm^{-1}, **(e)** sixth derivative, 1713 cm^{-1}.*

Larger areas of the same banknote were also analysed using FTIR chemical imaging (see Figure 4.21). Once again the fingerprint ridge detail is very clear even in areas that are almost exclusively printed in intaglio printing (see Figure 4.21*b*) or areas with very heavy intaglio printing (see Figure 4.21*c*).
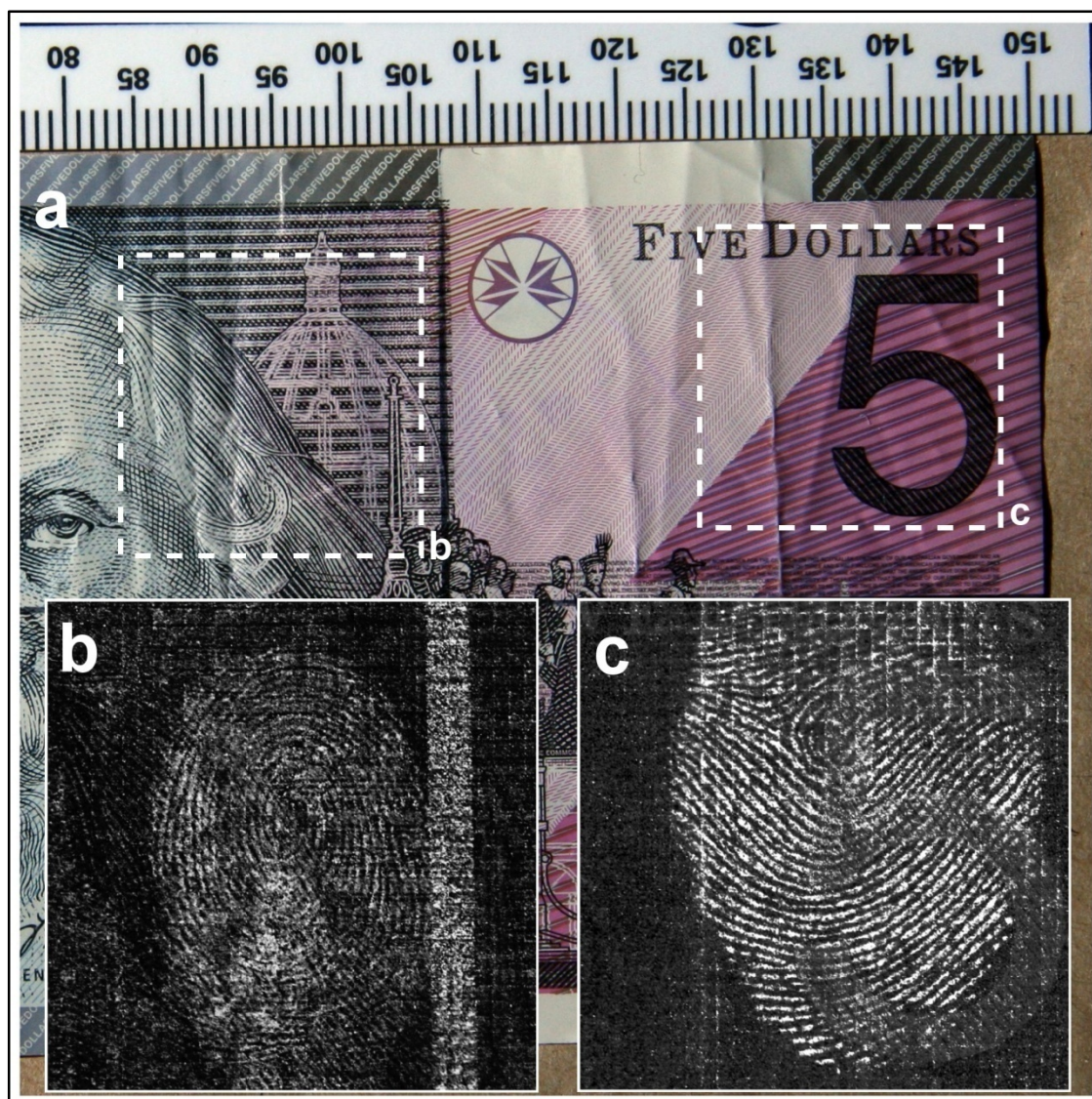
Figure 4.21: *Fingerprints (donor #5) treated with 1-cyanoethyl 2-cyanoacrylate on $5 Australian polymer banknote. **(a)** White light photograph with areas imaged using FTIR chemical imaging indicated. **(b)** Monochrome representation of FTIR chemical image (fourth derivative, 1713 cm^{-1}). **(c)** Monochrome representation of FTIR chemical image (fourth derivative, 1713 cm^{-1}).*

The results shown in Figure 4.20 and Figure 4.21 for fingerprints fumed with 1-CECA are superior to results obtained using conventional cyanoacrylate (and 2-CECA). Interestingly the contrast was not achieved using an absorption band within the 'region of interest' as originally planned. Instead it appears that the absorption band for the carbonyl group in poly-1-CECA is sufficiently resolved from any absorption due to the polymer banknotes (and its printing) to provide good contrast images of the treated fingerprint. This is not the case for conventional cyanoacrylate or 2-CECA. The shift in frequency observed for the carbonyl band is likely due to the close proximity of the additional electron-withdrawing nitrile functional group, which effectively increases the bond strength of the C=O bond and

increases its fundamental vibrational frequency. This is clearly seen in the FTIR spectrum of the precursor anthracene adduct (A/1-CECA), which shows a C=O stretch at 1763 cm^{-1} compared to 1753 cm^{-1} for A/2-CECA or 1747 cm^{-1} for A/ECA (the anthracene adduct of conventional (ethyl) cyanoacrylate). This is discussed in Section 3.5.3 above. Furthermore, the FTIR spectrum of a 1-CECA-fumed fingerprint on a reflective slide (see Figure 4.14 above) shows a carbonyl absorption of around 1750 cm^{-1}. Although this peak does not show the same shift in frequency as that seen for A/1-CECA, the absorption is very broad compared to that of poly-2-CECA for example (see Figure 4.11 above). At this stage it is unclear whether the contrast between the polymer banknote background and the poly-1-CECA on the ridges of the treated print is due to a shift in frequency or simply the broad absorption. In any case, at least part of the carbonyl peak from poly-1-CECA is resolved from any absorption from the polymer banknote background, particularly when higher order derivatives are used.

4.3.5 Trideuteromethyl 2-cyanoacrylate (MCA-d$_3$)

Monomeric trideuteromethyl 2-cyanoacrylate (MCA-d$_3$) was obtained in crude form from its anthracene adduct (A/MCA-d$_3$). As reported in Section 3.6, the crude monomer was found (by NMR) to be a mixture of approximately 70% w/w MCA-d$_3$ and 30% w/w anthracene / trideuteromethyl 2-cyanoacrylate adduct (A/MCA-d$_3$), the precursor compound. As expected, it was possible to fume MCA-d$_3$ monomer at moderate temperatures (less than 150 °C) and therefore avoid the thermal degradation of the anthracene adduct (A/MCA-d$_3$).

Using the custom-made cyanoacrylate fuming cabinet described earlier (see Figure 4.7), approximately 2.15 g of crude MCA-d$_3$ was charged into the wells of the aluminium heating block. A number of samples bearing freshly deposited fingerprints from two donors (#3 and #5) were placed inside the cabinet prior to sealing the chamber and heating the monomer. The samples treated with MCA-d$_3$ included an infrared reflective slide, glossy playing cards, plastic-coated playing cards, white opaque PMMA, translucent blue fluorescent PMMA, translucent green fluorescent PMMA, translucent red fluorescent PMMA, reflective gift wrap and an Australian polymer $5 banknote.

As with 1-CECA (see Section 4.3.4 above), recovery and analysis of the residue (0.65 g) remaining in the heater after fuming confirmed that A/MCA-d$_3$ remained behind while the monomer volatilised and developed the latent fingerprints. It was also possible to recover the residual A/MCA-d$_3$ and, after recrystallisation, reuse it in subsequent reactions. The mass

of A/MCA-d$_3$ recovered is also further evidence that the original sample was a 70:30 mixture of the monomer and anthracene adduct.

Figure 4.22*a* shows a fingerprint (donor #5) developed with MCA-d$_3$ on an infrared reflective slide. This white light photograph clearly shows the development achieved by the selective polymerisation of MCA-d$_3$ on the ridges of the latent fingerprint. This confirms that MCA-d$_3$ reacts in a manner similar to conventional (ethyl) cyanoacrylate (and, for that matter, methyl cyanoacrylate) and can render latent fingerprints visible to the naked eye. Figure 4.22*b* shows an FTIR chemical image of the same fingerprint. This is a high quality fingerprint with excellent second and third level detail. This FTIR chemical image was generated using the carbonyl band at 1743 cm^{-1} (second derivative data). FTIR chemical images of this fingerprint were also obtained at a number of other frequencies near this maxima as well as those corresponding to the ester C–O stretch near 1188 cm^{-1} among others. An image could be obtained using the C–D stretching band at 2182 cm^{-1} but this was of poorer quality. As with 2-CECA and 1-CECA the bands in the region of interest (the ones owing to the C–D stretching modes in this case) were present but had relatively low intensity even in spectra from a reflective surfaces such as this (see Figure 4.23 and caption). On less reflective surfaces, these bands were undetectable and therefore could not be used to generate any FTIR chemical images.
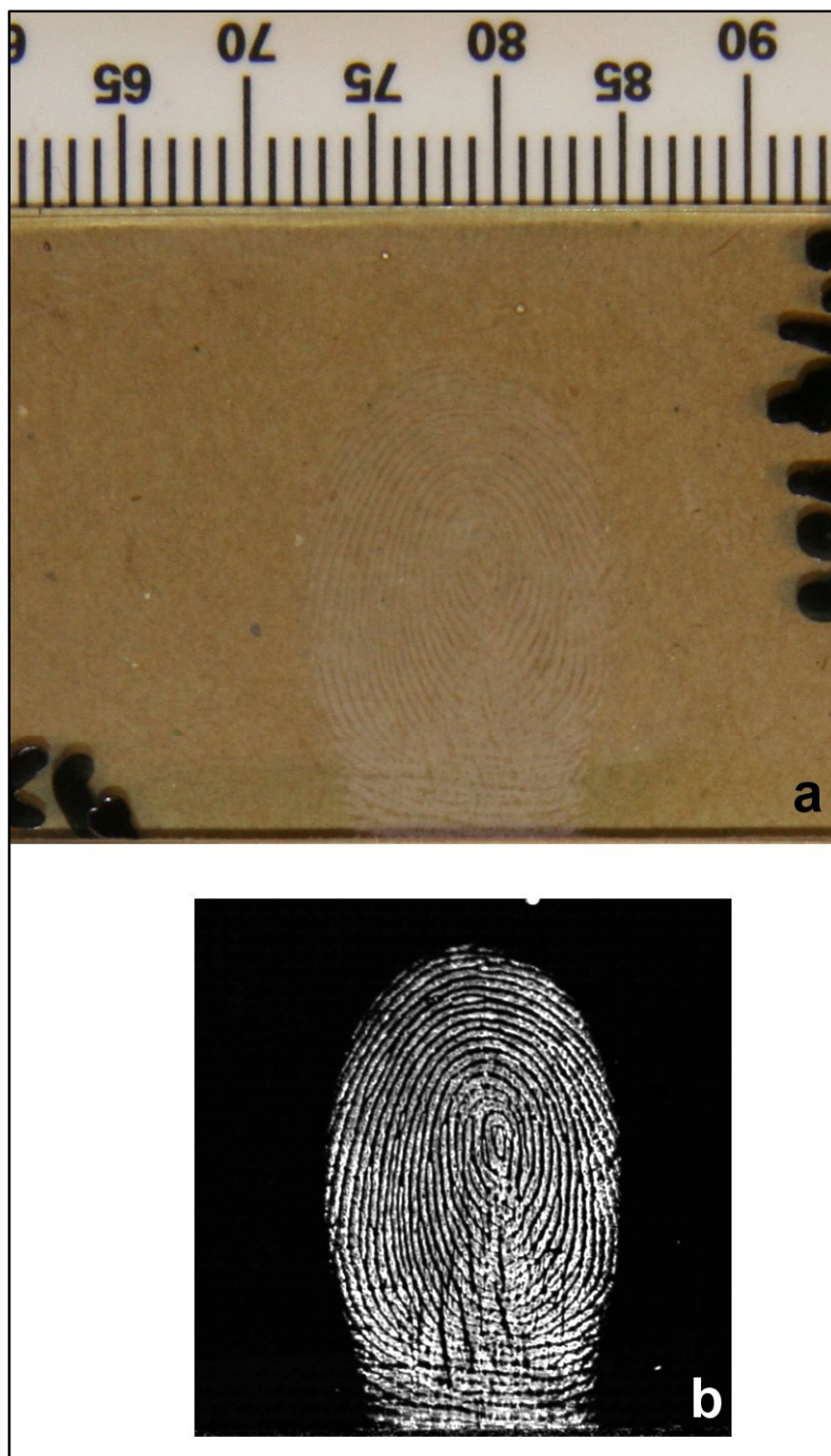
Figure 4.22: *Fingerprint (donor #5) treated with trideuteromethyl 2-cyanoacrylate on IR reflective slide.* **(a)** *White light photograph.* **(b)** *Monochrome representation of FTIR chemical image (second derivative, 1743 cm^{-1}).*
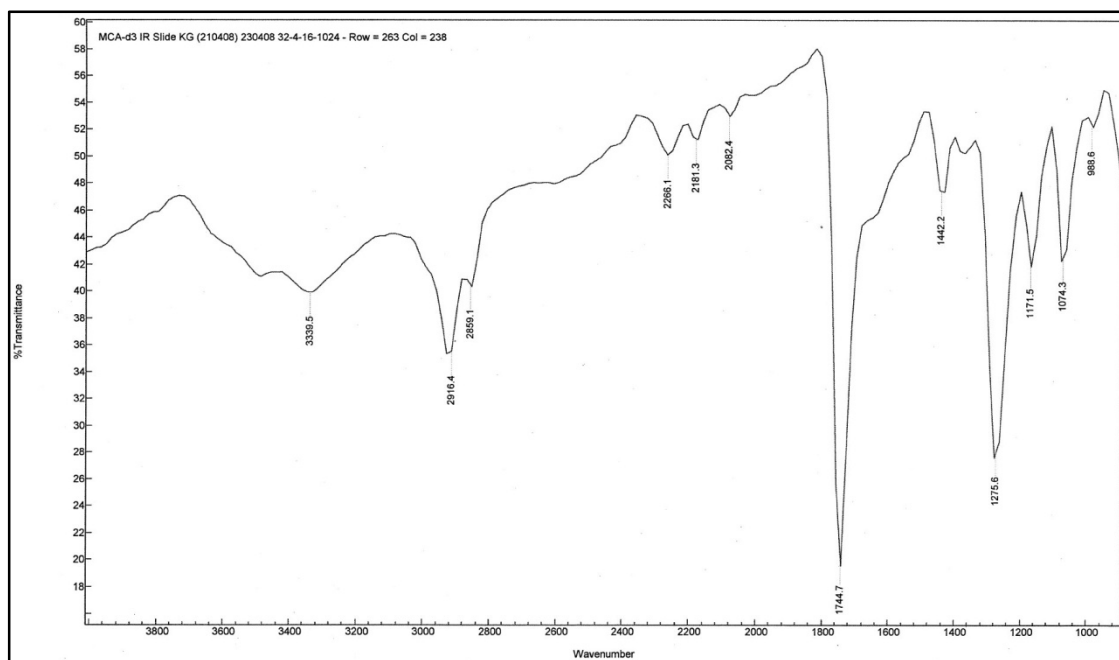
Figure 4.23: *FTIR spectrum from ridge of fingerprint on infrared reflective slide fumed with MCA-d_3 (poly- MCA-d_3).*

Figure 4.24 shows white light images and the corresponding FTIR chemical images of fingerprints from donors #5 and #3 on translucent red fluorescent PMMA. On this surface, some prints (such as the print in Figure 4.24*a*) were clearly visible to the naked eye while others (such as the print in Figure 4.24*b*) were much fainter. Since the background is highly fluorescent, the results are unlikely to improve with luminescent staining. In all cases FTIR chemical imaging gave high quality fingerprint images. These images, however, were formed by simply using the carbonyl region and hence similar results on these surfaces may be obtained using conventional cyanoacrylate. As discussed above, the intensity of the bands for the C–D stretch were too low to be utilised. For this reason it was not possible to obtain any clear images of prints treated with MCA-d_3 on polymer banknotes.
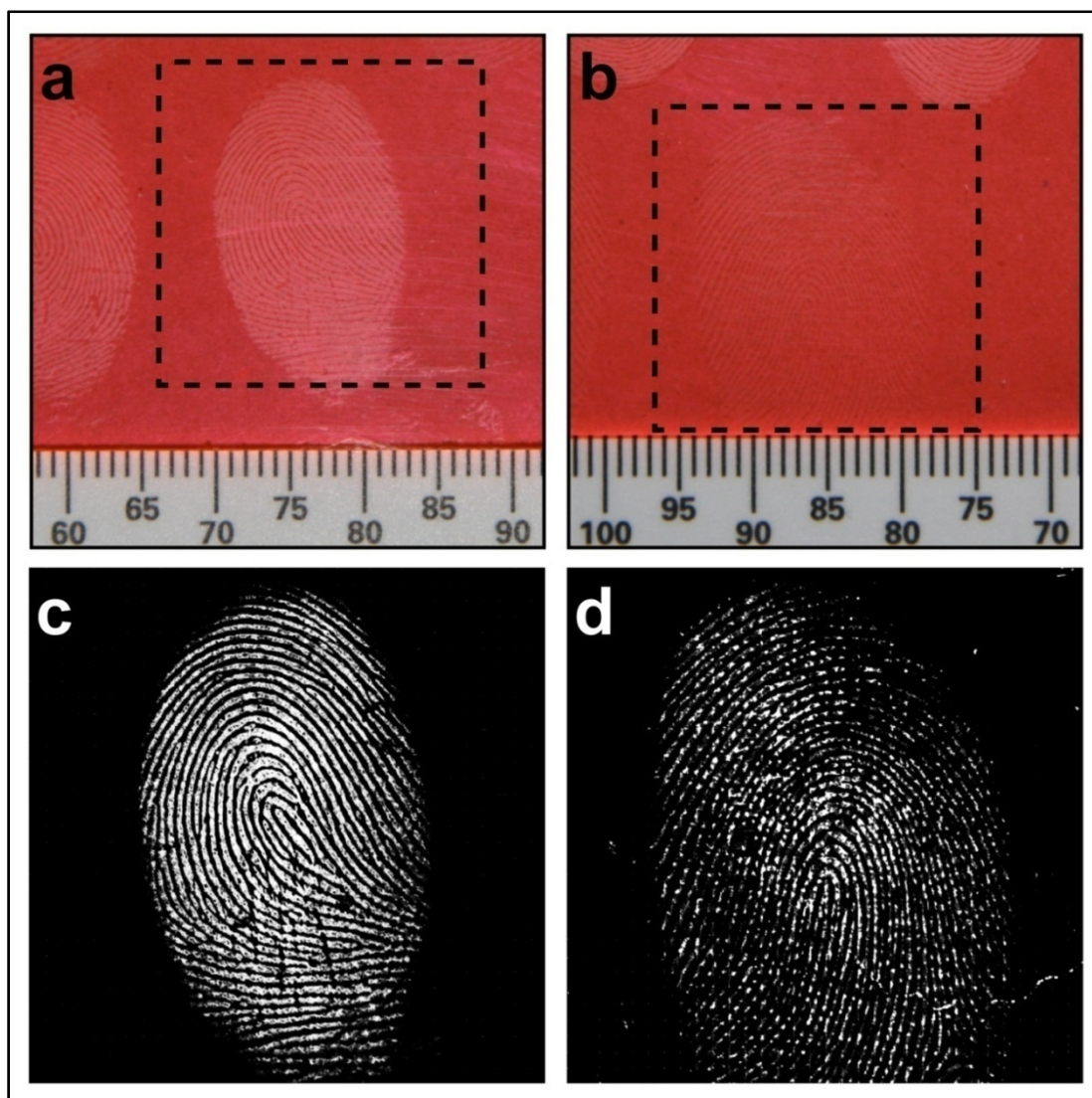
Figure 4.24: *Fingerprints (donor #5 (a, c) and #3 (b, d)) treated with trideuteromethyl 2-cyanoacrylate on red fluorescent PMMA. **(a)** and **(b)** White light photographs with areas imaged using FTIR chemical imaging indicated. **(c)** Monochrome representation of FTIR chemical image of fingerprint in (a) (second derivative, 1713 cm^{-1}). **(d)** Monochrome representation of FTIR chemical image of fingerprint in (b) (second derivative, 1728 cm^{-1}).*

4.3.6 Pentadeuteroethyl 2-cyanoacrylate (ECA-d$_5$)

Monomeric pentadeuteroethyl 2-cyanoacrylate (ECA-d$_5$) was obtained in crude form from its anthracene adduct (A/ECA-d$_5$). As reported in Section 3.6, the crude monomer was found (by NMR) to be a mixture of approximately 50% w/w ECA-d$_5$ and 50% w/w anthracene / pentadeuteroethyl 2-cyanoacrylate adduct (A/ECA-d$_5$), the precursor compound. As expected, it was possible to fume ECA-d$_5$ monomer at moderate temperatures (less than 160 °C) and therefore avoid the thermal degradation of the anthracene adduct (A/ECA-d$_5$).

Using the custom-made cyanoacrylate fuming cabinet described earlier (see Figure 4.7), crude monomeric ECA-d$_5$ was used to fume samples bearing latent fingerprints. During several attempts, a number of samples with fresh latent fingerprints from two donors (donors #3 and #5) were placed inside the fuming cabinet prior to sealing the chamber and heating the monomer. The samples treated with MCA-d$_3$ included an infrared reflective slide, glossy playing cards, plastic-coated playing cards, white opaque PMMA, translucent blue fluorescent PMMA, translucent green fluorescent PMMA, translucent red fluorescent PMMA, reflective gift wrap and an Australian polymer $5 banknote.

In one experiment, approximately 3.68 g of crude ECA-d$_5$ was charged into the wells of the aluminium heating block. The monomeric ECA-d$_5$ was heated to approximately 110 °C before some bubbling was observed and fumes began to evolve. Fumes continued to evolve from the heated monomer while the temperature was slowly increased to a maximum of 160 °C (after 20 minutes) before switching the heater unit off and allowing to cool.

As with 1-CECA (see Section 4.3.4 above) and MCA-d$_3$ (see Section 4.3.5 above), recovery and analysis of the residue (2.00 g) remaining in the heater after fuming confirmed that A/ECA-d$_3$ remained behind while the monomer volatilised and developed the latent fingerprints. It was also possible to recover the residual A/ECA-d$_5$ and, after recrystallisation, reuse it in subsequent reactions. The mass of A/ECA-d$_5$ recovered is also further evidence that the original sample was approximately a 50:50 (probably 45:55) mixture of the monomer and anthracene adduct.

Figure 4.25*a* shows a fingerprint (donor #5) developed with ECA-d$_5$ on an infrared reflective slide. This white light photograph clearly shows the development achieved by the selective polymerisation of ECA-d$_5$ on the ridges of the latent fingerprint. This confirms that ECA-d$_5$ reacts in a manner indistinguishable from that of conventional (ethyl) cyanoacrylate and can render latent fingerprints visible to the naked eye. Figure 4.25*b* shows an FTIR chemical image of the same fingerprint. This is a high quality fingerprint with excellent second and third level detail. This FTIR chemical image was generated using the C–D stretching band at 2182 cm^{-1} (peak area). This band was useful in forming images of the developed print on this reflective surface as its intensity was sufficient to provide a reasonable signal (see Figure 4.26 and caption). On less reflective surfaces, however, this band (and others corresponding to C–D stretches in this region) had a very low intensity and were generally undetectable and therefore could not be used to generate any FTIR chemical images.
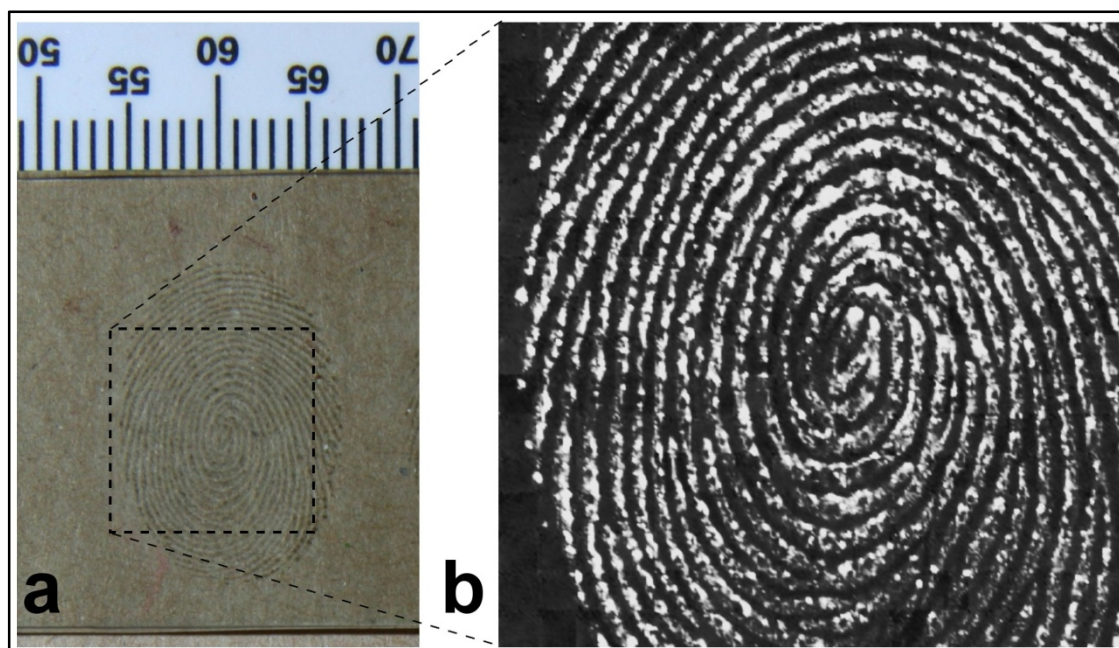
Figure 4.25: *Fingerprint (donor #5) treated with pentadeuteroethyl 2-cyanoacrylate on IR reflective slide. **(a)** White light photograph with area imaged using FTIR chemical imaging indicated. **(b)** Monochrome representation of FTIR chemical image (peak area 2248 cm^{-1}).*
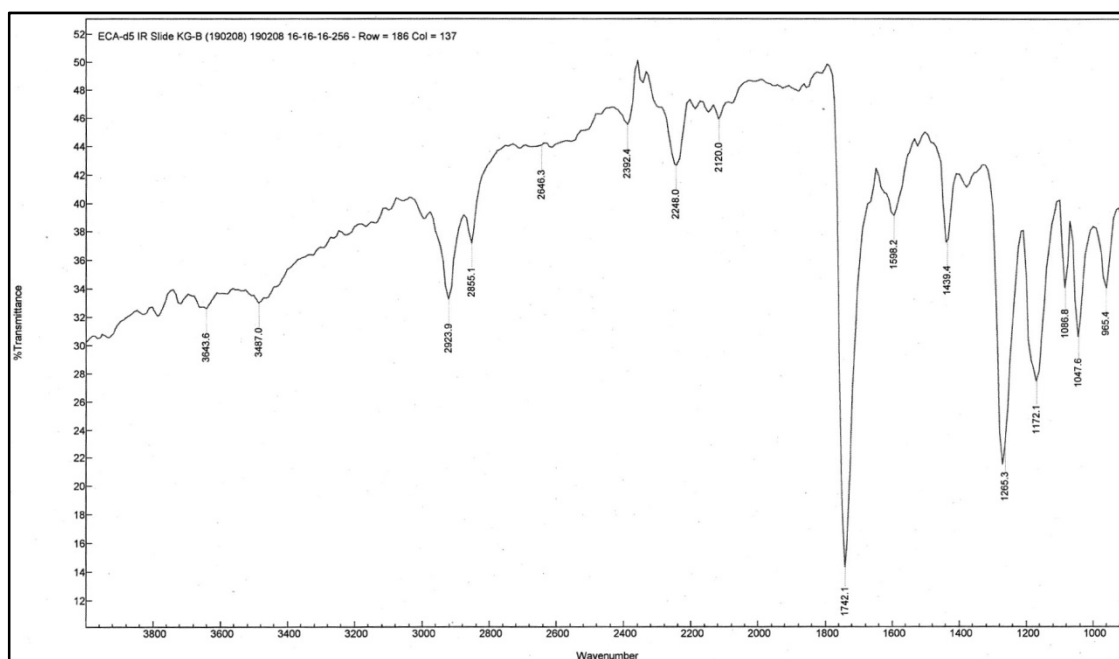
Figure 4.26: *FTIR spectrum from ridge of fingerprint on infrared reflective slide fumed with ECA-d$_5$ (poly- ECA-d$_5$).*

FTIR chemical images of the fingerprint shown in Figure 4.25 were also obtained at a number of other frequencies including those corresponding to the carbonyl (C=O) stretch and the ester C–O stretch. As discussed above, bands in this region are also present in conventional

cyanoacrylate and so do not provide any particular advantages. Nevertheless, Figure 4.27 and Figure 4.28 show fingerprints developed with ECA-d$_5$ on opaque white PMMA and a glossy playing card respectively. These developed fingerprints are difficult or impossible to see under white light but high quality images can be obtained using FTIR chemical imaging.
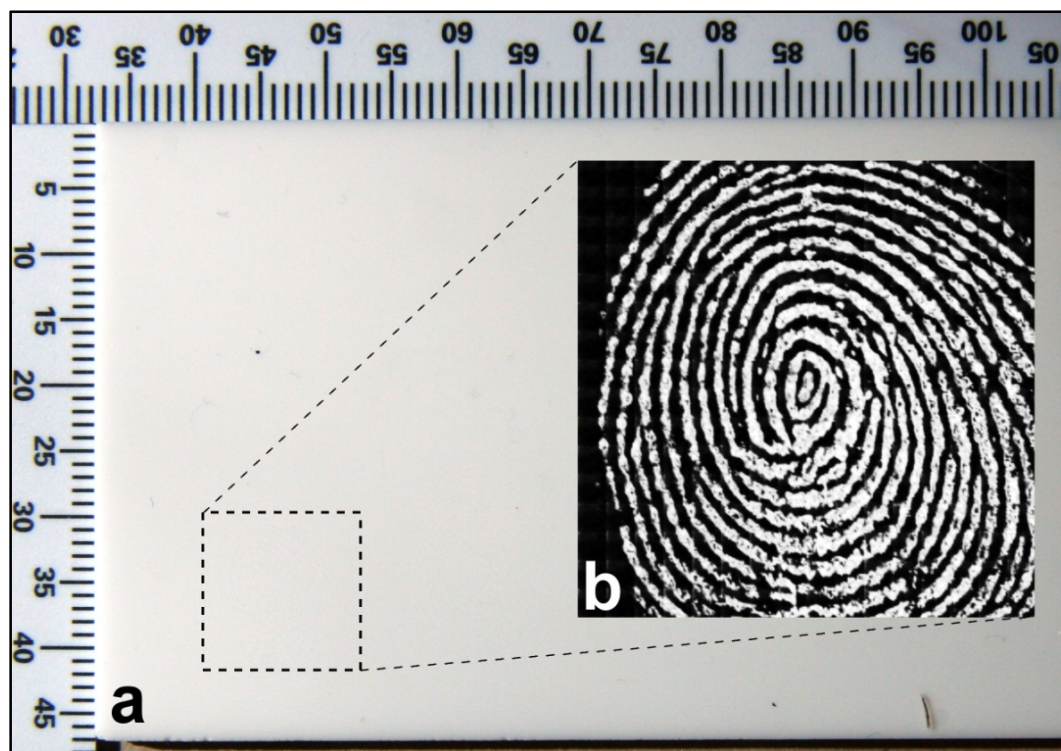
Figure 4.27:   *Fingerprint (donor #5) treated with pentadeuteroethyl 2-cyanoacrylate on opaque white PMMA. **(a)** White light photograph with area imaged using FTIR chemical imaging indicated. **(b)** Monochrome representation of FTIR chemical image (second derivative, 1728 cm^{-1}).*
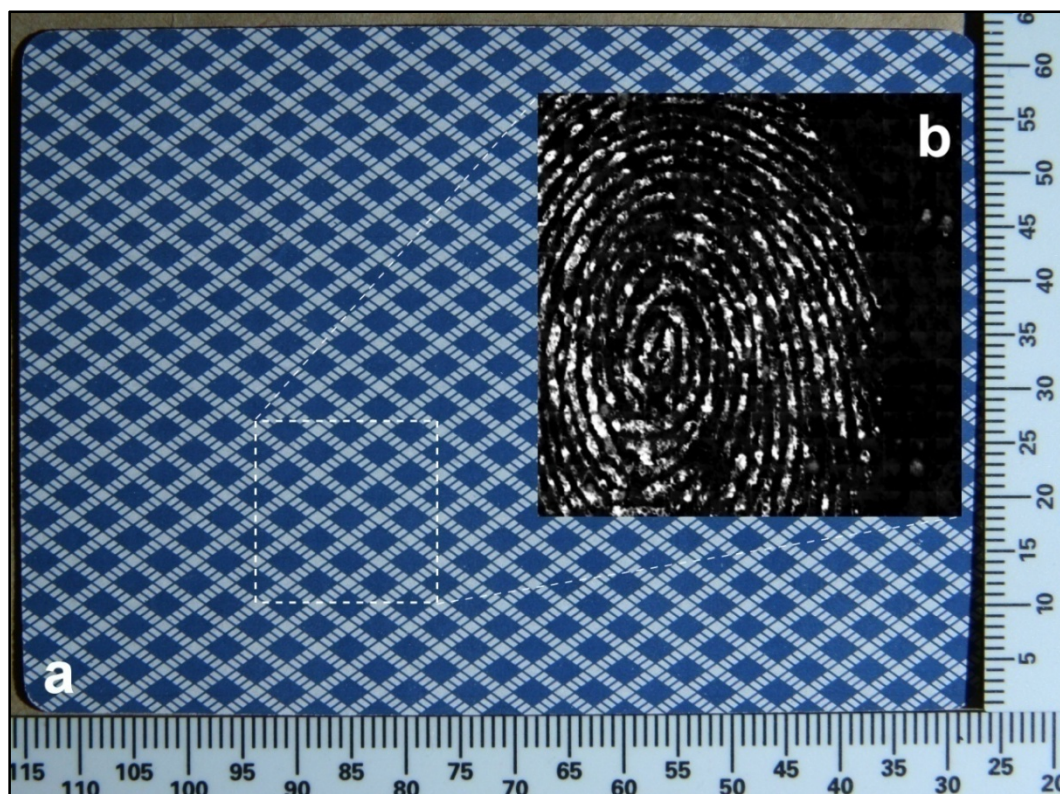
Figure 4.28:   *Fingerprint (donor #5) treated with pentadeuteroethyl 2-cyanoacrylate on glossy playing card. **(a)** White light photograph with area imaged using FTIR chemical imaging indicated. **(b)** Monochrome representation of FTIR chemical image (fourth derivative, 1651 cm^{-1}).*

The FTIR chemical imaging of one particular sample, which had been fumed with ECA-d$_5$, provided some interesting results.   Figure 4.29*a* shows a white light photograph of a fingerprint developed with ECA-d5 on a Vietnamese 10,000 dong polymer banknote. Figure 4.29*b* shows an FTIR chemical image of the region indicated, which has been formed using the band at 2252 cm^{-1} (this band is probably a C–D stretching mode but could also be a C≡N stretching mode). A faint partial fingerprint is seen in this example but, as with conventional cyanoacrylate, there is clear interference from the raised intaglio printing.
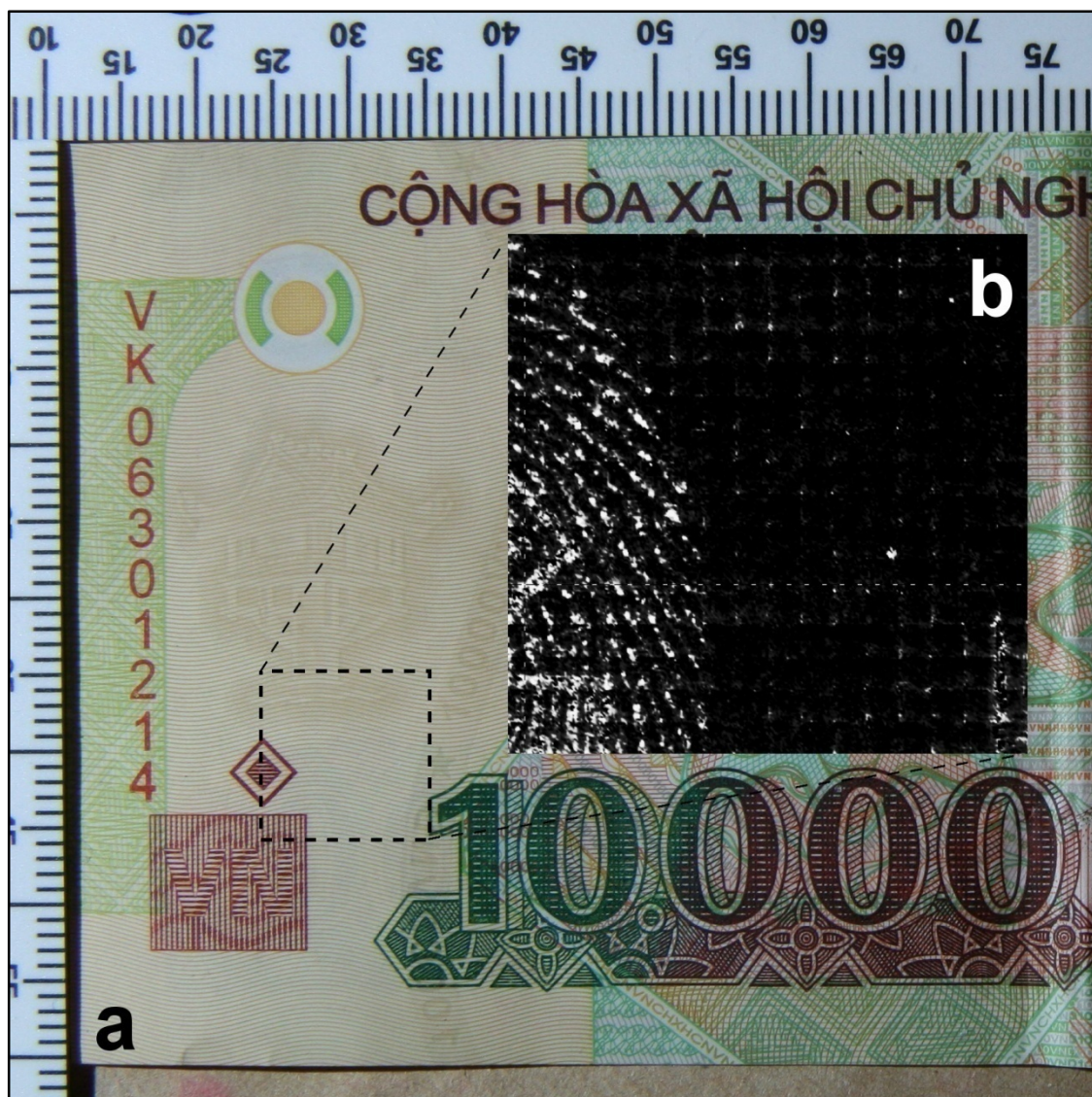
Figure 4.29: *Fingerprint (donor #5) treated with pentadeuteroethyl 2-cyanoacrylate on Vietnamese 10,000 dong polymer banknote. (a) White light photograph with area imaged using FTIR chemical imaging indicated. (b) Monochrome representation of FTIR chemical image (peak area 2252 cm^{-1}).*

This sample actually provided some interesting results that may help to explain why the raised intaglio printing is so problematic for the FTIR chemical imaging of fingerprints. Figure 4.30 shows the FTIR chemical image (Figure 4.30*a*) and two infrared spectra (Figure 4.30*b*) from the pixels indicated. The upper spectrum is from an area on a fingerprint ridge and, as expected, contains peaks characteristic of the pentadeuteroethyl 2-cyanoacrylate polymer (poly-ECA-d$_5$). In particular, a peak at 2250 cm^{-1} and a smaller one at 2120 cm^{-1} correspond to the nitrile and C–D stretches. The lower spectrum, from an area between fingerprint ridges but on the raised intaglio printing, also contains these peaks and is almost indistinguishable from the upper spectrum. This leads to the possibility that, when this sample was fumed with ECA-d$_5$ monomer, there was deposition of polymer on the ridges *and* on the inks of the

raised intaglio printing. The fact that both the ridges and the raised intaglio printing contain the same chemical deposit, and hence produce the same infrared spectral profile, explains the lack of contrast between the fingerprint ridge detail and the intaglio printing.
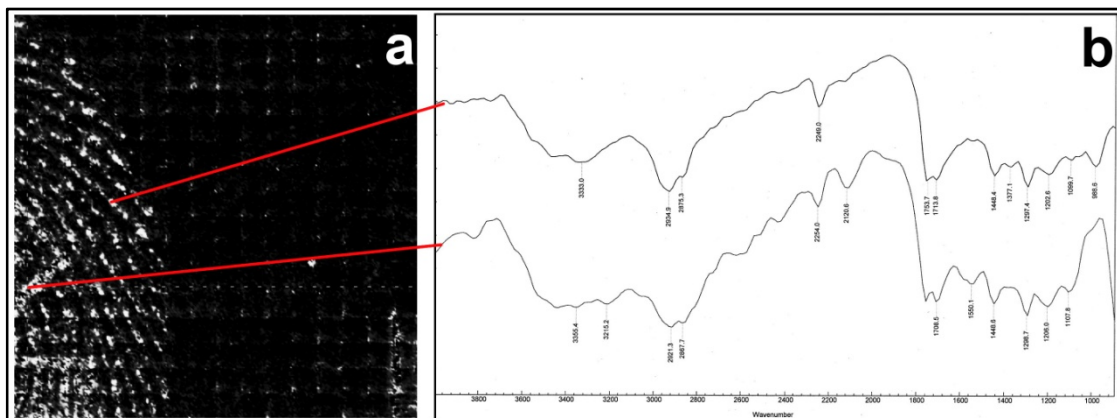
Figure 4.30: *Fingerprint (donor #5) treated with pentadeuteroethyl 2-cyanoacrylate on Vietnamese 10,000 dong polymer banknote. **a)** Monochrome representation of FTIR chemical image (peak area 2252 cm^{-1}). **b)** FTIR spectra from areas indicated; on fingerprint ridge (upper spectrum) and intaglio printing (lower spectrum).*

This finding could also explain the lack of contrast observed with conventional cyanoacrylate-fumed fingerprints on areas of polymer banknotes that contain raised intaglio printing. It also presents a possible solution to this problem. Perhaps by careful control of the fuming conditions (temperature, relative humidity etc), the attraction between the cyanoacrylate vapours and the intaglio printed areas can be minimised and selective deposition on the latent fingerprint deposits can be achieved. This would require a series of further carefully controlled experiments and is beyond the scope of this thesis. The new cyanoacrylate monomers discussed here, however, provide excellent tools for this kind of study. The advantage they can provide is that they have a unique infrared signature that can easily be identified by the presence of a few bands in key areas of the spectrum. When examined with FTIR chemical imaging, it is easy to ascertain where the cyanoacrylate has deposited.

4.3.7   Summary and general discussion on the use of novel cyanoacrylates for latent fingerprint enhancement

All four novel cyanoacrylates synthesised and tested in this study reacted with latent fingerprint deposits in a manner indistinguishable from conventional cyanoacrylate. The following is a summary of the results obtained and recommendations for each of these monomers.

The low volatility of 2-cyanoethyl 2-cyanoacrylate (2-CECA) made it difficult or impossible to fume latent fingerprints using the common heat acceleration method. Vacuum deposition was more successful and 2-CECA-fumed fingerprints on reflective surfaces and glass were successfully imaged. The intensity of the additional nitrile band was very low and was not detected on less reflective surfaces such as polymer banknotes. As with conventional cyanoacrylate, the carbonyl band overlapped with an interfering band from the polymer banknote (particularly on areas with raised intaglio printing). For these reasons, 2-CECA did not perform well on polymer banknotes.

In one experiment, involving the treatment of a reflective slide with 2-CECA in a round bottom flask under vacuum, a strange phenomenon was observed. As mentioned in Section 4.3.3 above, the preferential deposition of material on the ridges of the latent fingerprints in this sample were observed. In contrast to results using a more conventional experimental set-up or the reaction vessel discussed in Section 4.3.3 above (see Figure 4.8), the FTIR spectra (from the FTIR chemical images) of material preferentially deposited on the fingerprint ridges in this sample had very intense nitrile bands near 2255 cm^{-1}. A spectrum from a fingerprint treated with 2-CECA in this manner is shown in Figure 4.31. In addition to a large nitrile band, this spectrum also has a peak at ~1630 cm^{-1}, which can be attributed to an alkenyl (C=C) stretch. This tends to suggest that the material preferentially deposited on the fingerprint ridges is monomeric 2-CECA. Furthermore, this spectrum was collected three months after treatment, which indicates that the monomeric 2-CECA deposited on the ridges has not polymerised despite having had ample time to cure.
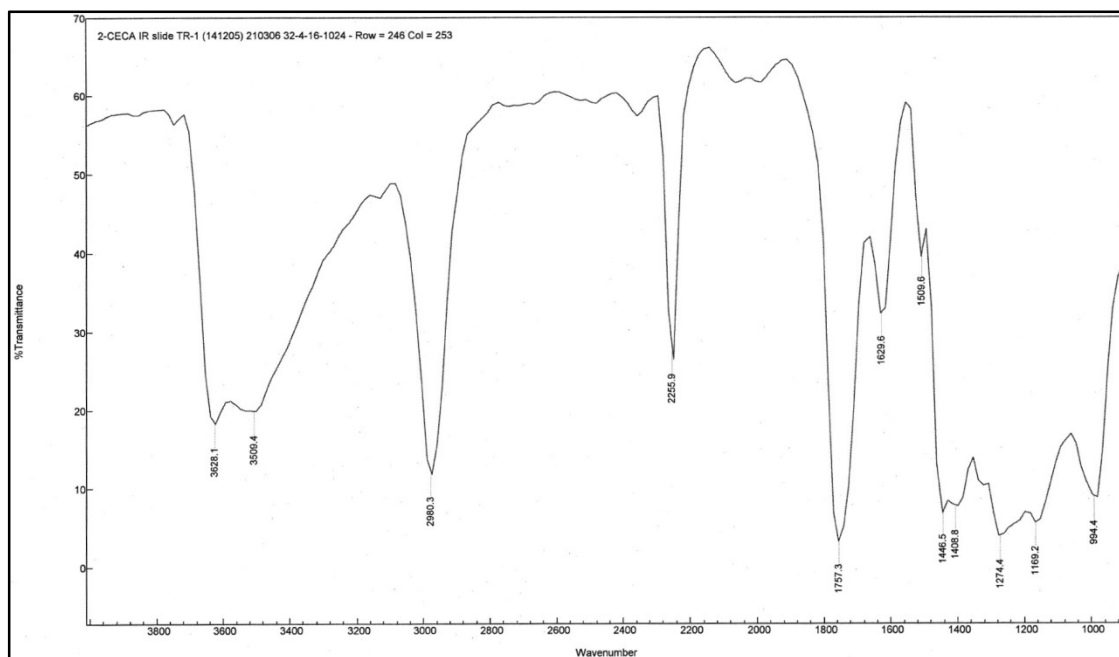
Figure 4.31: *FTIR spectrum of fingerprint treated with 2-CECA (three months after treatment).*

A spectrum collected from the same area 28 months after treatment still displays an intense nitrile band and, although its intensity has decreased somewhat, the C=C stretching frequency at around 1630 cm^{-1} (see Figure 4.32).
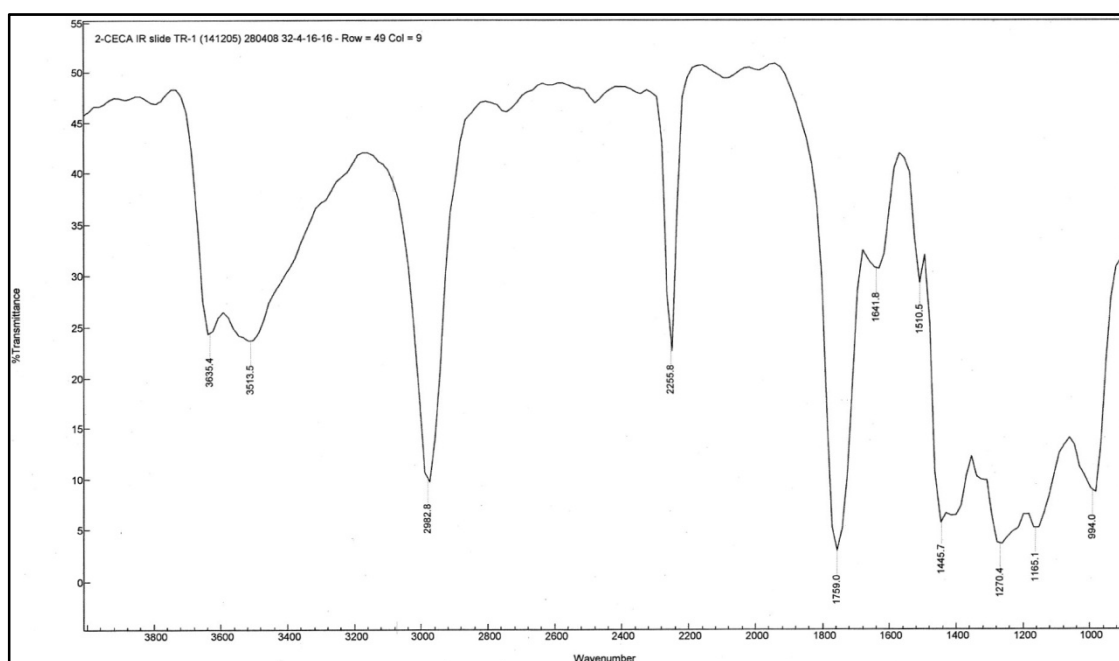
Figure 4.32: *FTIR spectrum of fingerprint treated with 2-CECA (28 months after treatment).*

Two main preliminary findings may be drawn from these results. The first it that this fingerprint has been developed by cyanoacrylate in a manner that is different to the generally accepted mechanism for the development of latent fingerprints via exposure to cyanoacrylate vapour. The generally accepted mechanism, discussed in Section 1.1.6.2.1 above, is that the monomeric cyanoacrylate vapour preferentially polymerises on the ridges of latent fingerprints, with polymerisation being initiated by a fingerprint component (e.g. moisture or an anion). The deposition of monomer in this case suggests that the monomeric cyanoacrylate is firstly attracted to the latent fingerprint deposit itself (possibly due to non-polar – non-polar attraction) before any reaction with initiators within the deposit and subsequent polymerisation. In fact, in this sample, the bulk of the monomer does not polymerise at all but is clearly still preferentially deposited along the ridges. Secondly, the presence of residual monomer months and even years after the treatment suggests that the bulk of the monomer deposited has not polymerised. This may be the result of being trapped beneath a thin but impenetrable 'skin' of polymer, or the monomer may be somehow immobilised in a viscous matrix as discussed in Section 4.1.1 above.

While this sample is interesting, it must be made clear that it was a one-off observation and no attempts have been made to replicate or further investigate this phenomenon. In any case, the possibility of selectively depositing an organic substance (not necessarily a cyanoacrylate), which may contain suitable infrared absorbances, on latent fingerprints by simply exposing it to a concentrated atmosphere of its vapour is appealing. It is, however, likely that the particular experimental setup in this case was favourable for this type of deposition to occur. The sample bearing the latent fingerprint was a clean, smooth non-porous surface and was in reasonably close proximity (within a sealed round bottom flask) to the vaporised monomer. The samples shown in Section 4.3.3 of fingerprints developed with 2-CECA within the one-litre reaction vessel show more typical preferential polymerisation on the ridges. This is evidenced by the difference in the FTIR spectrum from prints developed in the one-litre reaction vessel (see spectrum in Figure 4.11) compared to the FTIR spectrum from prints developed in the smaller flask (see spectrum in Figure 4.31). Note in particular the FTIR spectrum of the sample from the print treated in the reaction vessel (Figure 4.11) that has a much lower intensity nitrile band and no band near 1630 cm^{-1} that would be indicative of fully cured 2-cyanoethyl 2-cyanoacrylate polymer.

The second novel cyanoacrylate monomer tested, 1-cyanoethyl 2-cyanoacrylate (1-CECA) gave the best and most promising results of any of the monomers tested. This monomer was

volatile at a reasonable temperature (in a range similar to that typically used for conventional cyanoacrylate fuming) and gave high contrast FTIR chemical images of fingerprints on all surfaces tested. Of particular note, fingerprints on all areas of polymer banknotes (including areas with raised intaglio printing) that were treated with 1-CECA gave images with excellent ridge detail. This contrast was not based on the presence of an infrared absorption in the region of interest but is instead thought to be due to a shift in (and the broadness of) the carbonyl band, which was resolved from any interfering bands from the polymer banknote in this region. The shift in the carbonyl band, relative to say ethyl 2-cyanoacrylate, is due to the introduction of an electron-withdrawing nitrile functional group in close proximity to the carbonyl group. With the advantage of hindsight, the nitrile group was a good choice to achieve a shift in the carbonyl band but other cyanoacrylate monomers may produce a similar shift. For example some of the halo alkyl 2-cyanoacrylates listed in Table 3—1 above may be worth investigating for this purpose. In any case further testing of 1-CECA is warranted to explore its full potential for fingerprint development on difficult surfaces.

Finally the two deuterated cyanoacrylates, trideuteromethyl 2-cyanoacrylate (MCA-d_3) and pentadeuteroethyl 2-cyanoacrylate (ECA-d_5), were volatile and reacted with latent prints in a manner indistinguishable from conventional cyanoacrylate. Good quality FTIR chemical images of fingerprints on a number of difficult surfaces were collected from fingerprints fumed with these monomers. Unfortunately, however, the bands within the region of interest were very low in intensity (particularly an poorly reflective surfaces such as polymer banknotes) and hence were not able to be used for FTIR chemical imaging. The band used to generate contrast in most cases was the carbonyl band. Since conventional cyanoacrylate also contains a band in this region, no particular advantage was provided by these monomers. Furthermore, as with conventional cyanoacrylate, the carbonyl bands from fingerprints treated with MCA-d_3 or ECA-d_5 overlapped with bands from the polymer banknote background and led to a lack of contrast between the print and the background.

It may be possible to improve the results presented here for MCA-d_3 and ECA-d_5 by optimisation of the fuming procedure and or the image collection method. Improvements could lead to the detection of the bands due to C–D stretching vibrations, which would be resolved from any interfering peaks and therefore provide ideal target peaks for FTIR chemical imaging of fingerprints on a range of difficult surfaces.

Chapter 5: Conclusions and further work

Chapter 5:   Conclusions and further work

Fingerprint evidence continues to be of high value in forensic investigations. While there are a number of currently used fingerprint detection techniques, there is a need for new and innovative approaches to fingerprint detection, particularly on *'difficult'* surfaces.   FTIR chemical imaging has been shown to be an excellent technique for the enhancement of latent (untreated) and developed (treated) fingerprints on a number of difficult surfaces.

During this project, high quality fingerprint images were obtained of untreated fingerprints on reflective surfaces. The success of imaging untreated fingerprints is dependent on the background surface having few interfering absorbances in the region of the infrared spectrum used for imaging (typically the C–H stretching region around 2900 cm^{-1} is used). The imaging of untreated fingerprints via this technique is therefore most successful on surfaces such as metals and ceramics.

The FTIR chemical imaging of fingerprints treated with conventional (ethyl) cyanoacrylate has been successfully demonstrated. High quality images have been obtained of cyanoacrylate-fumed fingerprints on aluminium drink cans and certain areas of polymer banknotes. Prints aged up to one month have been imaged and this technique may even yield results on older prints, although this was not investigated.

The feasibility of using FTIR chemical imaging to image fingerprints on porous surfaces was also investigated. Problems were however encountered due to the high absorbance of the cellulose components of the paper over much of the spectrum in reflectance infrared spectroscopy.   FTIR chemical imaging of latent fingerprints or those pre-treated with ninhydrin or DFO on porous surfaces such as white copier paper, masking tape and thermal paper failed to yield any images of exploitable fingerprints.

During the course of this research, a systematic methodology for the optimisation of image collection and formation parameters was devised. This methodology allows the optimisation of parameters such as spectral resolution, number of co-added scans, spectral range, pixel aggregation and image formation parameters in order to minimise image collection time and file size while maintaining the quality of the fingerprint image produced. The optimisation procedure is recommended for each new fingerprint reagent / surface combination. Using an

optimised method, the collection of images (2.2 × 2.2 cm) of entire cyanoacrylate-fumed fingerprints on aluminium drink cans required just two and a half hours and the imaging of cyanoacrylate-fumed fingerprints on polymer banknotes required just over four hours. This represents a significant improvement on previously published, un-optimised settings. More importantly, the optimisation method described here allows the rapid, simple optimisation of new reagent / surface combinations, which greatly increases the utility of this technique.

Despite the success of using FTIR chemical imaging for fingerprints fumed with conventional cyanoacrylate on polymer banknotes, there were still problems on areas of the banknote that contained raised intaglio printing. On these areas, the contrast between the developed print and the background was reduced and, in some cases the raised intaglio printing totally obscured the developed print. For this reason, an alternative modified cyanoacrylate that contained a vibrational band in the 'region of interest' (2500 – 1800 cm^{-1}) was sought. This region is typically free from major interferences from backgrounds and hence, if present in the FTIR spectra of imaged fingerprint ridges, would provide good contrast between the print and the background.

The common route for the synthesis of alkyl 2-cyanoacrylates (i.e. Knoevenagel condensation of alkyl cyanoacetates with formaldehyde followed by thermal depolymerisation) was found to be unsatisfactory for the synthesis of small quantities of the targeted novel cyanoacrylates. A Diels-Alder protection / de-protection route involving the use of anthracene to protect (and later de-protect) the reactive vinyl group proved much more successful. In total four novel cyanoacrylates with potential as reagents for the FTIR chemical imaging of fingerprints on difficult surfaces were prepared. These were 2-cyanoethyl 2-cyanoacrylate (2-CECA), 1-cyanoethyl 2-cyanoacrylate (1-CECA), trideuteromethyl 2-cyanoacrylate (MCA-d$_3$) and pentadeuteroethyl 2-cyanoacrylate (ECA-d$_5$).

Each of the four novel monomers was tested a reagent for the detection and enhancement of latent fingerprints on a number of surfaces via FTIR chemical imaging. The 2-CECA monomer was found to be less volatile than conventional cyanoacrylate and thermally decomposed at the temperatures required to vaporise it. Treating latent fingerprints with this monomer at a reduced pressure (a technique known as vacuum cyanoacrylate deposition) yielded better results. Fingerprints on reflective surfaces that had been treated with 2-CECA were successfully imaged using FTIR chemical imaging. On less reflective surfaces, such as polymer

banknotes, however, the nitrile band of 2-CECA was almost undetectable and therefore could not be used for imaging the treated prints.

Fingerprints treated with the deuterated monomers (MCA-d_3 and ECA-d_5) showed characteristic bands in the region from 2300 – 1900 cm^{-1} owing to C–D stretching vibrations. Once again, however, the relatively low intensity of these bands meant that they were only detected from prints on reflective surfaces.

The monomer that produced the best results was 1-CECA. Surprisingly the contrast between the ridge detail and the background, was not generated by the nitrile band at 2250 cm^{-1} as anticipated. Instead it appears that the absorption band for the carbonyl group in poly-1-CECA is sufficiently resolved from any absorption within this region from the background surface (such as polymer banknotes) to provide good contrast images of the treated fingerprint. High quality fingerprint images were obtained of prints treated with 1-CECA on all difficult surfaces tested including white opaque acrylic sheets, fluorescent acrylic sheets and all areas of polymer banknotes including areas containing raised intaglio printing.

In all experiments during this project, the location of the latent or treated fingerprints was known. On certain surfaces, such as PMMA or glass, the fingerprints were somewhat visible to the naked eye even if the ridge detail was not very clear. In other cases, such as on polymer banknotes (with the exception of the clear plastic window) fingerprints were not visible whatsoever to the naked eye, nor could they be imaged using an alternative forensic light source. Under these circumstances, FTIR chemical imaging is at a disadvantage for the analysis of unknown or 'real' samples where the location of the fingerprint is unknown. There are however two approaches to resolve this issue.

The first approach is to set the spectral resolution as low as possible (32 cm^{-1} in our case) and have a minimal number of co-added scans (one or two). These settings would provide a rapid screen of the sample and, whilst the image produced may not necessarily produce a suitable fingerprint image, it should at least highlight a particular area of interest. This area (or areas) could then be re-imaged using a higher number of scans (to improve signal-to-noise) or better resolution if required.

The second approach is to follow a currently accepted fingerprint detection sequence for non-porous surfaces, which involves luminescent staining of fingerprints following

cyanoacrylate treatment. On as sample such as a polymer banknote, this technique alone may not reveal fingerprints of high quality under white light or in luminescence visualisation mode but may again highlight an area where a fingerprint may be located. This may appear as a smudge or partial print, which can then be imaged using FTIR chemical imaging. Of course, this approach would rely on the luminescent staining procedure giving no (or minimal) interference to subsequent FTIR chemical imaging. These are two approaches that can and should be investigated further.

Another area that warrants further investigation is the idea that monomeric cyanoacrylate (or another organic compound all together) can be preferentially deposited on the ridges of a latent fingerprint via vacuum deposition without subsequent polymerisation. This concept was highlighted by a strange result when testing the ability of the novel monomer 2-CECA to develop fingerprints under a reduced pressure. In one experiment, this monomer was found to have preferentially deposited on the ridges of a fingerprint on an infrared reflective slide and remained largely in its monomeric form (with an intense nitrile absorption band) for over two years. Further testing is required here to ascertain the mechanism of deposition and whether or not this could be utilised for the detection and enhancement of latent fingerprints.

One issue that has limited the success of certain monomers prepared during this project is the sensitivity of the infrared signal from samples imaged via the reflection FTIR chemical imaging and mosaicking technique describe here. To date, this technique is the only technique that allows the FTIR chemical imaging of large samples such as an entire fingerprints. Transmission mode can also be used but this has very limited application as it would require a sufficiently thin and infrared-transparent substrate.

Higher sensitivity (i.e. better signal-to-noise) is offered by attenuated total reflection (ATR) because it is a surface-preferenced technique but image sizes are limited by the dimensions of the ATR crystal and the focal plane array (FPA) detector, and the instrumental configuration and optics. Currently, the largest image possible using ATR-FTIR imaging is approximately 4.7×6.3 mm^2.[119] This area represents only a few ridges of an entire fingerprint. Improvements and advances in ATR crystals, instrumentation, optics and detectors may allow for the ATR-FTIR imaging of larger samples.

It is also envisaged that there will be marked improvements in other aspects of FTIR chemical imaging instruments. The next generation of FPA detectors for example, should offer increased sensitivity and possibly (in combination with advances in optics and instrumentation) increased image sizes. These advances, together with advances in computer processing, will lead to faster image collection times and higher quality spectral data, which, in turn, will lead to higher quality infrared chemical images of fingerprints on a range of surfaces. Furthermore, FTIR chemical imaging instruments (and imaging detectors) should become cheaper and more accessible to the average forensic laboratory. Most forensic laboratories already have the instrumentation and commonly perform FTIR spectroscopy and / or FTIR microspectroscopy. Over the past decade, new instruments have come equipped with the provisions to accommodate an FTIR imaging detector even if one is not purchased initially. FTIR imaging can then be thought of as an 'optional extra' on most modern instruments and this reduces the cost converting from a single-point to an imaging-capable instrument.

Another approach to achieving increased sensitivity is the use of thin films of certain metals (e.g. gold (Au) or silver (Ag)). This technique, known as surface-enhanced infrared absorption spectroscopy (SEIRAS), generally involves the deposition of an analyte on the surface of thin metallic films (such as Ag island films), which greatly increases the infrared signal of the analyte. Hatta et al. have reported the enhancement of the infrared intensity of poly-cyanoacrylate with underlying Ag island films.[59] This sort of approach may be adapted to enhance the signal from cyanoacrylate-fumed fingerprints. This may involve the deposition of an Ag island film prior to or following cyanoacrylate fuming.

During this project, for the first time, a number of reagents specifically designed for the FTIR chemical imaging of fingerprints have been prepared, tested and shown to yield impressive results. These reagents were all alkyl 2-cyanoacrylate monomers and there are a number of other currently available or novel alkyl 2-cyanoacrylate monomers that may also be useful as reagents for this purpose. These reagents may include one or more of the key functional groups that produce an infrared vibrational band (or bands) in the region of interest.

Another group of compounds that is worth investigating are compounds that contain these same functional groups, but may be applied to fingerprints that have been pre-treated by cyanoacrylate fuming. Analogous compounds already exist. There are a number of coloured and / or luminescent compounds or 'stains' that are applied to cyanoacrylate-fumed

fingerprints to enhance contrast in the visible / luminescence visualisation mode. A suitable compound for an *'infrared active stain'* would have a distinctive infrared absorption rather than a coloured or fluorescent one. Indeed it may even possible to select or synthesise a compound that has both coloured / luminescent properties *and* has a suitable infrared absorption. This would provide the best of both worlds, where commonly-used optical detection methods could be used and, if there is a need for improved contrast on a difficult surface or faint fingerprint, FTIR chemical imaging can then be employed.

Finally, it should be appreciated that FTIR chemical imaging should not be viewed as a technique to replace any of the currently used and accepted fingerprint detection and enhancement techniques. In most cases, the currently used techniques are capable of providing sufficient ridge detail for subsequent comparison and / or identification. FTIR chemical imaging should instead be considered in circumstances where the current techniques struggle or fail. Polymer banknotes are a good example but are merely a demonstration of the capabilities of this technique for the acquisition of high quality fingerprint images from difficult surfaces. In fact, polymer banknotes can even be considered as one of the *most* difficult surfaces for fingerprint detection and enhancement. On these surfaces the use of specific FTIR chemical imaging reagents such 1-CECA produces the best results. On the majority of other difficult surfaces, fuming with any one of the monomers discussed here (or, in many cases, conventional cyanoacrylate) followed by FTIR chemical imaging can produce high quality fingerprint images that are superior to those possible via traditional optical or luminescent visualisation methods.

References

References

1. Ashbaugh, D. R. *Quantitative-qualitative friction ridge analysis: an introduction to basic and advanced ridgeology;* CRC Press: Boca Raton, FL, 1999.

2. Knowles, A. M. Aspects of physicochemical methods for the detection of latent fingerprints. *J. Phys. [E]* **1978,** *11* (8), 713-721.

3. Berry, J.; Stoney, D. A. History and development of fingerprinting. In *Advances in fingerprint technology*, 2nd ed.; Lee, H. C.; Gaensslen, R. E., Eds.; CRC Press: Boca Raton, FL, 2001.

4. Champod, C.; Lennard, C.; Margot, P.; Stoilovic, M. *Fingerprints and other ridge skin impressions;* CRC Press: Boca Raton, FL, 2004.

5. Saferstein, R. *Criminalistics, An introduction to forensic science*, 7th ed.; Prentice Hall: New Jersey, 2001.

6. Voss-de Haan, P. Physics and fingerprints. *Contemp. Phys.* **2006,** *47* (4), 209-230.

7. Olsen, R. D.; Lee, H. C. Identification of latent prints. In *Advances in fingerprint technology*, 2nd ed.; Lee, H. C.; Gaensslen, R. E., Eds.; CRC Press: Boca Raton, FL, 2001.

8. Ramotowski, R. Composition of latent print residue. In *Advances in fingerprint technology*, 2nd ed.; Lee, H. C.; Gaensslen, R. E., Eds.; CRC Press: Boca Raton, FL, 2001.

9. Lewis, L. A.; Smithwick, R. W., 3rd; Devault, G. L.; Bolinger, B.; Lewis, S. A., Sr. Processes involved in the development of latent fingerprints using the cyanoacrylate fuming method. *J. Forensic Sci.* **2001,** *46* (2), 241-246.

10. Williams, D. K.; Schwartz, R. L.; Bartick, E. G. Analysis of latent fingerprint deposits by infrared microspectroscopy. *Appl. Spectrosc.* **2004,** *58* (3), 313-316.

11. Wilkinson, T. J.; Perry, D. L.; Martin, M. C.; McKinney, W. R.; Thompson, A. C. Applications of synchrotron technology to the study of latent human fingerprints.

Presented at 222nd National Meeting of the American Chemical Society, Chicago, IL, August 26-30, 2001; Paper IEC-036.

12.   Wilkinson, T. J.; Perry, D. L.; Martin, M. C.; McKinney, W. R. Applications of synchrotron IR microspectroscopy to the study of fingerprints. Presented at 221st National Meeting of the American Chemical Society, San Deigo, CA, April 1-5, 2001; Paper IEC-088.

13.   Wilkinson, T. J.; Martin, M. C.; McKinney, W. R.; Perry, D. L. Application of FTIR spectromicroscopy to the analysis of latent human fingerprints. Presented at 227th National Meeting of the American Chemical Society, Anaheim, CA, March 28 - April 1, 2004; Paper IEC-157.

14.   Wargacki, S.; Lewis, L. A.; Dadmun, M. D. Understanding the chemistry of fingerprints by superglue fuming. *J. Forensic Sci.* **2007,** *52* (5), 1057-1062.

15.   Ricci, C.; Phiriyavityopas, P.; Curum, N.; Chan, K. L. A.; Jickells, S.; Kazarian, S. G. Chemical imaging of latent fingerprint residues. *Appl. Spectrosc.* **2007,** *61* (5), 514-522.

16.   Jones, N.; Mansour, D.; Stoilovic, M.; Lennard, C.; Roux, C. The influence of polymer type, print donor and age on the quality of fingerprints developed on plastic substrates using vacuum metal deposition. *Forensic Sci. Int.* **2001,** *124* (2-3), 167-177.

17.   Mountfort, K. A.; Bronstein, H.; Archer, N.; Jickells, S. M. Identification of oxidation products of squalene in solution and in latent fingerprints by ESI-MS and LC/APCI-MS. *Anal. Chem.* **2007,** *79* (7), 2650-2657.

18.   Archer, N. E.; Charles, Y.; Elliott, J. A.; Jickells, S. Changes in the lipid composition of latent fingerprint residue with time after deposition on a surface. *Forensic Sci. Int.* **2005,** *154* (2-3), 224-239.

19.   Croxton, R. S.; Baron, M. G.; Butler, D.; Kent, T.; Sears, V. G. Development of a GC-MS method for the simultaneous analysis of latent fingerprint components. *J. Forensic Sci.* **2006,** *51* (6), 1329-1333.

20. Lee, H. C. G., R.E. Methods of latent fingerprint development. In *Advances in fingerprint technology*, 2nd ed.; Lee, H. C.; Gaensslen, R. E., Eds.; CRC Press: Boca Raton, FL, 2001.

21. Hansen, D. B.; Joullie, M. M. The development of novel ninhydrin analogues. *Chem. Soc. Rev.* **2005,** *34* (5), 408-417.

22. Joullie, M. M.; Thompson, T. R. Ninhydrin and ninhydrin analogs. Syntheses and applications. *Tetrahedron* **1991,** *47* (42), 8791-8830.

23. Schwarz, L.; Frerichs, I. Advanced solvent-free application of ninhydrin for detection of latent fingerprints on thermal paper and other surfaces. *J. Forensic Sci.* **2002,** *47* (6), 1274-1277.

24. Lennard, C. J.; Margot, P. A.; Sterns, M.; Warrener, R. N. Photoluminescent enhancement of ninhydrin developed fingerprints by metal complexation: structural studies of complexes formed between Ruhemann's purple and group IIb metal salts. *J. Forensic Sci.* **1987,** *32* (3), 597-605.

25. Hark, R. R.; Hauze, D. B.; Petrovskaia, O.; Joullie, M. M. Synthetic studies of novel ninhydrin analogs. *Can. J. Chem.* **2001,** *79* (11), 1632-1654.

26. Elber, R.; Frank, A.; Almog, J. Chemical development of latent fingerprints: Computational design of ninhydrin analogues. *J. Forensic Sci.* **2000,** *45* (4), 757-760.

27. Almog, J.; Hirshfeld, A.; Frank, A.; Grant, H.; Harel, Z.; Ittah, Y. 5-Methylthio ninhydrin and related compounds: a novel class of fluorogenic fingerprint reagents. *J. Forensic Sci.* **1992,** *37* (3), 688-694.

28. Almog, J.; Hirshfeld, A.; Klug, J. T. Reagents for the chemical development of latent fingerprints: synthesis and properties of some ninhydrin analogues. *J. Forensic Sci.* **1982,** *27* (4), 912-917.

29. Almog, J.; Sears, V. G.; Springer, E.; Hewlett, D. F.; Walker, S.; Wiesner, S.; Lidor, R.; Bahar, E. Reagents for the chemical development of latent fingerprints: scope and limitations of benzo[f]ninhydrin in comparison to ninhydrin. *J. Forensic Sci.* **2000,** *45* (3), 538-544.

30.   Almog, J.; Hirshfeld, A. 5-Methoxyninhydrin: a reagent for the chemical development of latent fingerprints that is compatible with the copper-vapor laser. *J. Forensic Sci.* **1988,** *33* (4), 1027-1030.

31.   Almog, J.; Hirshfeld, A.; Frank, A.; Sterling, J.; Leonov, D. Aminoninhydrins: fingerprint reagents with direct fluorogenic activity - preliminary studies. *J. Forensic Sci.* **1991,** *36* (1), 104-110.

32.   Almog, J. Reagents for chemical development of latent fingerprints: vicinal triketones - their reaction with amino acids and with latent fingerprints on paper. *J. Forensic Sci.* **1987,** *32* (6), 1565-1573.

33.   Kobus, H. J.; Pigou, P. E.; Jahangiri, S.; Taylor, B. Evaluation of some oxygen, sulfur, and selenium substituted ninhydrin analogues, nitrophenylninhydrin and benzo[f]furoninhydrin. *J. Forensic Sci.* **2002,** *47* (2), 254-259.

34.   Almog, J. Fingerprint development by ninhydrin and its analogues. In *Advances in fingerprint technology*, 2nd ed.; Lee, H. C.; Gaensslen, R. E., Eds.; CRC Press: Boca Raton, FL, 2001.

35.   Pomeroy, R. S.; Baker, M. E.; Radspinner, D. A.; Denton, M. B. Fluorescence imaging of latent fingerprints with a cooled charge-coupled device detector. *Proceedings of SPIE International conference on scientific optical imaging*, Georgetown, Grand Cayman Island, Bahamas, 28 November - 1 December, 1990; The International Society for Optical Engineering: Vol. 1439, 60-65.

36.   Wallace-Kunkel, C.; Lennard, C.; Stoilovic, M.; Roux, C. Optimisation and evaluation of 1,2-indanedione for use as a fingermark reagent and its application to real samples. *Forensic Sci. Int.* **2007,** *168* (1), 14-26.

37.   Wiesner, S.; Springer, E.; Sasson, Y.; Almog, J. Chemical development of latent fingerprints: 1,2-indanedione has come of age. *J. Forensic Sci.* **2001,** *46* (5), 1082-1084.

38.   Roux, C.; Jones, N.; Lennard, C.; Stoilovic, M. Evaluation of 1,2-indanedione and 5,6-dimethoxy-1,2-indanedione for the detection of latent fingerprints on porous surfaces. *J. Forensic Sci.* **2000,** *45* (4), 761-769.

39.   Almog, J.; Springer, E.; Wiesner, S.; Frank, A.; Khodzhaev, O.; Lidor, R.; Bahar, E.; Varkony, H.; Dayan, S.; Rozen, S. Latent fingerprint visualization by 1,2-indanedione and related compounds: preliminary results. *J. Forensic Sci.* **1999,** *44* (1), 114-118.

40.   Hauze, D. B.; Petrovskaia, O.; Taylor, B.; Joullie, M. M.; Ramotowski, R.; Cantu, A. A. 1,2-Indanediones: new reagents for visualizing the amino acid components of latent prints. *J. Forensic Sci.* **1998,** *43* (4), 744-747.

41.   Cantu, A. A.; Johnson, J. L. Silver physical development of latent prints. In *Advances in fingerprint technology*, 2nd ed.; Lee, H. C.; Gaensslen, R. E., Eds.; CRC Press: Boca Raton, FL, 2001.

42.   Jones, N.; Kelly, M.; Stoilovic, M.; Lennard, C.; Roux, C. The development of latent fingerprints on polymer banknotes. *J. Forensic Ident.* **2003,** *53* (1), 50-77.

43.   Geller, B. Commentary on: Lewis LA et al. Processes involved in the development of latent fingerprints using the cyanoacrylate fuming method. J. Forensic Sci. 2001, 46, (2), 241-246. *J. Forensic Sci.* **2002,** *47* (3), 700; author reply 701.

44.   Burns, D. T.; Brown, J. K.; Dinsmore, A.; Harvey, K. K. Base-activated latent fingerprints fumed with a cyanoacrylate monomer. A quantitative study using Fourier-transform infra-red spectroscopy. *Anal. Chim. Acta* **1998,** *362* (2-3), 171-176.

45.   Kendall, F.; Rehn, B. Rapid method of super glue® fuming application for the development of latent fingerprints. *J. Forensic Sci.* **1983,** *28* (3), 777-780.

46.   Yamashita, A. Use of a benchtop desiccator for vacuum cyanoacrylate treatment of latent prints. *J. Forensic Ident.* **1994,** *44* (2), 149-158.

47.   Almog, J.; Gabay, A. A modified Super Glue® technique - the use of polycyanoacrylate for fingerprint development. *J. Forensic Sci.* **1986,** *31* (1), 250-253.

48.   Watkin, J. E.; Wilkinson, D. A.; Misner, A. H.; Yamashita, A. B. Cyanoacrylate fuming of latent prints: vacuum versus heat/humidity. *J. Forensic Ident.* **1994,** *44* (5), 545-555.

49.   Canale, A. J.; Goode, W. E.; Kinsinger, J. B.; Panchak, J. R.; Kelso, R. L.; Graham, R. K. Methyl a-cyanoacrylate. I. Free-radical homopolymerization. *J. Appl. Polym. Sci.* **1960,** *4* (11), 231-236.

50.   Shibasaki, T.; Suetaka, W. Infrared spectra and adhesion strength of α-cyanoacrylate polymer films. *Chem. Lett.* **1975,** (2), 113-118.

51.   Donnelly, E. F.; Johnston, D. S.; Pepper, D. C.; Dunn, D. J. Ionic and zwitterionic polymerization of n-alkyl 2-cyanoacrylates. *J. Polym. Sci., Polym. Lett. Ed.* **1977,** *15* (7), 399-405.

52.   Pepper, D. C. Anionic and zwitterionic polymerization of a-cyanoacrylates. *J. Polym. Sci., Polym. Symp.* **1978,** *62* (Int. Symp. Macromol.), 65-77.

53.   Pepper, D. C. Kinetics and mechanism of zwitterionic polymerizations of alkyl cyanoacrylates. *Polym. J. (Tokyo, Jpn.)* **1980,** *12* (9), 629-637.

54.   Kusaka, I.; Suetaka, W. Infrared spectrum of α-cyanoacrylate adhesive in the first monolayer on a bulk aluminum surface. *Spectrochim. Acta, Part A* **1980,** *36A* (7), 647-648.

55.   Oxley, D. P. The application of inelastic electron tunnelling spectroscopy to a study of adhesives. *Adhesion (London)* **1982,** *6*, 123-134.

56.   Reynolds, S.; Oxley, D. P.; Pritchard, R. G. An adhesive study by electron tunneling: ethyl a-cyanoacrylate adsorbed on an oxidized aluminum surface. *Spectrochim. Acta, Part A* **1982,** *38A* (1), 103-111.

57.   Suetaka, W. Infrared spectroscopic investigation of polymer coating-metal substrate interaction. In *Adhesion aspects of polymeric coatings;* Mittal, K. L., Ed.; Plenum Press: New York, 1983; pp 225-33.

58.   Cronin, J. P.; Pepper, D. C. Zwitterionic polymerization of butyl cyanoacrylate by triphenylphosphine and pyridine. *Makromol. Chem.* **1988,** *189* (1), 85-102.

59.   Hatta, A.; Suzuki, N.; Suzuki, Y.; Suetaka, W. Infrared absorption of polycyanoacrylate enhanced by Ag island films in the Kretschmann's ATR geometry: the coverage dependence. *Appl. Surf. Sci.* **1989,** *37* (3), 299-305.

60.   Pepper, D. C. Zwitterionic chain polymerizations of cyanoacrylates. *Makromol. Chem., Macromol. Symp.* **1992,** *60* (Int. Symp. Cationic Polym. Relat. Ionic Processes, 10th, 1991), 267-277.

61.   Yang, D. B. Kinetic studies of photopolymerization using real time FT-IR spectroscopy. *J. Polym. Sci., Part A: Polym. Chem.* **1993,** *31* (1), 199-208.

62.   Yang, D. B. Direct kinetic measurements of vinyl polymerization on metal and silicon surfaces using real-time FT-IR spectroscopy. *Appl. Spectrosc.* **1993,** *47* (9), 1425-1429.

63.   Radhakrishnan, S.; Saini, D. R. Dielectric monitoring of the curing process in cyanoacrylate resin. *Polym. Eng. Sci.* **1993,** *33* (3), 125-131.

64.   Costa, G.; Loonan, C.; Pepper, D. End-group evidence of zwitterionic species in the anionic polymerization of cyanoacrylates by Lewis bases. *Macromol. Rapid Commun.* **1997,** *18* (9), 891-896.

65.   Arsu, N.; Oenen, A.; Yagci, Y. Photoinitiated zwitterionic polymerization of alkyl cyanoacrylates by pyridinium salts. *Macromolecules* **1996,** *29* (27), 8973-8974.

66.   Brookes, A.; Craston, D. The application of Raman spectroscopy to reacting systems. *Internet J. Vib. Spectrosc. [Online]* **1999,** *3* (3), Section 4. http://www.ijvs.com/volume3/edition3/section4.html (accessed Jun 5, 2007).

67.   Klemarczyk, P. The isolation of a zwitterionic initiating species for ethyl cyanoacrylate (ECA) polymerization and the identification of the reaction products between primary, secondary, and tertiary amines with ECA. *Polymer* **2001,** *42* (7), 2837-2848.

68.   Edwards, H. G. M.; Day, J. S. Fourier transform Raman spectroscopic studies of the curing of cyanoacrylate glue. *J. Raman Spectrosc.* **2004,** *35* (7), 555-560.

69.   Kato, H.; Tsuzi, I.; Azuma, K.; Tatemichi, H. Heat-resitant adhesive compositions containing radical polymerizable alpha-cyanoacrylates. U.S. Patent 3,825,580, July 23, 1974.

70.   Millet, G. H. Cyanoacrylate adhesives. In *Structural Adhesives: Chemistry and Technology;* Hartshorn, S. R., Ed.; Plenum: London, 1986.

71. Chappelow, C. C.; Pinzino, C. S.; Byerley, T. J.; Eick, J. D. Tri-n-butylborane oxide-initiated homopolymerization of vinyl monomers containing cyano or isocyanato groups. *J. Appl. Polym. Sci.* **1995,** *58* (7), 1147-1150.

72. Brinkmann, N. R.; Schaefer, H. F., III; Sanderson, C. T.; Kutal, C. Can the radical anion of alkyl 2-cyanoacrylates initiate anionic polymerization of these instant adhesive monomers? *J. Phys. Chem. A* **2002,** *106* (5), 847-853.

73. Sanderson, C. T.; Palmer, B. J.; Morgan, A.; Murphy, M.; Dluhy, R. A.; Mize, T.; Amster, I. J.; Kutal, C. Classical metallocenes as photoinitiators for anionic polymerization of an alkyl 2-cyanoacrylate. *Macromolecules* **2002,** *35* (26), 9648-9652.

74. Coover, H. W., Jr.; McIntire, J. M. Cyanoacrylate adhesives. In *Handbook of adhesives*, 2nd ed.; Van Nostrand Reinhold: New York, N.Y., 1977; pp 569-80.

75. Tahtouh, M.; Kalman, J. R.; Roux, C.; Lennard, C.; Reedy, B. J. The detection and enhancement of latent fingermarks using infrared chemical imaging. *J. Forensic Sci.* **2005,** *50* (1), 64-72.

76. Tahtouh, M.; Despland, P.; Shimmon, R.; Kalman, J. R.; Reedy, B. J. The application of infrared chemical imaging to the detection and enhancement of latent fingerprints: Method optimization and further findings. *J. Forensic Sci.* **2007,** *52* (5), 1089–1096.

77. Czekanski, P.; Fasola, M.; Allison, J. A mechanistic model for the superglue fuming of latent fingerprints. *J. Forensic Sci.* **2006,** *51* (6), 1323-1328.

78. Edwards, H. G. M.; Day, J. S. Anomalies in polycyanoacrylate formation studied by Raman spectroscopy: Implications for the forensic enhancement of latent fingerprints for spectral analysis. *Vib. Spectrosc.* **2006,** *41* (2), 155-159.

79. Mankidy, P. J.; Rajagopalan, R.; Foley, H. C. Facile catalytic growth of cyanoacrylate nanofibers. *Chem. Commun.* **2006,** (10), 1139-1141.

80. Day, J. S.; Edwards, H. G. M.; Dobrowski, S. A.; Voice, A. M. The detection of drugs of abuse in fingerprints using Raman spectroscopy I: latent fingerprints. *Spectrochim. Acta. A. Mol. Biomol. Spectrosc.* **2004,** *60* (3), 563-568.

81.   Day, J. S.; Edwards, H. G. M.; Dobrowski, S. A.; Voice, A. M. The detection of drugs of abuse in fingerprints using Raman spectroscopy II: cyanoacrylate-fumed fingerprints. *Spectrochim. Acta, Part A* **2004,** *60* (8-9), 1725-1730.

82.   Mankidy, P. J.; Rajagopalan, R.; Foley, H. C. Influence of initiators on the growth of poly(ethyl 2-cyanoacrylate) nanofibers. *Polymer* **2008,** *49* (9), 2235-2242.

83.   Note Printing Australia home page. http://www.noteprinting.com (accessed January 22, 2008).

84.   Reserve Bank of Australia. A new era – polymer currency notes: 1988 Onwards. http://www.rba.gov.au/Museum/Displays/1988_onwards_polymer_currency_notes/export_of_notes.html (accessed May 11, 2006).

85.   Hardwick, B.; Ghioghiu. *Guardian^{TM} substrate as an optical medium for security devices*; Technical Report for Note Printing Australia: Craigieburn, Victoria, 2004; 1-5 http://www.noteprinting.com/presentations.html (accessed January 8, 2008).

86.   Flynn, J.; Stoilovic, M.; Lennard, C. Detection and enhancement of latent fingerprints on polymer banknotes: A preliminary study. *J. Forensic Ident.* **1999,** *49* (6), 594-613.

87.   Jones, N. E.; Davies, L. M.; Russell, C. A. L.; Brennan, J. S.; Bramble, S. K. A systematic approach to latent fingerprint sample preparation for comparative chemical studies. *J. Forensic Ident.* **2001,** *51* (5), 504-515.

88.   Pavia, D. L.; Lampman, G. M.; Kriz, G. S. *Introduction to spectroscopy: A guide for students of organic chemistry*, 3rd ed.; Harcourt College Publishers: Fort Worth, Tex., 2001.

89.   Skoog, D. A.; Holler, F. J.; Nieman, T. A. *Principles of instrumental analysis*, Fifth ed.; Saunders College Publishing: Orlando, FL, 1998; p 849.

90.   Campbell, J. B. *Introduction to remote sensing*, 4th ed.; The Guilford Press: New York, 2006.

91.   Wood, B. R.; McNaughton, D. FPA imaging and spectroscopy for monitoring chemical changes in tissue. In *Spectrochemical analysis using infrared multichannel detectors;* Bhargava, R.; Levin, I. W., Eds.; Blackwell: Oxford, 2005; pp 204-233.

92. Romeo, M. J.; Diem, M. Infrared spectral imaging of lymph nodes: strategies for analysis and artifact reduction. *Vib. Spectrosc.* **2005,** *38* (1-2), 115-119.

93. Lasch, P.; Haensch, W.; Naumann, D.; Diem, M. Imaging of colorectal adenocarcinoma using FT-IR microspectroscopy and cluster analysis. *Biochim. Biophys. Acta, Mol. Basis Dis.* **2004,** *1688* (2), 176-186.

94. Bhargava, R. Towards a practical Fourier transform infrared chemical imaging protocol for cancer histopathology. *Anal. Bioanal. Chem.* **2007,** *389* (4), 1155-1169.

95. Kong, S. G.; Chen, Y.-R.; Kim, I.; Kim, M. S. Analysis of hyperspectral fluorescence images for poultry skin tumor inspection. *Appl. Opt.* **2004,** *43* (4), 824-833.

96. Gowen, A. A.; O'Donnell, C. P.; Cullen, P. J.; Downey, G.; Frias, J. M. Hyperspectral imaging - an emerging process analytical tool for food quality and safety control. *Trends Food Sci. Technol.* **2007,** *18* (12), 590-598.

97. Burger, J.; Geladi, P. Hyperspectral NIR imaging for calibration and prediction: A comparison between image and spectrometer data for studying organic and biological samples. *Analyst* **2006,** *131* (10), 1152-1160.

98. Beekes, M.; Lasch, P.; Naumann, D. Analytical applications of Fourier transform-infrared (FT-IR) spectroscopy in microbiology and prion research. *Vet. Microbiol.* **2007,** *123* (4), 305-319.

99. Kazarian, S. G.; Chan, K. L. A. Sampling approaches in fourier transform infrared imaging applied to polymers. *Prog. Colloid Polym. Sci.* **2006,** *132*, 1-6.

100. Kazarian, S. G.; Chan, K. L. A. Applications of ATR-FTIR spectroscopic imaging to biomedical samples. *Biochim. Biophys. Acta, Biomembr.* **2006,** *1758* (7), 858-867.

101. Roggo, Y.; Gendrin, C.; Spiegel, C. Near infrared chemical imaging for the pharmaceutical industry. *Spec. Anal.* **2007,** *36* (258), 26-30.

102. Gomez, R. B.; Dasgupta, S. Use of hyperspectral remote sensing for detection and monitoring of chemical and biological agents - a survey. *Proc. SPIE-Int. Soc. Opt. Eng.* **2004,** *5584* (Chemical and Biological Standoff Detection II), 276-285.

103. Exline, D. L.; Wallace, C.; Roux, C.; Lennard, C.; Nelson, M. P.; Treado, P. J. Forensic applications of chemical imaging: latent fingerprint detection using visible absorption and luminescence. *J. Forensic Sci.* **2003,** *48* (5), 1047-1053.

104. Miskelly, G. M.; Wagner, J. H. Using spectral information in forensic imaging. *Forensic Sci. Int.* **2005,** *155* (2-3), 112-118.

105. Payne, G.; Reedy, B.; Lennard, C.; Comber, B.; Exline, D.; Roux, C. A further study to investigate the detection and enhancement of latent fingerprints using visible absorption and luminescence chemical imaging. *Forensic Sci. Int.* **2004,** *150* (1), 33-51.

106. Payne, G.; Wallace, C.; Reedy, B.; Lennard, C.; Schuler, R.; Exline, D.; Roux, C. Visible and near-infrared chemical imaging methods for the analysis of selected forensic samples. *Talanta* **2005,** *67* (2), 334-344.

107. Wagner, J., H.; Miskelly, G., M. Background correction in forensic photography. II. Photography of blood under conditions of non-uniform illumination or variable substrate color--practical aspects and limitations. *J. Forensic Sci.* **2003,** *48* (3), 604-613.

108. Wagner, J., H.; Miskelly, G., M. Background correction in forensic photography. I. Photography of blood under conditions of non-uniform illumination or variable substrate color--theoretical aspects and proof of concept. *J. Forensic Sci.* **2003,** *48* (3), 593-603.

109. Dubois, J.; Wolff, J.-C.; Warrack, J. K.; Schoppelrei, J.; Lewis, E. N. NIR chemical imaging for counterfeit pharmaceutical products analysis. *Spectroscopy (Duluth, MN, US)* **2007,** *22* (2), 40, 42-46, 48, 50.

110. Lee, E.; Kidder, L. H.; Kalasinsky, V. F.; Schoppelrei, J. W.; Lewis, E. N. Forensic visualization of foreign matter in human tissue by near-infrared spectral imaging: methodology and data mining strategies. *Cytometry A* **2006,** *69A* (8), 888-896.

111. Sobanska, S.; Falgayrac, G.; Laureyns, J.; Bremard, C. Chemistry at level of individual aerosol particle using multivariate curve resolution of confocal Raman image. *Spectrochim. Acta, Part A* **2006,** *64A* (5), 1102-1109.

112.   Treado, P. J.; Nelson, M. P. Raman imaging. In *Handbook of vibrational spectroscopy;* Chalmers, J. M.; Griffiths, P. R., Eds.; John Wiley & Sons, LTD: New York, 2002; Vol. 2.

113.   Bojko, K.; Roux, C.; Reedy, B. J. An examination of the sequence of intersecting lines using attenuated total reflectance – Fourier transform infrared spectral imaging. *J. Forensic Sci.* **2008,** *In press*.

114.   Chan, K. L. A.; Kazarian, S. G. Detection of trace materials with Fourier transform infrared spectroscopy using a multi-channel detector. *Analyst (Cambridge, U. K.)* **2006,** *131* (1), 126-131.

115.   Crane, N. J.; Bartick, E. G.; Perlman, R. S.; Huffman, S. Infrared spectroscopic imaging for noninvasive detection of latent fingerprints. *J. Forensic Sci.* **2007,** *52* (1), 48-53.

116.   Flynn, K.; O'Leary, R.; Lennard, C.; Roux, C.; Reedy, B. J. Forensic applications of infrared chemical imaging: Multi-layered paint chips. *J. Forensic Sci.* **2005,** *50* (4), 832-841.

117.   Flynn, K.; O'Leary, R.; Roux, C.; Reedy, B. J. Forensic analysis of bicomponent fibers using infrared chemical imaging. *J. Forensic Sci.* **2006,** *51* (3), 586-596.

118.   Ricci, C.; Chan, K. L. A.; Kazarian, S. G. Combining the tape-lift method and Fourier transform infrared spectroscopic imaging for forensic applications. *Appl. Spectrosc.* **2006,** *60* (9), 1013-1021.

119.   Ricci, C.; Bleay, S.; Kazarian, S. G. Spectroscopic imaging of latent fingermarks collected with the aid of a gelatin tape. *Anal. Chem.* **2007,** *79* (15), 5771-5776.

120.   Lasch, P.; Wasche, W.; Muller, G.; Naumann, D. FT-IR microspectroscopic imaging of human melanoma thin sections. *AIP Conf. Proc.* **1998,** *430* (Fourier Transform Spectroscopy), 308-311.

121.   Haap, W. J.; Walk, T. B.; Jung, G. FTIR mapping - A new tool for spatially resolved characterization of polymer-bound combinatorial compound libraries with IR microscopy. *Angew. Chem., Int. Ed.* **1998,** *37* (23), 3311-3314.

122.   Sammon, C.; Boussetta, S.; Melia, C. Mapping the distribution of components in formulated polymeric membranes using FTIR-ATR microscopy. *Macromol. Symp.* **2002,** *184* (14th European Symposium on Polymer Spectroscopy, 2001), 357-370.

123.   Kalasinsky, K. S.; Magluilo, J., Jr.; Schaefer, T. Study of drug distribution in hair by infrared microscopy visualization. *J. Anal. Toxicol.* **1994,** *18* (6), 337-341.

124.   Mazzeo, R.; Joseph, E.; Prati, S.; Millemaggi, A. Attenuated total reflection-Fourier transform infrared microspectroscopic mapping for the characterisation of paint cross-sections. *Anal. Chim. Acta* **2007,** *599* (1), 107-117.

125.   Bhargava, R.; Wall, B. G.; Koenig, J. L. Comparison of the FT-IR mapping and imaging techniques applied to polymeric systems. *Appl. Spectrosc.* **2000,** *54* (4), 470-479.

126.   Bartick, E. G. Applications of vibrational spectroscopy in criminal forensic analysis. In *Handbook of vibrational spectroscopy;* Chalmers, J. M.; Griffiths, P. R., Eds.; John Wiley & Sons, LTD: New York, 2002; Vol. 4, pp 2993-3004.

127.   Wilkinson, J. M.; Locke, J.; Laing, D. K. The examination of paints as thin sections using visible microspectrophotometry and Fourier transform infrared microscopy. *Forensic Sci. Int.* **1988,** *38* (1-2), 43-52.

128.   Suzuki, E. M.; Brown, J. A. Forensic science applications of diffuse reflectance infrared Fourier transform spectroscopy (DRIFTS). V. Direct analysis of metallic paints-screening of panels. *J. Forensic Sci.* **1989,** *34* (1), 180-196.

129.   Suzuki, E. M. Forensic science applications of diffuse reflectance infrared Fourier transform spectroscopy (DRIFTS). IV. Direct analysis of metallic paints-sampling considerations. *J. Forensic Sci.* **1989,** *34* (1), 164-179.

130.   Zieba-Palus, J. Application of transmittance and reflectance FT-IR microscopy to examination of paints transferred onto fabrics. *Mikrochim. Acta, Suppl.* **1997,** *14* (Progress in Fourier Transform Spectroscopy), 361-362.

131.   Zieba-Palus, J. The use of micro Fourier-transform infrared spectroscopy and scanning electron microscopy with X-ray microanalysis for the identification of automobile

paint chips. *Mikrochim. Acta, Suppl.* **1997,** *14* (Progress in Fourier Transform Spectroscopy), 357-359.

132. Beveridge, A.; Fung, T.; Macdougall, D. Use of infrared spectroscopy for the characterisation of paint fragments. In *Forensic examination of glass and paint;* Caddy, B., Ed.; Taylor and Francis: London, 2001.

133. Beauchaine, J. P.; Peterman, J. W.; Rosenthal, R. J. Applications of FT-IR/microscopy in forensic analysis. *Mikrochim. Acta* **1988,** *1* (1-6), 133-138.

134. Kirkbride, K. P.; Tungol, M. W. Infrared microspectroscopy of fibres. In *Forensic examination of fibres*, Second ed.; Robertson, J.; Grieve, M., Eds.; Taylor & Francis: London, 1999; pp 179-222.

135. Grieve, M. C.; Dunlop, J.; Kotowski, T. M. Bicomponent acrylic fibers - their characterization in the forensic science laboratory. *J. Forensic Sci. Soc.* **1988,** *28* (1), 25-33.

136. Brenner, L.; Squires, P. L.; Garry, M.; Tumosa, C. S. A measurement of human hair oxidation by Fourier transform infrared spectroscopy. *J. Forensic Sci.* **1985,** *30* (2), 420-426.

137. Wielbo, D.; Tebbett, I. R. The use of microcrystal tests in conjunction with Fourier transform infrared spectroscopy for the rapid identification of street drugs. *J. Forensic Sci.* **1992,** *37* (4), 1134-1148.

138. Suzuki, E. M. Fourier transform infrared analyses of some particulate drug mixtures using a diamond anvil cell with a beam condenser and an infrared microscope. *J. Forensic Sci.* **1992,** *37* (2), 467-487.

139. Compton, S.; Powell, J. Forensic applications of IR microscopy. *Am. Lab.* **1991,** *23* (17), 41-46, 48-51.

140. Maynard, P.; Gates, K.; Roux, C.; Lennard, C. Adhesive tape analysis: establishing the evidential value of specific techniques. *J. Forensic Sci.* **2001,** *46* (2), 280-287.

141. Merrill, R. A.; Bartick, E. G. Analysis of pressure-sensitive adhesive tape: I. Evaluation of infrared ATR accessory advances. *J. Forensic Sci.* **2000,** *45* (1), 93-98.

142.   Lennard, C. J.; Mazzella, W. D. A simple combined technique for the analysis of toners and adhesives. *J. Forensic Sci. Soc.* **1991,** *31* (3), 365-371.

143.   Kher, A.; Mulholland, M.; Reedy, B.; Maynard, P. Classification of document papers by infrared spectroscopy and multivariate statistical techniques. *Appl. Spectrosc.* **2001,** *55* (9), 1192-1198.

144.   Andrasko, J. Microreflectance FTIR techniques applied to materials encountered in forensic examination of documents. *J. Forensic Sci.* **1996,** *41* (5), 812-823.

145.   Wang, J.; Luo, G.; Sun, S.; Wang, Z.; Wang, Y. Systematic analysis of bulk blue ballpoint pen ink by FTIR spectrometry. *J. Forensic Sci.* **2001,** *46* (5), 1093-1097.

146.   Merrill, R. A.; Bartick, E. G.; Mazzella, W. D. Studies of techniques for analysis of photocopy toners by IR. *J. Forensic Sci.* **1996,** *41* (2), 264-271.

147.   Merrill, R. A.; Bartick, E. G.; Taylor, H. J., III. Forensic discrimination of photocopy and printer toners. I. The development of an infrared spectral library. *Anal. Bioanal. Chem.* **2003,** *376* (8), 1272-1278.

148.   Egan, W. J.; Morgan, S. L.; Bartick, E. G.; Merrill, R. A.; Taylor, H. J., III. Forensic discrimination of photocopy and printer toners. II. Discriminant analysis applied to infrared reflection-absorption spectroscopy. *Anal. Bioanal. Chem.* **2003,** *376* (8), 1279-1285.

149.   Kalasinsky, K. S.; Magluilo, J., Jr.; Schaefer, T. Hair analysis by infrared microscopy for drugs of abuse. *Forensic Sci. Int.* **1993,** *63* (1-3), 253-260.

150.   Kalasinsky, K. S. Drug distribution in human hair by infrared microscopy. *Cell. Mol. Biol. (Paris, Fr., Print)* **1998,** *44* (1), 81-87.

151.   Suzuki, E. M. Forensic applications of infared spectroscopy. In *Forensic science handbook, Volume III;* Saferstein, R., Ed.; Prentice-Hall: New York, 1993; pp 71-195.

152.   Bartick, E. G.; Tungol, M. W. Infared microscopy and its forensic applications. In *Forensic science handbook, Volume III;* Saferstein, R., Ed.; Prentice-Hall: New York, 1993; pp 196-252.

153.   Roux, C.; Maynard, P.; Dawson, M. FTIR spectroscopy applications in forensic science. *Chem. Aust.* **1999,** *66* (2), 11-15.

154.   Koenig, J. L.; Wang, S.-Q.; Bhargava, R. FTIR Images. *Anal. Chem.* **2001,** *73* (13), 360A-369A.

155.   Kidder, L. H.; Haka, A. S.; Lewis, N. E. Instrumentation for FT-IR imaging. In *Handbook of vibrational spectroscopy;* John Wiley & Sons, LTD: Nottingham, 2002; Vol. 2, pp 1386-1404.

156.   Miseo, E. V.; Wright, N. A. Developing a chemical imaging camera. *Ind. Phys.* **2003,** *9* (5), 29-32.

157.   Lewis, E. N.; Levin, I. W. Real-time, mid-infrared spectroscopic imaging microscopy using indium antimonide focal-plane array detection. *Appl. Spectrosc.* **1995,** *49* (5), 672-678.

158.   Lewis, E. N.; Kidder, L. H.; Arens, J. F.; Peck, M. C.; Levin, I. W. Si:As focal-plane array detection for Fourier transform spectroscopic imaging in the infrared fingerprint region. *Appl. Spectrosc.* **1997,** *51* (4), 563-567.

159.   Lewis, E. N.; Treado, P. J.; Reeder, R. C.; Story, G. M.; Dowrey, A. E.; Marcott, C.; Levin, I. W. Fourier transform spectroscopic imaging using an infrared focal-plane array detector. *Anal. Chem.* **1995,** *67* (19), 3377-3381.

160.   Bennett, C. L.; Carter, M.; Fields, D.; Hernandez, J. Imaging Fourier transform spectrometer. *Proc. SPIE-Int. Soc. Opt. Eng.* **1993,** *1937* (Imaging Spectrometry of the Terrestrial Environment), 191-200.

161.   Snively, C. M.; Katzenberger, S.; Oskarsdottir, G.; Lauterbach, J. Fourier-transform infrared imaging using a rapid-scan spectrometer. *Opt. Lett.* **1999,** *24* (24), 1841-1843.

162.   Snively, C. M.; Koenig, J. L. Characterizing the performance of a fast FT-IR imaging spectrometer. *Appl. Spectrosc.* **1999,** *53* (2), 170-177.

163.   Koenig, J. L.; Snively, C. M. Fast FT-IR imaging: theory and applications. *Spectroscopy (Eugene, Oregon)* **1998,** *13* (11), 22-28.

164. Bhargava, R.; Ribar, T.; Koenig, J. L. Towards faster FT-IR imaging by reducing noise. *Appl. Spectrosc.* **1999,** *53* (11), 1313-1322.

165. Bhargava, R.; Schaeberle, M. D.; Fernandez, D. C.; Levin, I. W. Novel route to faster Fourier transform infrared spectroscopic imaging. *Appl. Spectrosc.* **2001,** *55* (8), 1079-1084.

166. Bhargava, R.; Wang, S.-Q.; Koenig, J. L. Route to higher fidelity FT-IR imaging. *Appl. Spectrosc.* **2000,** *54* (4), 486-495.

167. Bhargava, R.; Wang, S.-Q.; Koenig, J. L. Processing FT-IR imaging data for morphology visualization. *Appl. Spectrosc.* **2000,** *54* (11), 1690-1706.

168. Bhargava, R.; Levin, I. W. Fourier transform infrared imaging: a new spectroscopic tool for microscopic analyses of biological tissue. *Trends Appl. Spectrosc.* **2001,** *3*, 57-71.

169. Marcott, C.; Reeder, R. C. FT-IR spectroscopic imaging microscopy using an MCT focal-plane array detector. *Proceedings of The 11th international conference on Fourier transform spectroscopy*, Athens, Georgia (USA), June 1, 1998; AIP: Vol. 430 (1), 377-378.

170. Marcott, C.; Reeder, R. C. Industrial applications of FT-IR microspectroscopic imaging using a mercury-cadmium-telluride focal-plane array detector. *Proceedings of SPIE Conference on infrared technology and applications XXIV*, San Diego, California, July 19-24, 1998; The International Society for Optical Engineering: Vol. 3436 (1), 285-289.

171. Buice, R. G., Jr.; Cassis, L. A.; Lodder, R. A. Near-IR and IR imaging in lipid metabolism and obesity. *Cell. Mol. Biol.* **1998,** *44* (1), 53-64.

172. Atti, E.; Gomez, S.; Wahl, S. M.; Mendelsohn, R.; Paschalis, E.; Boskey, A. L. Effects of transforming growth factor-b deficiency on bone development: A Fourier transform-infrared imaging analysis. *Bone* **2002,** *31* (6), 675-684.

173. Zhang, L.; Small, G. W.; Haka, A. S.; Kidder, L. H.; Lewis, E. N. Classification of Fourier transform infrared microscopic imaging data of human breast cells by cluster analysis and artificial neural networks. *Appl. Spectrosc.* **2003,** *57* (1), 14-22.

174.	Gupper, A.; Kazarian, S. G. Study of solvent diffusion and solvent-induced crystallization in syndiotactic polystyrene using FT-IR spectroscopy and imaging. *Macromolecules* **2005,** *38* (6), 2327-2332.

175.	Kazarian, S. G.; Chan, K. L. A. FTIR imaging of polymeric materials under high-pressure carbon dioxide. *Macromolecules* **2004,** *37* (2), 579-584.

176.	Kazarian, S. G.; Chan, K. L. A. "Chemical photography" of drug release. *Macromolecules* **2003,** *36* (26), 9866-9872.

177.	Patterson, B. M.; Havrilla, G. J. Integrating X-ray fluorescence and infrared imaging microspectroscopies for comprehensive characterization of an acetaminophen model pharmaceutical. *Appl. Spectrosc.* **2006,** *60* (5), 471-478.

178.	Bartick, E.; Schwartz, R.; Bhargava, R.; Schaeberle, M.; Fernandez, D.; Levin, I. Spectrochemical analysis and hyperspectral imaging of latent fingerprints. Presented at 16th Meeting of the International Association of Forensic Sciences, Montpellier, France, September 2-7, 2002.

179.	Anderson, A. S.; Fulton, J. E., Jr. Sebum: Analysis by infrared spectroscopy. *J. Invest. Dermatol.* **1973,** *60* (3), 115-120.

180.	Hemmila, A.; McGill, J.; Ritter, D. Fourier transform infrared reflectance spectra of latent fingerprints: a biometric gauge for the age of an individual. *J. Forensic Sci.* **2008,** *53* (2), 369-376.

181.	Bartick, E.; Schwartz, R.; Bhargava, R.; Schaeberle, M.; Fernandez, D.; Levin, I. Spectral imaging of latent fingerprints. Presented at 29th Annual FACSS meeting, Providence, RI, October 13-17, 2002.

182.	Bartick, E. G.; Williams, D. K.; Peters, H. L.; Schwartz, R. L.; Crane, N. J.; Bhargava, R.; Fernandez, D.; Huffman, S. W.; Levin, I. Spectrochemical analysis and spectral imaging of latent fingerprints and trace evidence included within the prints. Presented at 37th Middle Atlantic regional meeting of the American Chemical Society, New Brunswick, NJ, May 22-25, 2005; GENE-757.

183. Mercado, A. G.; Janni, J.; Gilbert, B. Image analysis of explosives fingerprint contamination using a Raman imaging spectrometer. *Proc. SPIE-Int. Soc. Opt. Eng.* **1995,** *2511*, 142-152.

184. Cheng, C.; Kirkbride, T. E.; Batchelder, D. N.; Lacey, R. J.; Sheldon, T. G. In situ detection and identification of trace explosives by Raman microscopy. *J. Forensic Sci.* **1995,** *40* (1), 31-37.

185. West, M. J.; Went, M. J. The spectroscopic detection of exogenous material in fingerprints after development with powders and recovery with adhesive lifters. *Forensic Sci. Int.* **2008,** *174* (1), 1-5.

186. Grant, A.; Wilkinson, T. J.; Holman, D. R.; Martin, M. C. Identification of recently handled materials by analysis of latent human fingerprints using infrared spectromicroscopy. *Appl. Spectrosc.* **2005,** *59* (9), 1182-1187.

187. Ricci, C.; Chan, K. L. A.; Kazarian, S. G. Fourier transform infared spectroscopic imaging for the identification of concealed drug residue particles and fingerprints. *Proceedings of SPIE-Optics and photonics for counterterrorism and crime fighting II*, Stockholm, Sweden, September 11-12, 2006; SPIE: Vol. 6402 (1), Paper 64020M-9.

188. Ricci, C.; Kazarian, S. G. Enhancing forensic science with spectroscopic imaging. *Proceedings of SPIE-Optics and photonics for counterterrorism and crime fighting II*, Stockholm, Sweden, September 11-12, 2006; SPIE: Vol. 6402 (1), Paper 64020J-10.

189. Ricci, C.; Eliasson, C.; Macleod, N. A.; Newton, P. N.; Matousek, P.; Kazarian, S. G. Characterization of genuine and fake artesunate anti-malarial tablets using Fourier transform infrared imaging and spatially offset Raman spectroscopy through blister packs. *Anal. Bioanal. Chem.* **2007,** *389* (5), 1525-1532.

190. Ricci, C.; Nyadong, L.; Fernandez, F. M.; Newton, P. N.; Kazarian, S. G. Combined Fourier-transform infrared imaging and desorption electrospray-ionization linear ion-trap mass spectrometry for analysis of counterfeit antimalarial tablets. *Anal. Bioanal. Chem.* **2007,** *387* (2), 551-559.

191. Chan, K. L. A.; Kazarian, S. G.; Mavraki, A.; Williams, D. R. Fourier transform infrared imaging of human hair with a high spatial resolution without the use of a synchrotron. *Appl. Spectrosc.* **2005,** *59* (2), 149-155.

192. Coates, J. Interpretation of infrared spectra, a practical approach. In *Encyclopedia of analytical chemistry;* Meyers, R. A., Ed.; John Wiley & Sons Ltd: Chichester, 2000; pp 10815-10837.

193. Ley, L.; Mantel, B. F.; Matura, K.; Stammler, M.; Janischowsky, K.; Ristein, J. Infrared spectroscopy of C-D vibrational modes on diamond (100) surfaces. *Surf. Sci.* **1999,** *427-428*, 245-249.

194. Tadokoro, H.; Kobayashi, M.; Kawaguchi, Y.; Kobayashi, A.; Murahashi, S. Normal vibrations of polymer molecules of helical configuration. III. Polyoxymethylene and polyoxymethylene-d2. *J. Chem. Phys.* **1963,** *38*, 703-721.

195. Bruker Optics home page. http://www.brukeroptics.com/hyperion/3000.html (accessed May 18, 2006).

196. Perkin Elmer home page. http://las.perkinelmer.com (accessed May 18, 2006).

197. Bertie, J. E. Optical constants. In *Handbook of vibrational spectroscopy;* Chalmers, J. M.; Griffiths, P. R., Eds.; John Wiley & Sons, LTD: New York, 2002; Vol. 1.

198. Long, J. R. Derivatives of fatty acids and methods of preparing same. U.S. Patent 2,391,251, December 18, 1945.

199. Ardis, A. E. Preparation of monomeric alkyl alpha-cyano-acrylates. U.S. Patent 2,467,926, April 19, 1949.

200. Ardis, A. E. Preparation of monomeric alkyl alpha-cyano-acrylates. U.S. Patent 2,467,927, April 19, 1949.

201. Joyner, F. B.; Hawkins, G. F. Method of making α-cyanoacrylates. U.S. Patent 2,721,858, October 25, 1955.

202. Coover, H. W., Jr.; Dickey, J. B. Stabilized alpha-cyanoacrylate adhesive compositions. U.S. Patent 2,765,332, October 2, 1956.

203. Coover, H. W., Jr.; Shearer, N. H., Jr. Single-stage mixed-monomer adhesives. U.S. Patent 2,763,585, September 18, 1956.

204. Jeremias, C. G. Process for making monomeric α-cyanoacrylates. U.S. Patent 2,763,677, September 18, 1956.

205. Joyner, F. B.; Shearer, N. H., Jr. Preparation of monomeric α-cyanoacrylates. U.S. Patent 2,756,251, July 24, 1956.

206. Coover, H. W., Jr.; Shearer, N. H., Jr. Adhesive compositions containing alkyl esters of cyanoacrylic acid. U.S. Patent 2,794,788, June 4, 1957.

207. Joyner, F. B. Monomeric esters of α-cyanoacrylic acid and their preparation. U.S. Patent 2,784,215, March 5, 1957.

208. Joyner, F. B.; Coover, H. W., Jr. Plasticized monomeric adhesive compositions and articles prepared there-from. U.S. Patent 2,784,127, March 5, 1957.

209. Lee, H. *Cyanoacrylate resins - The instant adhesives: A monograph of their applications and technology;* Pasadena Technology Press: Los Angeles, CA, 1986.

210. Leonard, F.; Kulkarni, R. K.; Brandes, G.; Nelson, J.; Cameron, J. T. Synthesis and degradation of poly(alkyl α-cyanoacrylates). *J. Appl. Polym. Sci.* **1966,** *10* (2), 259-272.

211. McKeever, C. H. Preparation of alkyl α-cyanoacrylates. U.S. Patent 2,912,454, November 10, 1959.

212. Robertson, J. E.; Harrington, J. K.; Banitt, E. H. Fluorocyanoacrylates. U.S. Patent 3,639,361, February 1, 1972.

213. Chang, R. W. H.; Banitt, E. H.; Joos, R. W. Fluoroalkoxyalkyl 2-cyanoacrylate compositions used in tooth treatment. U.S. Patent 3,540,126, November 17, 1970.

214. Banitt, E. H. Cyanoacrylate monomer process. U.S. Patent 3,654,340, April 4, 1972.

215. Halpern, B. D.; Dickstein, J.; Hoegerle, R. M. Cyanoacrylate esters. U.S. Patent 3,142,698, July 28, 1964.

216. Vijayalakshmi, V.; Vani, J. N. R.; Krishnamurti, N. Alkyl and substituted alkyl 2-cyanoacrylates. Part 1. Synthesis and properties. *J. Adhes. Sci. Technol.* **1990,** *4* (9), 733-750.

217. Hawkins, G. F.; McCurry, H. F. Esters of alpha-cyanoacrylic acid and process for the manufacture thereof. U.S. Patent 3,254,111, May 31, 1966.

218. Coover, H. W., Jr.; Wicker, T. H., Jr. Stabilized cyanoacrylate adhesives. U.S. Patent 3,355,482, November 28, 1967.

219. Coover, H. W.; McIntire, J. M. Cyanoacrylate adhesive compositions. U.S. Patent 3,728,375, October 2, 1973.

220. Hawkins, G. F. Process for manufacture of high purity α-cyanoacrylates. U.S. Patent 3,465,027, September 2, 1969.

221. McKeever, C. H.; Raterink, H. R. Process for preparing α-cyanoacrylates. U.S. Patent 2,926,188, February 23, 1960.

222. Ito, K.; Kondo, K. Stabilized alpha-cyanoacrylate adhesive compositions. U.S. Patent 3,557,185, January 19, 1971.

223. Hwang, Y.-H.; Hwang, C.-P.; Tsiang, R. C.-C.; Chen, M. Synthesis and characterization of ethoxyethyl α-cyanoacrylate and reaction intermediates. *J. Appl. Polym. Sci.* **2003,** *87* (11), 1758-1773.

224. Kimura, K.; Sugiura, K. Adhesive composition. U.S. Patent 4,321,180, March 23, 1982.

225. Woods, J. G.; Coakley, P. Anionically polymerizable monomers, polymers thereof and use of such polymers in photoresists. U.S. Patent 5,359,101, October 25, 1994.

226. Rabinowitz, R. Preparation of alkyl and aryl alpha-cyanoacrylates. U.S. Patent 3,444,233, May 13, 1969.

227. Buck, C. J. Modified cyanoacrylate monomers and methods of preparation. U.S. Patent 4,041,061, August 9, 1977.

228.   Ray, N. H.; Doran, P. Preparation of α-cyanoacrylic esters. U.S. Patent 3,463,804, August 26, 1969.

229.   Harris, S. The preparation of thiocyanoacrylates. *J. Polym. Sci., Polym. Chem. Ed.* **1981,** *19* (10), 2655-2656.

230.   Buck, C. J. Preparation of bis(2-cyanoacrylate)monomers. U.S. Patent 3,975,422, August 17, 1976.

231.   Kronenthal, R. L.; Schipper, E. Surgical adhesives. U.S. Patent 3,995,641, December 7, 1976.

232.   Warrener, R. N.; Yong, S. J. Products and methods for development of latent fingerprints with cyanoacrylates. WO 88/01616, 10 March, 1988.

233.   De Keyser, J. L.; De Cock, C. J. C.; Poupaert, J. H.; Dumont, P. Synthesis of ^{14}C labeled acrylic derivatives: diethyl [3-^{14}C] methylidenemalonate and isobutyl [3-^{14}C] cyanoacrylate. *J. Labelled Compd. Radiopharm.* **1989,** *27* (8), 909-916.

234.   Buck, C. J. Unequivocal synthesis of bis(2-cyanoacrylate) monomers. I. Via anthracene adducts. *J. Polym. Sci., Polym. Chem. Ed.* **1978,** *16* (10), 2475-2507.

235.   Kennedy, J. P.; Midha, S.; Gadkari, A. Macromers by carbocationic polymerization. X. Synthesis, characterization, and polymerizability of cyanoacrylate-capped polyisobutylenes. *J. Macromol. Sci., Pure Appl. Chem.* **1991,** *A28* (2), 209-224.

236.   Giral, L.; Malicorne, G.; Montginoul, C.; Sagnes, R.; Serre, B.; Schue, F. Synthesis of fluoroalkyl α-cyanoacrylates: demonstration of an experimental process. *Ann. Pharm. Fr.* **1986,** *43* (5), 439-449.

237.   Kennedy, J. P.; Midha, S.; Gadkari, A. Macromers by carbocationic polymerization. IX. The synthesis and characterization of a cyanoacrylate-capped polyisobutylene. *Polym. Prepr. (Am. Chem. Soc., Div. Polym. Chem.)* **1990,** *31* (2), 655-656.

238.   Dyatlov, V. A.; Maleev, V. Manufacture of 2-cyanoacryloyl chloride and its use for preparation of 2-cyanoacrylate esters. WO 95/32183, November 30, 1995.

239. Gololobov, Y.; Gruber, W.; Nicolaisen, H. C. Process for the production of biscyanoacrylates. U.S. Patent 6,096,848, August 1, 2000.

240. Malofsky, B.; Badejo, I. T. Transesterification method and for making cyanoacrylates. U.S. Patent 6,245,933, June 12, 2001.

241. Klemarczyk, P. Synthesis of cyanoacrylate esters by oxidation of aromatic selenyl cyanopropionates. U.S. Patent 5,504,252, April 2, 1996.

242. Klemarczyk, P. A general synthesis of 1,1 disubstituted electron deficient olefins and their polymer properties. *Polymer* **1998,** *39* (1), 173-181.

243. Harth, H.; Wuest, W.; Bruhn, H. A.; Danielisz, M.; Heinrich, E. Process for production of 2-cyanoacrylates from 2,4-dicyanoglutarates. U.S. Patent 4,587,059, May 6, 1984.

244. Denchev, Z. Z.; Kabaivanov, V. On the synthesis of ethyl-2-cyanoacrylate from waste residue. *J. Appl. Polym. Sci.* **1992,** *44* (10), 1829-1835.

245. Klemarczyk, P. Cyanoacrylate instant adhesives. In *Adhesion science and engineering;* Chaudhury, M.; Pocius, A. V., Eds.; Elsevier: Boston, 2002; Vol. 2, pp 847-867.

246. Denchev, Z. Z.; Kotsev, D.; Serafimov, B. Synthesis and properties of allyloxyethyl 2-cyanoacrylate adhesive. *J. Adhes. Sci. Technol.* **1988,** *2* (3), 157-165.

247. Coover, H. W., Jr.; Joyner, F. B.; Shearer, N. H., Jr.; Wicker, T. H., Jr. Chemistry and performance of cyanoacrylate adhesives. *SPE Tech. Pap.* **1959,** *5*, No. 92, 5 pp.

248. Shantha, K. L.; Thennarasu, S.; Krishnamurti, N. Developments and applications of cyanoacrylate adhesives. *J. Adhes. Sci. Technol.* **1989,** *3* (4), 237-260.

249. Al-Khawam, E. M.; Brewis, O. M.; Glasse, M. D. Cyanoacrylate adhesives of potential medical use. *Adhesion (London)* **1983,** *7*, 109-133.

250. Askill, I. N.; Greff, R. J.; Byram, M. M. Methods for closing suturable wounds by use of cyanoacrylate ester compositions comprising an antimicrobial agent. U.S. Patent 6,214,332, April 10, 2001.

251. Montanaro, L.; Arciola, C. R.; Cenni, E.; Ciapetti, G.; Savioli, F.; Filippini, F.; Barsanti, L. A. Cytotoxicity, blood compatibility and antimicrobial activity of two cyanoacrylate glues for surgical use. *Biomaterials* **2000,** *22* (1), 59-66.

252. Mungiu, C.; Gogalniceanu, D.; Leibovici, M.; Negulescu, I. On the medical use of cyanoacrylic esters: toxicity of pure n-butyl-α-cyanoacrylate. *J. Polym. Sci., Polym. Symp.* **1979,** *66* (Med. Polym.: Chem. Probl.), 189-193.

253. Shalaby, S. W.; Shalaby, W. S. W. Cyanoacrylate-based systems as tissue adhesives. In *Absorbable and biodegradable polymers;* Shalaby, S. W.; Burg, K. J. L., Eds.; CRC Press: Boca Raton, FL, 2004; pp 59-75.

254. Lherm, C.; Muller, R. H.; Puisieux, F.; Couvreur, P. Alkyl cyanoacrylate drug carriers: II. Cytotoxicity of cyanoacrylate nanoparticles with different alkyl chain lengths. *Int. J. Pharm.* **1992,** *84* (1), 13-22.

255. Damge, C.; Aprahamian, M.; Balboni, G.; Hoeltzel, A.; Andrieu, V.; Devissaguet, J. P. Poly(alkyl cyanoacrylate) nanocapsules increase the intestinal absorption of a lipophilic drug. *Int. J. Pharm.* **1987,** *36* (2-3), 121-125.

256. Simeonova, M.; Velichkova, R.; Ivanova, G.; Enchev, V.; Abrahams, I. Study on the Role of 5-fluorouracil in the Polymerization of Butylcyanoacrylate during the Formation of Nanoparticles. *J. Drug Targeting* **2004,** *12* (1), 49-56.

257. Denchev, Z. Z.; Kabaivanov, V. S. Thermal behavior and adhesive properties of some cyanoacrylate adhesives with increased heat resistance. *J. Appl. Polym. Sci.* **1993,** *47* (6), 1019-1026.

258. Kotzev, D. L.; Ward, T. C.; Dwight, D. W. Assessment of the adhesive bond properties of allyl 2-cyanoacrylate. *J. Appl. Polym. Sci.* **1981,** *26* (6), 1941-1949.

259. Attarwala, S.; Klemarczyk, P. T. Cyanoacrylate adhesives with improved cured thermal properties. Eur. Patent 579,476, January 19, 1994.

260. Mikuni, H.; Chikusa, T. Silicon-containing alpha-cyanoacrylates. U.S. Patent 5,140,084, August 18, 1992.

261. Kinsinger, J. B.; Panchak, J. R.; Kelso, R. L.; Bartlett, J. S.; Graham, R. K. Methyl α-cyanoacrylate. II. Copolymerization studies. *J. Appl. Polym. Sci.* **1965,** *9* (2), 429-437.

262. Katti, D.; Krishnamurti, N. Anionic polymerization of alkyl cyanoacrylates: in vitro model studies for in vivo applications. *J. Appl. Polym. Sci.* **1999,** *74* (2), 336-344.

263. Blais, P.; Campbell, R. W. Cyanoacrylates in medicine. *Can. Med. Assoc. J.* **1982,** *126* (3), 227-228.

264. Kotsev, D.; Novakov, P.; Kabaivanov, V. Synthesis and properties of some alkenyl and alkynyl 2-cyanoacrylates. *Angew. Makromol. Chem.* **1980,** *92*, 41-52.

265. Lees, W. A. The science of acrylic adhesives. *Brit. Polym. J.* **1979,** *11* (2), 64-71.

266. Coover, H. W.; McIntire, J. M. Acrylic and methacrylic ester polymers, 2-cyanoacrylic ester polymers. In *Encyclopedia of polymer science and engineering*, 2nd ed.; Interscience, New York: 1985; Vol. 1, pp 299-305.

267. Martin, F. R. Cyanoacrylate adhesives. In *Encyclopedia of materials science and engineering*, 1 ed.; Bever, M. B., Ed.; MIT Press: Cambridge, 1986; Vol. 2, pp 1012-1015.

268. Goodman, M.; Wartman, A. Morpholineamide of α-cyanoacrylates and polymers thereof. U.S. Patent 3,711,448, January 16, 1973.

269. Kotsev, D.; Kabaivanov, V.; Novakov, P. Kinetics of propargyl 2-cyanoacrylate synthesis. *Dokl. Bolg. Akad. Nauk* **1980,** *33* (6), 803-806.

270. Rooney, J. M. Thermal degradation of methyl and ethyl cyanoacrylate oligomers. *Brit. Polym. J.* **1981,** *13* (4), 160-163.

271. Donnelly, E. F.; Pepper, D. C. Solubilities, viscosities, and unperturbed dimensions of poly(ethyl and poly(butyl cyanoacrylate)s. *Makromol. Chem., Rapid Commun.* **1981,** *2* (6-7), 439-442.

272. Birkinshaw, C.; Pepper, D. C. The thermal degradation of polymers of n-butyl cyanoacrylate prepared using tertiary phosphine and amine initiators. *Polym. Degrad. Stab.* **1986,** *16* (3), 241-259.

273. Guthrie, J.; Otterburn, M. S.; Rooney, J. M.; Tsang, C. N. The effect of heat on the molecular weight of poly(ethyl 2-cyanoacrylate) adhesive. *J. Appl. Polym. Sci.* **1985,** *30* (7), 2863-2867.

274. Negulescu, I. I.; Calugaru, E. M.; Vasile, C.; Dumitrescu, G. Thermal behavior of poly(α-cyanoacrylate)s. *J. Macromol. Sci., Pure Appl. Chem.* **1987,** *A24* (1), 75-83.

275. Chorbadjiev, K. G.; Novakov, P. C. Study of the thermal degradation of poly(alkyl α-cyanoacrylate)s. *Eur. Polym. J.* **1991,** *27* (10), 1009-1015.

276. Stein, M. Thermal behavior of various poly(2-cyanoacrylates). *J. Appl. Polym. Sci.: Appl. Polym. Symp.* **1991,** *48* (Polym. Anal. Charact. 3), 441-447.

277. Ryan, B.; McCann, G. Novel sub-ceiling temperature rapid depolymerization-repolymerization reactions of cyanoacrylate polymers. *Macromol. Rapid Commun.* **1996,** *17* (4), 217-227.

278. Guseva, T. I.; Senchenya, N. G.; Gololobov, Y. G.; Gol'ding, I. R.; Shchegolikhin, A. N. Investigation of thermal destruction of polycyanoacrylates. *Russ. Polym. News* **1999,** *4* (2), 6-13.

279. Robello, D. R.; Eldridge, T. D.; Swanson, M. T. Degradation and stabilization of polycyanoacrylates. *J. Polym. Sci., Part A: Polym. Chem.* **1999,** *37* (24), 4570-4581.

280. Hickey, A.; Leahy, J. J.; Birkinshaw, C. End-group identity and its effect on the thermal degradation of poly(butyl cyanoacrylate). *Macromol. Rapid Commun.* **2001,** *22* (14), 1158-1162.

281. Strobel, A. F.; Catino, S. C. α-cyano-β,β-diphenylacrylic acid esters. U.S. Patent 3,644,466, February 22, 1972.

282. Etlis, V. S.; Degtyareva, L. M.; Trofimov, N. N. Preparation of cyanoacetic acid esters. *Zh. Prikl. Khim. (Leningrad)* **1971,** *44* (4), 937-939.

283. Tahtouh, M. Fingerprint reagents for infrared chemical imaging. Honours Thesis, University of Technology, Sydney, Broadway, NSW, 2003.

284. Ono, N.; Yamada, T.; Saito, T.; Tanaka, K.; Kaji, A. A convenient procedure for esterification of carboxylic acids. *Bull. Chem. Soc. Jpn.* **1978,** *51* (8), 2401-2404.

285. Rao, C. G. A new rapid esterification procedure utilizing exceptionally mild reaction conditions. *Org. Prep. Proced. Int.* **1980,** *12* (3-4), 225-228.

286. Pfeffer, P. E.; Silbert, L. S. Esterification by alkylation of carboxylate salts. Influence of steric factors and other parameters on reaction rates. *J. Org. Chem.* **1976,** *41* (8), 1373-1379.

287. Shaw, J. E.; Kunerth, D. C. Quantitative conversion of carboxylic acids and phenols to esters and ethers by reaction of their salts with alkyl halides. *J. Org. Chem.* **1974,** *39* (13), 1968-1970.

288. Bedeschi, A.; Visentin, G.; Perrone, E.; Giudici, F.; Zarini, F.; Franceschi, G.; Meinardi, G.; Castellani, P.; Jabes, D.; et al. Synthesis and structure-activity relations in the class of 2-(pyridyl)penems. *J. Antibiot.* **1990,** *43* (3), 306-313.

289. Paul, R. B.; Kelly, J. M.; Pepper, D. C.; Long, C. Photoinduced anionic polymerization of cyanoacrylates using substituted pyridine pentacarbonyl complexes of tungsten or chromium. *Polymer* **1997,** *38* (8), 2011-2014.

290. Jarikov, V. V.; Neckers, D. C. Anionic photopolymerization of methyl 2-cyanoacrylate and simultaneous color formation. *Macromolecules* **2000,** *33* (21), 7761-7764.

291. Johnston, D. S.; Pepper, D. C. Polymerization via macrozwitterions. 1. Ethyl and butyl cyanoacrylates polymerized by triethyl and triphenylphosphines. *Makromol. Chem.* **1981,** *182* (2), 393-406.

292. Johnston, D. S.; Pepper, D. C. Polymerization via macrozwitterions. 2. Ethyl and butyl cyanoacrylates polymerized by pyridine and poly(vinylpyridine). *Makromol. Chem.* **1981,** *182* (2), 407-420.

293. Johnston, D. S.; Pepper, D. C. Polymerization via macrozwitterions. 3. Ethyl and butyl cyanoacrylates polymerized by benzyldimethyl, triethyl, and tribenzylamines. *Makromol. Chem.* **1981,** *182* (2), 421-435.

294.   Wargacki, S.; Dadmun, M.; Lewis, L. Cyanoacrylate fuming from model fingerprint systems. *Polym. Prepr. (Am. Chem. Soc., Div. Polym. Chem.)* **2005,** *46* (1), 373-374.

295.   Khanna, S. K.; Lambe, J. Inelastic electron tunneling spectroscopy. *Science (Washington, DC, U. S.)* **1983,** *220* (4604), 1345-1351.

296.   Bellamy, L. J. *The infrared spectra of complex molecules*, 3rd ed.; Chapman & Hall: London, 1975.

297.   Tomlinson, S. K.; Ghita, O. R.; Hooper, R. M.; Evans, K. E. The use of near-infrared spectroscopy for the cure monitoring of an ethyl cyanoacrylate adhesive. *Vib. Spectrosc.* **2006,** *40* (1), 133-141.

298.   Tomlinson, S. K.; Ghita, O. R.; Hooper, R. M.; Evans, K. E. Investigation of the dual setting mechanism of a novel dental cement using infrared spectroscopy. *Vib. Spectrosc.* **2007,** *45* (1), 10-17.

299.   Hummel, D. O. *Infrared spectra of polymers in the medium and long wavelength regions;* Interscience: New York, 1966.

cyanoacetic acid

3-hydroxypropionitrile
(3-HPN)

2-hydroxypropionitrile
(2-HPN)

2-cyanoethyl cyanoacetate
(2-CECAc)

oligo-2-cyanoethyl 2-cyanoacrylate
(oligo-2-CECA)

anthracene / ethyl
2-cyanoacylate adduct
(A/ECA)

3-bromopropionitrile
(3-BPN)

formaldehyde

paraformaldehyde

anthracene / 2-cyanoacrylic
acid adduct
(A/CAA)

anthracene / 2-cyanoacylic acid
potassium salt adduct
(A/CAA-K)

anthracene / 2-cyanoacyloyl
chloride adduct
(A/CAC)

hydroquinone

sulfur dioxide
(SO$_2$)

thionyl chloride
(SOCl$_2$)

anthracene / 2-cyanoethyl
2-cyanoacylate adduct
(A/2-CECA)

anthracene / 1-cyanoethyl
2-cyanoacylate adduct
(A/1-CECA)

anthracene / methyl
2-cyanoacylate adduct
(A/MCA)

ethyl 2-cyanoacrylate
superglue
(ECA)

methyl 2-cyanoacrylate
(MCA)

maleic anhydride

anthracene / trideuteromethyl
2-cyanoacylate adduct
(A/MCA-d$_3$)

anthracene / pentadeuteroethyl
2-cyanoacylate adduct
(A/ECA-d$_5$)

2-cyanoethyl 2-cyanoacrylate
(2-CECA)

anthracene

1,8-diazobicyclo[5,4,0]undec-7-ene
(DBU)

anthracene / maleic anhydride adduct
(A/MA)

1-cyanoethyl 2-cyanoacrylate
(1-CECA)

trideuteromethyl 2-cyanoacrylate
(MCA-d$_3$)

pentadeuteroethyl 2-cyanoacrylate
(ECA-d$_5$)